

# **A practical guide to multi-dimensional ERT surveys, interpretation and data integration**

**EAGE-GSM ASIA PACIFIC MEETING ON NEAR SURFACE  
GEOSCIENCE AND ENGINEERING,  
Kula Lumpur, Malaysia  
22<sup>nd</sup> April 2019**

**M.H. Loke, Geotomo Software Sdn Bhd  
T. Søltoft, Aarhus Geosoftware**

# Workshop outline

- 1) Brief introduction to the resistivity method.
- 2) Progress of electrical methods 1920s to 2010s, from 1-D to 4-D
- 3) 2-D surveys, data and inversion
- 4) 3-D surveys, data and inversion
- 5) 4-D surveys, data and inversion

## Special Topics (own reading)

- 1). Model reliability
- 2). Banding effects in 3-D surveys

# **Part 1**

## **Brief introduction to resistivity surveys.**

# Overview of geophysical exploration methods

Geophysical methods measure some physical (physics) property of materials within the earth (geo). The physical property is related to the geological structures that are of interest.

**Seismic** – speed of P and S waves (elastic properties and density).

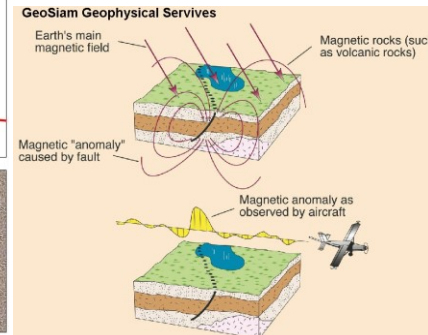
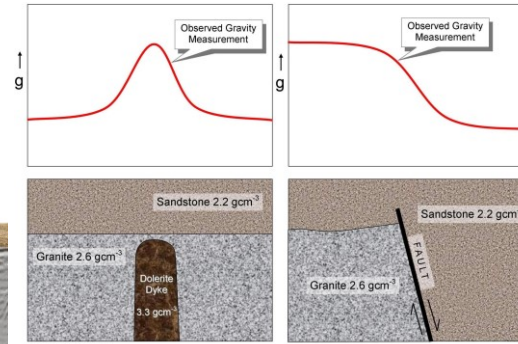
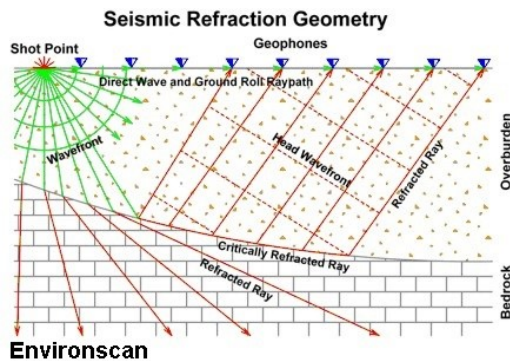
**Electromagnetic, GPR** – electrical and magnetic properties.

**Magnetic** – magnetic properties (magnetite)

**Gravity** – density

**Electrical** – electrical properties

There must be a change (contrast) in the physical property of the soils/rocks for the geophysical method to be used. The seismic and electrical methods are widely used by small survey companies.

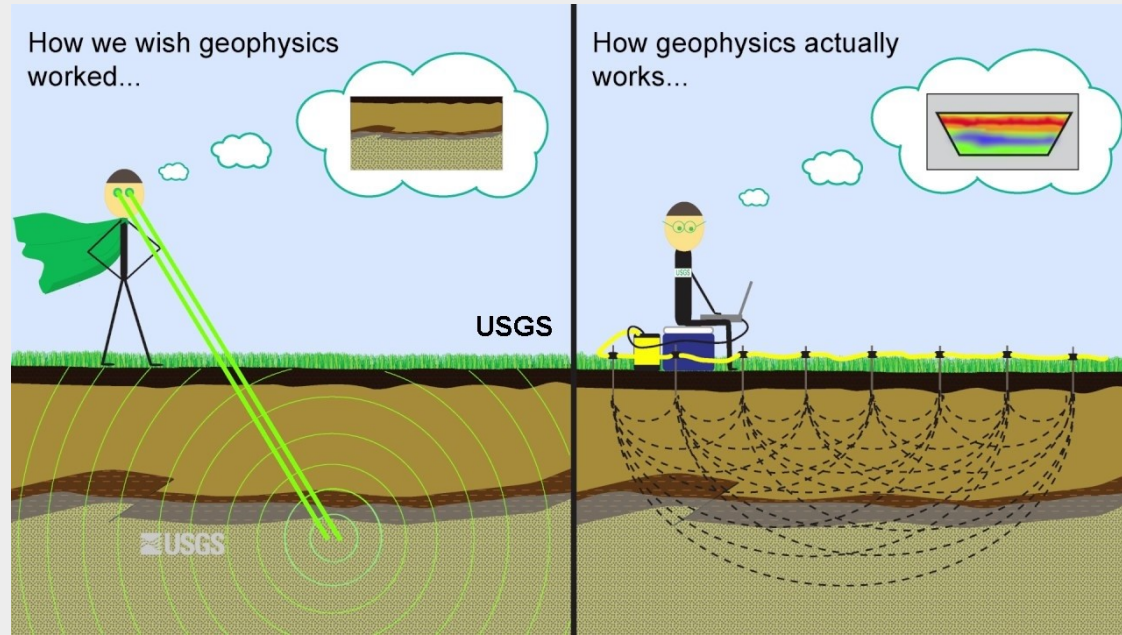
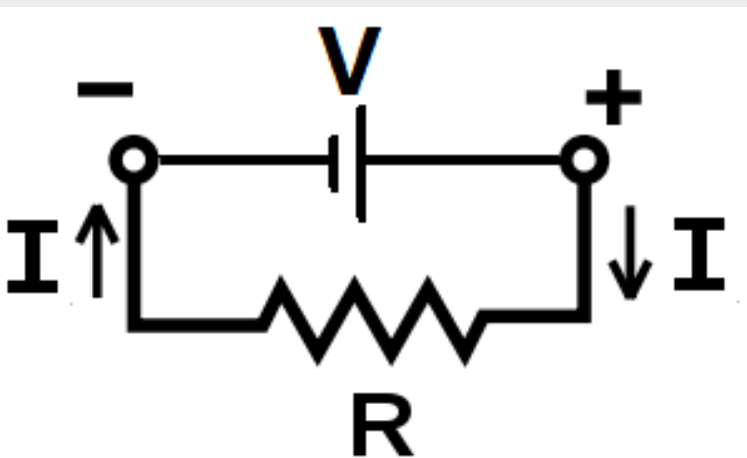


# The electrical method – Ohm's Law

The electrical method measures the resistivity of soils and rocks. The basic physical law used is Ohm's Law. Ohm's Law gives the relationship between the voltage (**V**), current (**I**) and resistance (**R**). It is given by

$$V = R I$$

This form of Ohm's Law is for a current flow in an electrical circuit through a resistor. However, in a field survey the current flows through a continuous 3-D medium.



# Resistivity measurements in a laboratory

In a laboratory, the resistivity of a material  $\rho$  can be determined from the resistance  $R$  between two opposite faces of a prism cut out of that material. Each face has surface area  $A$ , and the two faces are separated by distance  $l$ . Then  $\rho = R A / l$

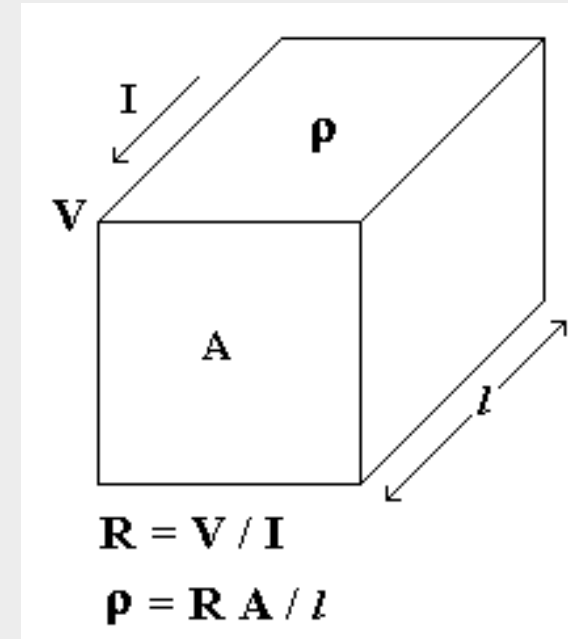
The unit of resistivity is ohm.meter ( $\Omega.m$ ).

Sometimes the conductivity,  $s$ , which is the reciprocal of the resistivity is used.

$$s = 1 / \rho$$

A common unit used for conductivity is milliSeimen/cm ( $mS/cm$ ).

Resistivity is a basic property of the material, similar to density and elastic parameters.

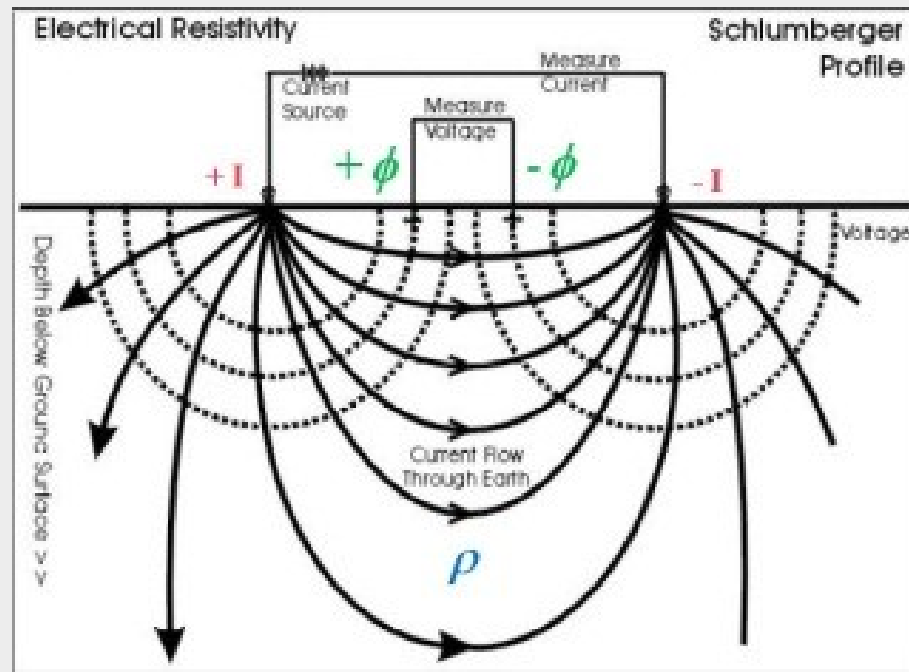


# Ohm's Law in geophysics

In the earth, the current does not pass through a single resistor, but spreads out in all directions. The equation for Ohm's Law for current flow through a continuous medium is given by

$$-\nabla \cdot \left[ \frac{1}{\rho(x,y,z)} \nabla \Phi(x,y,z) \right] = I_c$$

$\rho$  is the resistivity of the medium,  $\phi$  is the potential due to a current source  $I$ .

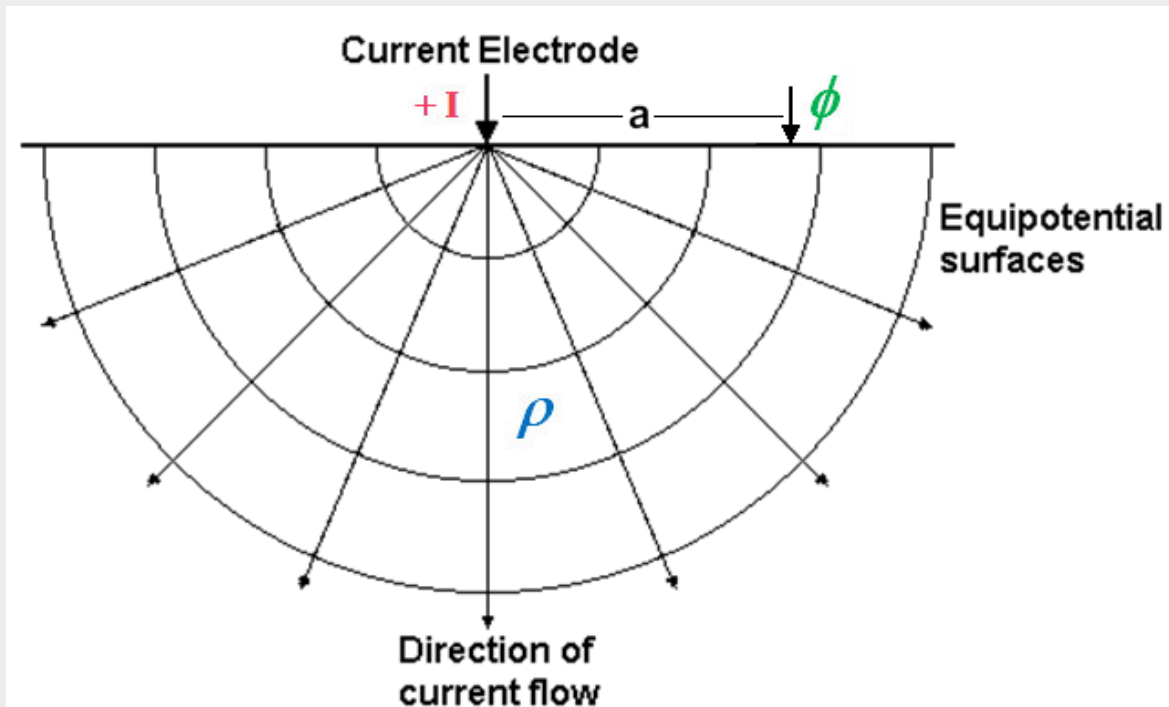


# Electrical potential for a homogeneous medium

In a homogeneous half-space with resistivity  $\rho$ , the potential  $\phi$  due to a single current electrode  $I$  has a simple form

$$\phi = I \rho / 2\pi a$$

where 'a' is the distance between the current and potential electrodes.

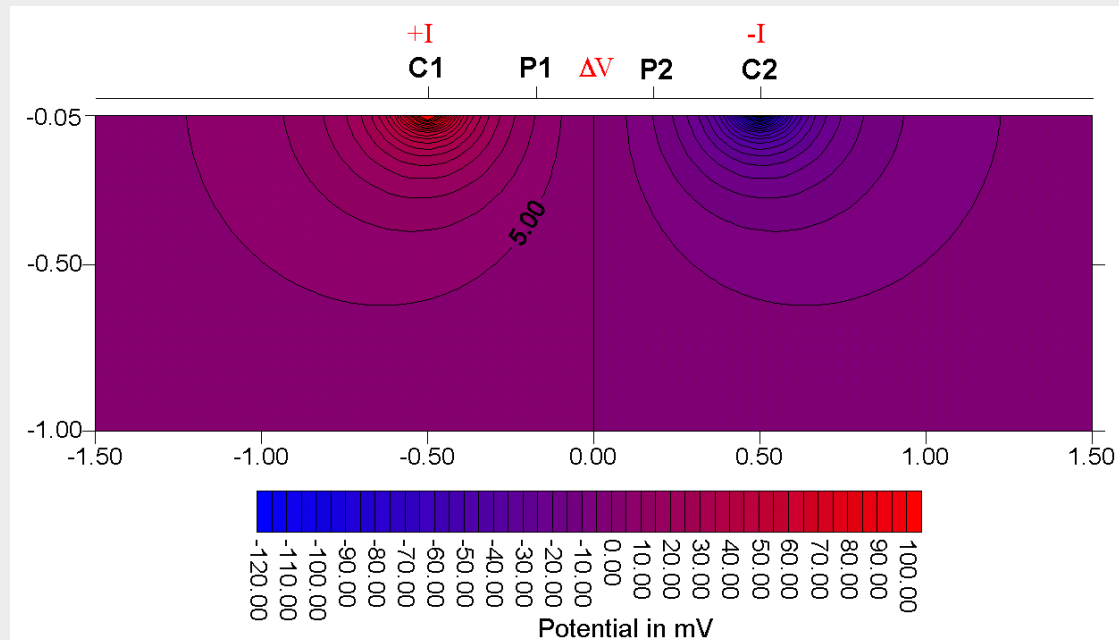


# Electrical potentials due to point current sources

In practice, positive (+I) and negative (-I) current sources are used. The voltage difference between two potential electrodes (P1,P2) is measured. From the current (I) and potential difference ( $\Delta V$ ) measurements, an apparent resistivity value is calculated. The apparent resistivity value  $\rho_a$  is calculated as

$$\rho_a = k \Delta V / I = k R$$

k = geometric factor, R = resistance

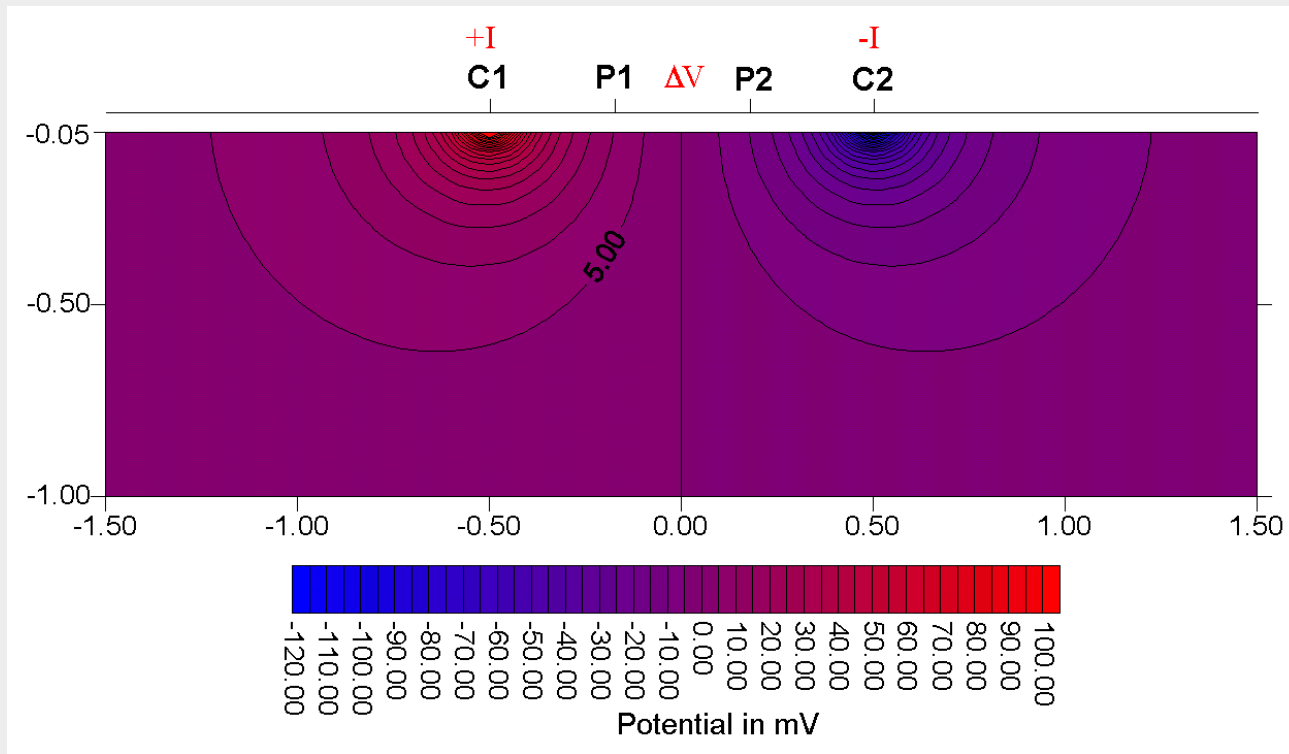


# Apparent resistivity

The apparent resistivity value  $\rho_a$  calculated by

$$\rho_a = k \Delta V / I = k R$$

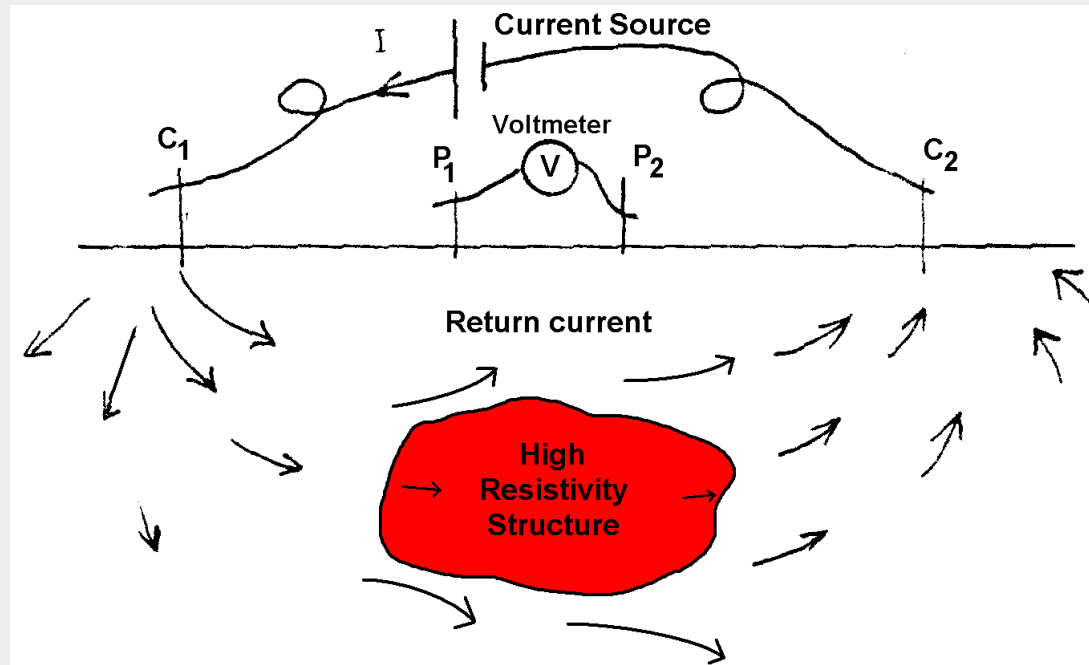
is only equal to the true resistivity for a homogeneous medium. The relationship between the apparent resistivity and the true resistivity is complex for a general non-homogeneous medium, as in all cases for measurements in the earth.



# Electrical field survey measurements

In a field survey, the resistivity of the subsurface is measured by passing a current through the ground. Four metal electrodes are planted into the ground. An electric current (10 mA to 1 A) is injected into the ground using electrodes  $C_1$  and  $C_2$ . The resulting voltage difference at two points on the ground surface is measured using two electrodes,  $P_1$  and  $P_2$ . Changes in the ground resistivity will cause deviations in the current flow and the resulting measured voltage difference  $\Delta V$ .

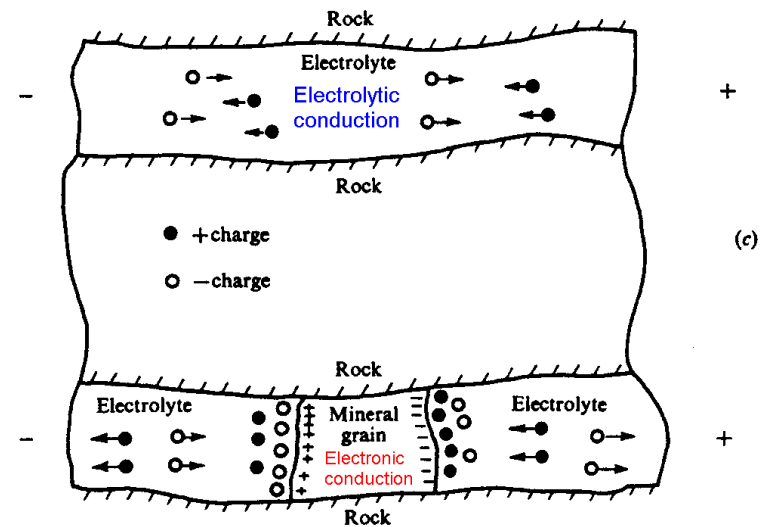
## Basic setup for a resistivity survey



# Current flow in the earth - electrolytic

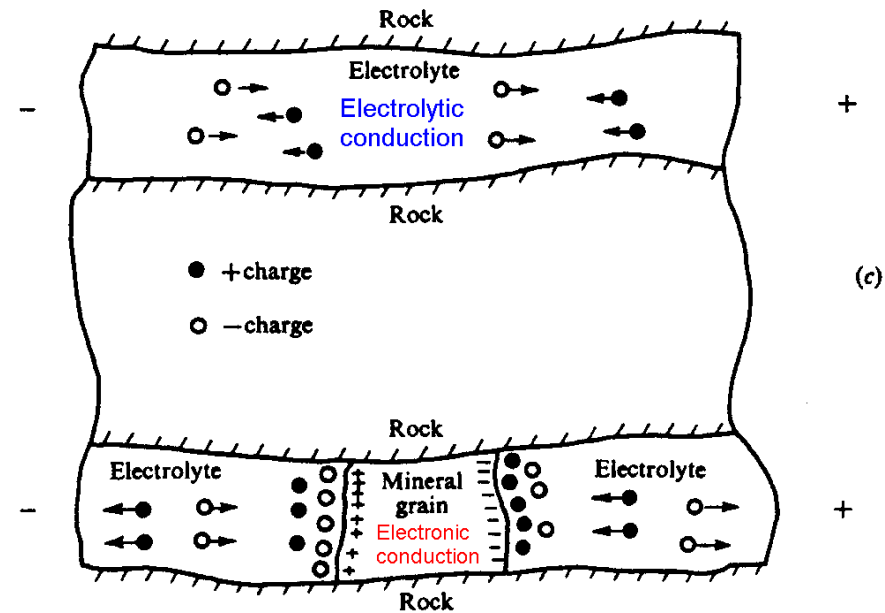
Electric current flows in the earth through two main methods, electrolytic and electronic conduction.

The most common method is electrolytic conduction where the current flow is via the movement of ions in groundwater. Changes in the ground fluid content causes changes in the electrical conductivity. This could be due to changes in the porosity (space between the solid matrix), or nature of the fluid (water with dissolved minerals, hydrocarbons), or solid matrix (sand to clay).



# Current flow in the earth - electronic

In electronic conduction, the current flow is via free electrons, such as in metals. Electronic conduction is important when conductive minerals are present, such as metallic sulfides and graphite in mineral exploration surveys. In environmental and engineering surveys industrial metals (such as pipes and scrap metals) show a distinct low resistivity anomaly.

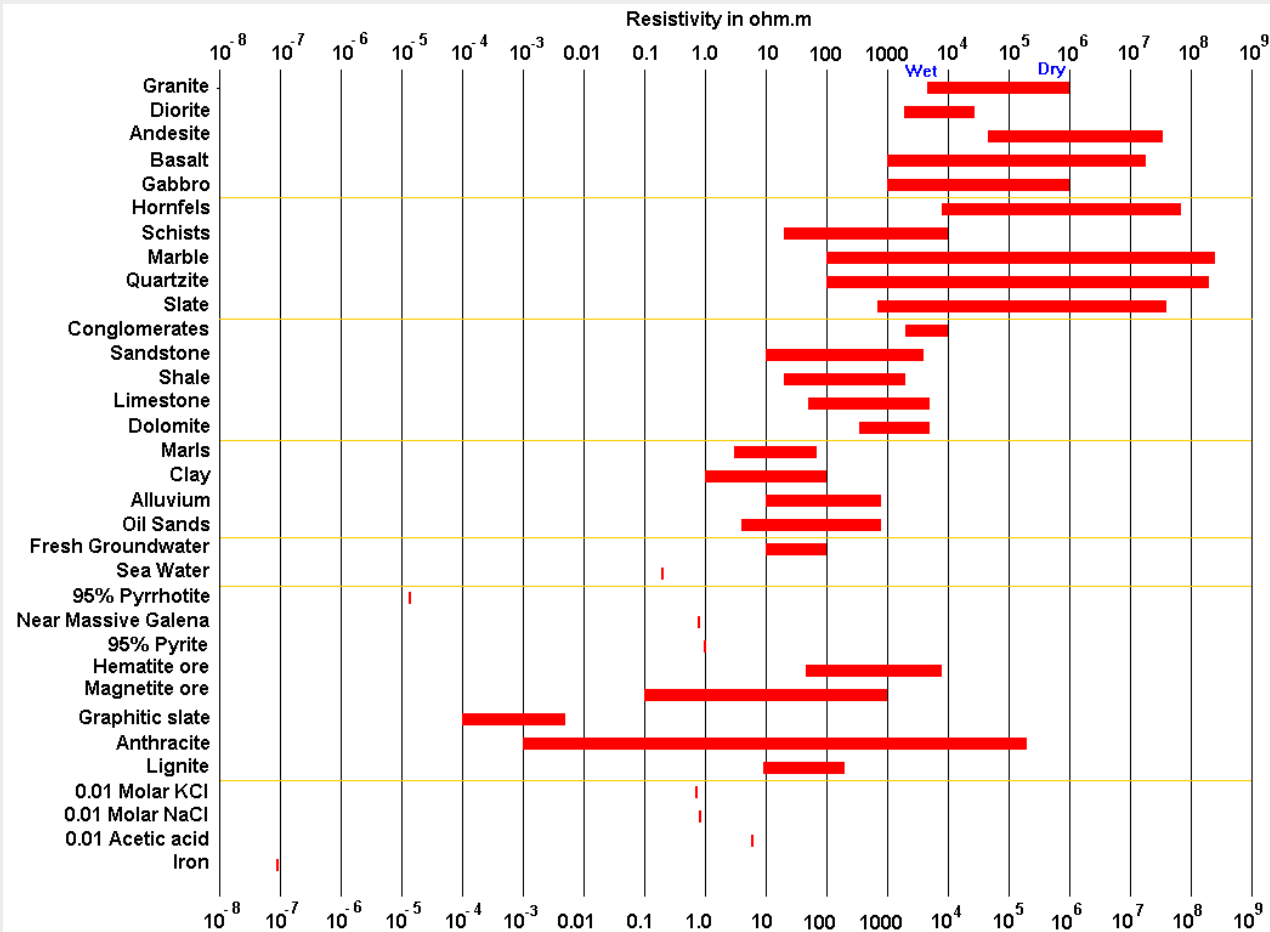


# Electrical properties of rocks and soils

The resistivity of a soil or rock depends on the nature of the solid matrix, porosity and pore fluid. Except for conductive minerals (sulfides, graphite, clay, etc) the main effect is the pore fluid (usually water). As a general rule, igneous/metamorphic rocks have the highest resistivity, followed by sedimentary rocks and soils.

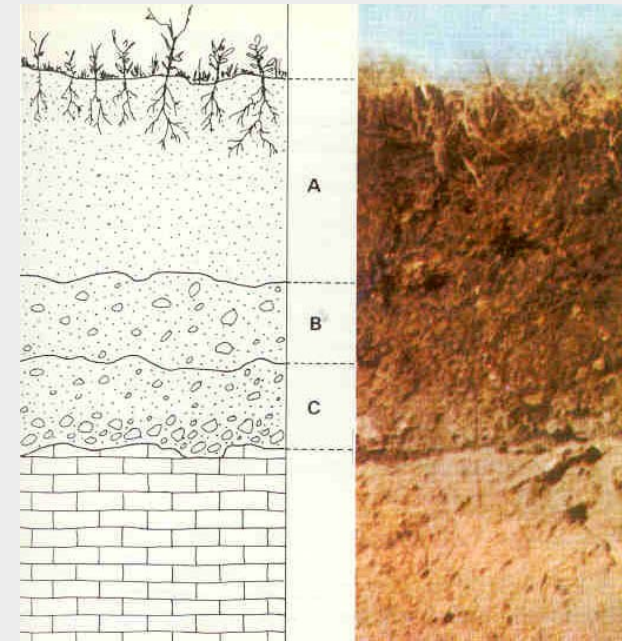
Resistivity values of geological materials have a large range, from millions of  $\Omega.m$  for dry hard-rocks, to less than 1  $\Omega.m$  for saline water and conductive minerals.

This makes the resistivity method a versatile tool.



# Electrical properties of water and sediments

The resistivity of groundwater depends mainly on the concentration of dissolved salts. Fresh groundwater has a resistivity of 10 to 100  $\Omega\cdot\text{m}$ . Seawater has a resistivity of about 0.2  $\Omega\cdot\text{m}$ . Brackish water has a resistivity of about 1 to 10  $\Omega\cdot\text{m}$ . The resistivity of sediments/soils depends on the porosity, fluid and clay content, with most values ranging from 10 to 1000  $\Omega\cdot\text{m}$ . Resistivity decreases with increasing clay content. Clays have resistivity of 1 to 10  $\Omega\cdot\text{m}$ . For clay free rocks and sediments, the electrical conduction is mainly through the fluids in the pores of the soil or rock.



# Electrical properties of sedimentary rocks

The resistivity of sedimentary rocks is generally higher than comparable sediments due to compaction and lithification that reduces the porosity in the rocks (A=gravel, B=conglomerate). Resistivity values are usually between 10 to 1000  $\Omega$ .m. For clastic rocks, the resistivity largely depends on the porosity and the resistivity of the fluids within the pores. The lower resistivity values of shale and marls are due to the clay minerals content.

Limestone



Shale



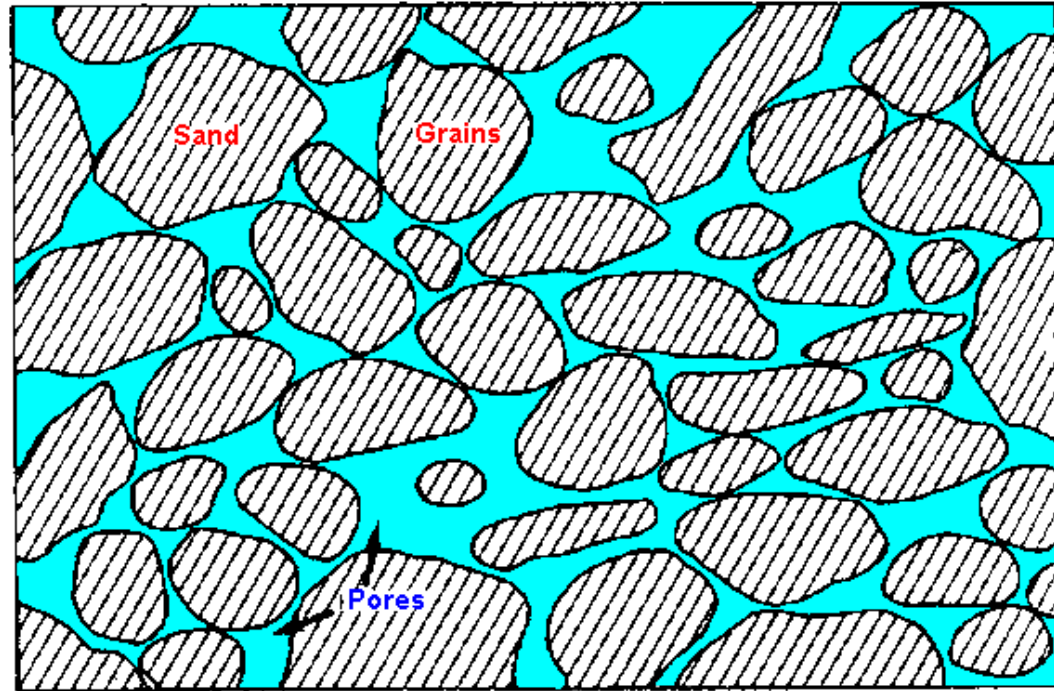
# Electrical properties of sediments and sedimentary rocks

For clay free soils or rocks, the relationship between resistivity and porosity is given by Archie's Law.  $\rho_r = a \rho_w \phi^{-m}$

$\rho_r$  = rock resistivity,  $\rho_w$  = fluid resistivity,  $a \approx 1$ ,  $m \approx 2$

$\phi$  = fraction of the rock filled with fluid

The resistivity of the pore fluid varies from 10 to 100  $\Omega \cdot m$  for fresh groundwater, and as low as 0.2  $\Omega \cdot m$  for seawater.



# Electrical properties of metamorphic and igneous rocks

Igneous and metamorphic rocks usually have high resistivity values of over  $1000 \Omega \cdot \text{m}$ . The resistivity of these rocks is greatly dependent on the degree of fracturing and weathering, and the percentage of the fractures filled with ground water. A given rock type can have a large range of resistivity, from about 1000 to 10 million  $\Omega \cdot \text{m}$ , depending on whether it is wet or dry. In areas with hard bedrock, aquifers are frequently found in the weathering zones associated with fractures or faults which can be mapped by resistivity surveys.

**Granite**



**Marble with fractures**



# Electrical properties of metallic mineral ores

Metallic sulfides (such as pyrrhotite, galena and pyrite) have typically low resistivity values of less than  $1 \Omega \cdot \text{m}$ . The resistivity value of a particular ore body can differ greatly from the resistivity of the individual crystals. Other factors, such as the nature of the ore body (massive or disseminated) have a significant effect. I.P. measurements are frequently made together with the resistivity measurements in mineral exploration surveys, particular for disseminated minerals.

Copper ore



Galena ore



# Electrical properties of metals and chemicals

Metals, such as iron, have extremely low resistivity values.

Soluble chemicals that are strong electrolytes, such as potassium chloride and sodium chloride, can greatly reduce the resistivity of ground water to less than  $10 \Omega \cdot \text{m}$  even at fairly low concentrations.

ERT surveys are widely used in landfill surveys, such as in mapping low resistivity leachate plumes.



# Electrical properties of natural hydrocarbons

Hydrocarbons typically have very high resistivity values. The effect of the hydrocarbons depends on its concentration. Natural occurrences, such as near surface seepage from reservoir or tar sands, can have very high concentrations. Hydrocarbon-bearing oil sands have a significantly higher resistivity so electrical imaging surveys are widely used in its exploration.

**Oil shale**



**Oil sands**



# Electrical properties of industrial hydrocarbons

The effect of industrial hydrocarbons leakage depends on the concentration. New leakages at high concentrations might appear as high resistivity zones. If the percentage of hydrocarbons from the spillage is small, it might not have a significant effect on the bulk resistivity.

In some areas, alteration of insoluble organic compounds by bacteria over time can produce chemicals that lower the soil resistivity.



## **Part 2**

**Progress of electrical methods, from  
1910s to 2010s, from 1-D to 4-D**

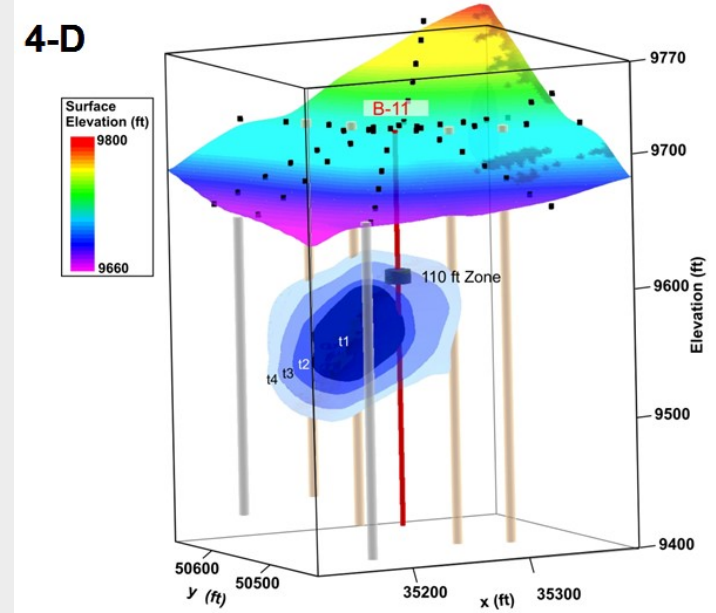
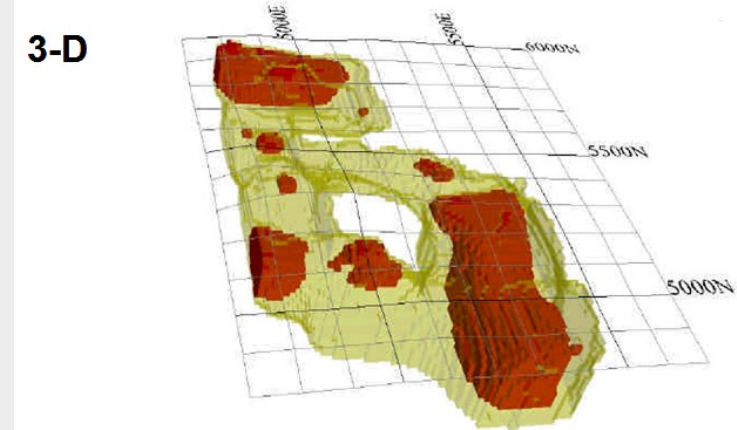
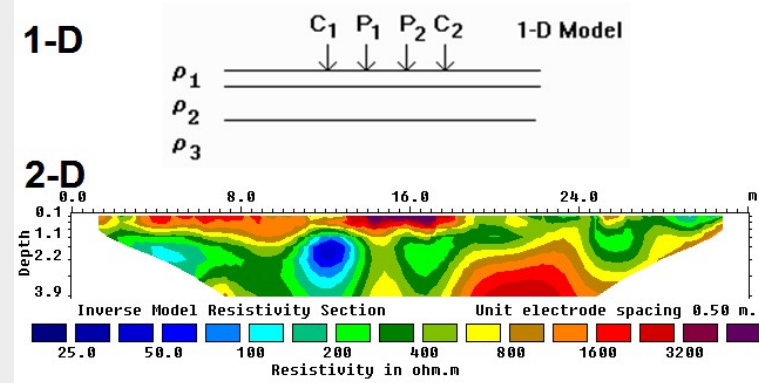
# Progress of the electrical method : 1910s to 2010s

1910s to 1980s : 1-D. Sounding and profiling surveys using 4 electrode resistivity meters.

1990s : 2-D. Major change with multi-electrode systems. Widespread use, more realistic images.

2000s : 3-D. Multi-channel meters. Dense areal data coverage. Mineral exploration with offset pole-dipole layouts. Able to resolve complex mineral systems.

2010s : 4-D. Environmental monitoring (landslides, aquifers, landfills). Remote systems with wireless control.



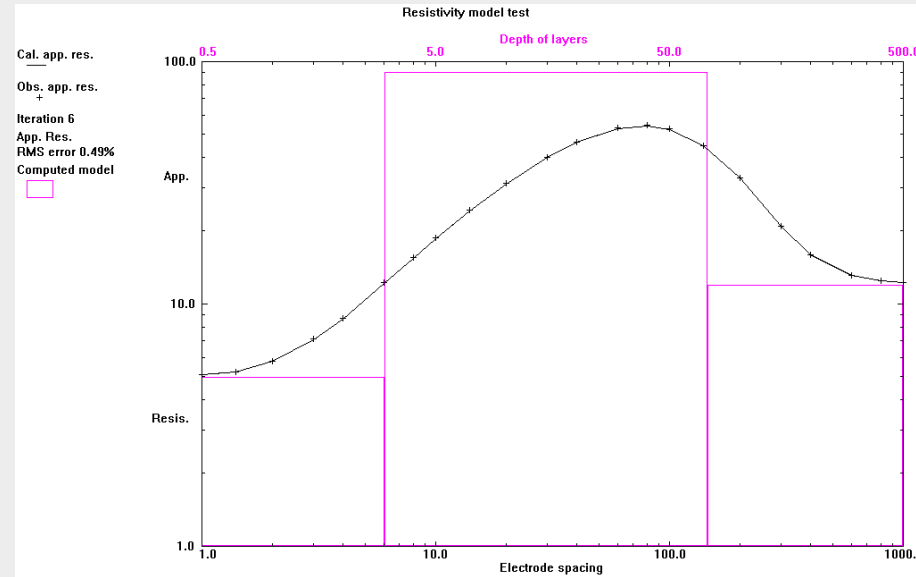
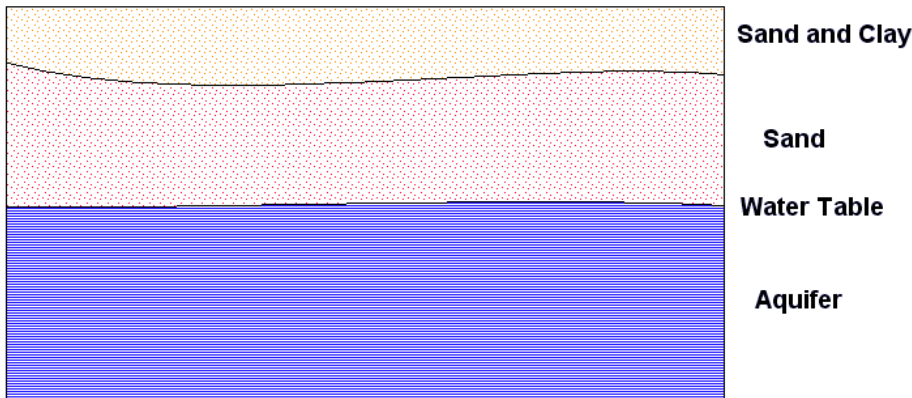
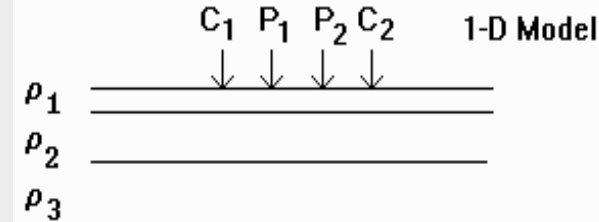
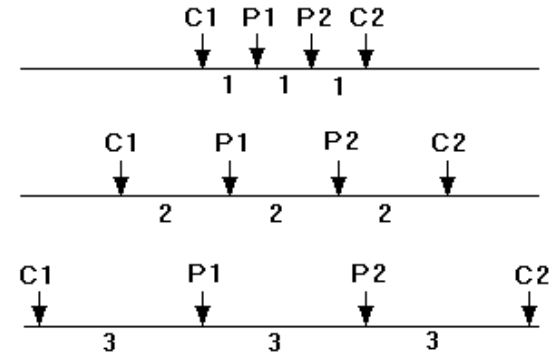
# 1910s to 1980s : 1-D resistivity method

1-D sounding surveys carry out measurements with different spacings between electrodes but with a common center. The data is usually plotted as a sounding curve.

Assume a simplified mathematical model for the subsurface that consists of horizontal layers.

Correlate model properties with known geology.

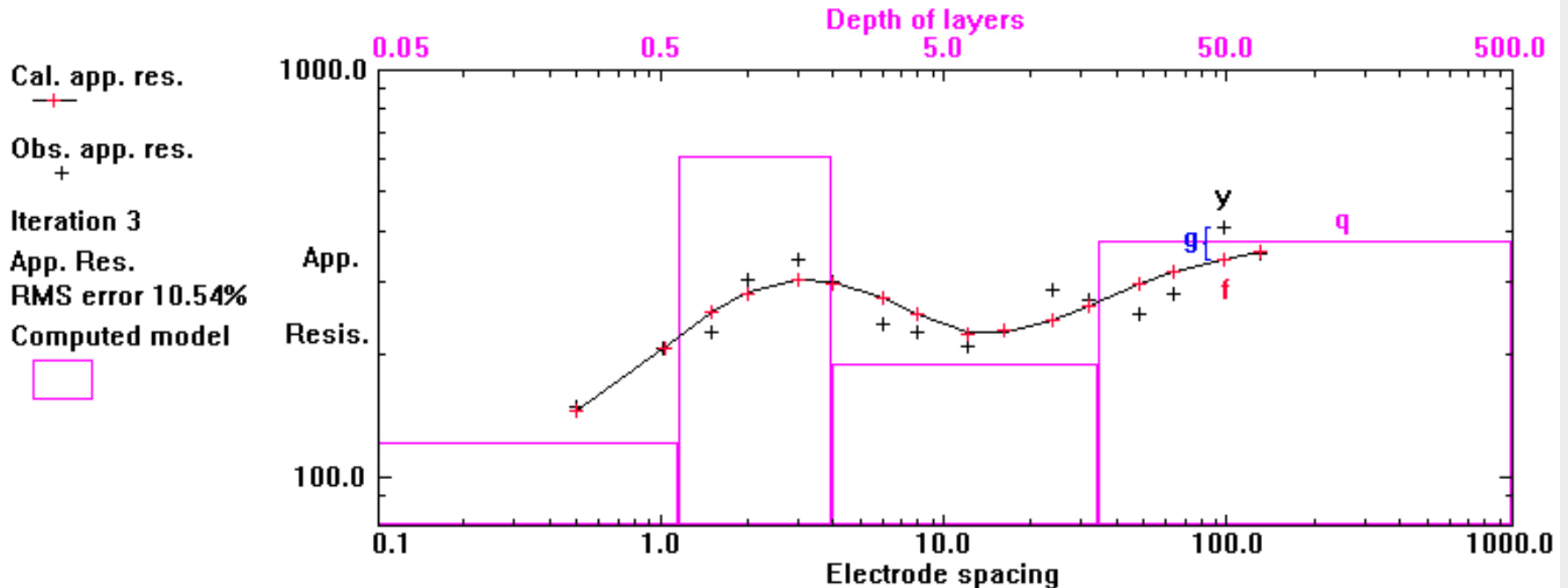
Wenner array sounding survey



# Example of 1-D inversion

The interpretation of data from 1-D sounding surveys can be automatically done using an inversion program. The user enters the data (apparent resistivity values and electrode spacings), together with a starting model (number of layers with estimated thickness and resistivity). The program then automatically adjust the thickness and resistivity of the layers until the calculated apparent resistivity values are 'close' to the measured values.

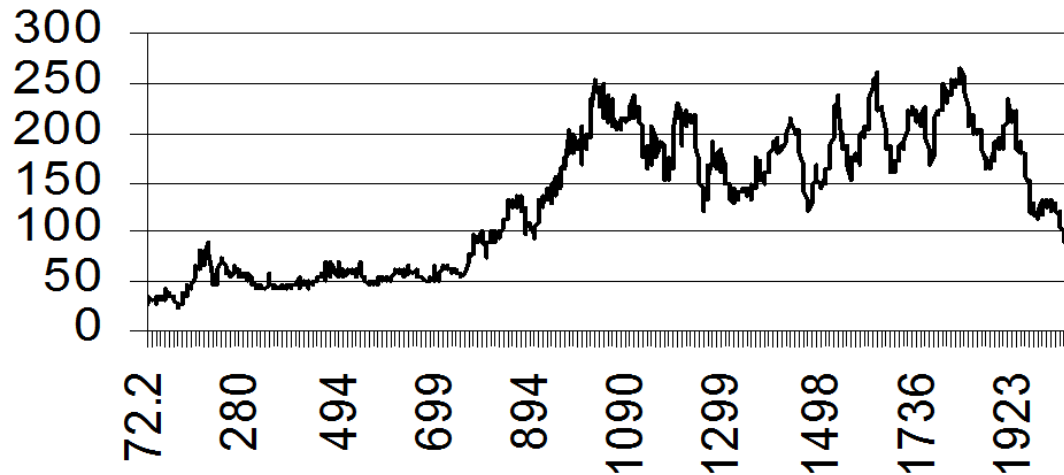
Offset Wenner data set



# Traditional 1-D profiling surveys

The distances between the electrodes are kept fixed, and the electrodes are moved along the survey line. The data interpretation for profiling surveys was mainly qualitative using profile plots. They illustrate qualitatively the change of resistivity with horizontal distance but gives no depth resolution.

**OhmMapper Data, Vignolo, Dipole = 10,  
N = 2.5**

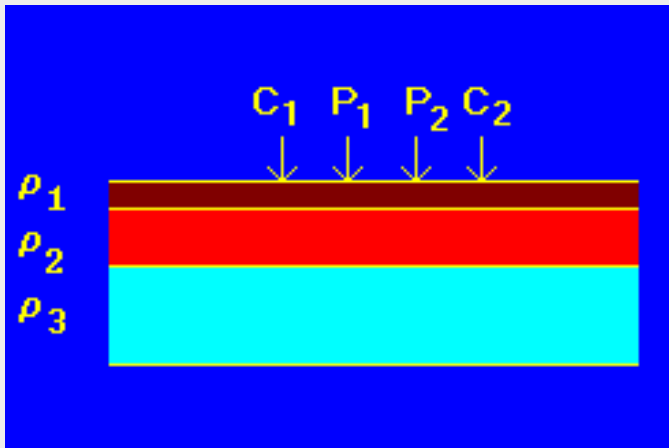


Profiling survey with the OhmMapper Capacitively Coupled Resistivity System, Geometrics

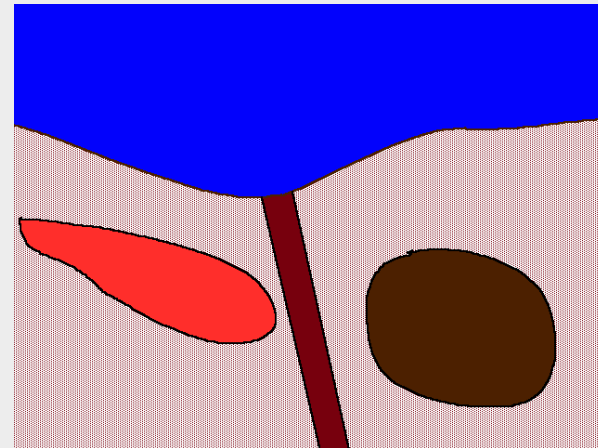
# Limitations of 1-D surveys

Traditional resistivity sounding surveys only give a 1-D picture of the subsurface, which is probably too simple in many cases.

**Sounding 1-D Model**



**Real Situation**

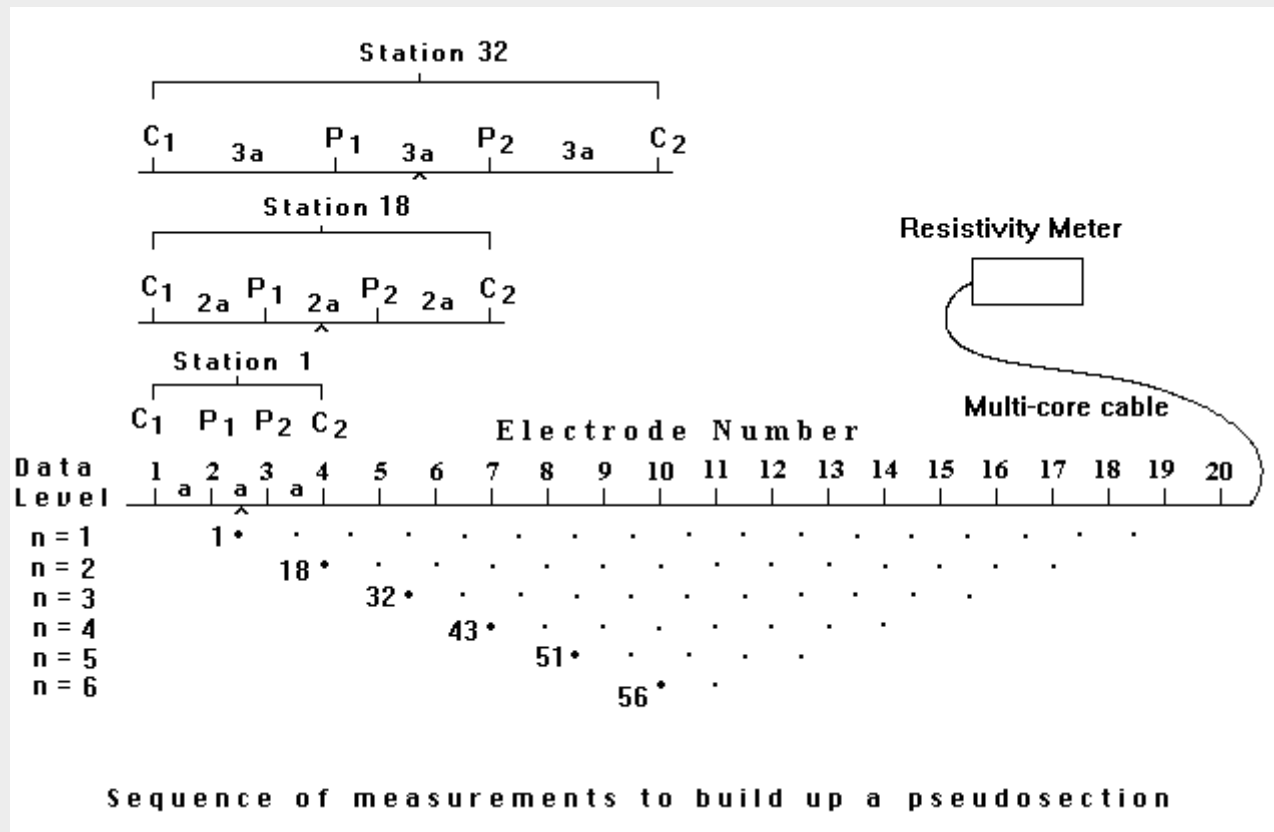


1-D models are probably too inaccurate for most areas where there are significant lateral and vertical variations.

This method is still used for extremely deep aquifers and in many developing parts of the world where access to multi-electrode resistivity meter systems is limited.

# 1990s : 2-D electrical imaging surveys

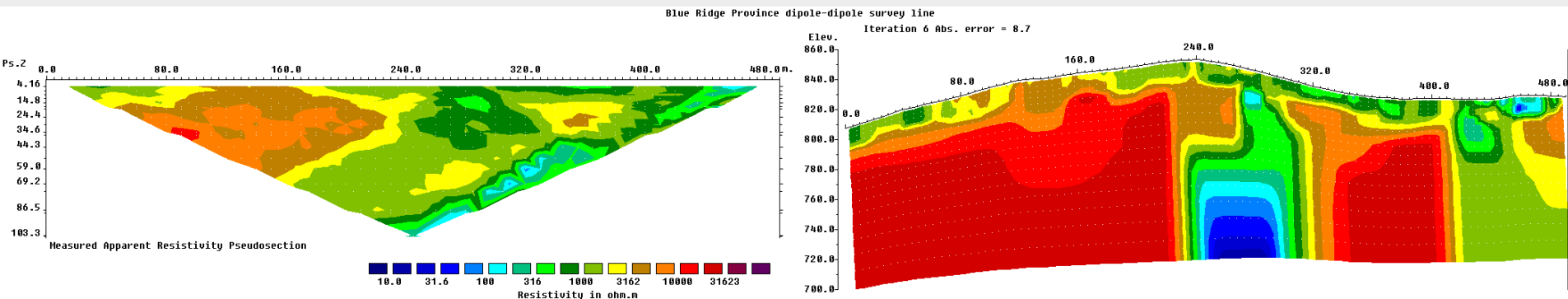
The 1990s saw a rapid growth in 2-D surveys driven by availability of multi-electrode instruments, fast PCs and automatic inversion software. A computer control program automatically selects the appropriate 4 electrodes for each measurement to give a 2-D coverage of the subsurface. A large variety of arrays and survey arrangements can be used with such a system.



# 2-D survey example - Groundwater

Since the mid-1990s 2-D surveys have become a 'standard' geophysical tool for small companies in the hydrological, environmental and engineering sectors. It has enabled the mapping of complex structures previously not possible with 1-D surveys. Together with seismic surveys, 2-D ERT surveys are now offered by most small geophysical survey companies particularly for groundwater related problems.

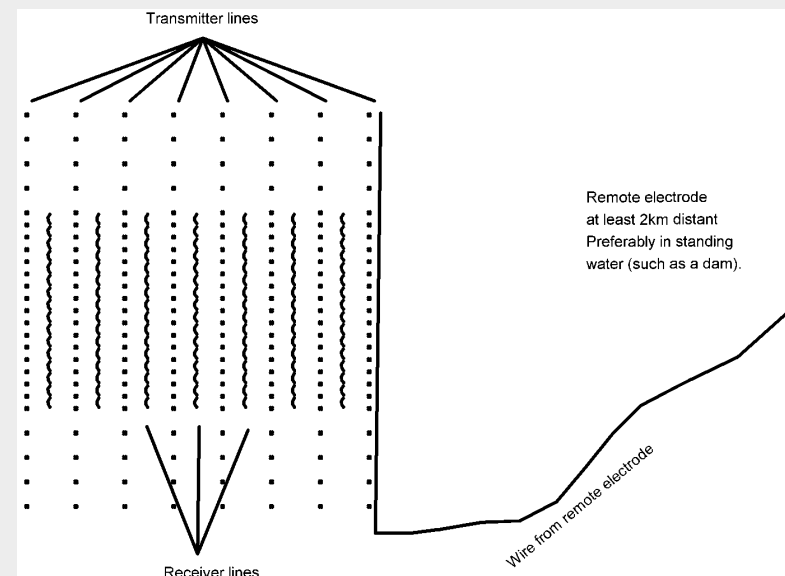
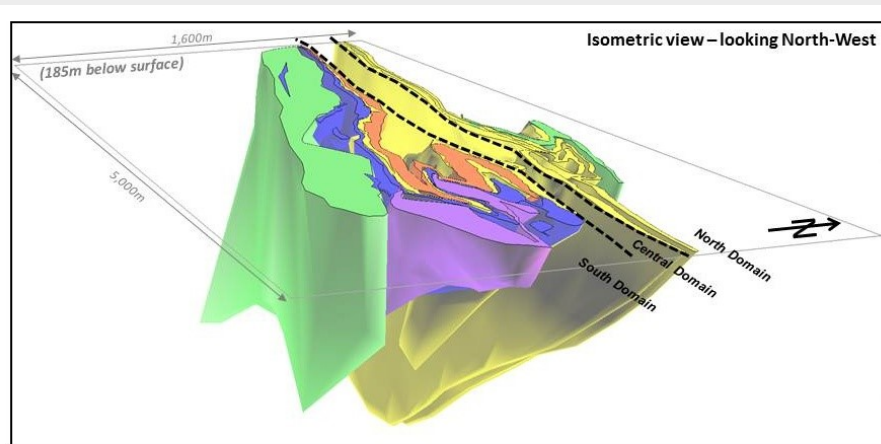
Below is an example of a survey to map fractures filled with groundwater in a hard-rock environment in the Blue Ridge mountain area in eastern USA.



# 2000s : 3-D surveys

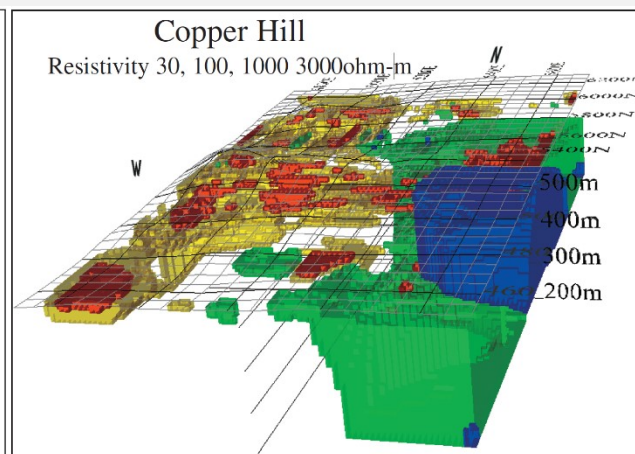
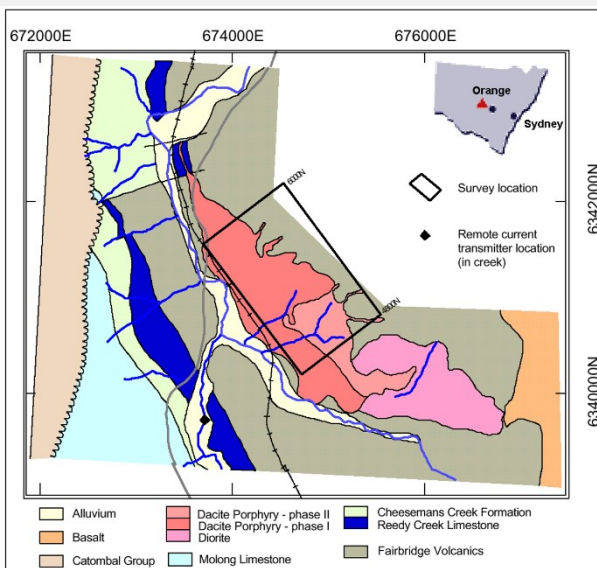
All geological structures are 3-D in nature. For very complex structures, a 3-D resistivity survey and inversion model is required for accurate results. 3-D surveys are not as commonly carried out as 2-D surveys, mainly due higher costs. Recent developments in instrumentation and field techniques have reduced the costs.

The mineral exploration industry was one of the early users of 3-D surveys. The data used was collated from previous 2-D surveys, or measured using new survey protocols such as the offset pole-dipole or dipole-dipole arrays, or the new 'distributed arrays'.

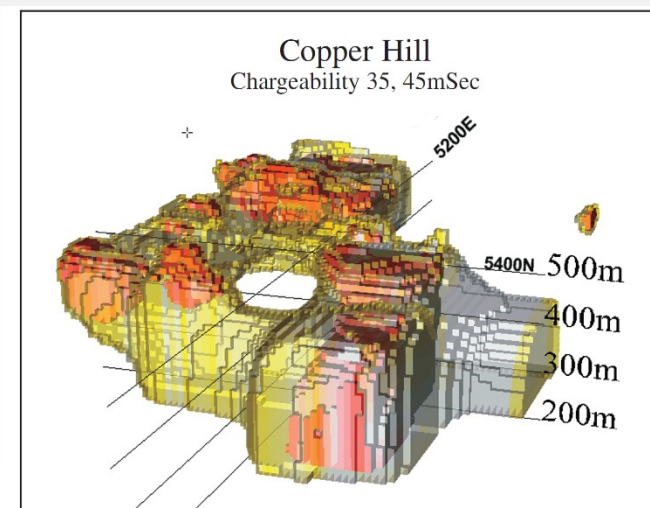


# 3-D survey example – mineral exploration

Copper hill is the oldest copper mine in NSW, Australia dating back to 1845. Gold and copper are found in structurally controlled fractures and quartz veins. However, due to the complex geology, large differences in ore grades were found in drill-holes that were less than 200 m apart. In the late 1990s, a 3-D I.P. survey was conducted using the offset pole-dipole layout. The I.P. model shows 2 en-echelon N-S and E-W trends forming an annular zone of high chargeability. The high model I.P. anomalies agrees well with mineralized zones in existing drill-holes.



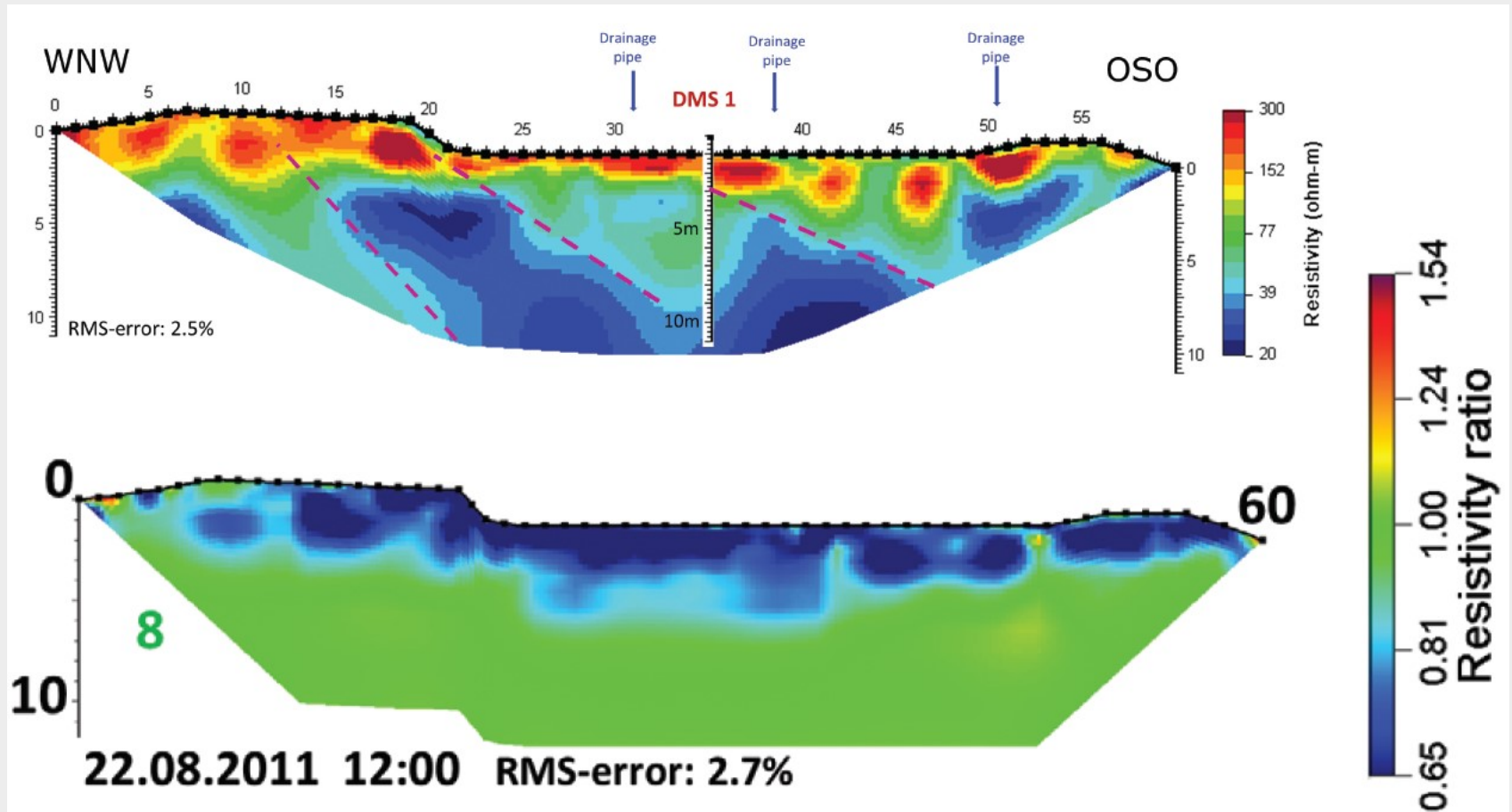
Resistivity Model. Red low to blue high resistivity. the green and blue areas are coincident with the volcanics.



3D Chargeability IP model of Copper Hill with sensitivity controlling the colour saturation.

# 2010s : 4-D surveys

Time-lapse surveys are used to detect changes with time to monitor flow of fluids, possible landslides, landfill changes, leakage from dams. Below is a landslide monitoring example from Austria that shows resistivity change after 1.5 years.



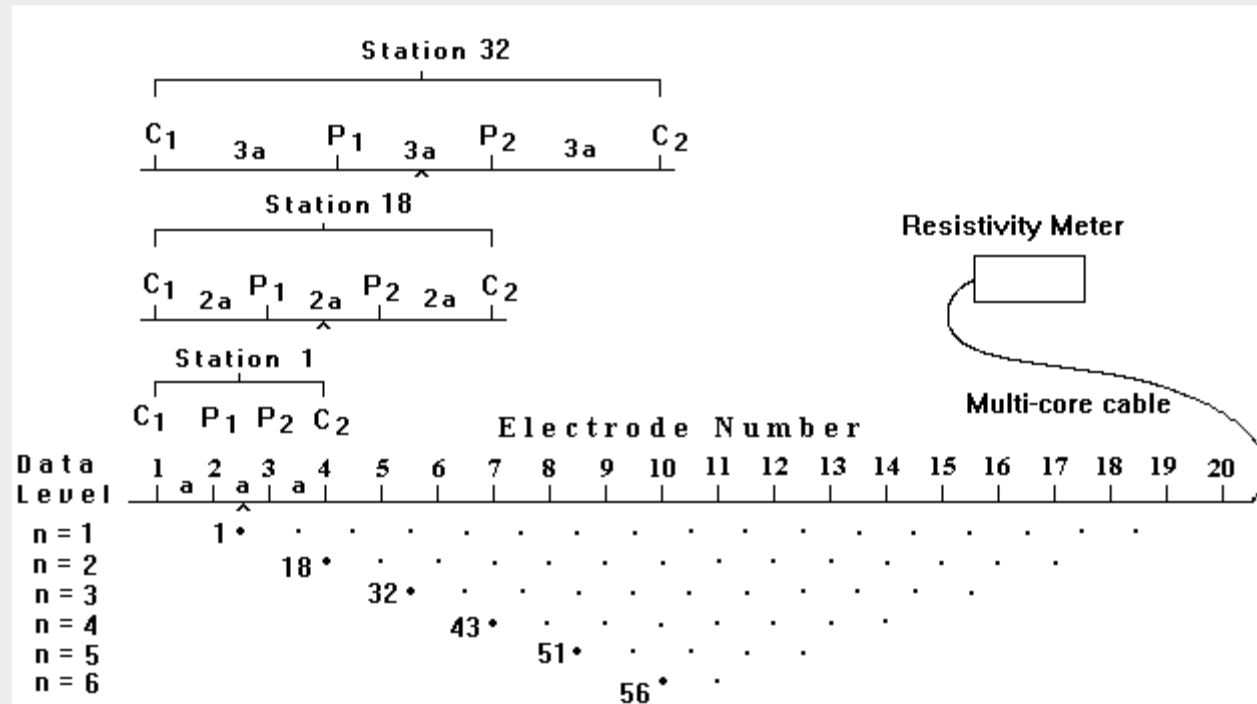
# **Part 3**

## **2-D surveys, data and inversion**

**How 2-D surveys are carried out, the models used, inversion and interpretation.**

# What is a 2-D electrical imaging survey?

A 2-D imaging survey is usually carried out with a computer controlled resistivity meter system connected to a multi-electrode cable system. The control software automatically selects the appropriate four electrodes for each measurement to give a 2-D coverage of the subsurface. A large variety of arrays and survey arrangements can be used with such a system.

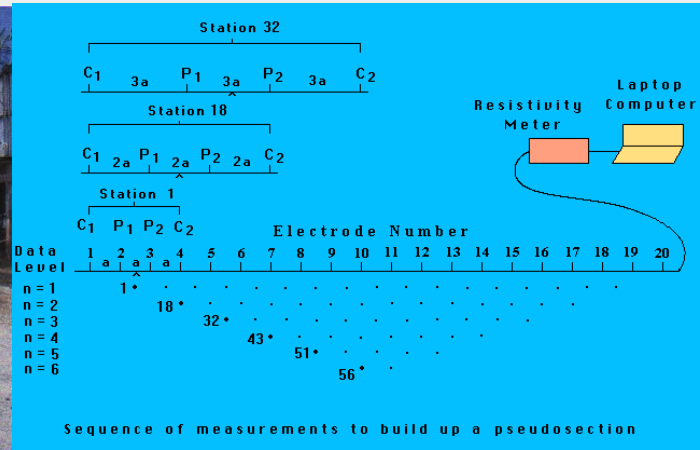


Sequence of measurements to build up a pseudosection

# 2-D imaging survey - instrumentation

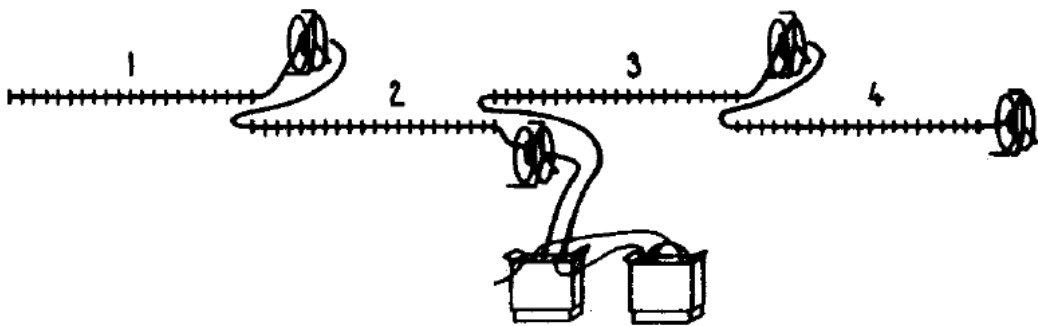
At present, field techniques and equipment to carry out 2-D resistivity surveys are fairly well developed. Commercial multi-electrode systems typically costs from about US\$12,000 to \$100,000. The more expensive systems support multi-channel measurements, and I.P. readings.

To obtain a good 2-D picture of the subsurface, the coverage of the measurements must be 2-D as well. The figure shows a sequence of measurements for the Wenner electrode array for a system with 20 electrodes where all the possible spacings from  $1a$  to  $6a$  are measured across the line.



# 2-D surveys – typical multi-electrode systems

Two of the most widely used ‘high-end’ systems are the Abem Terrameter and Iris Syscal systems. Many system has a ‘center-spread’ arrangement using two cables with take-outs attached to the main resistivity meter placed at the center. The systems can have 24 to 256 electrodes, but 32 is probably the practical minimum. One common system is the Abem SAS and LS series that uses a time-domain I.P. measuring system. The Abem SAS4000 system is an example that uses a 4-cable system. In a 2-D survey, the cables are laid out along a straight line, and an internal computer automatically selects the electrodes for each measurement using a control file provided.



# Prosys system by Iris Instruments

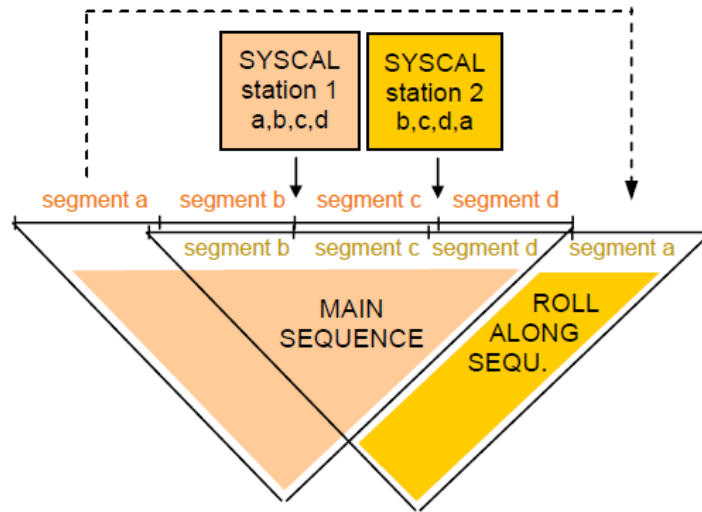
Another example is the Syscal series by Iris Instrument that uses cable segments each with 12 electrodes. Systems come with 48 to 128 electrodes. This is one of the more powerful battery based systems. The multielectrode cable system has been used with node spacings of up to 20 m for surveys up to about 300 m deep.



The **SYSCAL Pro Switch** units use segments (seg) of multi-core cable which are reversible and interchangeable.

For instance, the **SYSCAL Pro Switch 48** with 10m spacing has 4 segments of cable a, b, c, d, with 12 electrodes each, for a total line length of 480m. The SYSCAL is placed in the middle of the line, between segments b and c.

If the profile to measure is longer than the line length, a **ROLL ALONG** technique can be applied where, after a first set of readings with (a, b, c, d), segment a is placed after segment d to form a new (b, c, d, a) combination etc.



SYSCAL Pro Switch	48	72	96	120
5m spacing total line length	2 seg x 24 elect 240m	4 seg x 18 elect 360m	6 seg x 16 elect 480m	12 seg x 10 elect 600m
10m spacing total line length	4 seg x 12 elect 480m	8 seg x 9 elect 720m	12 seg x 8 elect 960m	24 seg x 5 elect 1 200m

# Other multi-electrode systems

There are many other commercial multi-electrode systems :- GF Instruments, Lippmann, Pasi Geophysics, Allied Associates, Siber, ZZ, Geomative, Langeo etc. A typical system has a central control box and multi-electrode cables. Some systems such as by Pasi, have both seismic and resistivity functions.



Lippmann (Germany)



Langeo (China)



Allied (U.K.)



Siber-48 & Siber-64

Siber (Russia)



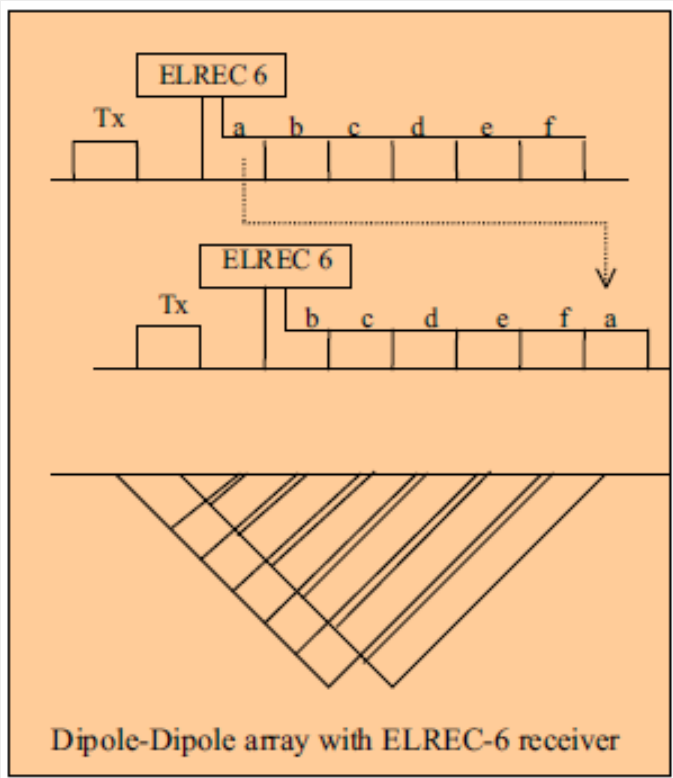
Geomative (China)



Polares (Italy)

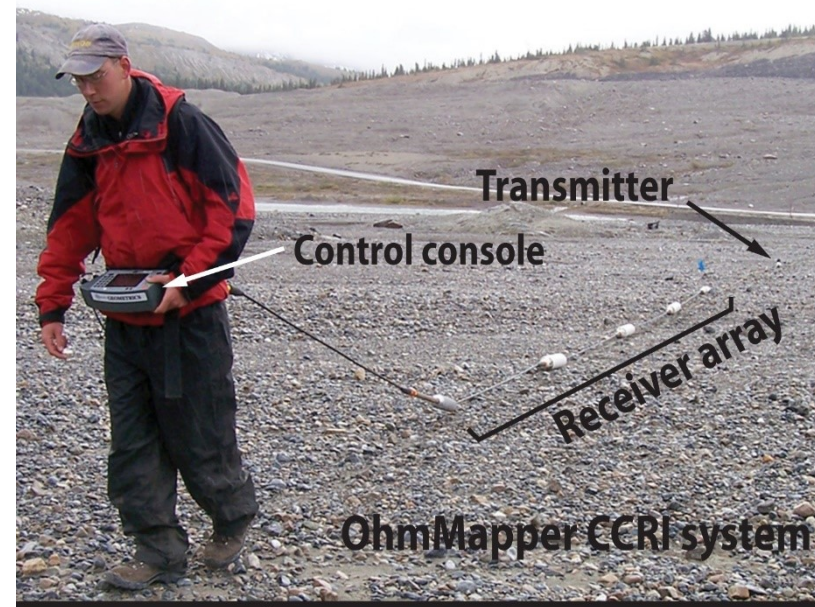
# More powerful and expensive systems

For deeper surveys using larger spacings, separate current and potential measurement units are used. The current source is usually a petrol generator that can produce high currents of up to about 10 Amps, commonly used in I.P. mineral surveys. Example systems are the Iris Elrec and Full-Waver, Quantec Geoscience Titan, GDD and Scintrex IPR-12 system. They are used for survey depths up to about 500 to 1000 m for mineral exploration.



# Mobile systems

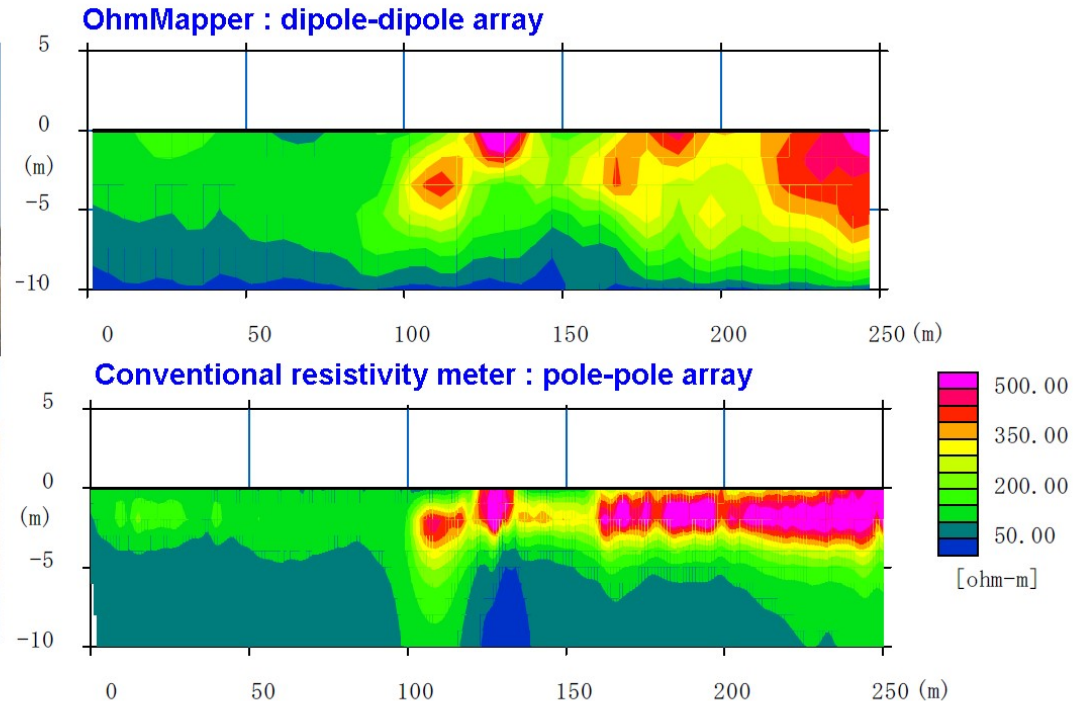
The Geometrics OhmMapper uses a capacitively coupled system that does not require direct ground contact, such as on roads or concrete floors. This system can cover a large area in a short time, but has a more limited depth penetration (3-15m).



Geometrics (USA)



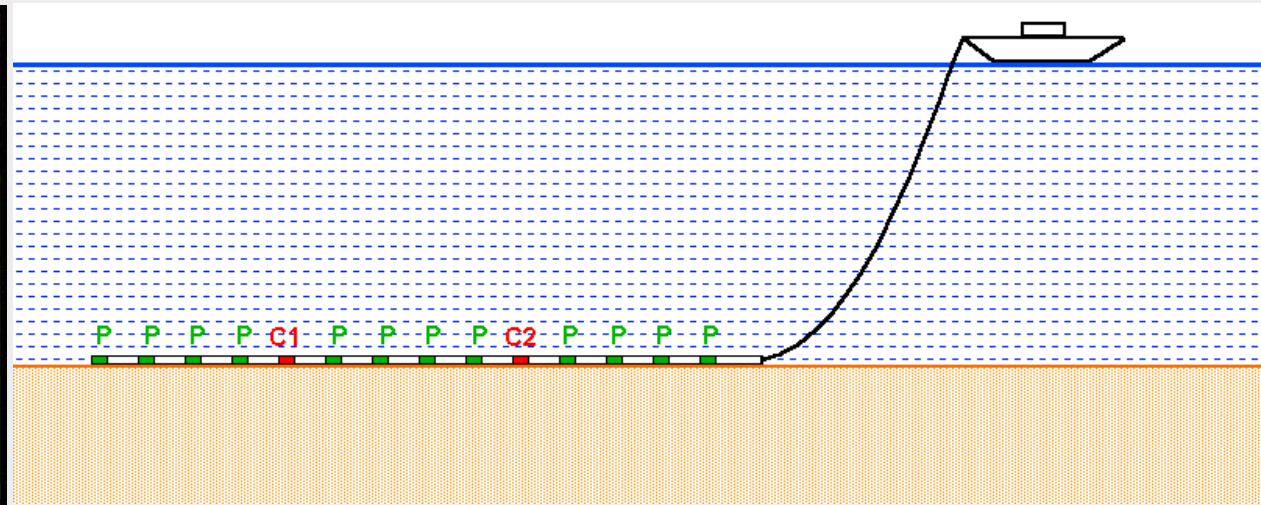
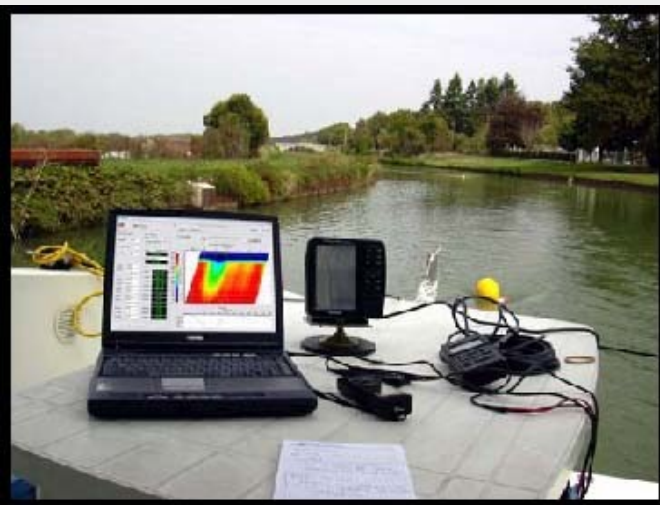
Survey lines on levee (Kokai river, Japan)



Oyo Corporation (Japan) and Geometrics, Inc (USA)

# More mobile 2-D surveys - aquatic systems

Surveys have also been carried out in areas covered by water. A boat pulls a cable with a number of nodes. Two of the nodes are used as current electrodes while the rest are used as potential electrodes. There are now several multi-channel marine systems available, complete with GPS and software on a laptop that controls a resistivity-meter that takes readings automatically. Surveys have also been carried out with the electrodes floating on the surface, dragged along the bottom, or suspended between the water surface and bottom.

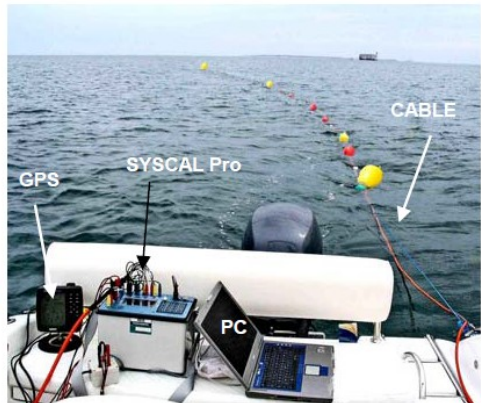
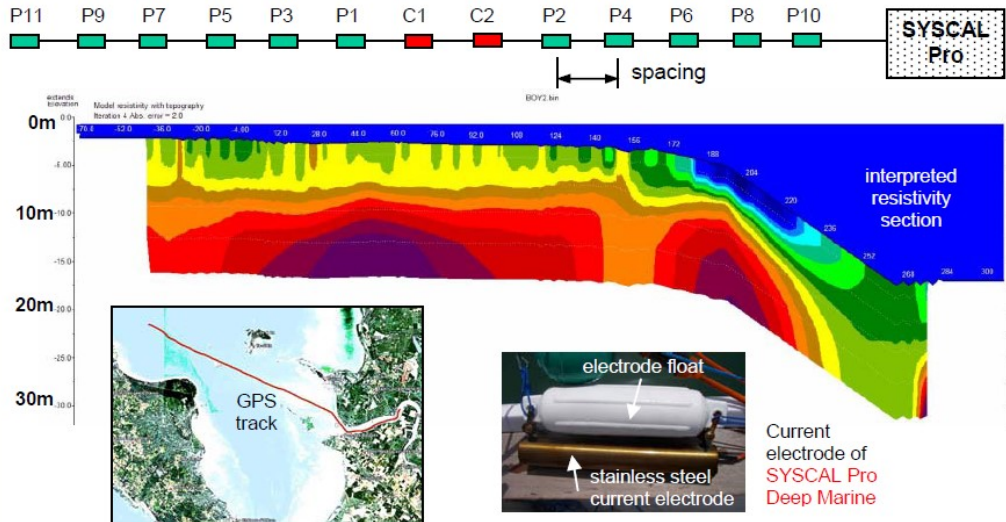


# Example of commercial water survey system

Below is an example with the Syscal system with PC and GPS together with a streamer using graphite electrodes used for a water-borne survey. Note the cable tends to bend due to water currents.

## SYSCAL Pro for river and sea survey

- DYNAMIC ACQUISITION for RIVER & SEA SURVEYS**
- The SYSCAL Pro can be used with a specific cable pulled on the surface of water (lake, river or sea) by a light boat, for a continuous acquisition of resistivity readings.
  - The cable features 13 cylindrical graphite electrodes (4cm diameter, 10cm length) at 5m spacing:
    - 2 for transmitting the current,
    - 11 for simultaneously measuring ten potential channels.
  - A PC continuously records the 10 resistivity / IP values and the GPS data, displays profiles in real time
  - GPS track visualisation on Google Earth
  - Recommended electrode array: reciprocal Wenner Schlumberger
  - Penetration depth: about 15m with a 100m total length cable
  - Acquisition speed: typ. 3km/h



**SYSCAL Pro Deep Marine** is a SYSCAL Pro dedicated to measurement in sea water:

- with outputs of 50V, 50A, 2500W
- for higher penetration
- for higher speed (up to 10km/h)
- with reciprocal Wenner-Schlumb & dip-dip

It uses the same graphite electrode cable as the SYSCAL Pro for the measurement of the potential, but stainless steel electrodes for the current (5cm diameter, 30cm length)

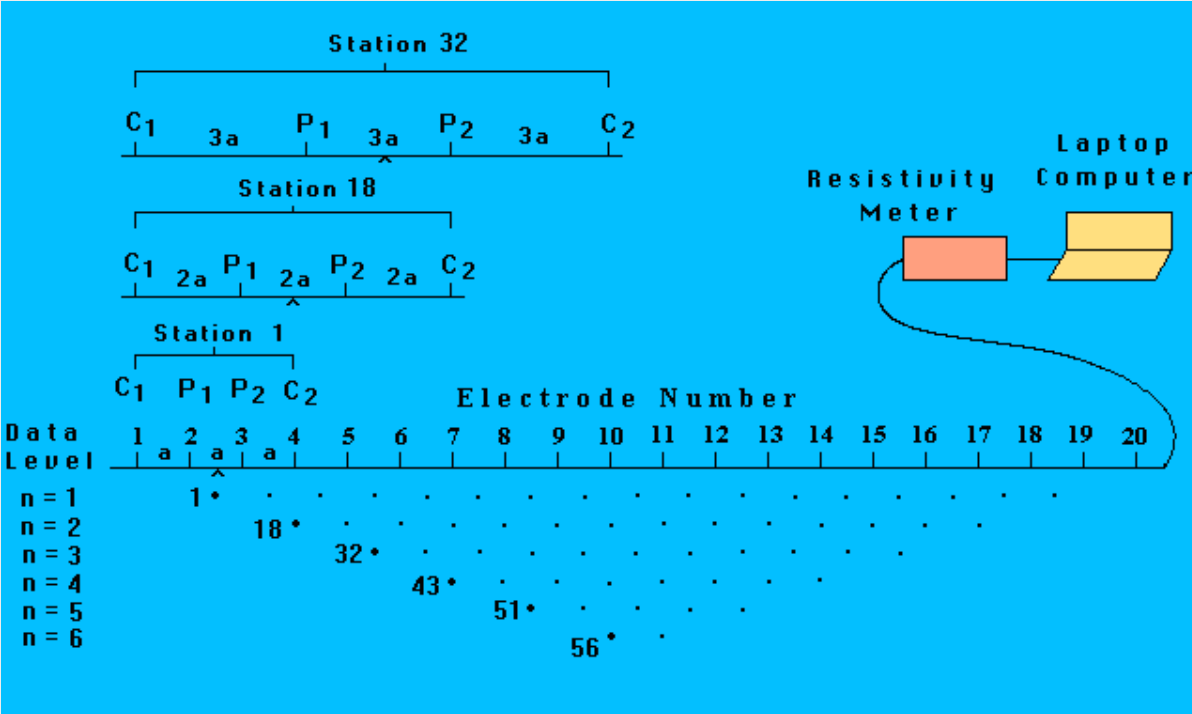
It can be used with a cable of 25m spacing between electrodes (total cable length 350m), for a depth of penetration of about 60m

# Presentation of 2-D survey data

## The pseudosection plotting method

# Pseudosection data plotting method

To plot the data from a 2-D imaging survey, the pseudosection contouring method is normally used. The horizontal location of the point is placed at the mid-point of the set of electrodes used to make that measurement. The vertical location of the plotting point is placed at the median depth of investigation of the array used. For example, the data point measured by electrodes 1, 2, 3 and 4 are plotted at the mid-point between electrodes 2 and 3 in the diagram below.

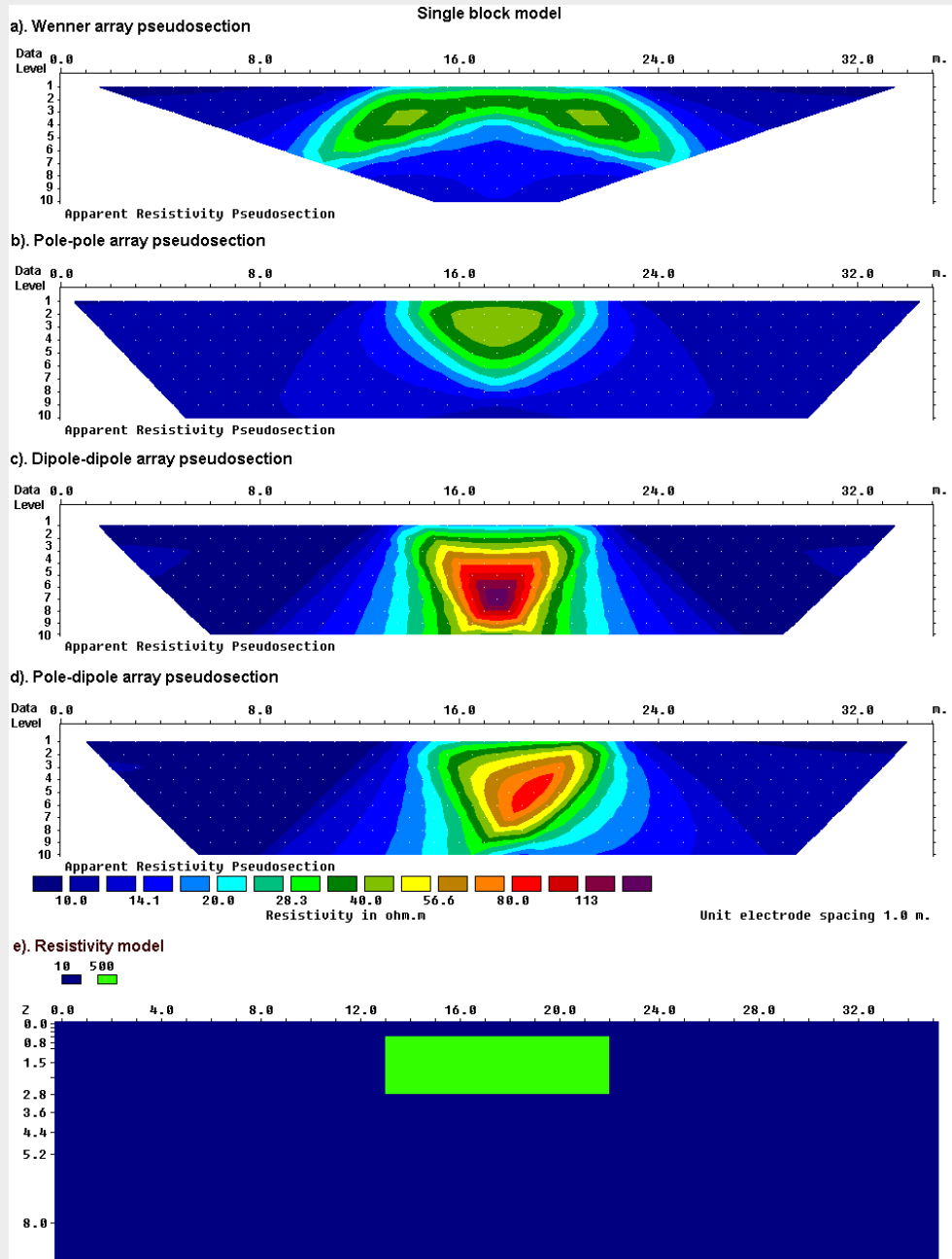


Sequence of measurements to build up a pseudosection

# Pseudosection data plotting method - usage

The pseudosection gives a very rough picture of the true subsurface resistivity structures, as the shapes of the contours depend on the type of array used as well as the true subsurface resistivity.

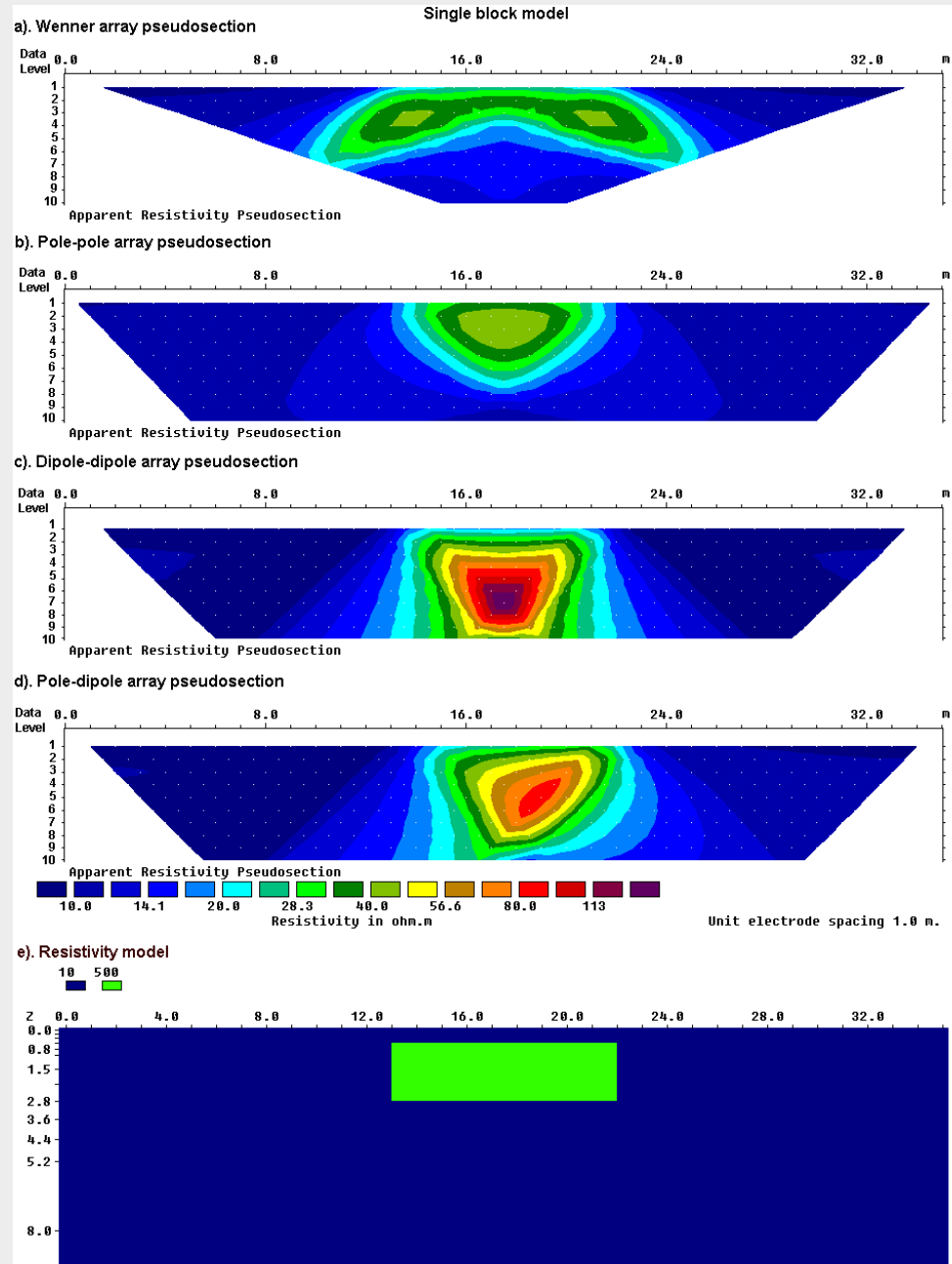
The pseudosection is useful as a means to present the measured apparent resistivity values in a pictorial form, and as an initial guide for further quantitative interpretation.



# Pseudosection data plotting method - limitations

The figure also gives you an idea of the data coverage that can be obtained with different arrays. The pole-pole array gives the widest horizontal coverage, while the coverage obtained by the Wenner array decreases more rapidly with increasing electrode spacing.

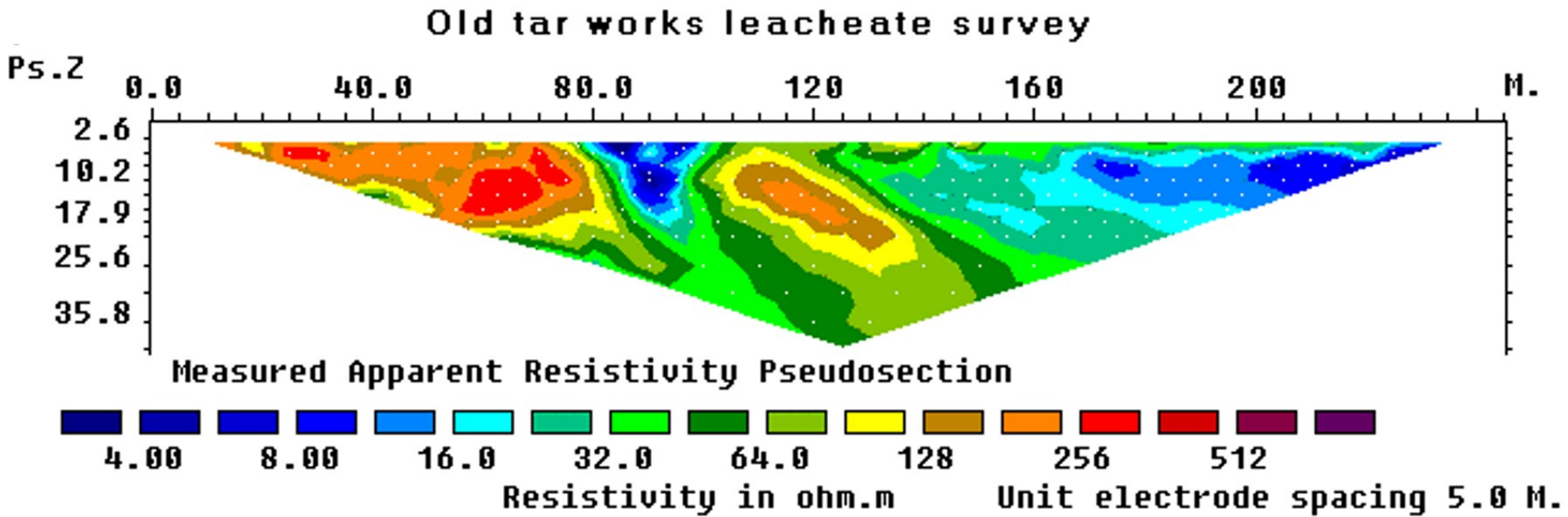
One useful practical application of the pseudosection plot is for picking out bad apparent resistivity data points, which have unusually high or low values.



# Example of a typical pseudosection

The pseudosection plot normally shows smoothly changing contours, particularly when a 'conventional' array is used, such as the Wenner array in the example below. There is a large variation of about 100 times in the apparent resistivity values, but they change in a smooth manner across the section.

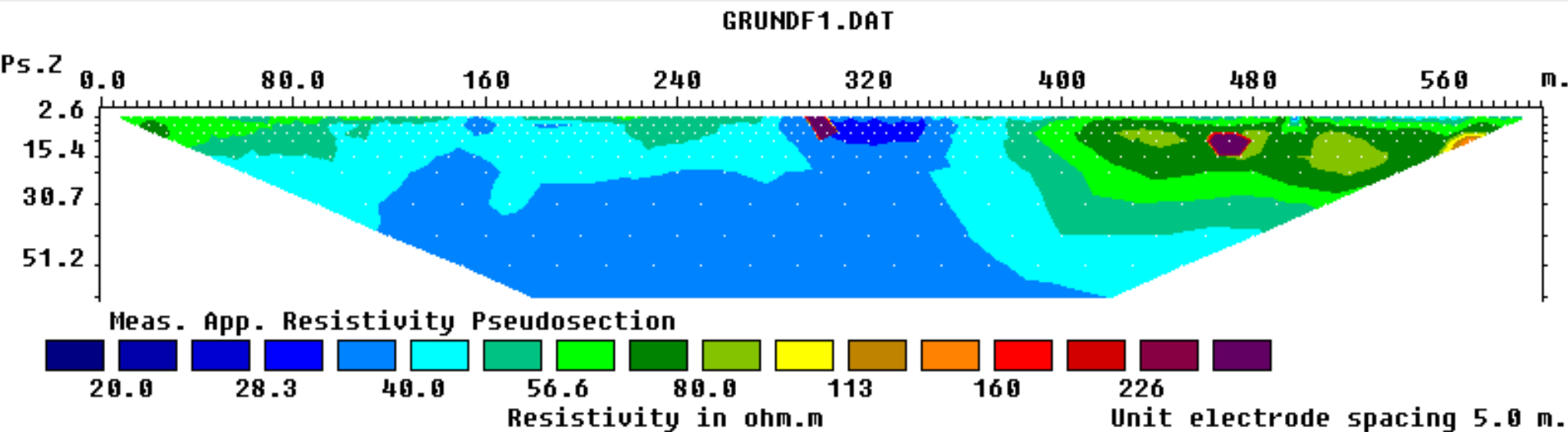
If there are sudden jumps in the apparent resistivity values, it is usually an indication of bad data.



# Using the pseudosection to identify bad data points

Bad data points fall into two broad categories, i.e. “systematic” and “random” noise. Systematic noise is usually caused by some sort of failure during the survey, and some of the apparent resistivity values are much higher or lower than other readings. Random noise include effects such telluric currents that affects all the readings, and the readings to be slightly lower or higher.

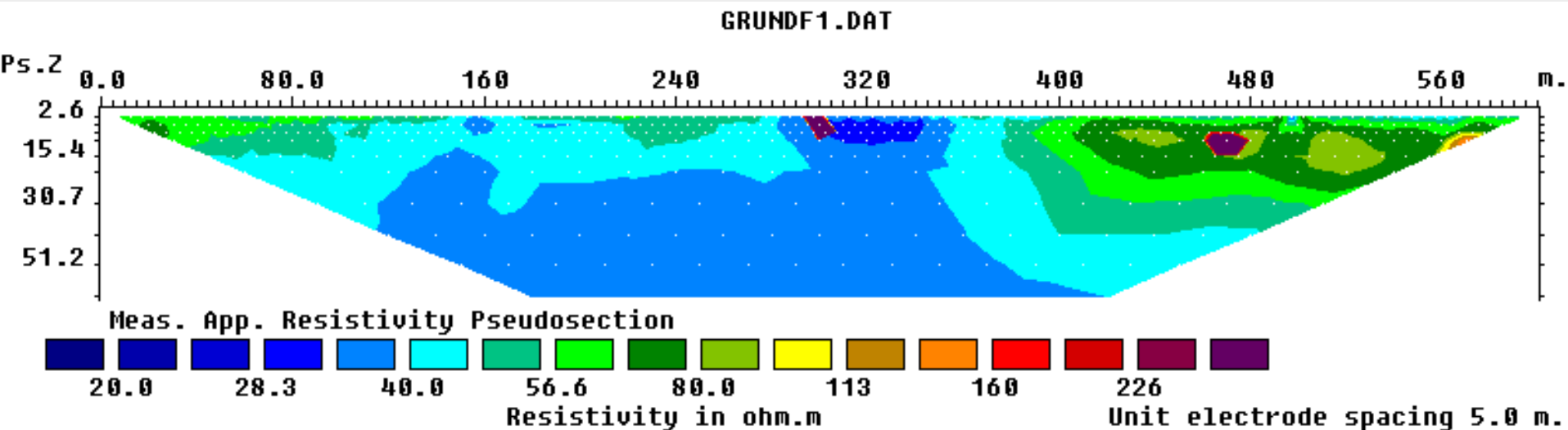
The pseudosection plot below two areas with unusually high values compared to neighboring points.



# Methods to remove bad data points

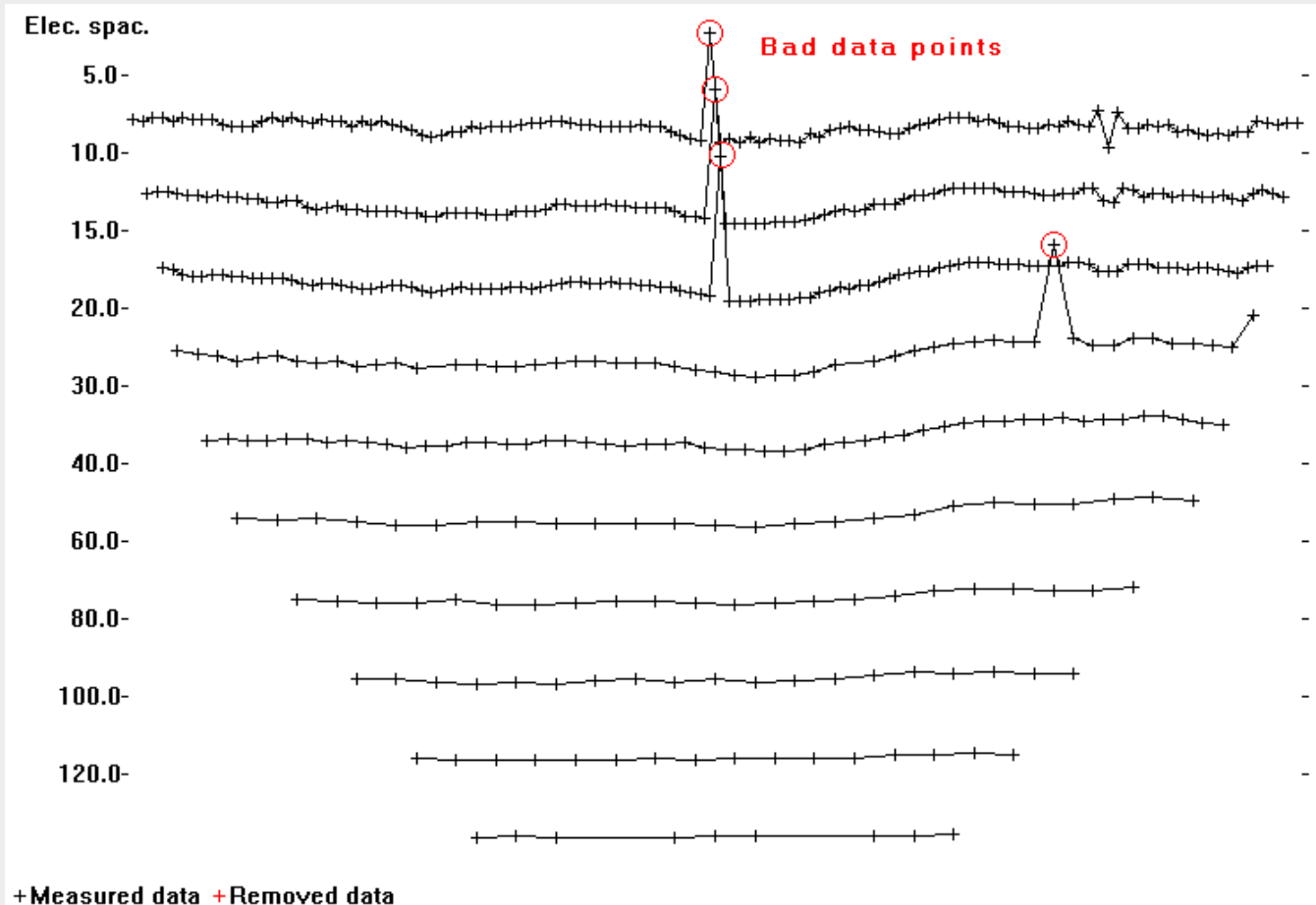
Before carrying out the inversion, you should first take a look at the data as a pseudosection plot or a profile plot. This option is possible for surveys carried out with one of the standard arrays, such as Wenner, Schlumberger, dipole-dipole, pole-dipole and gradient.

The bad data points with “systematic” noise show up as spots with unusually low or high values in the pseudosection, such as the example below. Note a few points with very high resistivity values which are bad data points. They are probably caused by equipment problems rather than random background noise.



# Method to remove bad data points before inversion

One method is to remove the bad data points manually, particular if there only a small number of bad data points, is to plot the data as profiles. The bad data points are usually much higher or lower than the other data points. The bad data points can be removed by clicking them with the mouse within the Res2dinvx64 program.

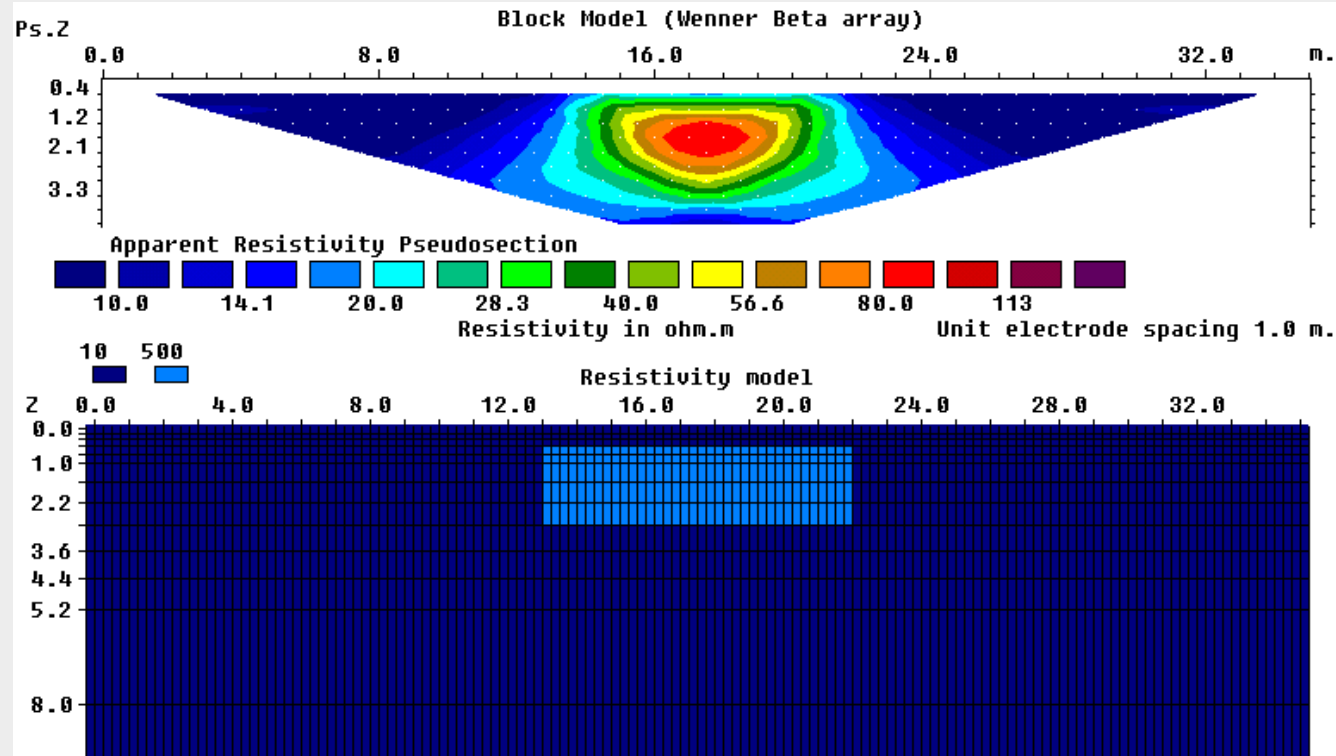


# **2-D forward modeling**

**The finite-difference and  
finite-element methods**

# 2-D forward modeling

In the inversion of a data set, it is necessary to calculate the apparent resistivity values for the model used – this is the forward modeling problem. In forward modeling, the subsurface resistivity distribution is specified and the purpose is to calculate the apparent resistivity that would be measured by a survey over such a structure. The 2-D subsurface is divided into many cells, and the finite-difference or finite-element method is used to calculate the apparent resistivity values.



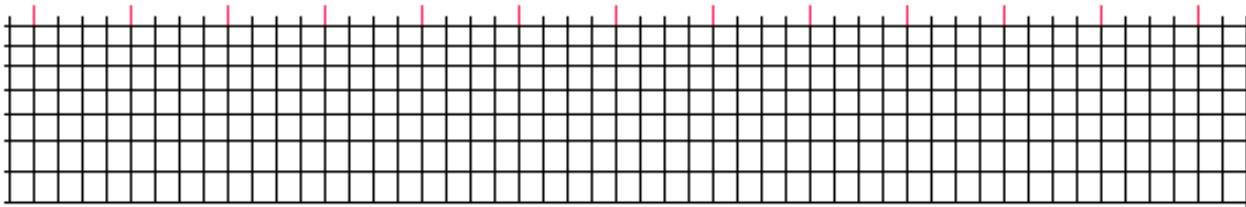
# The finite-difference and finite-element methods

Both methods solve the following Poisson's equation :-

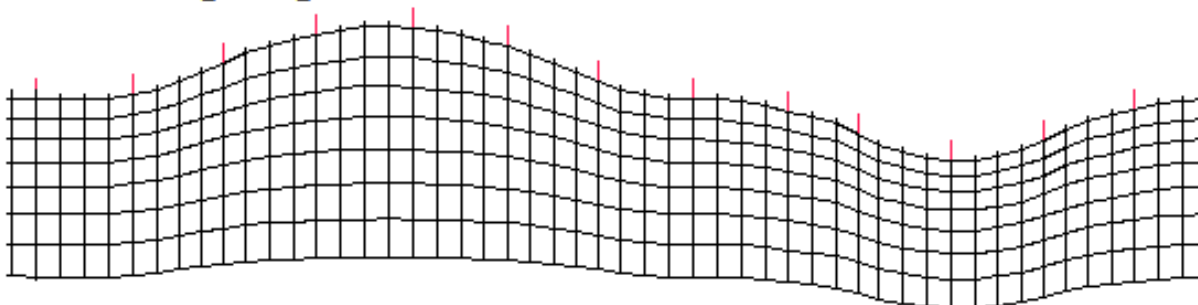
$$-\nabla \cdot \left[ \frac{1}{\rho(x,y)} \nabla \Phi(x,y,z) \right] = I_c$$

$I_c$  is the current and  $\rho(x,y)$  is the resistivity.  $\Phi(x,y,z)$  is the potential at the nodes that is to be calculated. The subsurface is divided into a large number of cells and each model cell can have a different resistivity value.

**Rectangular grid**



**Non-rectangular grid**



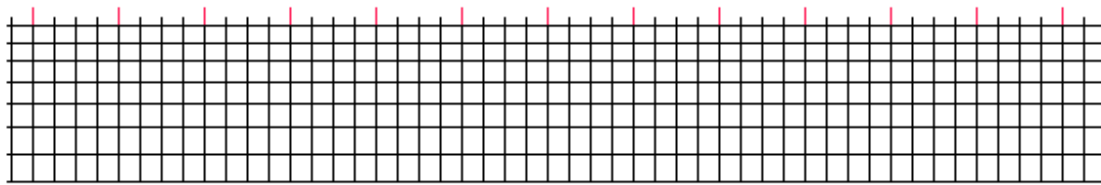
| Electrode    □ Model cell    + Node

# Finite-difference/element methods - usage

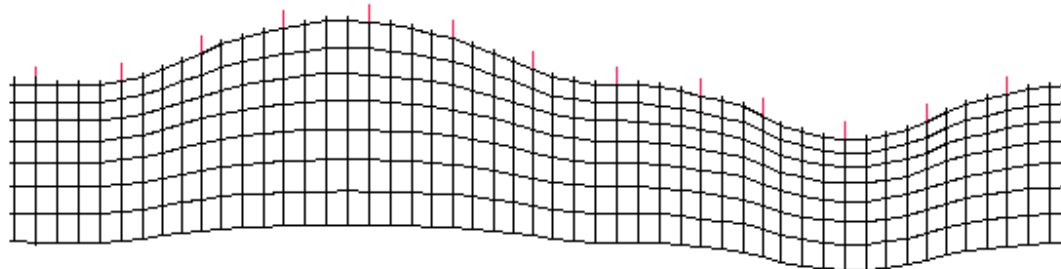
The Poisson's equation 
$$-\nabla \cdot \left[ \frac{1}{\rho(x, y)} \nabla \Phi(x, y, z) \right] = I_c$$

The finite-difference method is limited to rectangular grids. The finite-element method can have non-rectangular cells and thus is normally used when there is topography. The time taken by both methods depend on the number of nodes (cells) in the mesh used. The total number of nodes depend on the number of nodes in the horizontal and vertical directions. Normally 2 or 4 horizontal nodes are used between adjacent electrodes.

**Rectangular grid**



**Non-rectangular grid**

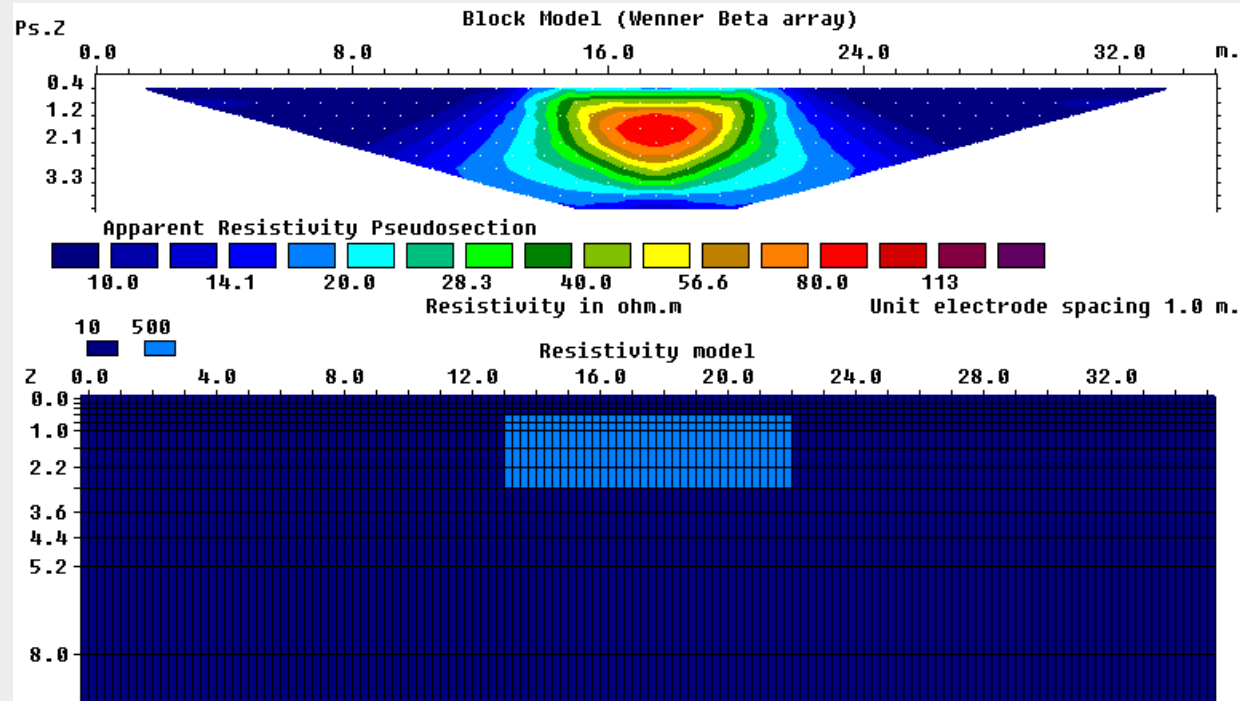


| Electrode    □ Model cell    + Node

# 2-D forward modeling program – applications

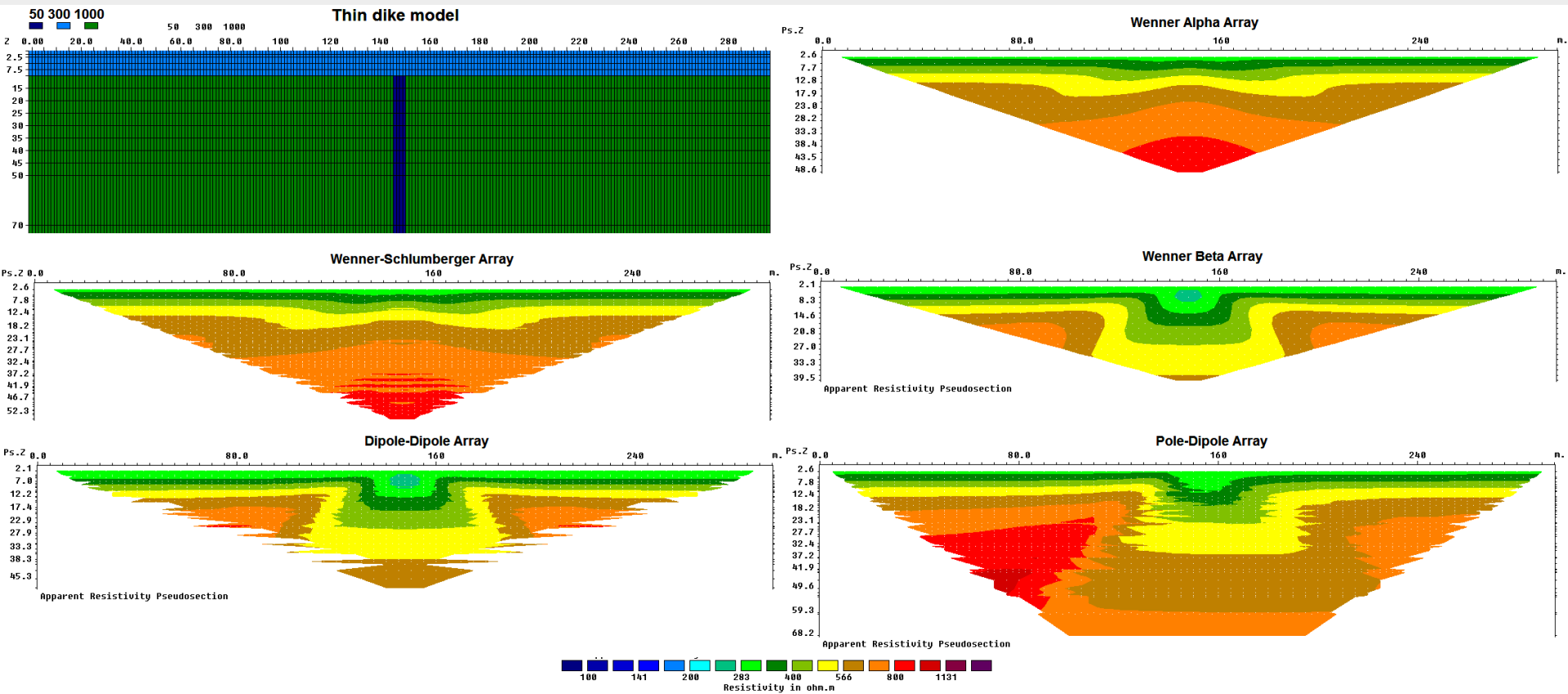
The forward modeling program is useful in the planning stage of the survey, if some information about the shape and size of expected targets is known.

By trying different arrays on the computer, we can avoid using an array that is unsuitable for the detection of the structures of interest. We can also have an idea of a suitable spacing between adjacent electrodes to use, the maximum electrode separation and cable length needed.



# 2-D forward modeling - example

Below is an example of pseudosections for different arrays over a thin low resistivity dike. Note the Wenner Alpha and Schlumberger arrays barely detects it, while the dipole-dipole and Wenner Beta (dipole-dipole array with  $n=1$ ) arrays show a clear anomaly. It also shows up in the pole-dipole array pseudosection.



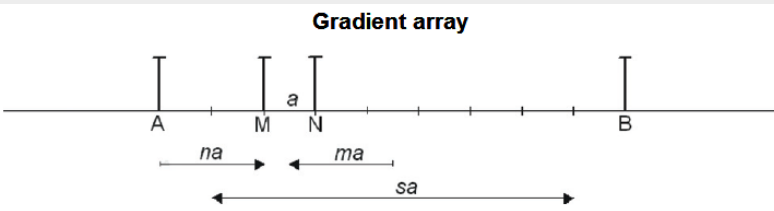
# Types of arrays used in 2-D surveys

## Brief summary of common arrays

- 1). Wenner
- 2). Wenner-Schlumberger
- 3). Dipole-dipole
- 4). Pole-dipole
- 5). Pole-pole
- 6). Multiple gradient

# Array types for 2-D surveys

The multi-electrode systems can be programmed to use almost any array. Most surveys use the Wenner (alpha), dipole-dipole, Wenner-Schlumberger and pole-dipole array. A new addition for multi-channel systems is the multiple gradient array, which is a non-symmetrical form of the Schlumberger. The dipole-dipole and pole-dipole arrays are also widely used with multi-channel systems.



- a). **Wenner Alpha**  

$$\begin{array}{ccccccc} \text{C1} & & \text{P1} & & \text{P2} & & \text{C2} \\ \bullet \leftarrow a \rightarrow \bullet & \bullet \end{array}$$

$$k = 2 \pi a$$
- b). **Wenner Beta**  

$$\begin{array}{ccccccc} & & \text{C1} & & \text{P1} & & \\ \text{C2} & & \leftarrow a \rightarrow \bullet & \bullet \end{array}$$

$$k = 6 \pi a$$
- c). **Wenner Gamma**  

$$\begin{array}{ccccccc} \text{C1} & & \text{P1} & & \text{C2} & & \text{P2} \\ \bullet \leftarrow a \rightarrow \bullet & \bullet \end{array}$$

$$k = 3 \pi a$$
- d). **Pole - Pole**  

$$\begin{array}{ccc} \text{C1} & & \text{P1} \\ \bullet \leftarrow a \rightarrow \bullet & & \bullet \end{array}$$

$$k = 2 \pi a$$
- e). **Dipole - Dipole**  

$$\begin{array}{ccccccc} & & \text{C1} & & \text{P1} & & \text{P2} \\ \bullet \leftarrow a \rightarrow \bullet & \leftarrow na \rightarrow \bullet & \leftarrow a \rightarrow \bullet & \bullet \end{array}$$

$$k = \pi n(n+1)(n+2)a$$
- f). **Pole - Dipole**  

$$\begin{array}{ccccccc} & & \text{C1} & & \text{P1} & & \text{P2} \\ \bullet \leftarrow na \rightarrow \bullet & \leftarrow a \rightarrow \bullet & \bullet \end{array}$$

$$k = 2 \pi n(n+1)a$$
- g). **Wenner - Schlumberger**  

$$\begin{array}{ccccccc} \text{C1} & & \text{P1} & & \text{P2} & & \text{C2} \\ \bullet \leftarrow na \rightarrow \bullet & \leftarrow a \rightarrow \bullet & \leftarrow a \rightarrow \bullet & \leftarrow na \rightarrow \bullet & \leftarrow na \rightarrow \bullet & \leftarrow na \rightarrow \bullet & \bullet \end{array}$$

$$k = \pi n(n+1)a$$
- h). **Equatorial Dipole - Dipole**  

$$\begin{array}{ccc} & & \text{P2} \\ \uparrow & & \uparrow \\ \text{C2} & \xleftarrow{b} & \text{C1} \\ \uparrow & & \uparrow \\ \bullet & \xleftarrow{na} & \bullet \\ \downarrow & & \downarrow \\ \text{C1} & & \text{P1} \end{array}$$

$$b = na$$

$$k = 2 \pi b L / (L - b)$$

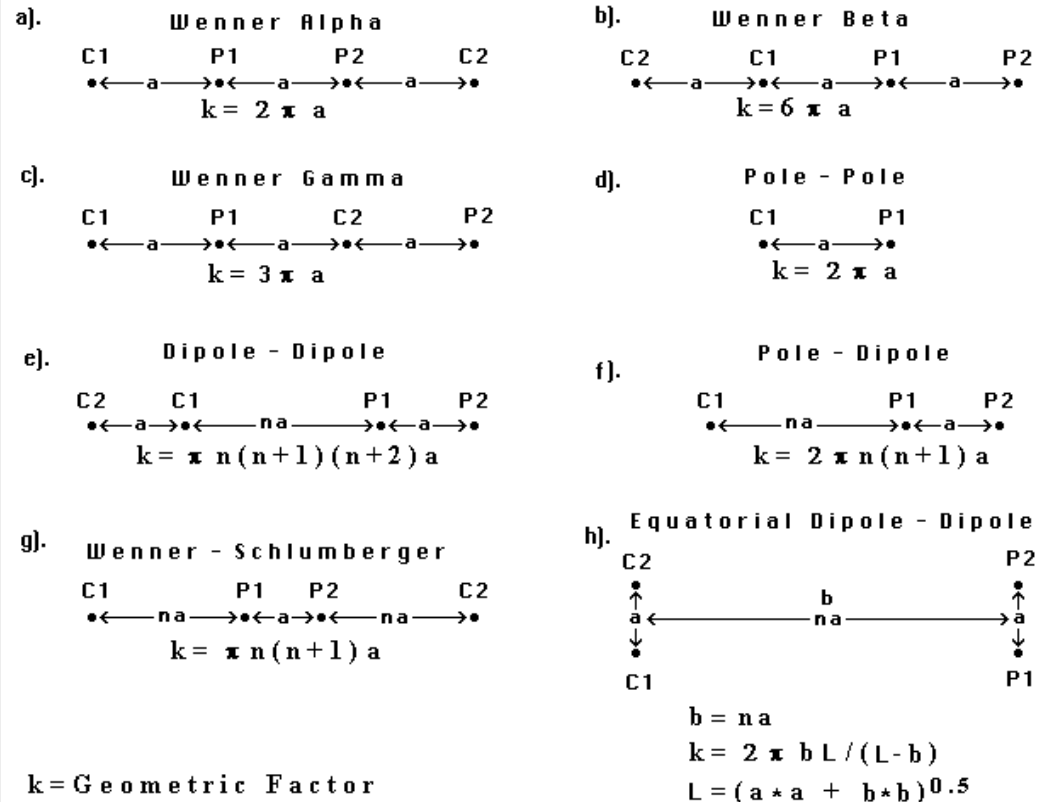
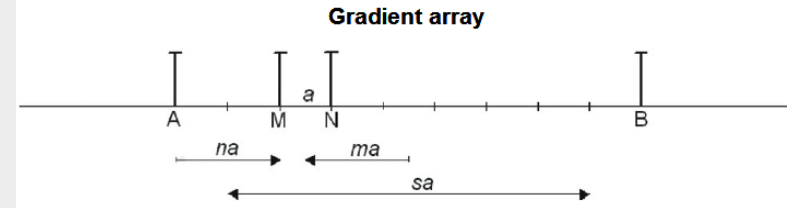
$$L = (a * a + b * b)^{0.5}$$
- $k = \text{Geometric Factor}$

# 2D surveys - array types

Among the characteristics of an array that should be considered are

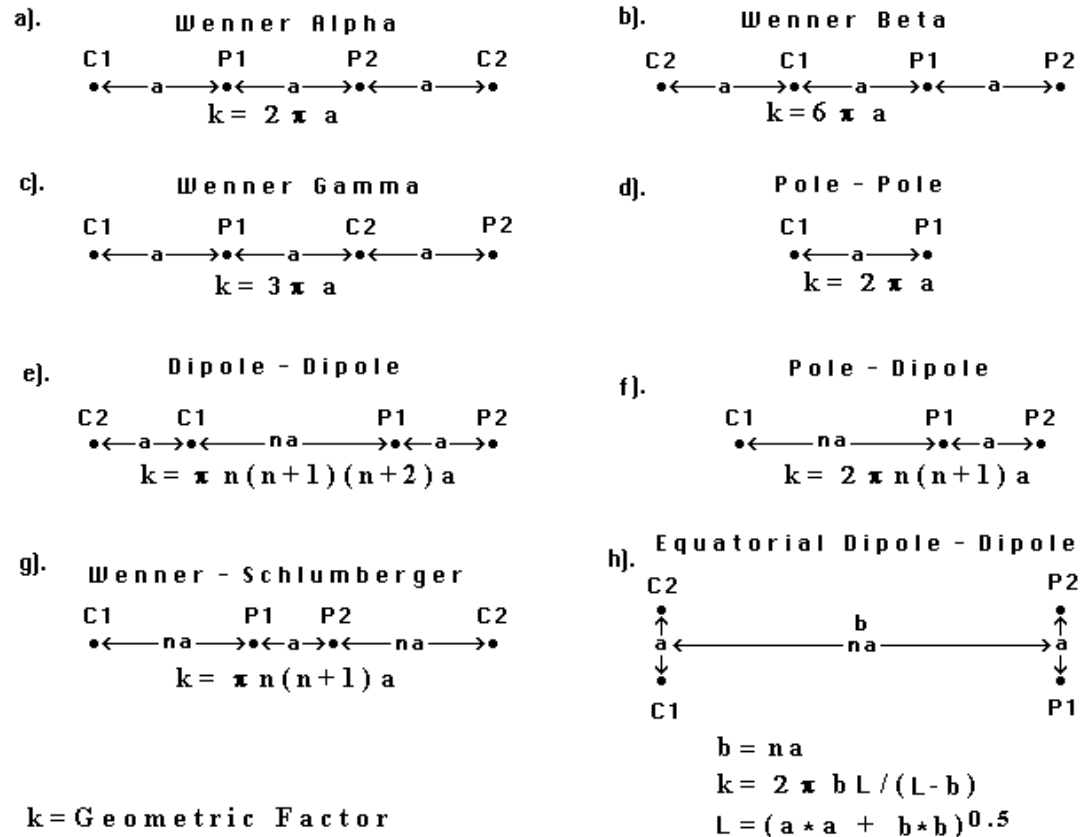
- (i) the depth of investigation,
- (ii) the sensitivity of the array to vertical and horizontal changes in the subsurface resistivity,
- (iii) the signal strength.

A new consideration is the efficiency in which it can be implemented for multi-channel systems, i.e. the number of simultaneous readings that can be made with a common pair of current electrodes.



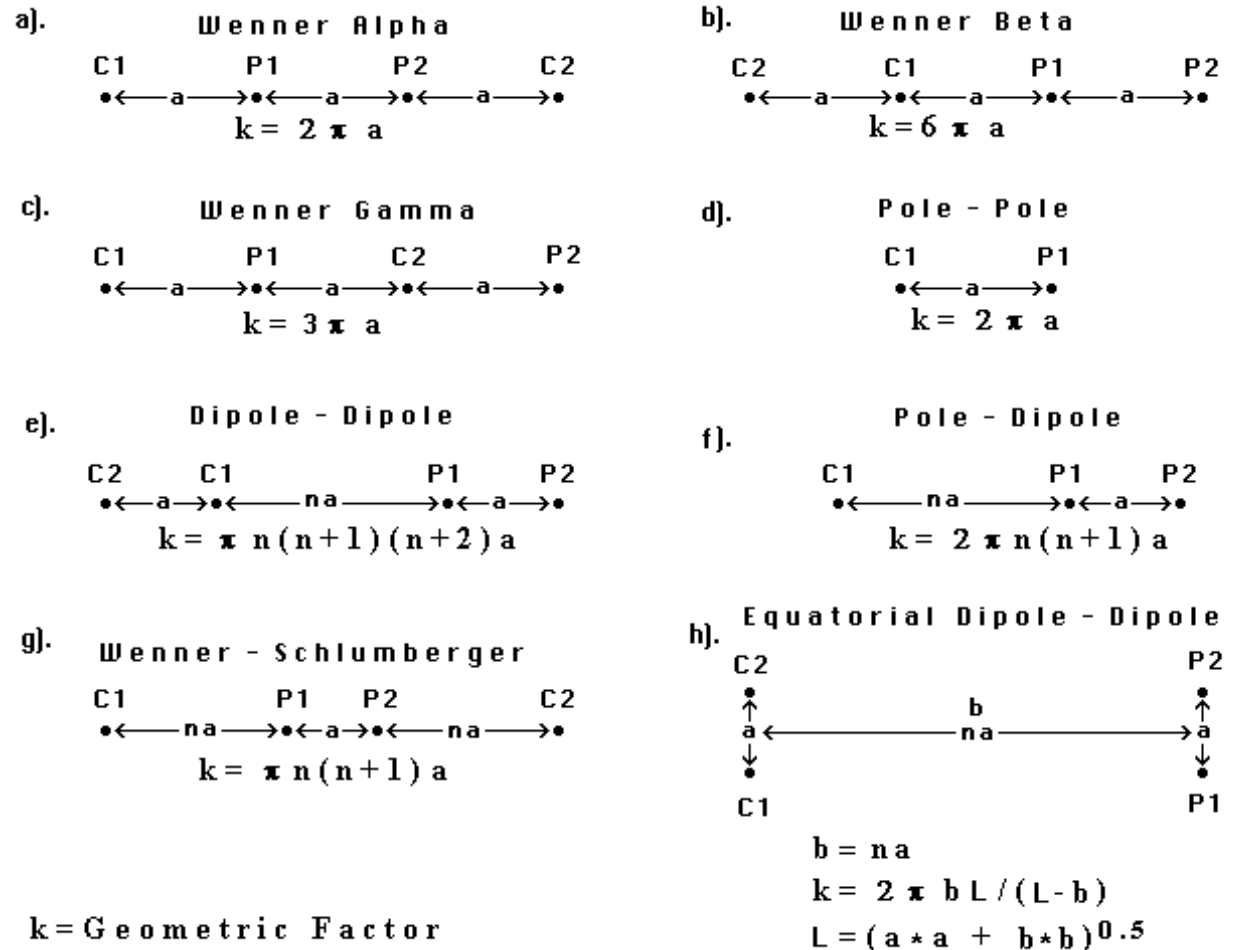
# How to select an array? – Signal strength

The signal strength is an important factor in noisy areas, or when large electrode spacings are used or for surveys in conductive areas. The signal strength is inversely proportional to the geometric factor, so it can be easily estimated. The Wenner (alpha) array has the smallest geometric factor, and thus the highest signal strength. This means surveys with the Wenner array are generally less noisy.



# Pole-pole array signal strength

The pole-pole array has the same geometric factor as the Wenner (alpha) array but it has higher telluric noise due to the large distance between the potential electrodes. In practice it might be difficult to place the C2 and P2 electrodes at sufficiently far distances from the survey area.



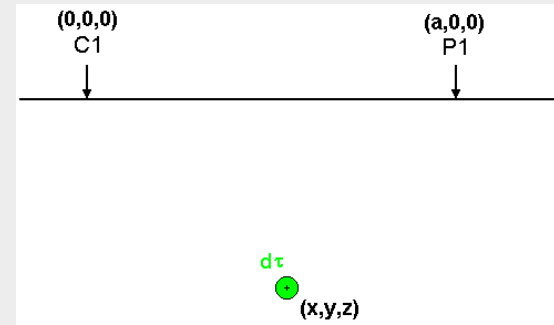


# Depth of investigation and sensitivity

These characteristics can be determined from the sensitivity function of the array for a homogeneous earth model. The sensitivity function tells us the degree to which a change in the resistivity of a section of the subsurface will influence the potential measured by the array. The higher the value of the sensitivity function, the greater is the influence of the subsurface region on the measurement. A current of 1 Amp injected into the ground through the C1 current electrode results in a potential  $\phi$  observed at the potential P1 electrode. If the resistivity within a small volume ( $\delta\tau$ ) of the ground located at  $(x,y,z)$  is changed by a small amount,  $\delta\rho$ , the change in the potential,  $\delta\phi$ , measured at P1 due to a current source at C1 is given by the equation below. **Sensitivity =  $\delta\phi / \delta\rho$**

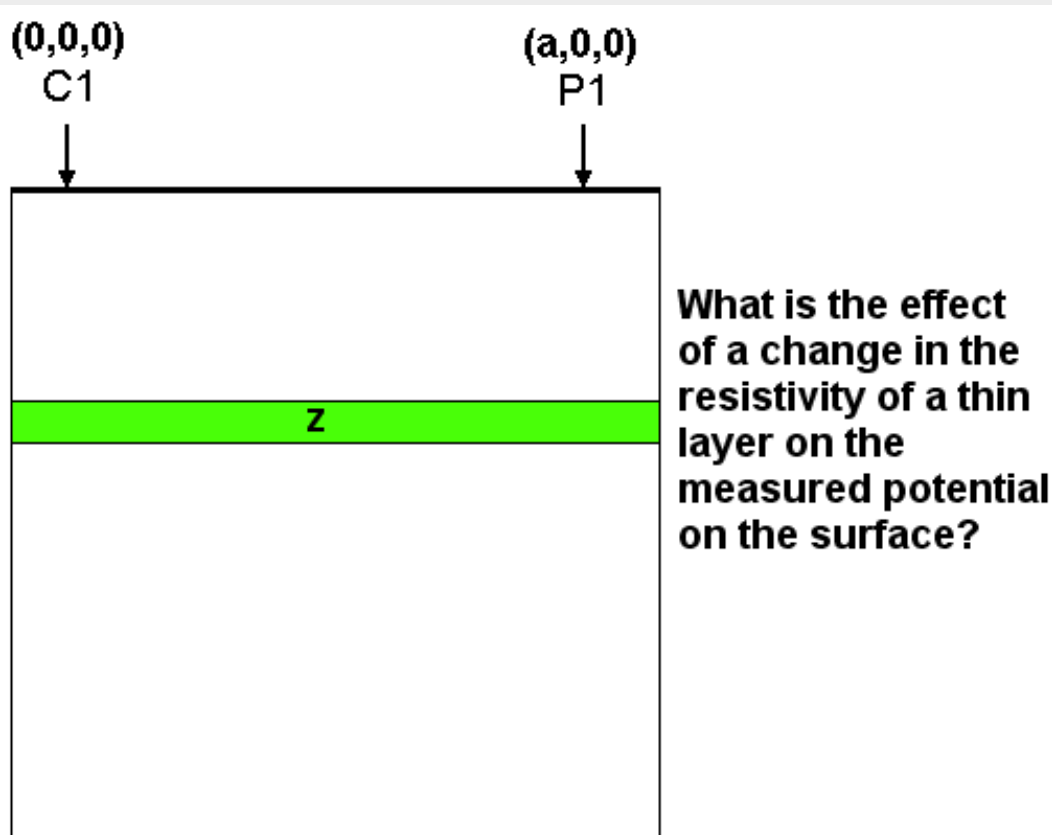
$$\delta\phi = \frac{\delta\rho}{\rho^2} \int_V \nabla\phi \cdot \nabla\phi' d\tau$$

$$\frac{\delta\phi}{\delta\rho} = F_{3D}(x, y, z) = \frac{1}{4\pi^2} \cdot \frac{x(x-a) + y^2 + z^2}{\left[x^2 + y^2 + z^2\right]^{1.5} \left[(x-a)^2 + y^2 + z^2\right]^{1.5}}$$



# Depth of investigation – the 1-D sensitivity function

In resistivity sounding surveys, it is well known as the separation between the electrodes is increased, the array senses the resistivity of increasingly deeper layers. One method to calculate the depth of investigation is by using the 1-D version of the sensitivity function. The sensitivity function for a thin horizontal layer is obtained by integrating the 3-D sensitivity function in the  $x$  and  $y$  directions.



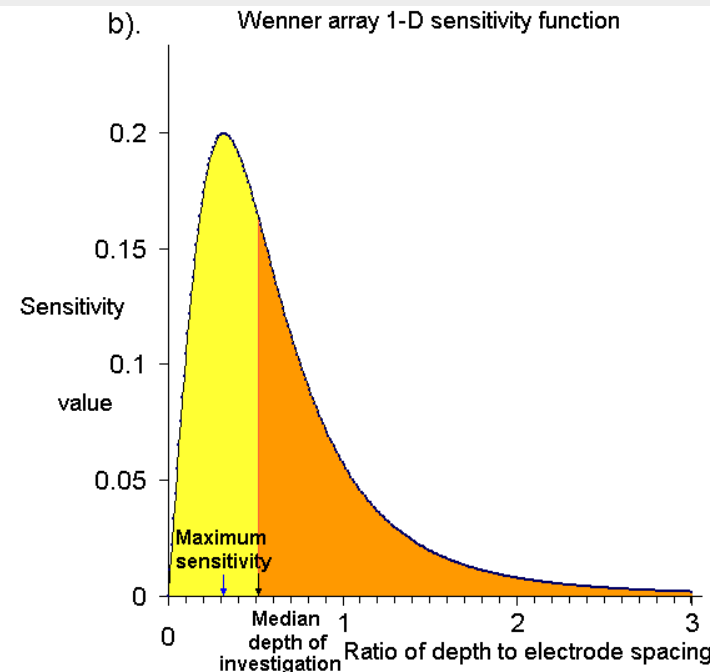
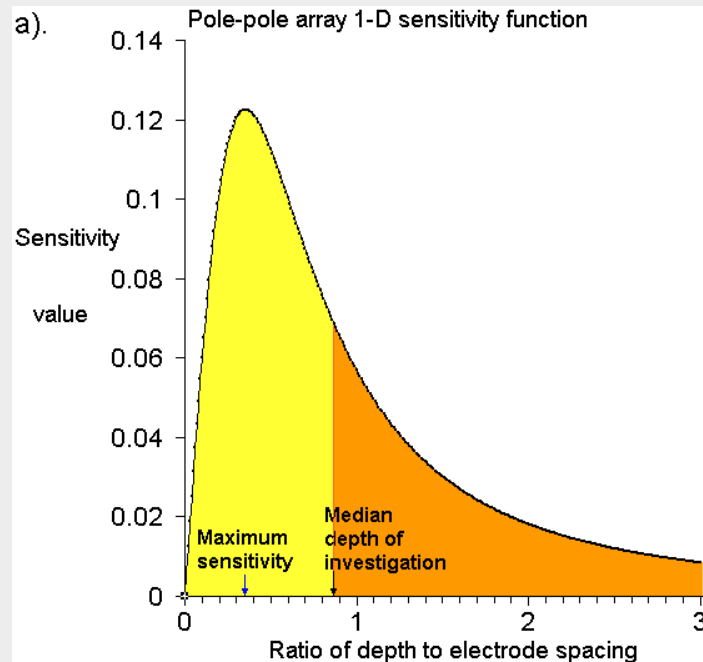
$$F_{1D}(z) = \frac{2}{\pi} \cdot \frac{z}{(a^2 + 4z^2)^{1.5}}$$

# 1-D depth of investigation

The 1-D sensitivity function is given by

$$F_{1D}(z) = \frac{2}{\pi} \cdot \frac{z}{(a^2 + 4z^2)^{1.5}}$$

The "median depth of investigation" of an array is the depth above which the area under the sensitivity function curve is equal to half the total area under the curve. The upper section of the earth above the "median depth of investigation" has the same influence on the measured potential as the lower section. This is roughly how deep we can see with an array, assuming the subsurface is homogeneous.



# The depth of investigation of different arrays

The "median depth of investigation",  $z_e$ , can be easily calculated for different arrays, as listed in the table below. The depths are given as the ratio to the 'a' spacing or the total length 'L' of the array. To calculate the actual depth of investigation, just multiply this ratio by the 'a' spacing or 'L' length used in the field survey.

Array	$z_e/a$	$z_e/L$
Wenner Alpha	0.519	0.173
Wenner Beta	0.416	0.139
Wenner Gamma	0.594	0.198
Dipole-dipole		
n = 1	0.416	0.139
n = 2	0.697	0.174
n = 3	0.962	0.192
n = 4	1.220	0.203
n = 5	1.476	0.211
n = 6	1.730	0.216
n = 7	1.983	0.220
n = 8	2.236	0.224
Pole-Pole	0.867	0.867

Array	$z_e/a$	$z_e/L$
Wenner - Schlumberger		
n = 1	0.519	0.173
n = 2	0.925	0.186
n = 3	1.318	0.189
n = 4	1.706	0.190
n = 5	2.093	0.190
n = 6	2.478	0.191
n = 7	2.863	0.191
n = 8	3.247	0.191
n = 9	3.632	0.191
n = 10	4.015	0.191
Pole-dipole		
n = 1	0.519	0.260
n = 2	0.925	0.308
n = 3	1.318	0.330
n = 4	1.706	0.341
n = 5	2.093	0.349
n = 6	2.478	0.354
n = 7	2.863	0.358
n = 8	3.247	0.361

# Comparison of the depth of investigation for arrays

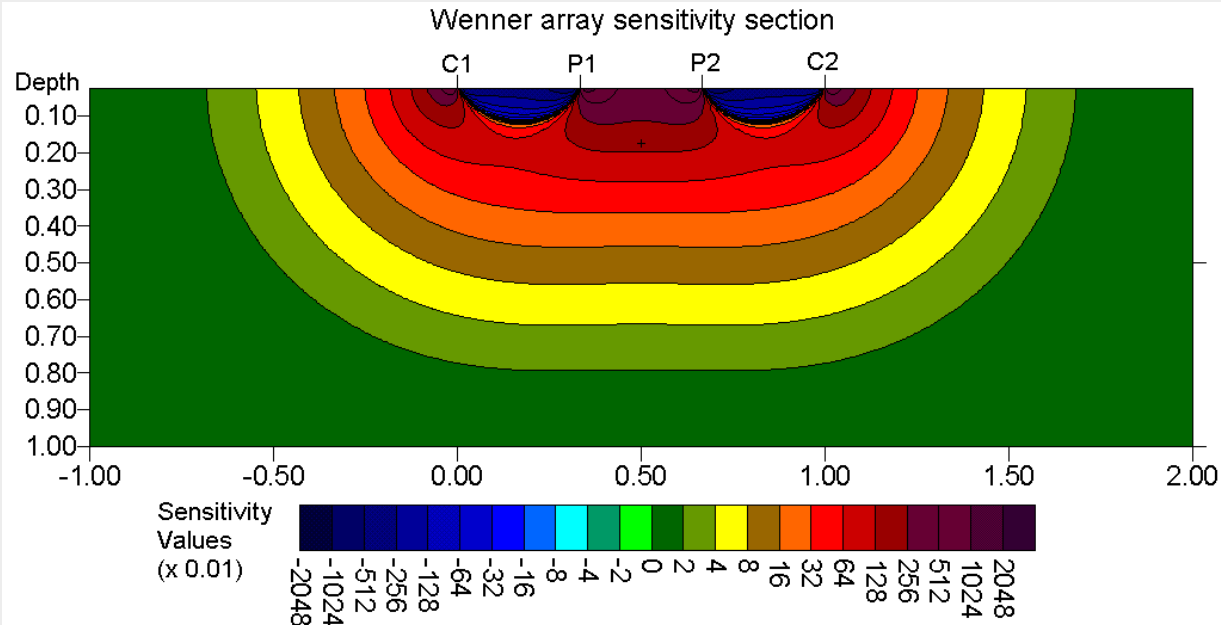
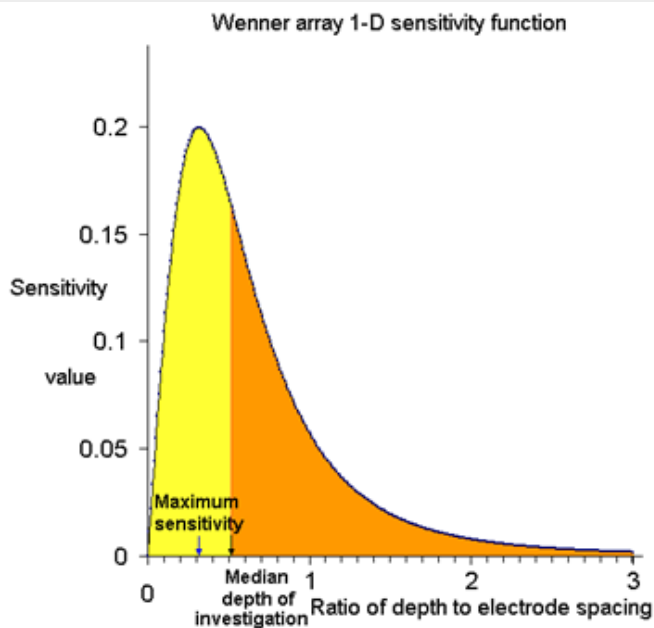
The depth of investigation of the Wenner alpha array is about half the 'a' spacing between the electrodes. The pole-pole array has the deepest depth of investigation (excluding the distances to the C2 and P2 electrodes). The 'median depth of investigation' for the dipole-dipole array is probably an underestimate, due to the extreme form of the shape of the sensitivity function (which we shall see next). Note the depth of investigation for the Wenner and Schlumberger arrays is about one-sixth the array length.

Array	$z_e/a$	$z_e/L$
Wenner Alpha	0.519	0.173
Wenner Beta	0.416	0.139
Wenner Gamma	0.594	0.198
Dipole-dipole		
1	n = 0.416	0.139
2	n = 0.697	0.174
3	n = 0.962	0.192
4	n = 1.220	0.203
5	n = 1.476	0.211
6	n = 1.730	0.216
	n = 1.983	0.220

Array		$z_e/a$	$z_e/L$
Wenner - Schlumberger			
	n = 1	0.519	0.173
	n = 2	0.925	0.186
	n = 3	1.318	0.189
	n = 4	1.706	0.190
	n = 5	2.093	0.190
	n = 6	2.478	0.191
	n = 7	2.863	0.191
	n = 8	3.247	0.191
	n = 9	3.632	0.191
	n = 10	4.015	0.191
Pole-dipole			
	n = 1	0.519	0.260
	n = 2	0.925	0.308
	n = 3	1.318	0.330
	n = 4	1.706	0.341
	n = 5	2.093	0.349
	n = 6	2.478	0.354
	n = 7	2.863	0.358
	n = 8	3.247	0.361

# The 1-D and 2-D sensitivity functions

The plot of the 1-D sensitivity function shows that the sensitivity of an array to the topmost layer is very small. The plot actually gives the *net* contribution calculated by summing up the contribution for all  $x$ - and  $y$ -values at the same depth, and the small value near the surface is caused by the addition of large positive and negative sensitivity values. The *net* contribution for the topmost layer is small only if the ground is completely homogeneous. Below are plots of the Wenner array sensitivity in 1-D and 2-D. There are actually regions with large positive and negative values near the surface.



# The 2-D sensitivity function

To study the effect of changes in the resistivity in the vertical and one horizontal direction, the 2-D sensitivity function is used. This is obtained by integrating the 3-D sensitivity function in the y-direction. It is given by

$$F_{2D}(x, z) = \frac{1}{4\pi^2} \int_{-\infty}^{+\infty} \frac{x(x-a) + y^2 + z^2}{\left[x^2 + y^2 + z^2\right]^{1.5} \left[(x-a)^2 + y^2 + z^2\right]^{1.5}} dy$$

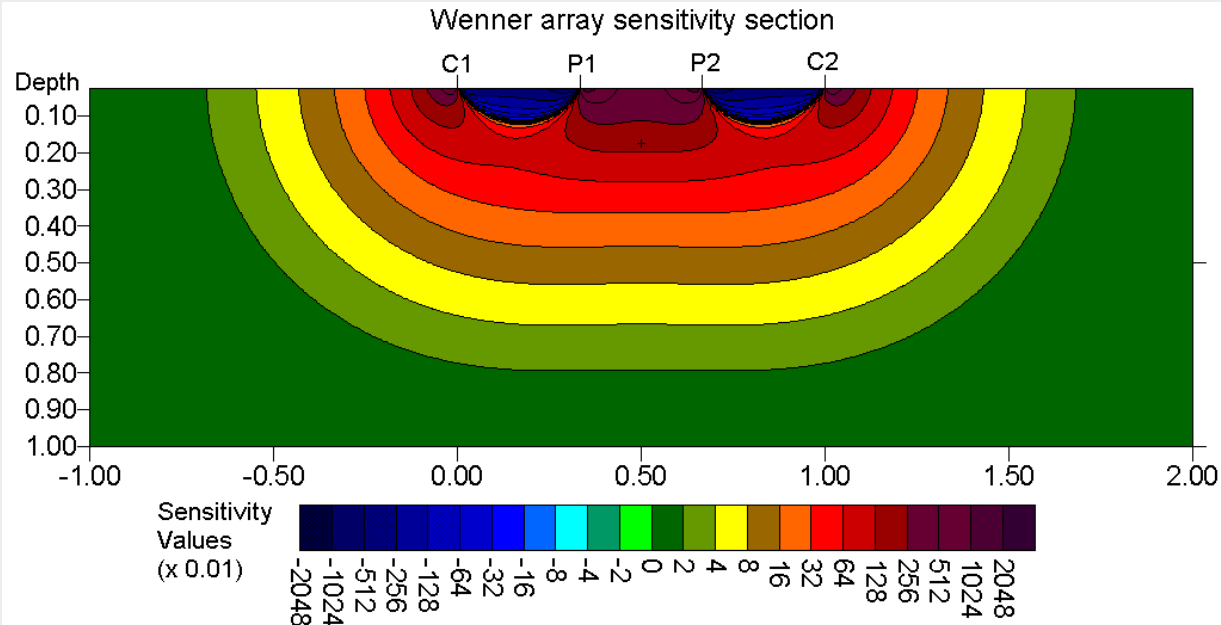
that gives

$$F_{2D}(x, z) = \frac{2}{\alpha\beta^2} \left[ \frac{\alpha^2 E(k) - \beta^2 K(k)}{(\alpha^2 - \beta^2)} - \frac{\gamma [(\alpha^2 + \beta^2)E(k) - 2\beta^2 K(k)]}{(\alpha^2 - \beta^2)^2} \right]$$

The equation involves elliptic integrals, and the details are given in the Tutorial Notes. Here, we will just use it to explain the behavior of the different arrays. It gives the effect of a section of the subsurface that extends in the y-direction perpendicular to the survey line.

# The Wenner alpha array : 2-D sensitivity

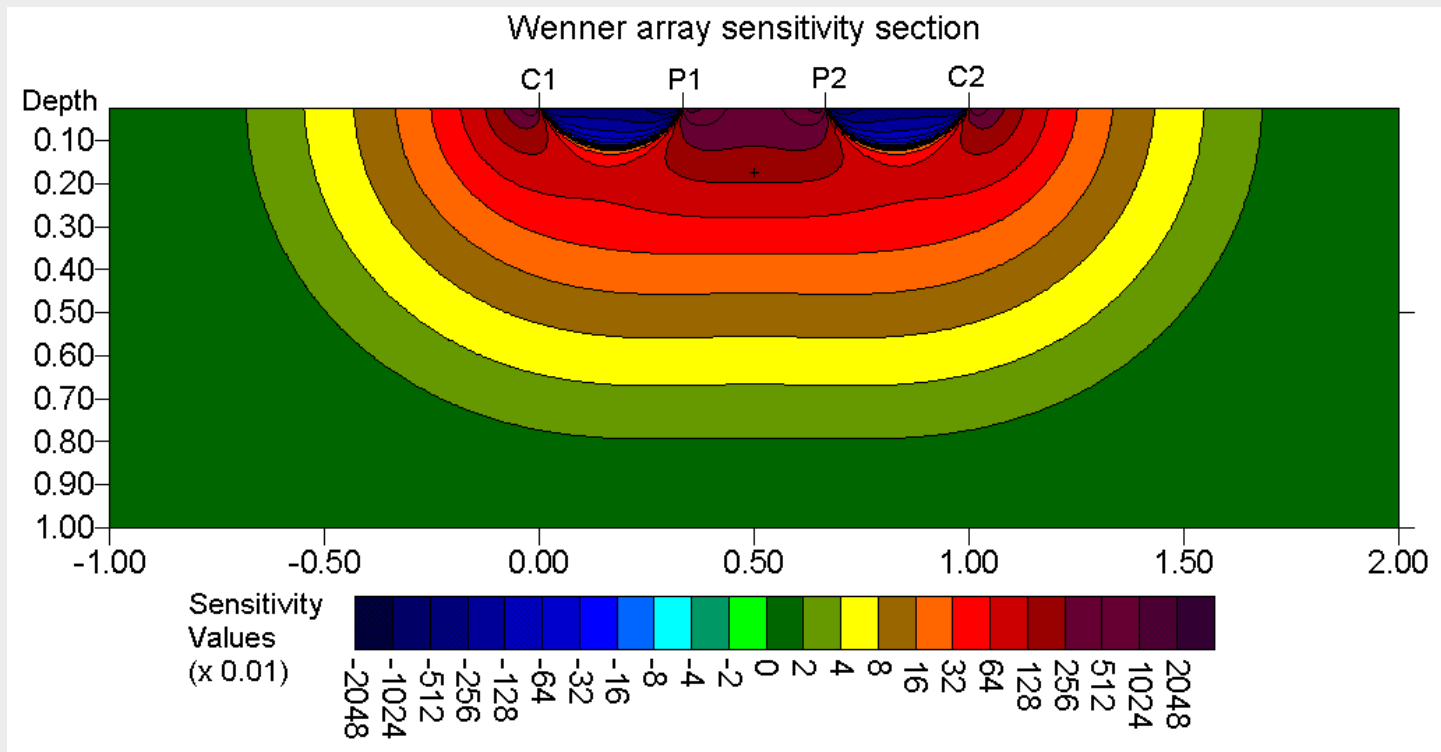
The plot of the 2-D sensitivity function shows that the sensitivity of an array to 2-D structures at different (x,z) locations. This shows the sensitivity of the array to different types of structures. The sensitivity plot for this array has almost horizontal contours beneath the center of the array. It is relatively sensitive to vertical changes in the subsurface resistivity below the center of the array, but is less sensitive to horizontal changes in the subsurface resistivity. The Wenner is good in resolving vertical changes (horizontal structures), but relatively poor in detecting horizontal changes (narrow vertical structures).



# Wenner array – depth of investigation and signal strength

The median depth of investigation for the Wenner Alpha array is approximately 0.5 times the “a” spacing (or one-sixth the array length) used, and this array has a moderate depth of investigation.

Among the common arrays, the Wenner array has the strongest signal strength. This can be an important factor if the survey is carried in areas with high background noise.

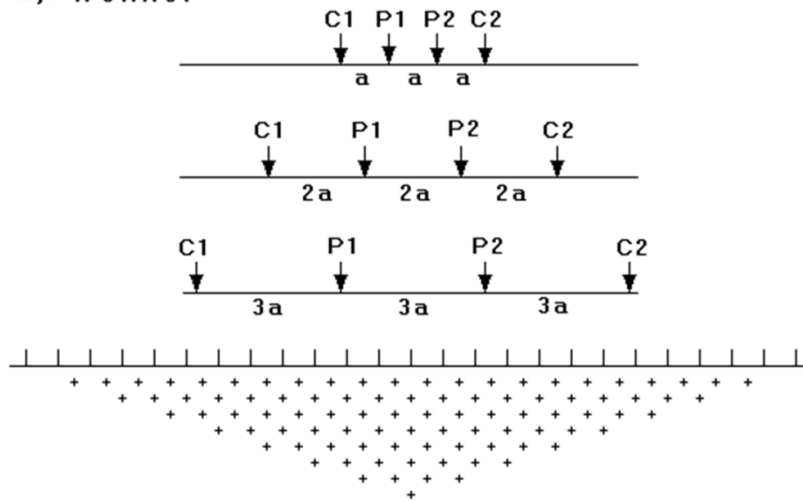


# The Wenner-Schlumberger array

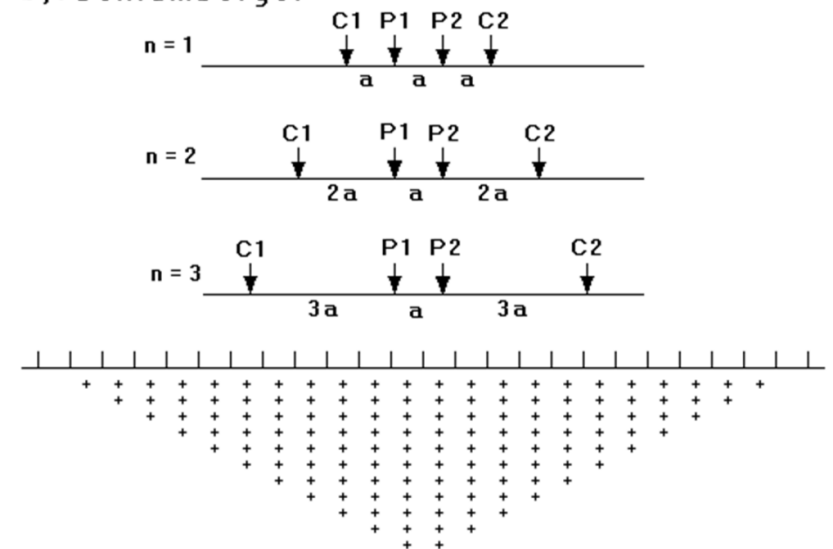
This is a combination of the Wenner and Schlumberger arrays. The “ $n$ ” factor for this array is the ratio of the distance between the C1-P1 (or P2-C2) electrodes to the spacing (“ $a$ ”) between the P1-P2 potential pair.

The depth of investigation for this array is about 10% larger than that for the Wenner array for the same array length for large “ $n$ ” values. The signal strength decreases with  $n^2$ . It is weaker than the Wenner array, but higher than the dipole-dipole and pole-dipole arrays.

a). Wenner



b). Schlumberger

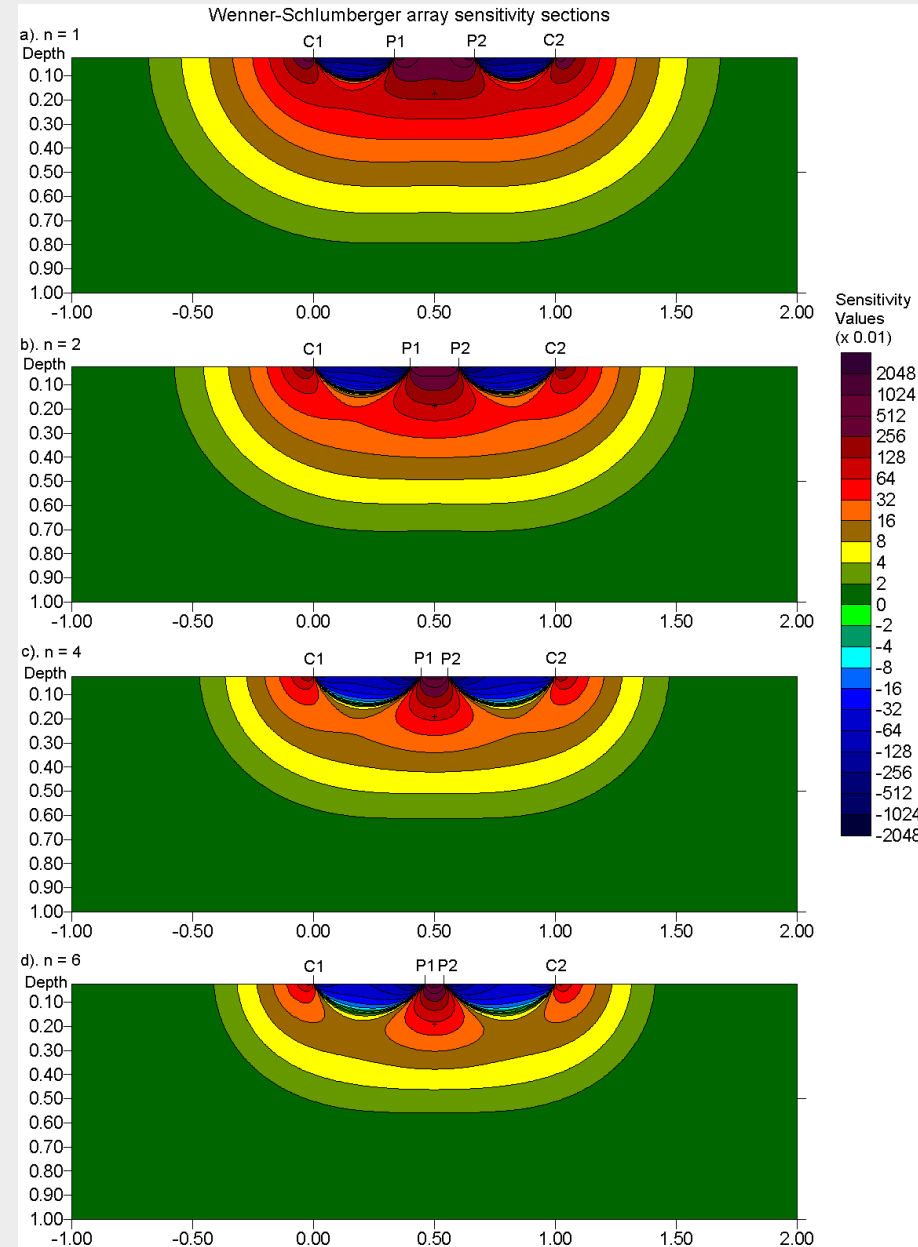


⊥ Electrode + Datum point in pseudosection

# The Wenner-Schlumberger array – sensitivity pattern

The figure shows the sensitivity pattern as the " $n$ " factor is increased from 1 (Wenner array) to 6 (the Schlumberger array). The flat sensitivity pattern for low " $n$ " values means that this array is moderately sensitive to horizontal structures, and also to vertical structures for high " $n$ " values where the pattern is more vertical.

In areas where both types of geological structures are expected, this array might be a good compromise between the Wenner and the dipole-dipole arrays.



# The dipole-dipole array – arrangement

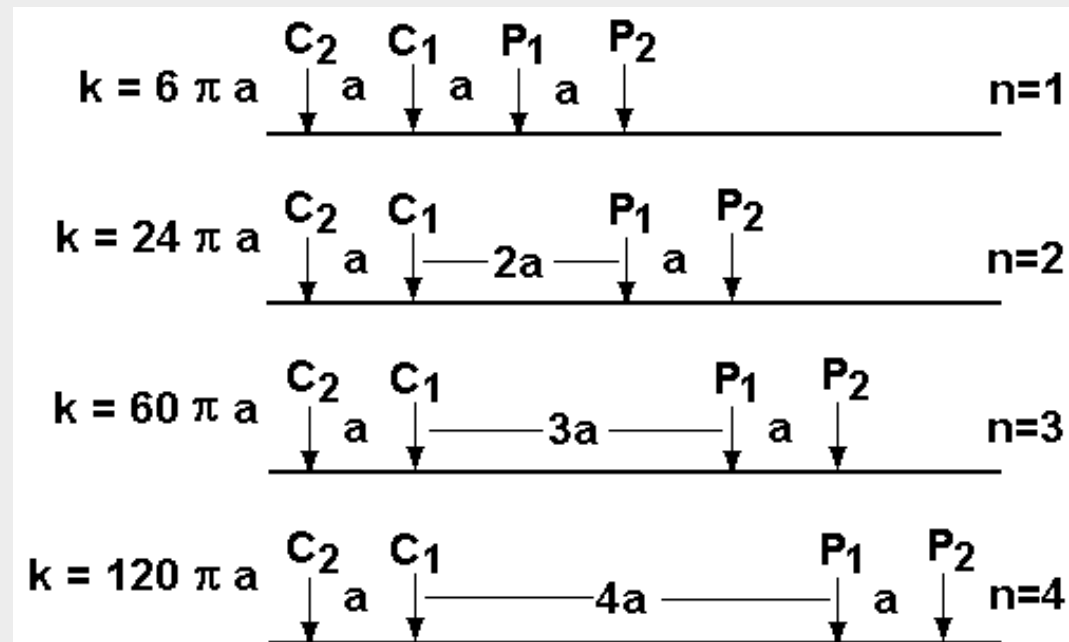
This array is widely used in I.P. surveys because of the low EM coupling between the current and potential circuits. The spacing between the C2-C1 (and P1-P2) electrodes is given as “ $a$ ”. The “ $n$ ” factor is the ratio of the C1-P1 distance the dipole length “ $a$ ”. For surveys, the “ $a$ ” spacing is initially kept fixed at the smallest unit electrode spacing and the “ $n$ ” factor is increased from 1 to 2 until about 6 to increase the depth of investigation. Note the large increase in the geometric  $k$  by 20 times when  $n$  increases from 1 to 4.

For  $n=6$ ,  $k= 336 \pi a$ ,

For  $n=8$ ,  $k= 720 \pi a$ ,

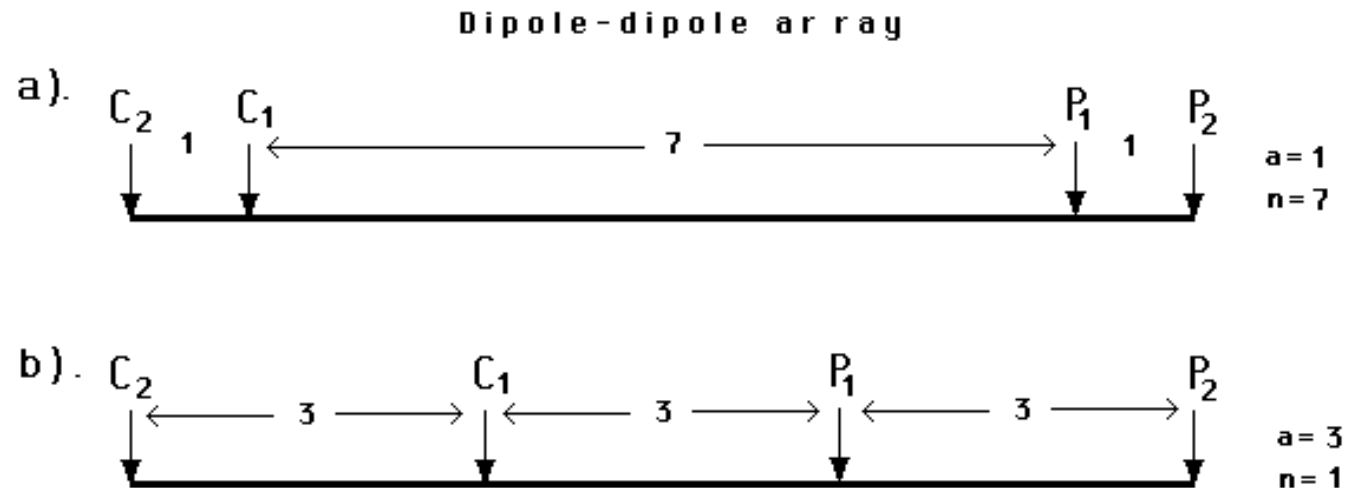
or 120 times larger than

for  $n=1$ .



# The dipole-dipole array – arrangement

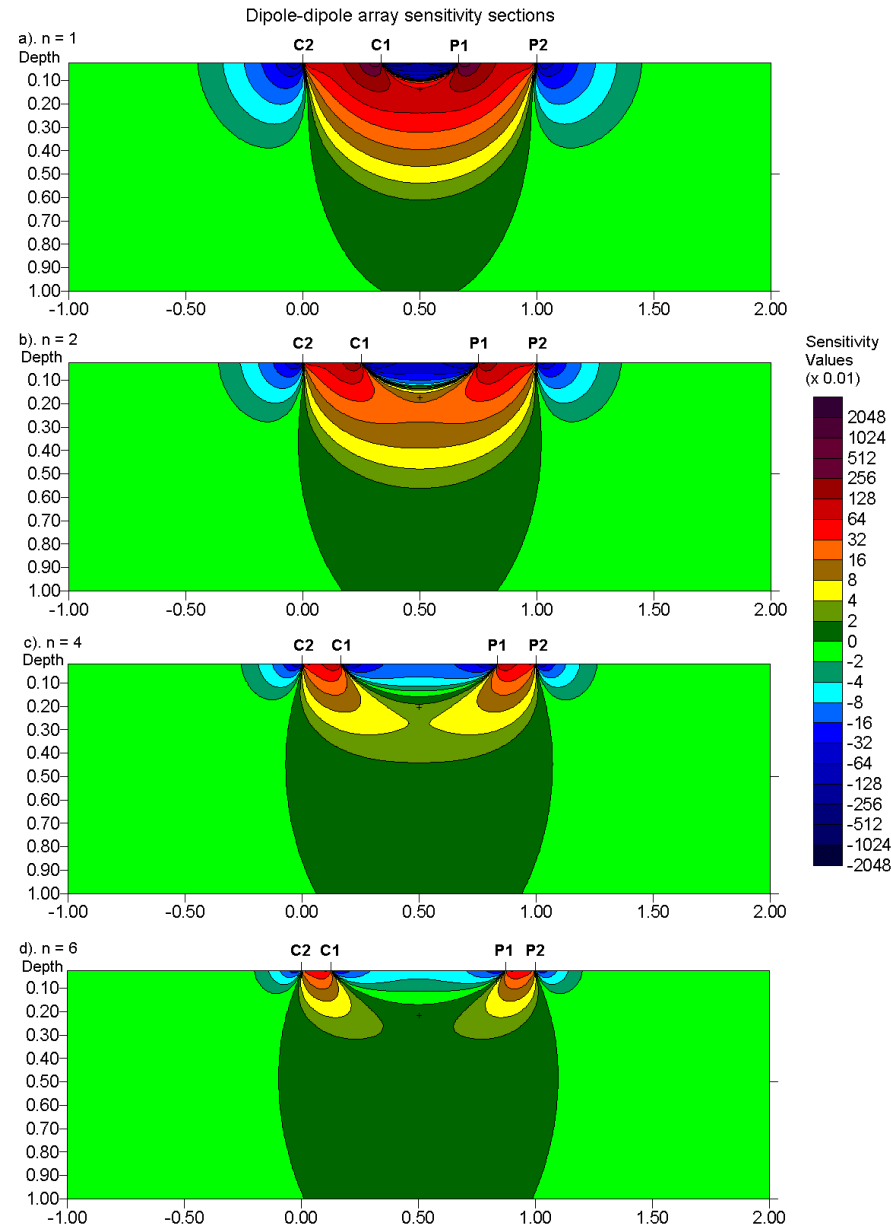
One disadvantage of this array is the low signal strength. It decreases with the cube of the “ $n$ ” factor. The voltage measured by the resistivity meter drops by about 56 times when “ $n$ ” is increased from 1 to 6. To overcome this problem, the “ $a$ ” spacing between the C1-C2 (and P1-P2) dipole pair can be increased. The two different arrangements for the dipole-dipole array with the same array length but with different “ $a$ ” and “ $n$ ” factors. The signal strength of the array with the smaller “ $n$ ” factor is about 28 times stronger than the one with the larger “ $n$ ” factor.



# The dipole-dipole array – sensitivity pattern

The figure shows the sensitivity sections for this array for "n" values of 1 to 6. The largest sensitivity values are generally located between the C1-C2 dipole pair, and also between the P1-P2 pair.

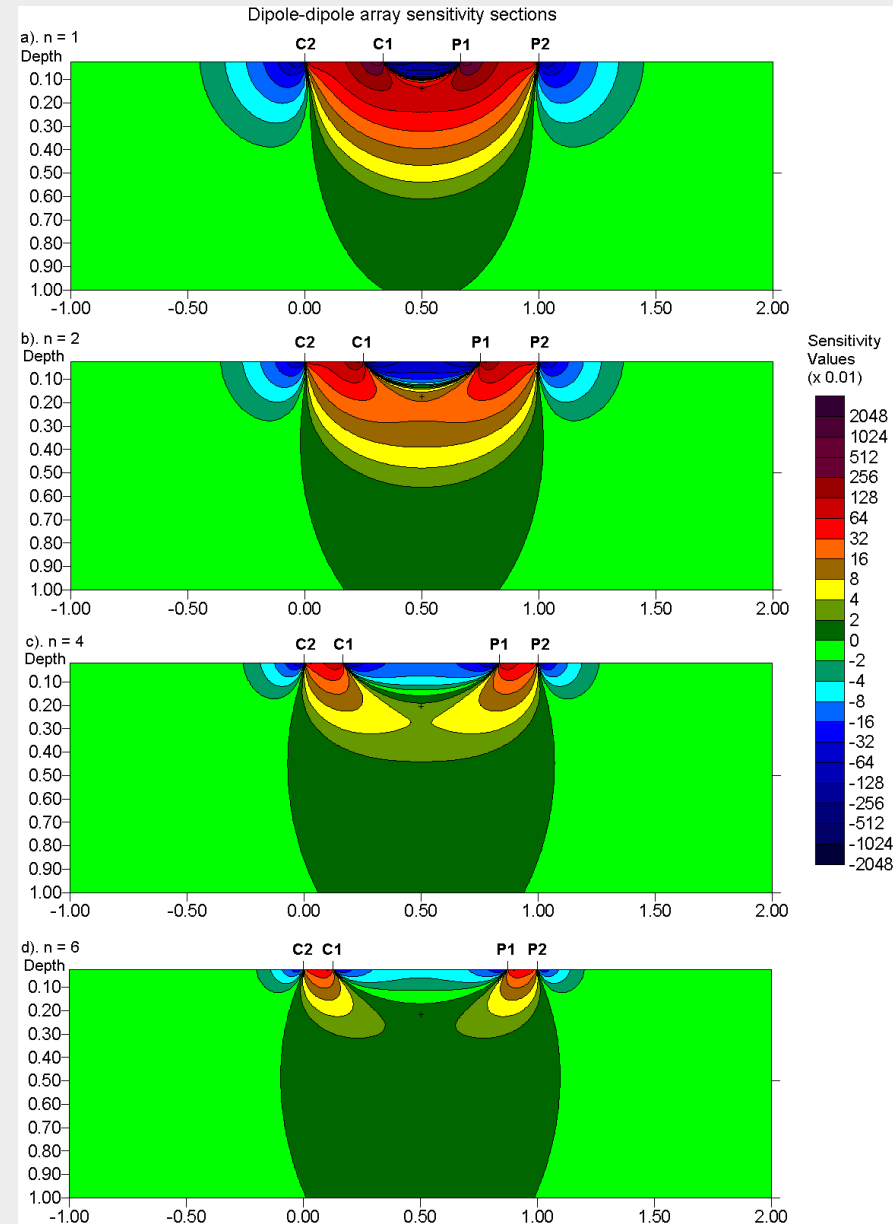
This means that this array is most sensitive to resistivity changes below each dipole pair.



# The dipole-dipole array – sensitivity pattern

As the " $n$ " factor is increased, the high sensitivity values become increasingly more concentrated beneath the C1-C2 and P1-P2 dipoles, while the sensitivity values beneath the center of the array between the C1-P1 electrodes decreases.

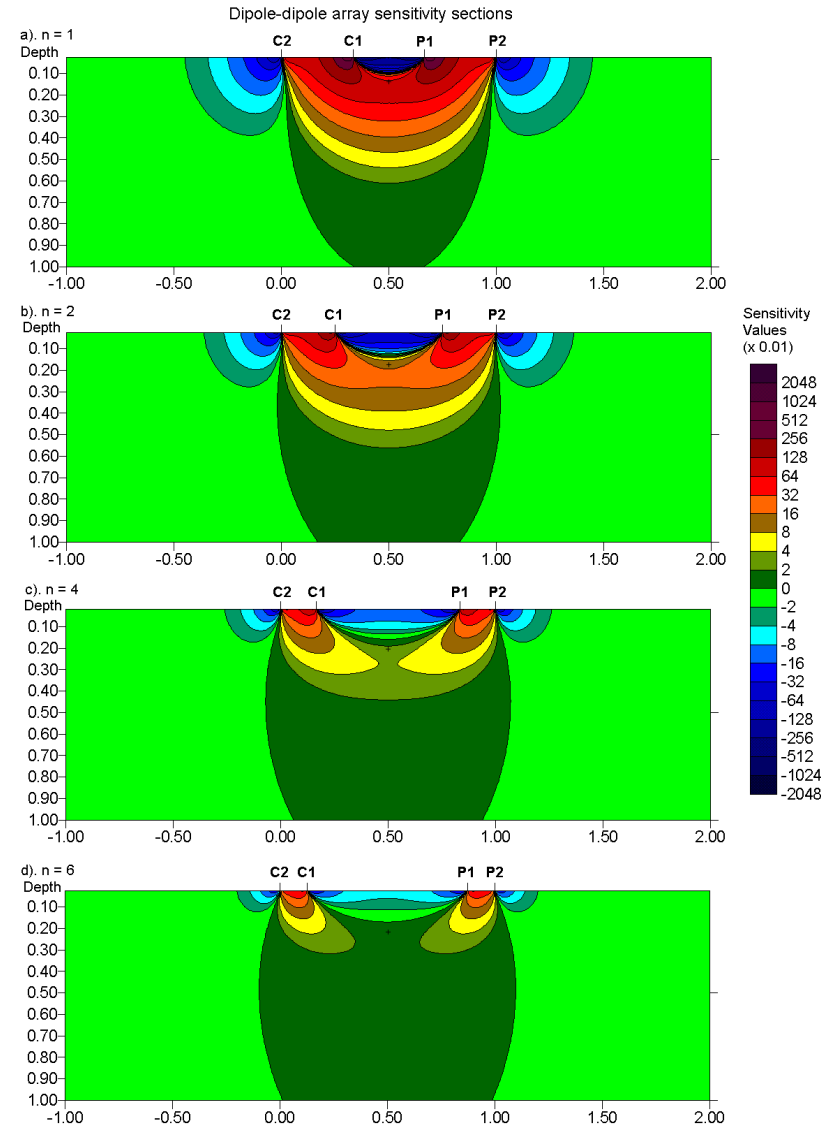
For " $n$ " values of greater than 2, the sensitivity values at the pseudosection data plotting point becomes negligible. The sensitivity contour pattern becomes almost vertical for " $n$ " values greater than 4.



# The dipole-dipole array – sensitivity to structures

Due to the almost vertical sensitivity pattern, this array is very sensitive to horizontal changes in resistivity, but relatively insensitive to vertical changes in the resistivity.

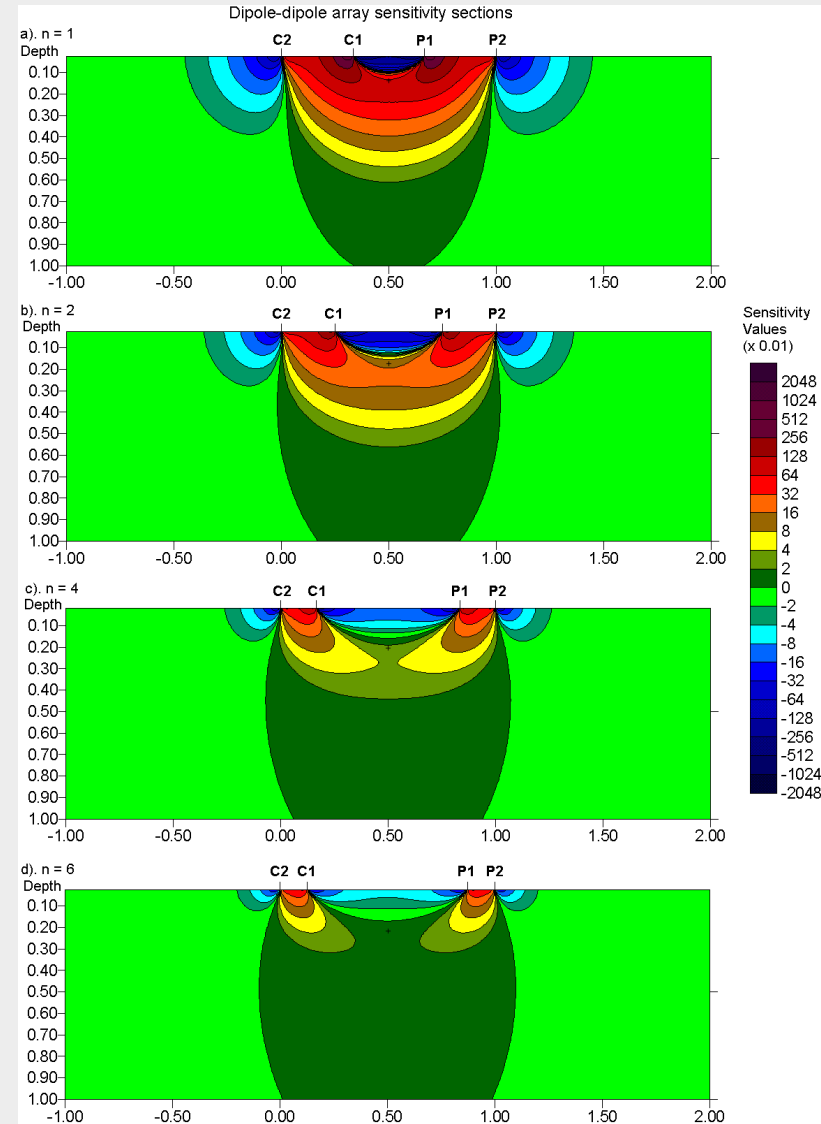
That means that it is good in mapping vertical structures, such as dykes and cavities, but poorer in mapping horizontal structures such as sedimentary layers.



# The dipole-dipole array – depth of investigation

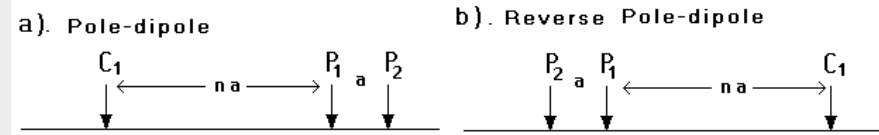
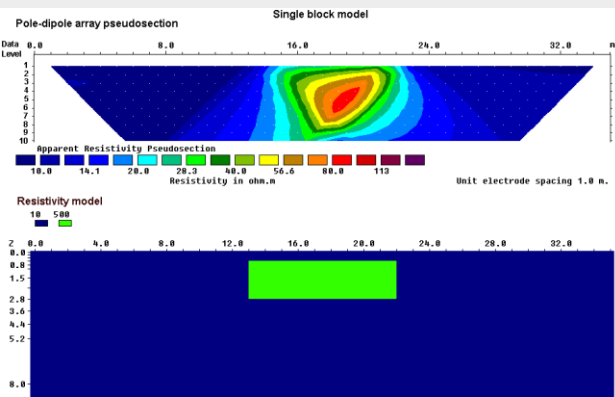
The depth of investigation of this array depends on both the “ $a$ ” spacing and the “ $n$ ” factor. For “ $n$ ” larger than 3, the depth of investigation is approximately 20% of the array length.

Due to the almost vertical pattern of the sensitivity contours, the median depth of investigation might underestimate the depth of structures sensed by this array by about 20% to 30% for large “ $n$ ” factors.

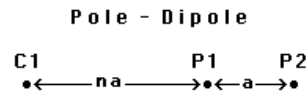


# The pole-dipole array – electrode arrangement

The pole-dipole array is an asymmetrical array. It requires a remote electrode (C2 electrode) that must be placed sufficiently far from the survey line (at least 5 times the maximum C1-P1 distance used). Over symmetrical structures the apparent resistivity anomalies in the pseudosection are asymmetrical, which could influence the inversion model. To remove the asymmetry, measurements are repeated with the electrodes arranged in the reverse manner. By combining the measurements with the “forward” and “reverse” pole-dipole arrays, any bias in the model due to the asymmetrical nature of this array would be removed. This will double the number of data points but it is not a significant problem with multi-channel instruments.



C2  
•

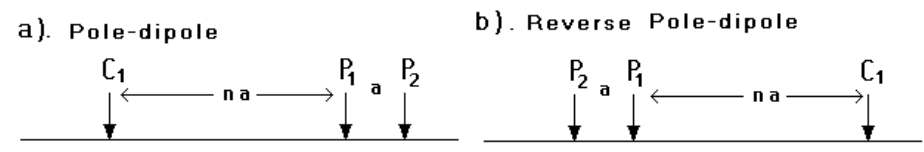
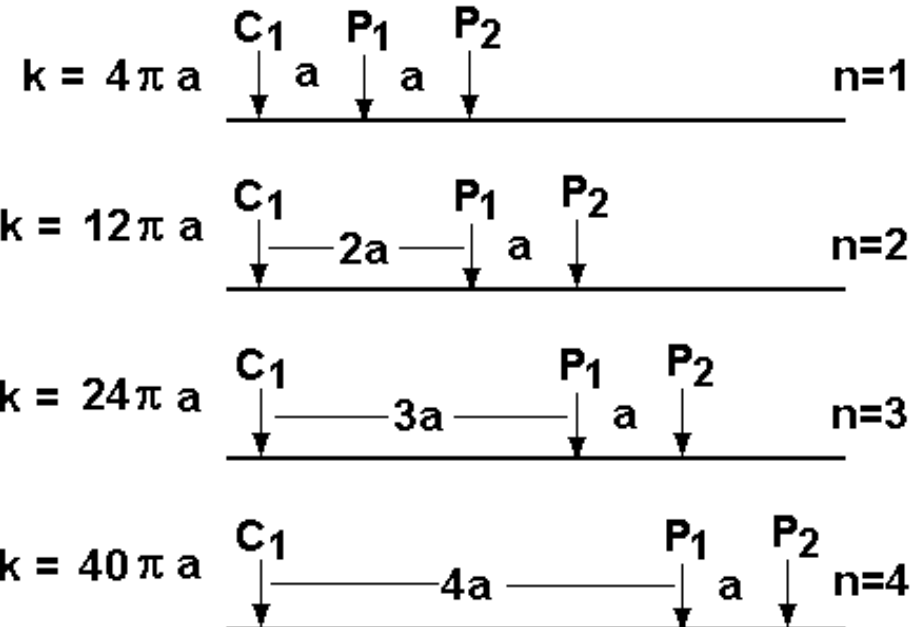


$$k = \text{Geometric Factor} = 2 \pi n(n+1)a$$

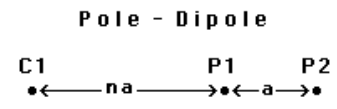
# The pole-dipole array – electrode arrangement

The pole-dipole array is an asymmetrical array. It requires a remote electrode (C2 electrode) that must be placed sufficiently far from the survey line (at least 5 times the maximum C1-P1 distance used).

The distance between the P1-P2 potential dipole from the C1 electrode is increased to increase the depth of investigation. The 'n' spacing usually starts with 1 and increased to 6 to 10. The geometric factor k also increases with the 'n' spacing factor but not as rapidly as the dipole-dipole array.



C2

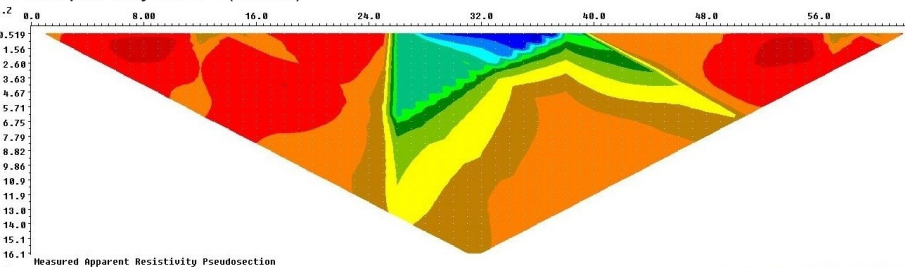


$k = \text{Geometric Factor} = 2\pi n(n+1)a$

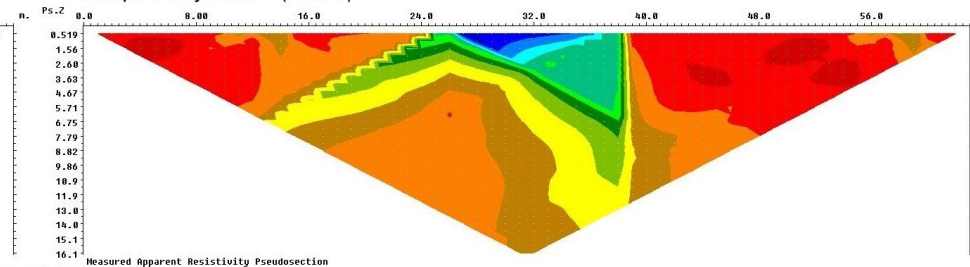
# The pole-dipole array – asymmetry

Over symmetrical structures the apparent resistivity anomalies in the pseudosection are asymmetrical, which could influence the inversion model. To remove the asymmetry, measurements are repeated with the electrodes arranged in the reverse manner. By combining the measurements with the “forward” and “reverse” pole-dipole arrays, any bias in the model due to the asymmetrical nature of this array would be removed. This will double the number of data points but it is not a significant problem with multi-channel instruments.

Pole-dipole array with n=1 (forward)

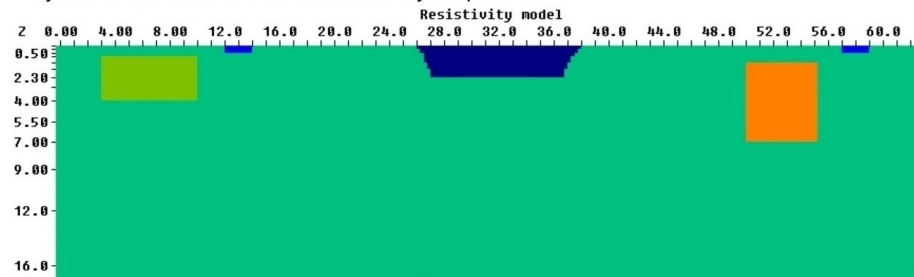


Pole-dipole array with n=1 (reverse)



Resistivity in ohm.m

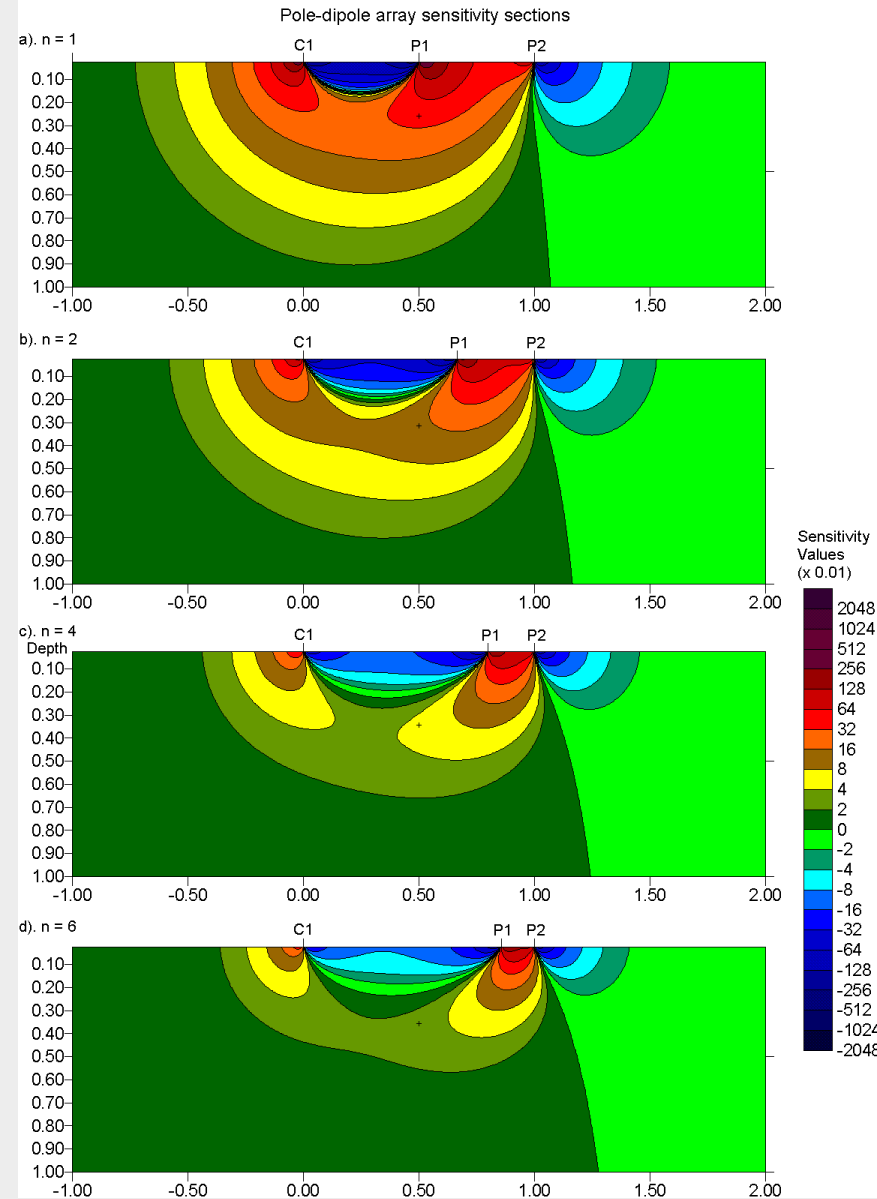
Synthetic model with near surface low resistivity dump site



Model Resistivity Values  
2.5 25 100 250 500

# The pole-dipole array – sensitivity pattern

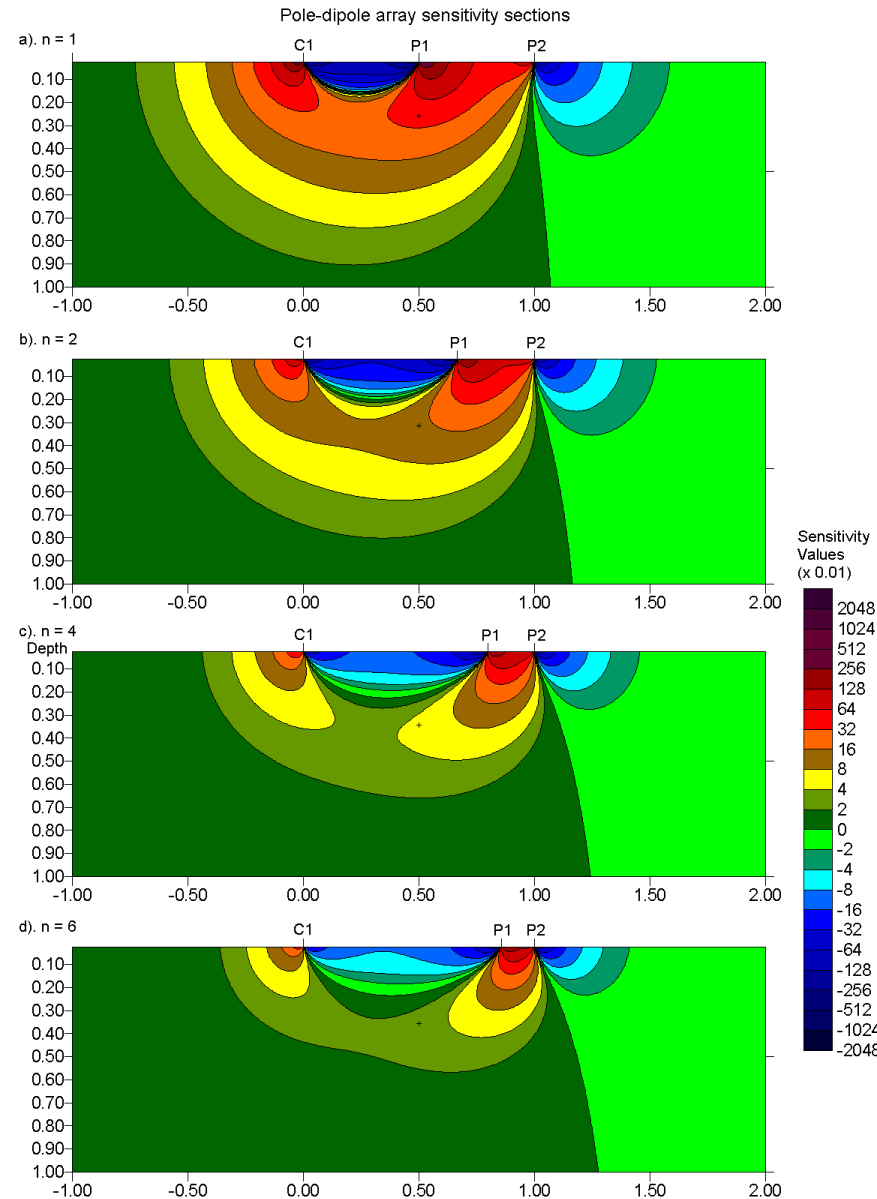
The areas with the greatest sensitivity lies beneath P1-P2 dipole pair, particularly for large “ $n$ ” factors. For “ $n$ ” values of 4 and higher, the high positive sensitive region beneath the P1-P2 dipole becomes increasingly vertical. Thus this array is more sensitive to vertical structures, particularly below the P1-P2 potential dipole.



# The pole-dipole array – sensitivity pattern

For very large ' $n$ ' factors, the array becomes very sensitive to near surface features between the P1-P2 electrodes, and less sensitive to deeper structures. This means beyond a certain limit, the effective depth of investigation actually decreases with increasing ' $n$ '.

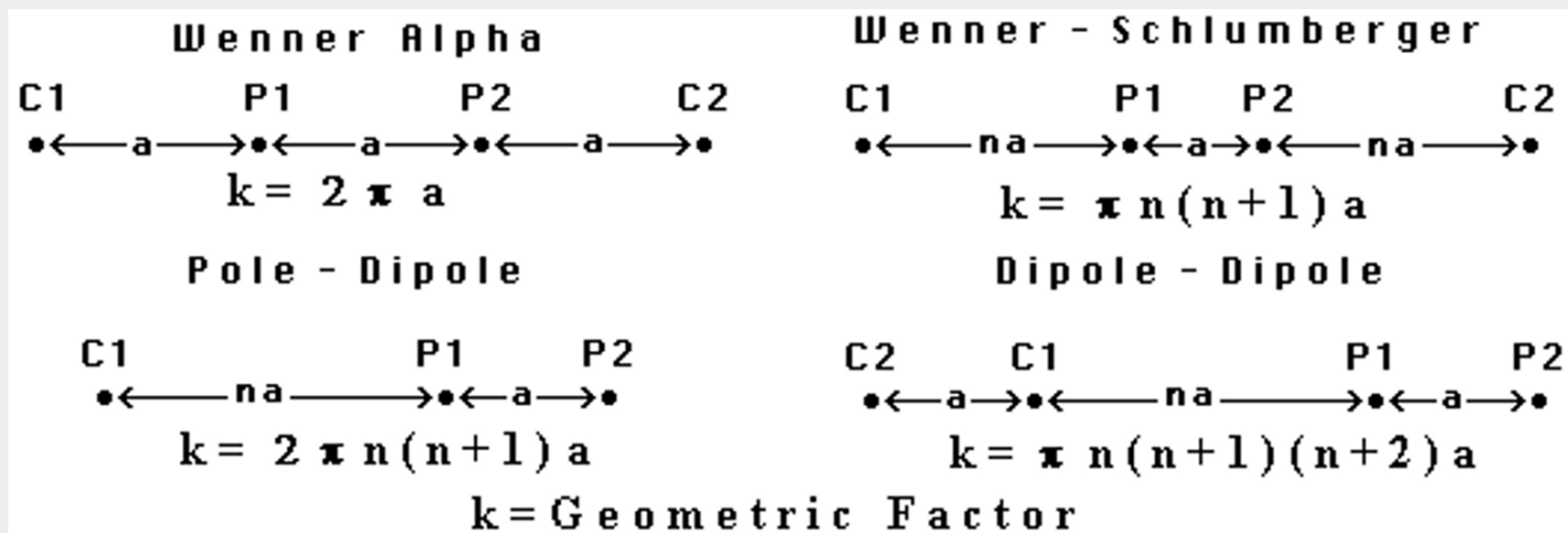
One result is that the ' $n$ ' factor used in a field survey should not exceed 8.



# The pole-dipole array – depth and signal strength

The signal strength for the pole-dipole array decreases with the *square* of the “*n*” factor. The maximum “*n*” value used should not exceed 8. Beyond this, the “*a*” spacing between the P1-P2 dipole pair should be increased to obtain a stronger signal strength.

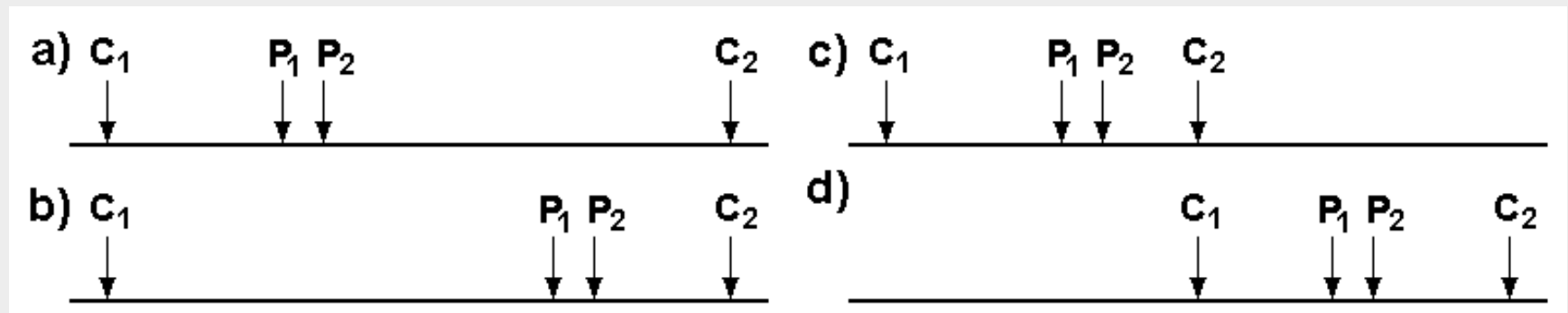
The signal strength is lower compared with the Wenner and Wenner-Schlumberger arrays but higher than the dipole-dipole array. The depth of investigation is about 30% of the C1 to P2 distance.



# The multiple gradient array

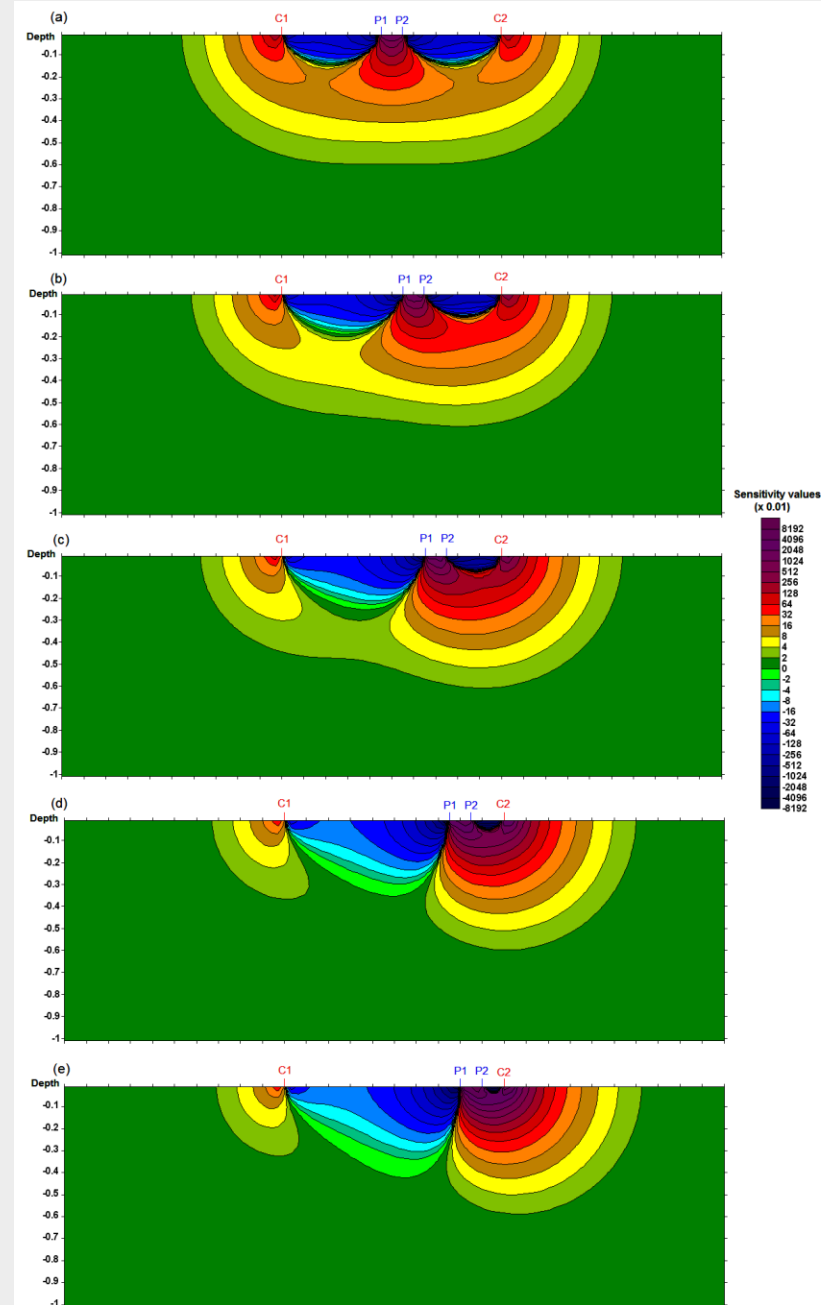
This is a relatively new array developed primarily for multi-channel resistivity meter systems. In the multiple gradient array, different sets of measurements are made with the potential electrodes at different locations for the same current electrodes. As an example, for a system with 32 electrodes, one set of measurements can be made with the current electrodes at nodes 1 and 32.

Next, another series of measurements are made with the current electrodes at nodes 1 and 16, as well as another with the current electrodes at 16 and 32. A similar set of measurements can be made with the C1-C2 electrodes at 1-8, 8-16, 16-24 and 2-32. This can be repeated using smaller distances between the current electrodes.



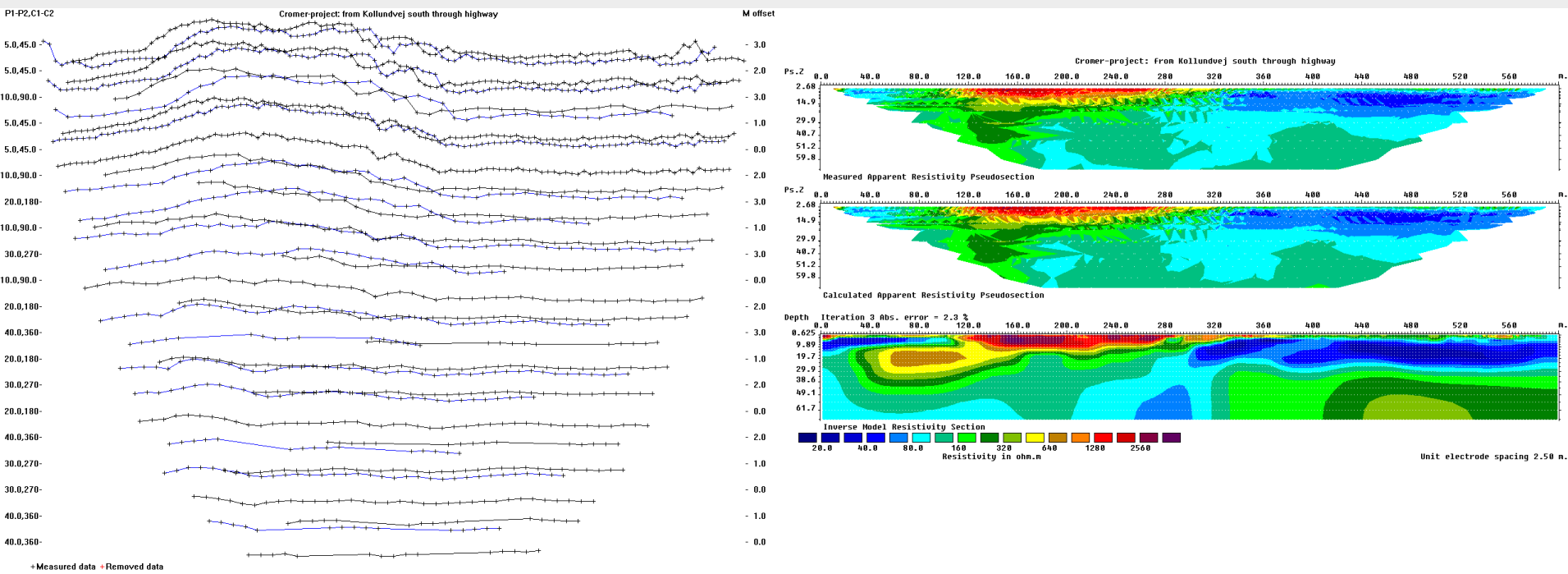
# The gradient array array - sensitivity

The figure shows sensitivity sections with the same positions of the C1-C2 current electrodes, but with the potential dipole P1-P2 being moved from the center to one end of the array. The sensitivity contour pattern slowly changes from a Wenner-Schlumberger pattern towards the pole-dipole pattern as the potential dipole moves closer to the current electrode at one end of the array. The results obtained by this array is comparable to those obtained by the Wenner-Schlumberger and pole-dipole arrays, but generally has better signal strength than the pole-dipole array.



# The multiple gradient array array - example

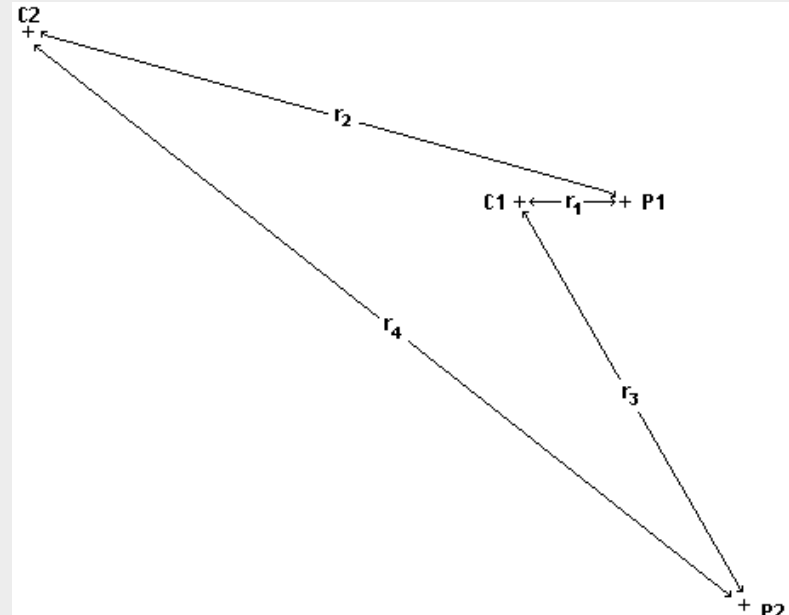
The figure shows the data from a survey using a multiple gradient array was carried out by Aarhus University. A plot of this data set in the form of profiles is also shown. This array is popular with the new multi-channel instruments. It allows a number of readings to be taken simultaneously with the same current electrodes positions, but gives a stronger signal strength compared to the dipole-dipole and pole-dipole arrays. The depth of investigation is similar to the Wenner-Schlumberger.



# The pole-pole array – arrangement

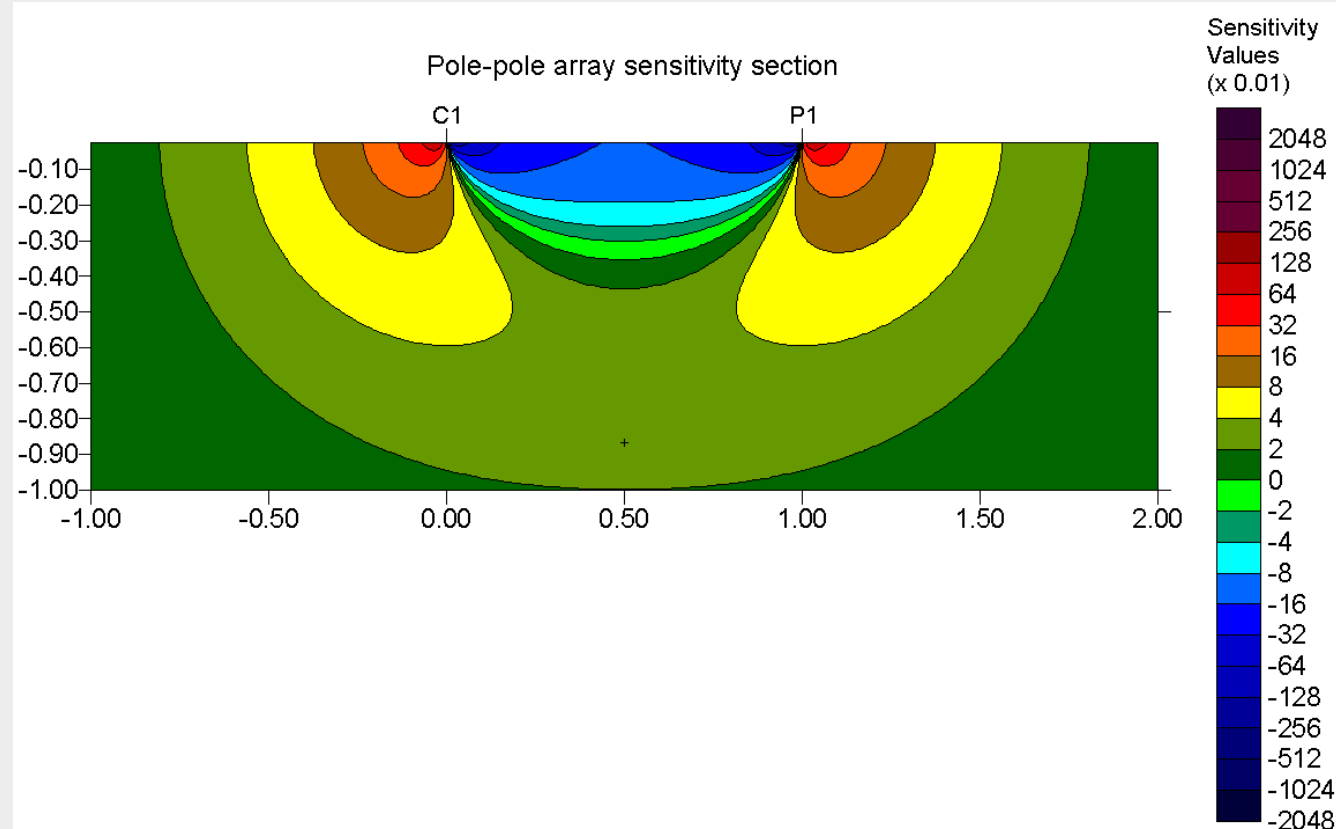
In practice the ideal pole-pole array, with only one current and one potential electrode, does not exist. To approximate the pole-pole array, the second current and potential electrodes (C2 and P2) must be placed at a distance that is more than 20 times the maximum separation between C1 and P1 electrodes used in the survey. When the inter-electrode spacing along the survey line is more than a few meters, finding suitable locations for the C2 and P2 electrodes to satisfy this requirement could be a major task.

Another possible disadvantage of this array is that because of the large distance between the P1 and P2 electrodes, it is can pick up a large amount of telluric noise (particularly near urban areas) that can severely degrade the quality of the measurements.



# The Pole-pole array – sensitivity pattern

This array is commonly used in surveys where small electrode spacings (less than a few meters) are used, such as archaeological surveys. This array has the deepest depth of investigation. However, it has the poorest resolution, which is reflected by the comparatively large spacing between the contours in the sensitivity function plot.

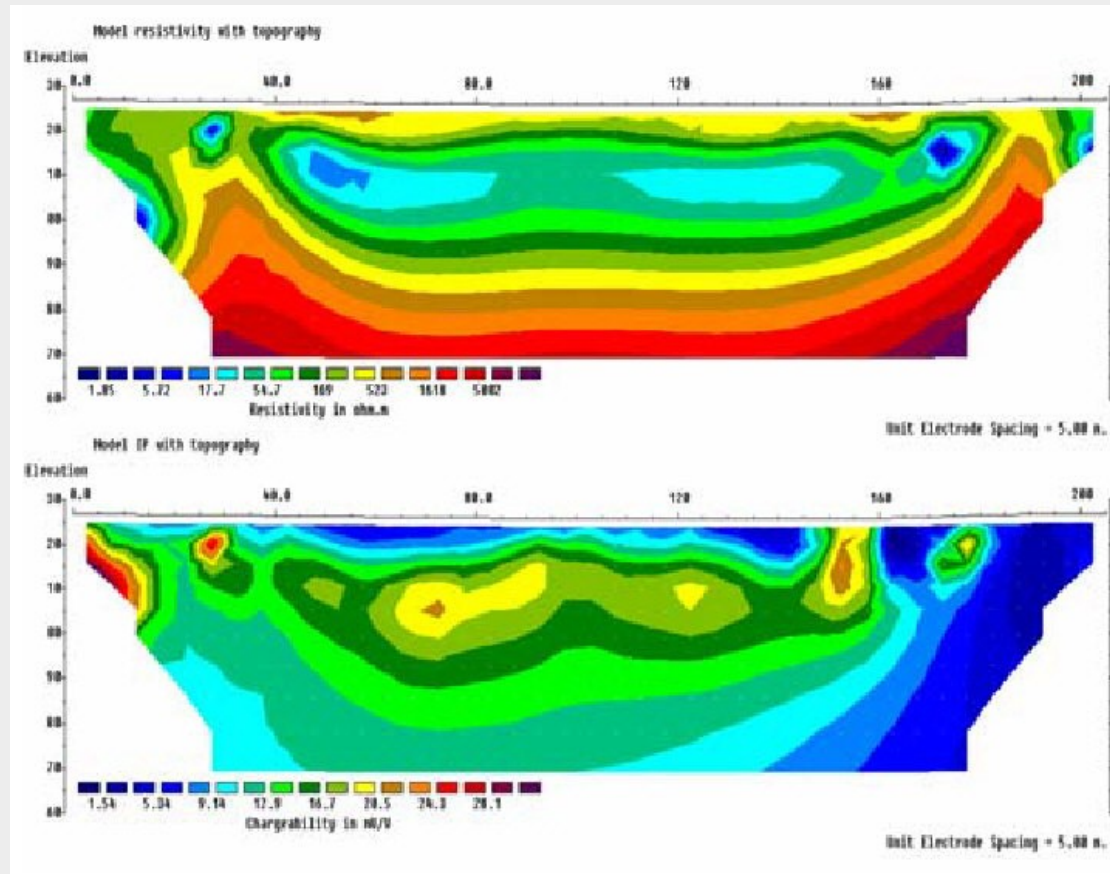


# Pole-pole array field example

Despite the potential problems, this arrays has been used in mineral exploration surveys. Below is an example from Peru where an IP survey was conducted to map mining wastes containing metallic sulphides using a 10 m. electrode spacing.

The success of the survey was partly due to the low telluric noise because of the remote location of the site from possible cultural EM noise.

Due to its large depth of investigation compared to the survey line length, it is an attractive alternative in remote areas.



# Summary of array types

The **Wenner** array is an attractive choice for a survey carried out in a noisy area (due to its high signal strength) and also if good vertical resolution is required. It is probably the most robust and simple array to use, and might be a 'safe' choice for beginners.

The **Wenner-Schlumberger** array is a reasonable alternative if both good horizontal and vertical resolutions are needed, particularly if good signal strength is also required.

The **multiple-gradient** array is useful with multi-channel systems. It has relatively good signal strength.

The **dipole-dipole** array might be a more suitable choice if good horizontal resolution is important (assuming your resistivity meter is sufficiently sensitive and there is good ground contact). However, special care must be taken for surveys with this array to avoid very noisy data.

# Summary of array types continued

The **pole-dipole** array has the advantage of a deeper depth of investigation, and only one remote C2 electrode. To avoid bias in the results, measurements in both the forward and reverse directions should be taken. It is an alternative to the dipole-dipole for I.P. surveys due to the stronger signal strength.

For surveys with small electrode spacings, the **pole-pole** array might be a suitable choice. However, it has two remote electrodes that must be placed at a sufficiently far distance which might be a problem in developed areas.

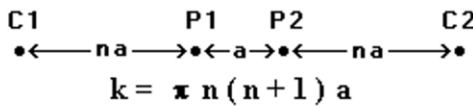
The new multi-electrode systems has modified the criteria for array choice. The arrays that are used are the dipole-dipole, pole-dipole, pole-pole, reverse Wenner-Schlumberger and multiple gradient.

# Arrays with with overlapping data levels

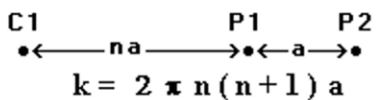
The Wenner-Schlumberger, dipole-dipole and pole-dipole arrays have 2 parameters, the ' $a$ ' spacing between the potential electrodes and an ' $n$ ' factor. Different combinations of ' $a$ ' and ' $n$ ' might have the same total array length, and similar depths of investigations.

A dipole-dipole array with a " $a$ " spacing of 10m and " $n$ " of 7 will have the same length as an array with  $a=30m$  and  $n=1$ . However, the array with  $n=1$  will have a signal strength that is 28 times larger than the array with  $n=7$ .

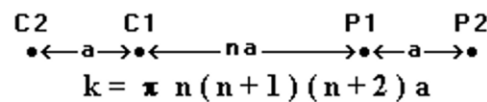
## Wenner - Schlumberger



## Pole - Dipole

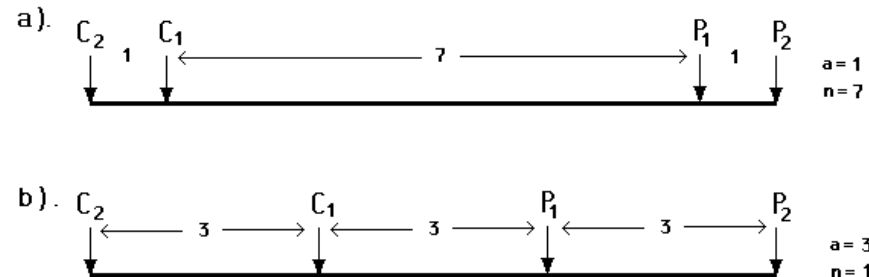


## Dipole - Dipole



$k = \text{Geometric Factor}$

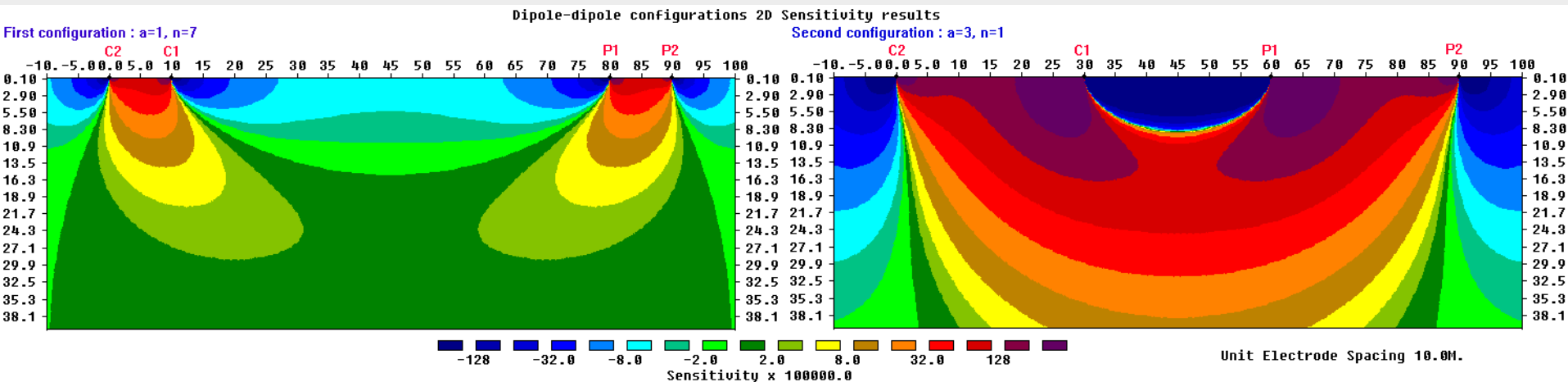
## Dipole-dipole array



# Dipole-dipole array sensitivity patterns

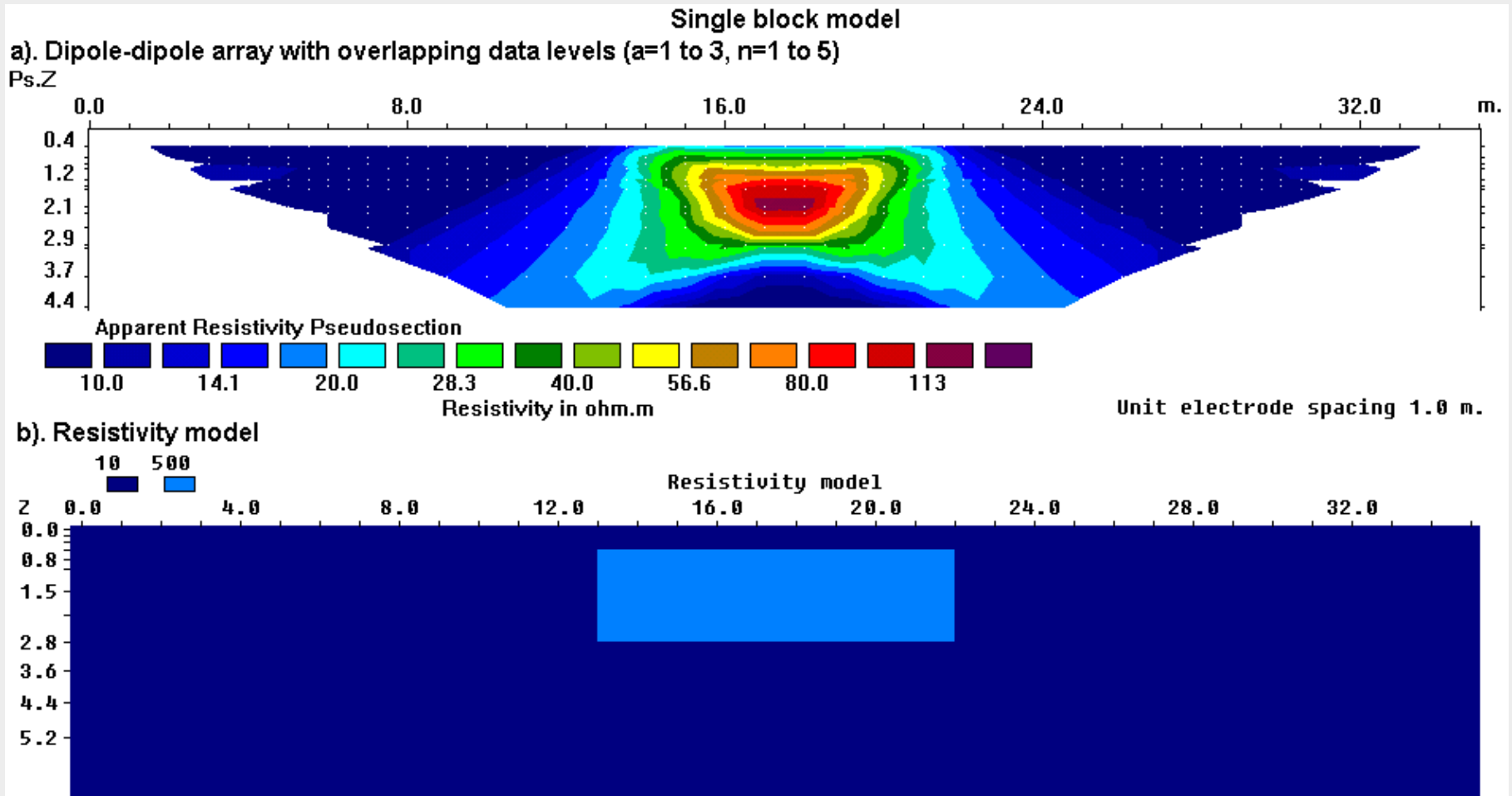
The two dipole-dipole arrays have sensitivity patterns that are very different. The array with  $n=7$  will be very sensitive to vertical structures below the C1-C2 and P1-P2 dipoles, while the other array will be more sensitive to deeper structures below the entire array.

To make use of both features, a “high-resolution” survey technique can be used by combining measurements with different “ $a$ ” and “ $n$ ” values to give overlapping data levels.



# High resolution survey example

The figure shows the apparent resistivity pseudosection for the dipole-dipole array using overlapping data levels over a rectangular prism. Values of 1 to 3 metres are used for the dipole length ' $a$ ', and the dipole separation factor ' $n$ ' varies from 1 to 5.



# **2-D Models & Data Inversion**

**Inversion methods**

**Models and Mathematics**

**Why we carry out inversions,  
the least-squares optimization method  
with different constraints and their  
effects on the model.**

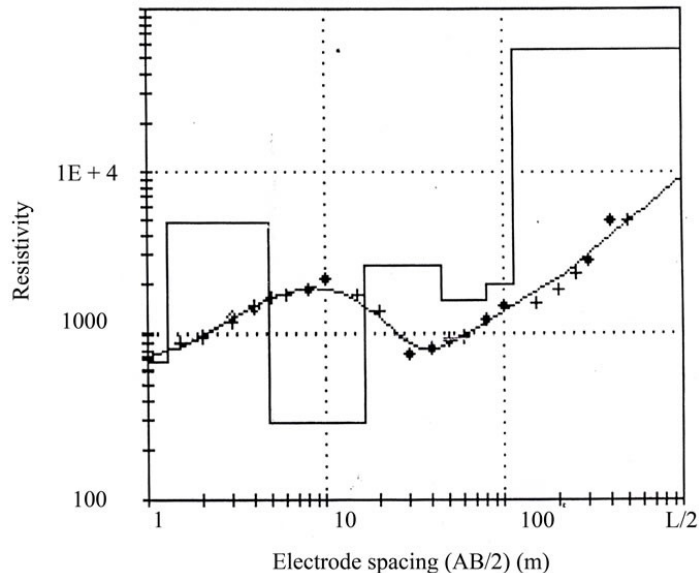
# What is inversion?

The purpose of an inversion program is to convert the apparent resistivity values into the true resistivity of the subsurface.

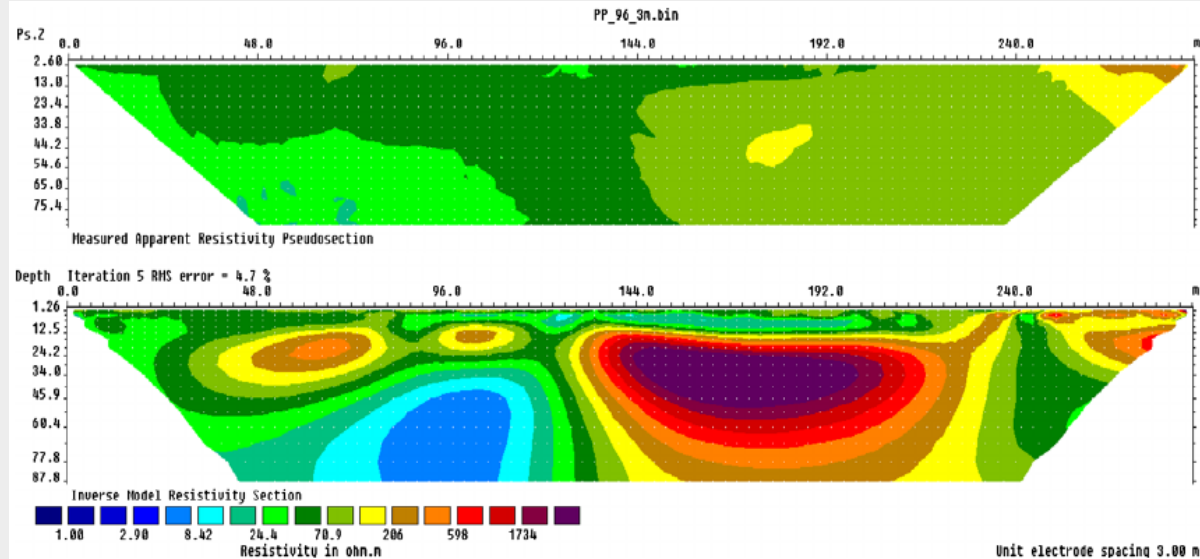
$$\rho_{\text{app}} \rightarrow \rho_{\text{true}}$$

The relationship between the apparent resistivity and the true resistivity is a very complex relationship, depending on whether the subsurface model is 1-D, 2-D or 3-D. Converting the data into a model is the inversion step.

## 1-D inversion example

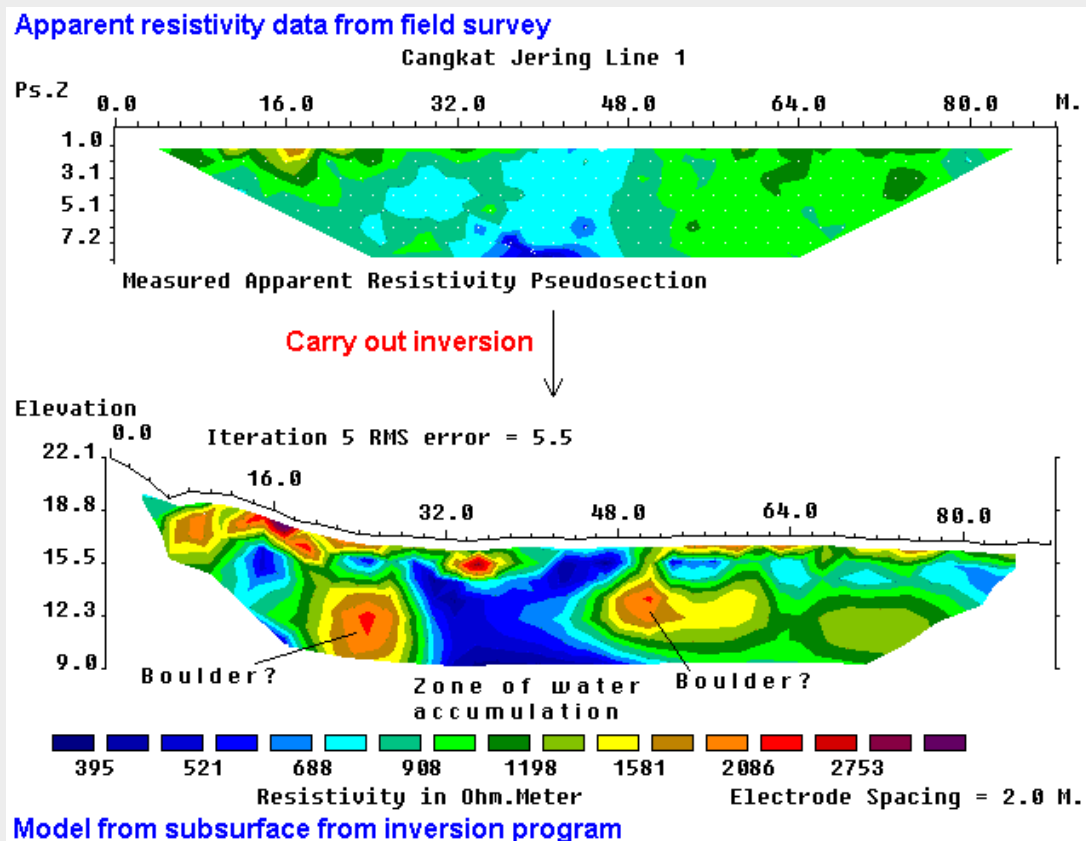


## 2-D inversion example



# From data to model : 2-D inversion

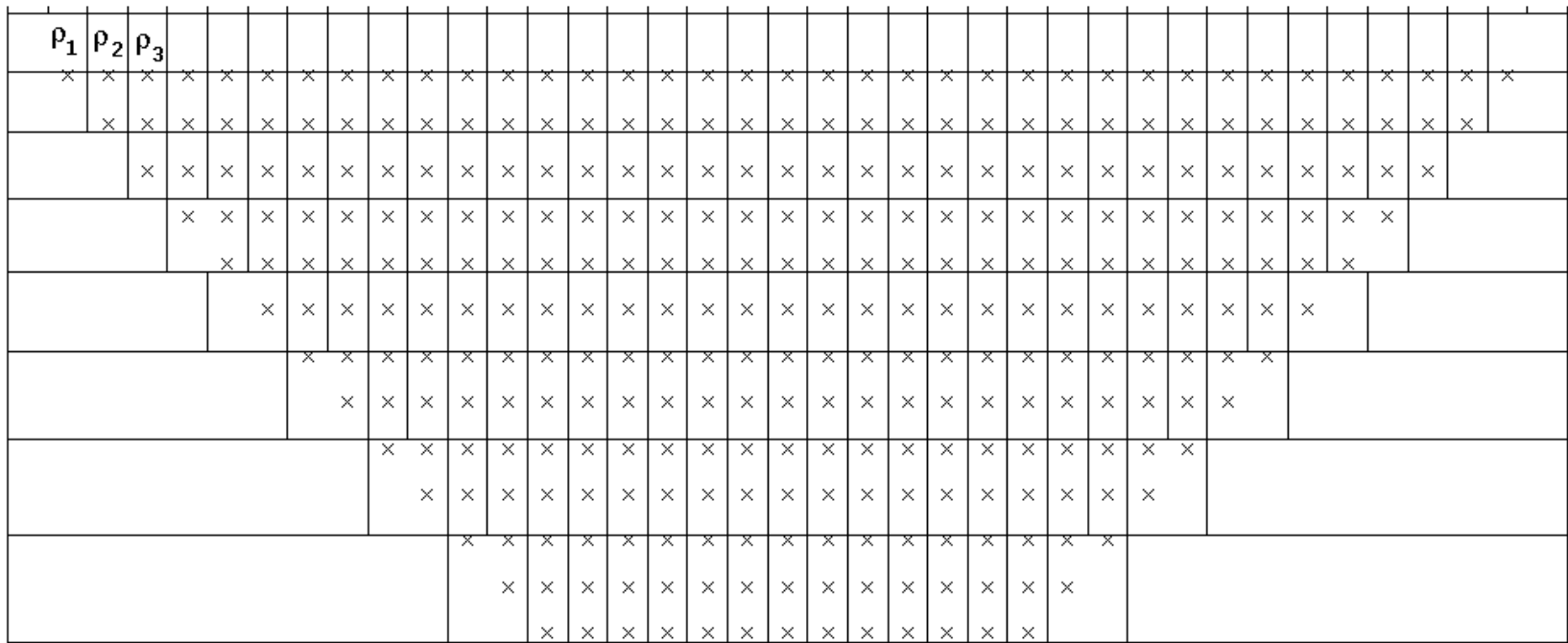
After the field survey, the resistance measurements are usually changed to apparent resistivity values. The purpose of the inversion is to convert the apparent resistivity values into a model section. The conversion of the apparent resistivity data to a model for the subsurface resistivity is carried out on a microcomputer using an automatic inversion program.



# What is a 2-D model?

A 2-D model is used to interpret the data from a 2-D imaging survey. The model usually consists of a large number of rectangular cells. The size and position of each cell is fixed. An inversion program is used to determine the resistivity of the cells from the measured apparent resistivity values.

ARRANGEMENT OF MODEL BLOCKS AND APPARENT RESISTIVITY DATUM POINTS



Model block



Datum point

Number of model blocks 232

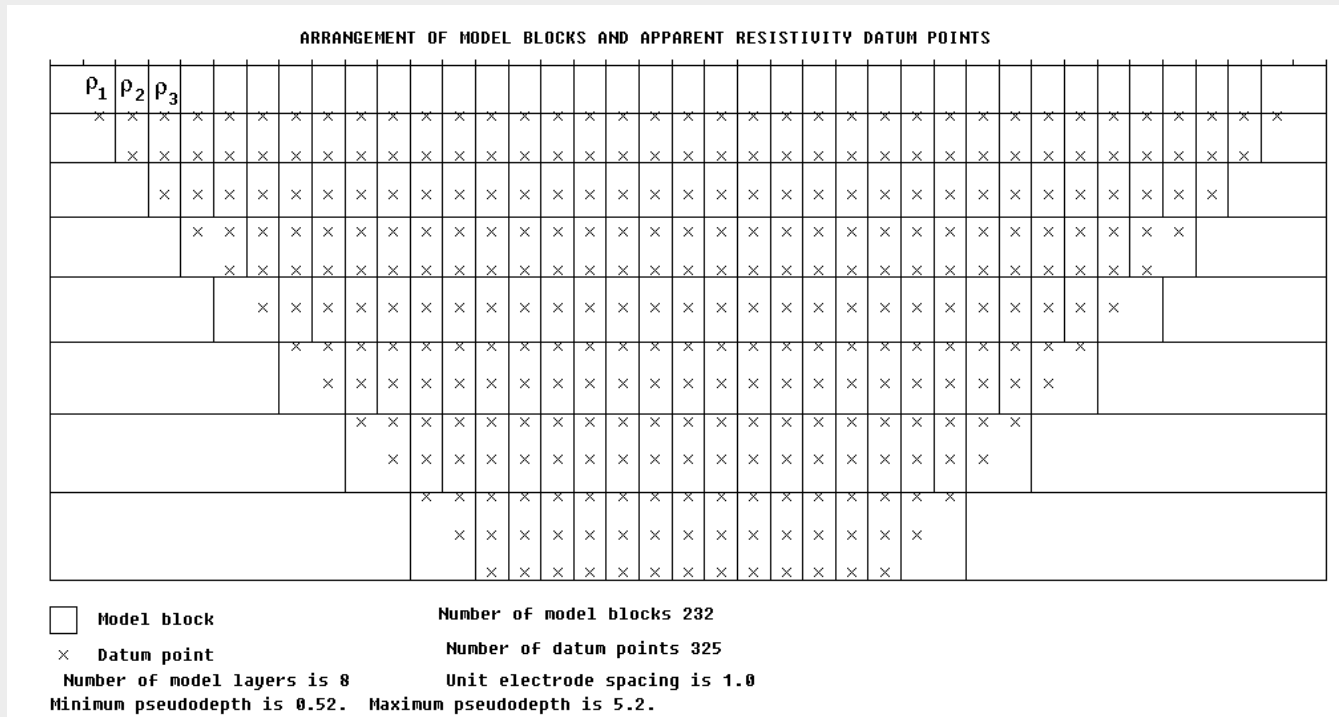
Number of datum points 325

Number of model layers is 8

Unit electrode spacing is 1.0

Minimum pseudodepth is 0.52. Maximum pseudodepth is 5.2.

# The 2-D model – some quantities



What we have : Observed data (logarithm of measured apparent resistivity values) :- **y**

What we want : Model parameters (logarithm of model cells resistivity values) :- **q**

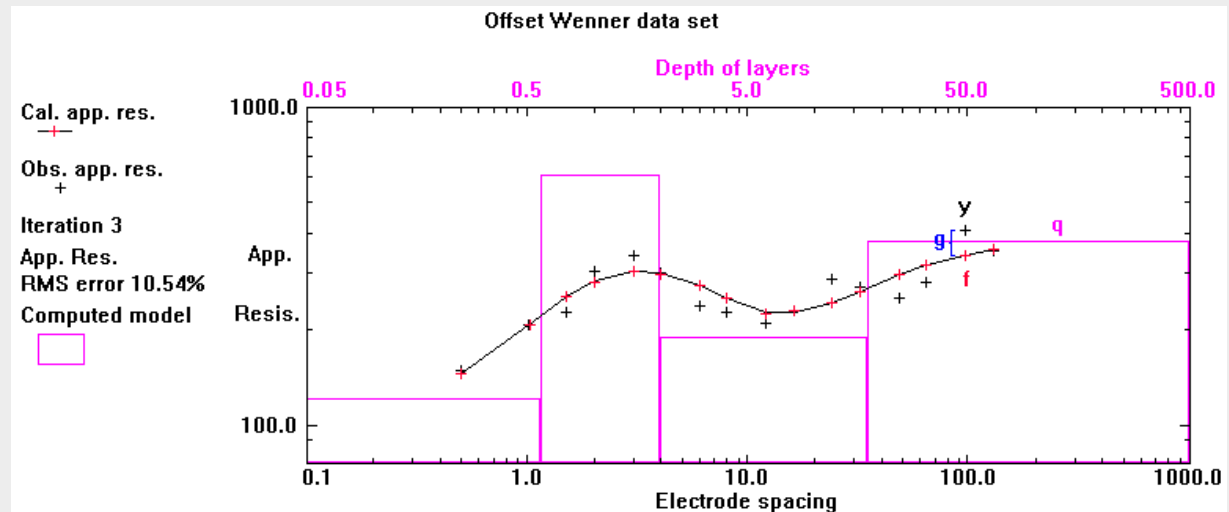
The connection between them : Model response (logarithm of calculated apparent resistivity values for a given model) :- **f**

# Starting an inversion

All inversion methods try to determine a model for the subsurface whose response agrees with the measured data subject to certain restrictions. The model parameters are the resistivity values of the model cells, while the data is the measured apparent resistivity values. An initial model (usually a simple model with same resistivity value for all the cells) is modified in an iterative manner so that the difference ( $g$ )

$$g = y - f$$

between the calculated ( $f$ ) and measured ( $y$ ) apparent resistivity values is reduced.



# Example of measured and calculated apparent resistivity

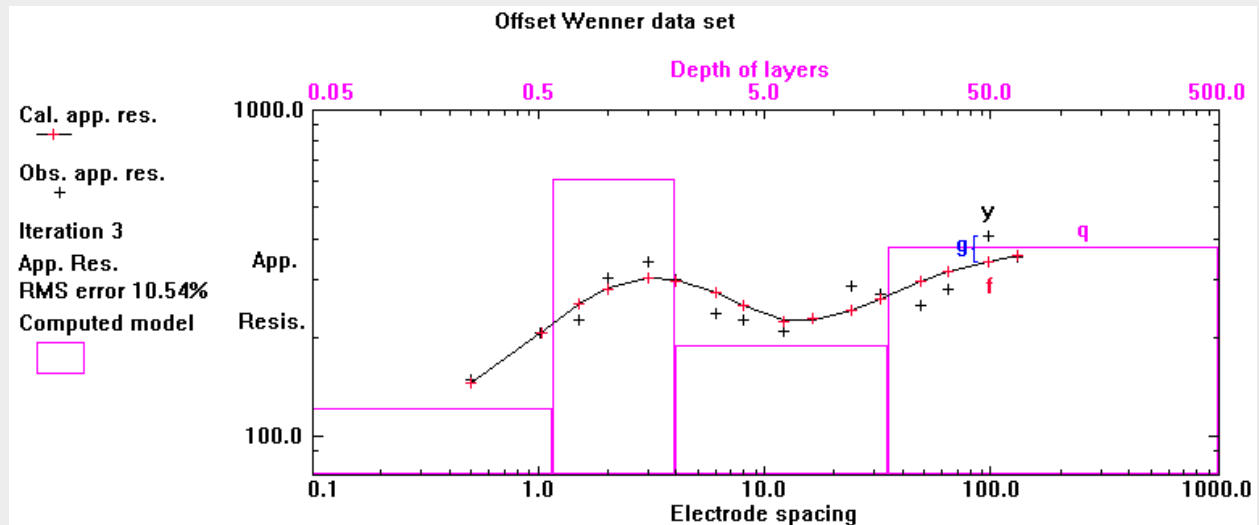
As a simple first example, we use a 1-D sounding survey that makes it easier to illustrate the different quantities. In this case

$y$  = input data is the measured apparent resistivity values

$f$  = model response, calculated apparent resistivity values

$g = y - f$  = data misfit, difference between measured and calculated apparent resistivity values

$q$  = model parameters, the resistivity and thickness of layers that we want to adjust so as to reduce  $g$

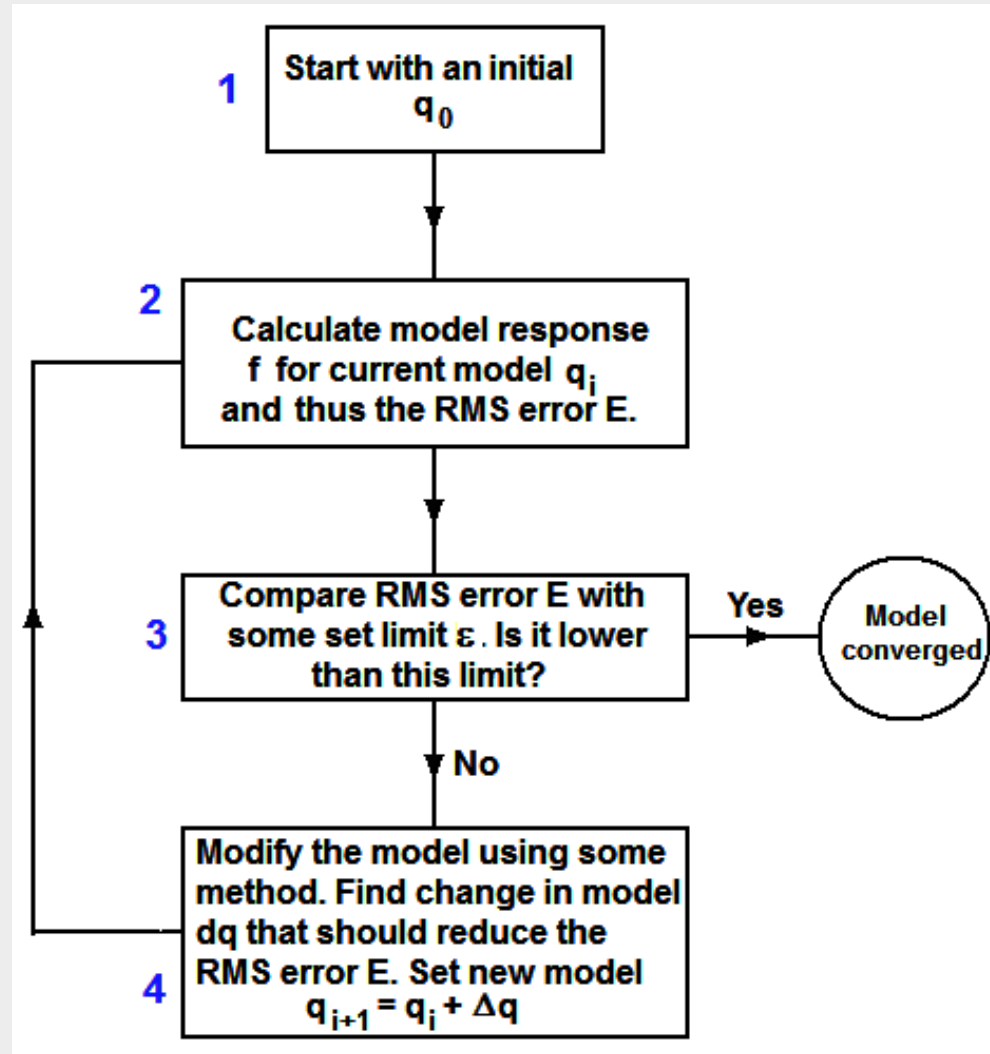


# The iterative inversion algorithm

The simplest initial model  $q_0$  is a homogenous earth model, set to the average apparent resistivity value.

The main difference in an inversion method is in step 4, the method used to determine the change in the model  $\Delta q$  that should improve the current model.

The Res2dinv and Res3dinv programs use the least-squares optimization method.

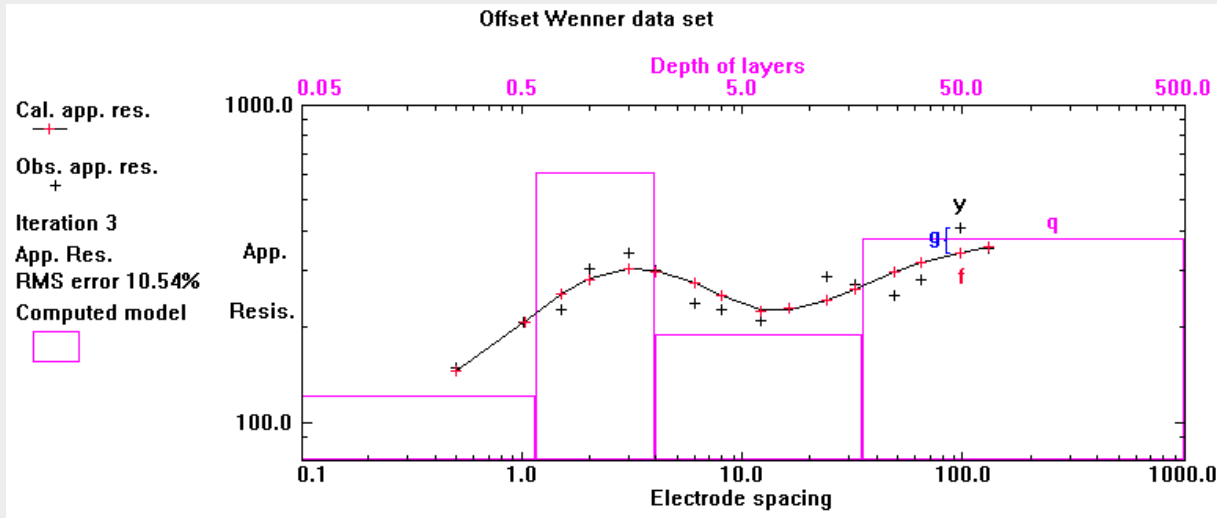
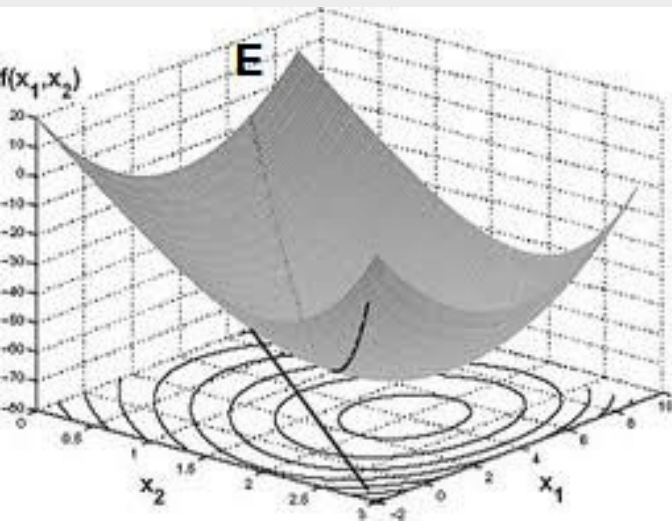


# The least-squares criterion

In the least-squares optimization method, the model ( $\mathbf{q}$ ) is modified such that the sum of squares error  $E$  of the difference between the model response and the observed data values ( $\mathbf{g} = \mathbf{y} - \mathbf{f}$ ) is minimized.

$$E = \mathbf{g}^T \mathbf{g} = \sum_{i=1}^n g_i^2$$

When the data misfit ( $\mathbf{g} = \mathbf{y} - \mathbf{f}$ ) is small, the model obtained ( $\mathbf{q}$ ) is a possible solution.  $n$  is the number of data points.



# The least-squares inversion method

The Gauss-Newton least-squares method uses the equation

$$\mathbf{J}^T \mathbf{J} \Delta \mathbf{q}_i = \mathbf{J}^T \mathbf{g}$$

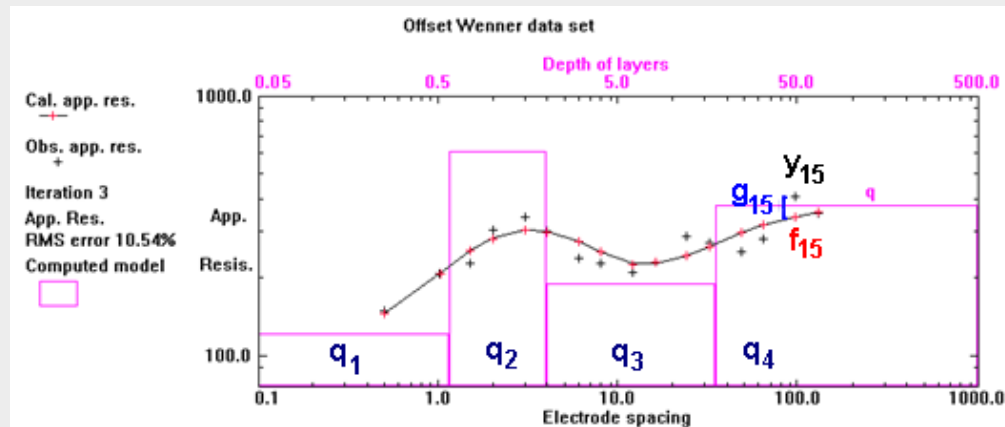
to calculate the change in the model resistivity values ( $\Delta \mathbf{q}$ ) that will reduce the sum of squares error  $E$ .  $\mathbf{J}$  is the Jacobian matrix (of size  $m$  by  $n$ ) of partial derivatives. The elements of the Jacobian matrix are given by

$$J_{ij} = \frac{\partial f_i}{\partial q_j}$$

that is the change in the  $i$ th calculated apparent resistivity value due to a change in the  $j$ th model resistivity value. After calculating the parameter change vector, a new model is obtained by

$$\mathbf{q}_{k+1} = \mathbf{q}_k + \Delta \mathbf{q}_k$$

$m$  is the number of model parameters.

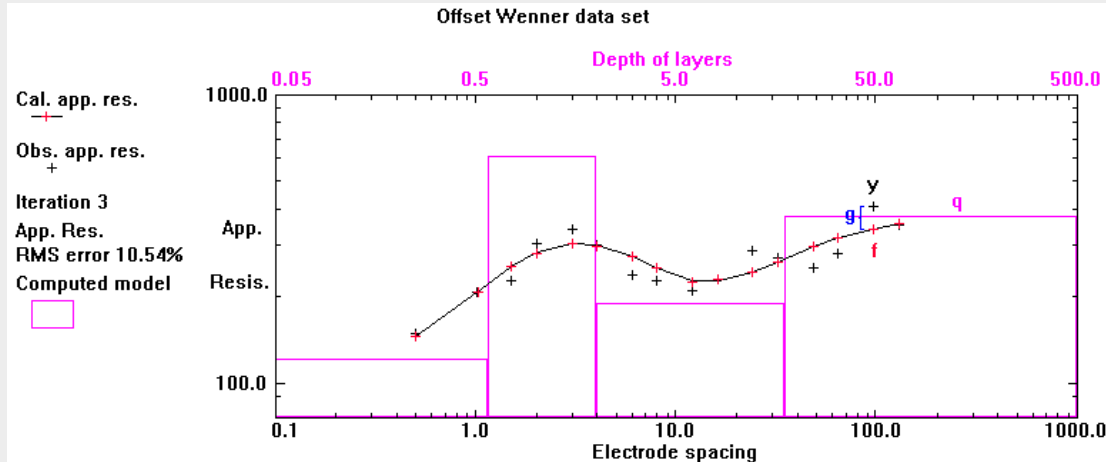
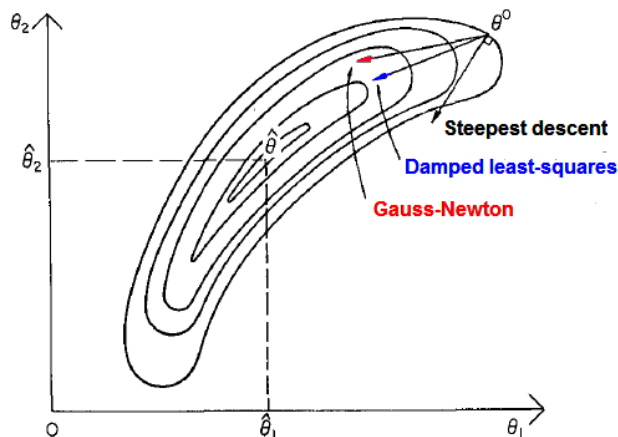


# The damped least-squares inversion method

The simple Gauss-Newton least-squares equation can result in very large and unrealistic variations in the model resistivity values. To overcome this problem, the damped least-squares or “ridge-regression” method is used.

$$(\mathbf{J}^T \mathbf{J} + \lambda \mathbf{I}) \Delta \mathbf{q}_k = \mathbf{J}^T \mathbf{g}$$

$\lambda$  is the damping factor that reduces the change in model resistivity values ( $\Delta \mathbf{q}$ ).  $\mathbf{I}$  is the identity matrix with 1 in the main diagonal and 0 elsewhere. It has been successfully used in cases with a small number of model parameters, such as in resistivity sounding inversions. However, for models with a large number of parameters, it can lead to very large and abrupt changes in model resistivity values.



# The smooth least-squares inversion method

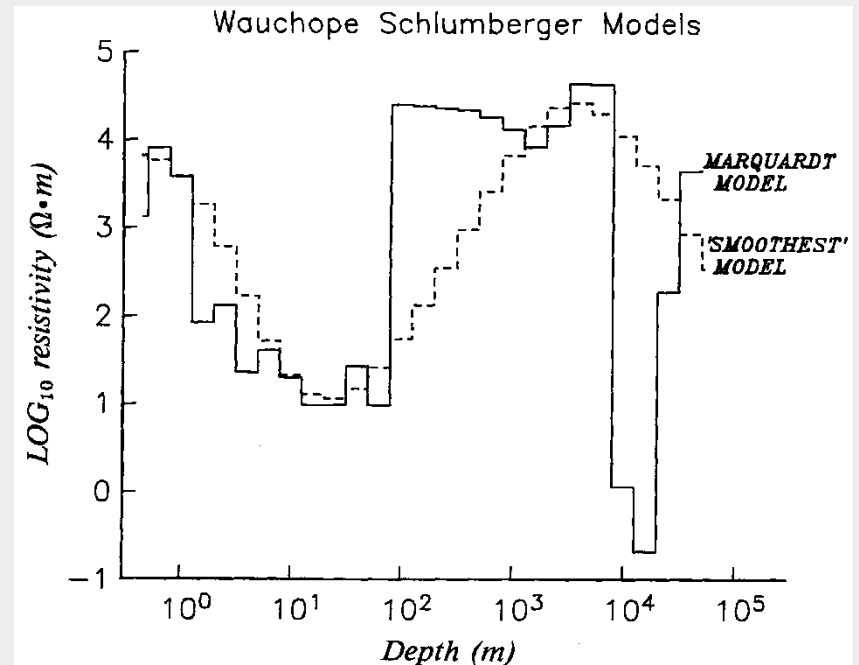
For models with a large number of parameters, the following smoothness-constrained least-squares equation can be used to ensure that the model resistivity changes in a smooth manner.

$$(\mathbf{J}^T \mathbf{J} + \lambda \mathbf{F}) \Delta \mathbf{q}_k = \mathbf{J}^T \mathbf{g} - \lambda \mathbf{F} \mathbf{q}_k,$$

$$\text{where } \mathbf{F} = \alpha_x \mathbf{C}_x^T \mathbf{C}_x + \alpha_y \mathbf{C}_y^T \mathbf{C}_y + \alpha_z \mathbf{C}_z^T \mathbf{C}_z$$

$\mathbf{C}_x$ ,  $\mathbf{C}_y$  and  $\mathbf{C}_z$  are the smoothing matrices in the  $x$ -,  $y$ - and  $z$ - directions. A first-order difference matrix is commonly used as the smoothing matrix.

$$\mathbf{C} = \begin{bmatrix} -1 & 1 & 0 & 0 & \dots & \dots & \dots & 0 \\ 0 & -1 & 1 & 0 & \dots & \dots & \dots & 0 \\ 0 & 0 & -1 & 1 & 0 & \dots & \dots & 0 \\ & & & \vdots & & & & \\ & & & & \vdots & & & \\ & & & & & \dots & & \\ & & & & & & \dots & \\ & & & & & & & \mathbf{0} \end{bmatrix}$$



# The $L_2$ norm least-squares inversion method

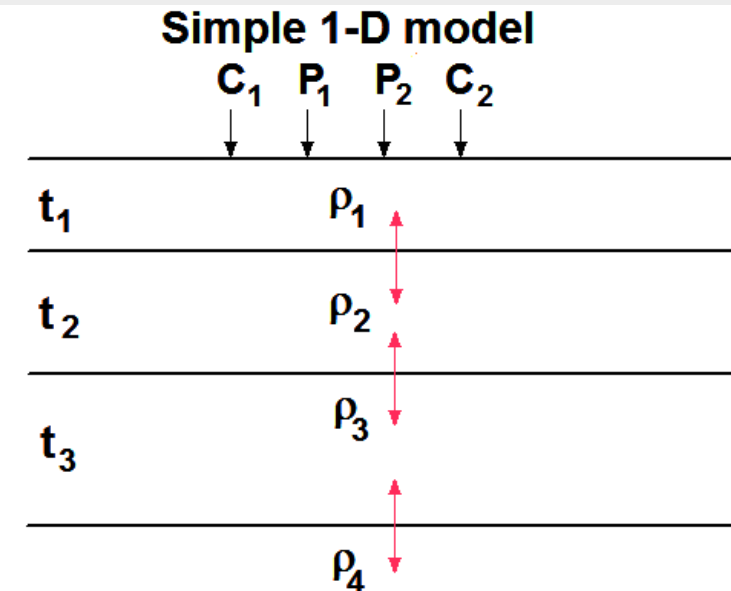
The smoothness-constrained least-squares equation.

$$(\mathbf{J}^T \mathbf{J} + \lambda \mathbf{F}) \Delta \mathbf{q}_k = \mathbf{J}^T \mathbf{g} - \lambda \mathbf{F} \mathbf{q}_k,$$

$$\text{where } \mathbf{F} = \alpha_x \mathbf{C}_x^T \mathbf{C}_x + \alpha_y \mathbf{C}_y^T \mathbf{C}_y + \alpha_z \mathbf{C}_z^T \mathbf{C}_z$$

For the simple case of a 1-D model, the  $\mathbf{C}_z$  matrix takes the difference between the (logarithm) of the resistivity of adjacent layers. Applying the  $\mathbf{C}_z$  matrix will form terms of the type  $(\mathbf{q}_{i+1} - \mathbf{q}_i)$ , and since we use  $\mathbf{C}^T \mathbf{C}$  we actually get  $(\mathbf{q}_{i+1} - \mathbf{q}_i)^2$ , i.e. we minimize the square of the changes so it is called a  $L_2$  norm method.

$$\mathbf{C} = \begin{bmatrix} -1 & 1 & 0 & 0 & \dots & \dots & \dots & 0 \\ 0 & -1 & 1 & 0 & \dots & \dots & \dots & 0 \\ 0 & 0 & -1 & 1 & 0 & \dots & \dots & 0 \\ & & & \dots & & & & \\ & & & & \dots & & & \\ & & & & & \dots & & \\ & & & & & & \dots & \\ & & & & & & & \dots & \\ & & & & & & & & \mathbf{0} \end{bmatrix}$$



# 2-D and 3-D roughness filters least-squares method

The smoothness-constrained least-squares equation is given by :-

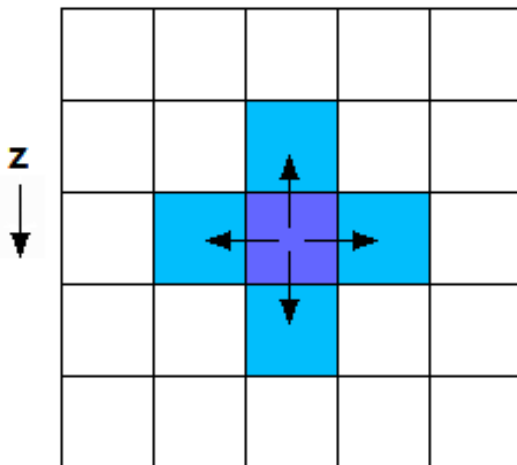
$$\left(\mathbf{J}^T \mathbf{J} + \lambda \mathbf{F}\right) \Delta \mathbf{q}_k = \mathbf{J}^T \mathbf{g} - \lambda \mathbf{F} \mathbf{q}_k,$$

where  $\mathbf{F} = \alpha_x \mathbf{C}_x^T \mathbf{C}_x + \alpha_y \mathbf{C}_y^T \mathbf{C}_y + \alpha_z \mathbf{C}_z^T \mathbf{C}_z$

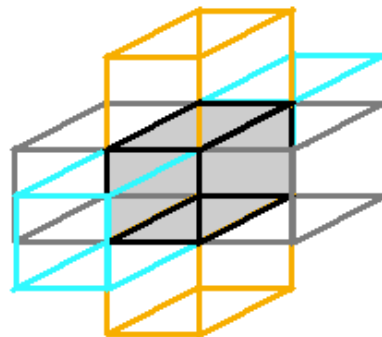
The diagrams below shows the coupling introduced by the  $\mathbf{C}_x$ ,  $\mathbf{C}_y$  and  $\mathbf{C}_z$  filters for 2-D and 3-D models. In 2-D models, the coupling is applied to adjacent cells horizontally and vertically. In the 3-D model, there is an additional coupling in the y-direction.

2-D roughness filter

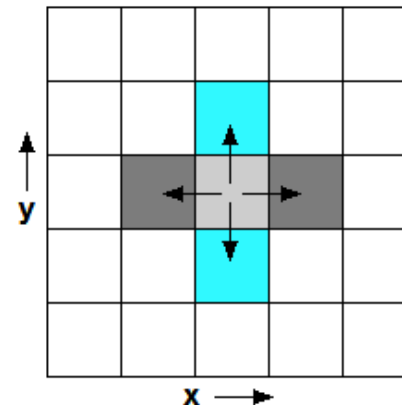
x →



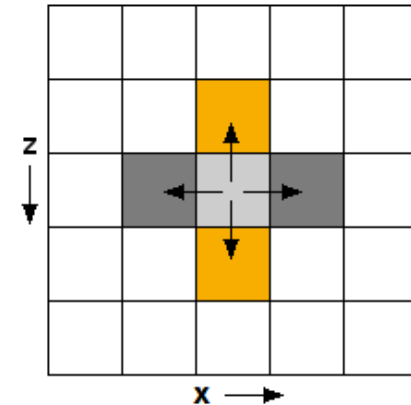
Coupling of 3-D model cells in roughness filter



Normal horizontal roughness filter x and y components



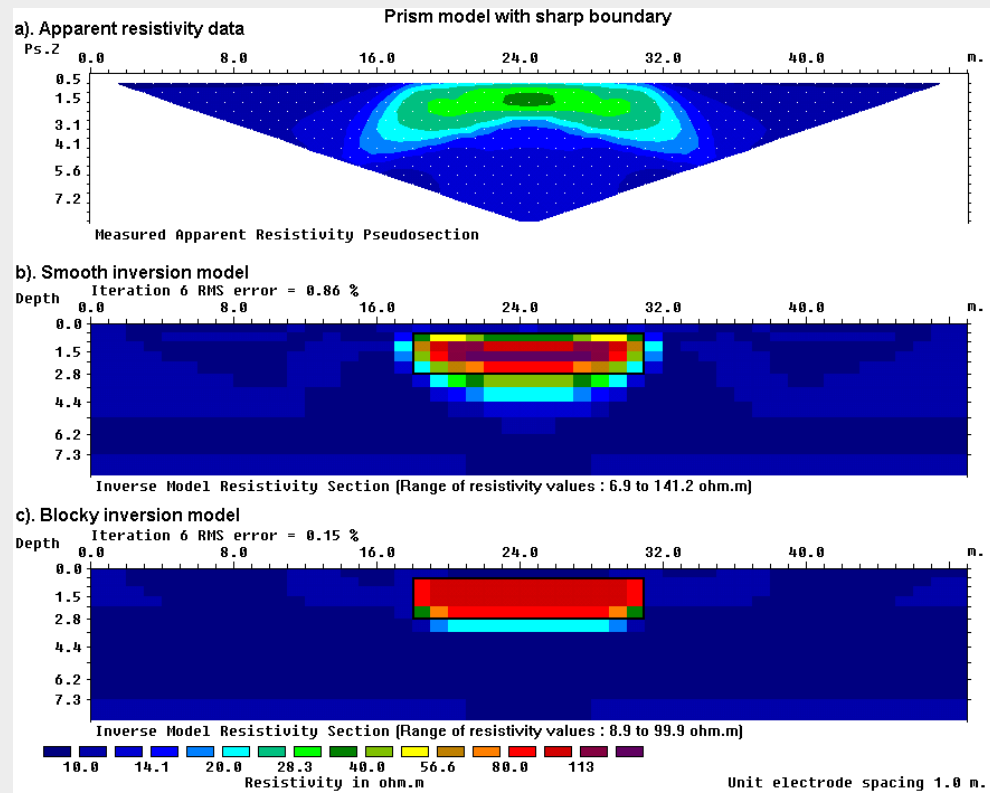
Normal vertical roughness filter with z component



# When smooth is too smooth

The smooth inversion method minimizes the sum-of-squares (a  $L_2$  norm) of the change in the model resistivity values (through the  $C^T C$  term). It gives accurate results in situations where the subsurface resistivity changes in a gradual manner. However, in situations with sharp boundaries, the results are less accurate.

The example below shows a rectangular block with sharp boundaries. The smooth inversion method produces a model with smeared boundaries.



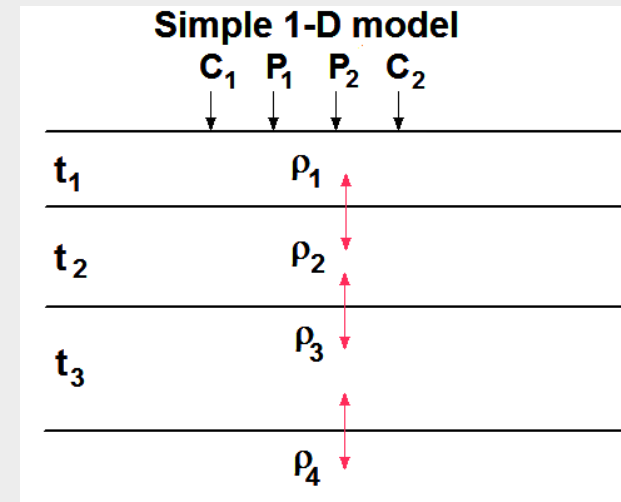
# The blocky least-squares inversion method

To overcome the problem of boundaries that are too smooth, the “blocky” inversion method is one possible solution. The least-squares equation is further modified to

$$\left( \mathbf{J}^T \mathbf{J} + \lambda \mathbf{F}_R \right) \Delta \mathbf{q}_k = \mathbf{J}^T \mathbf{g} - \lambda \mathbf{F}_R \mathbf{q}_k,$$

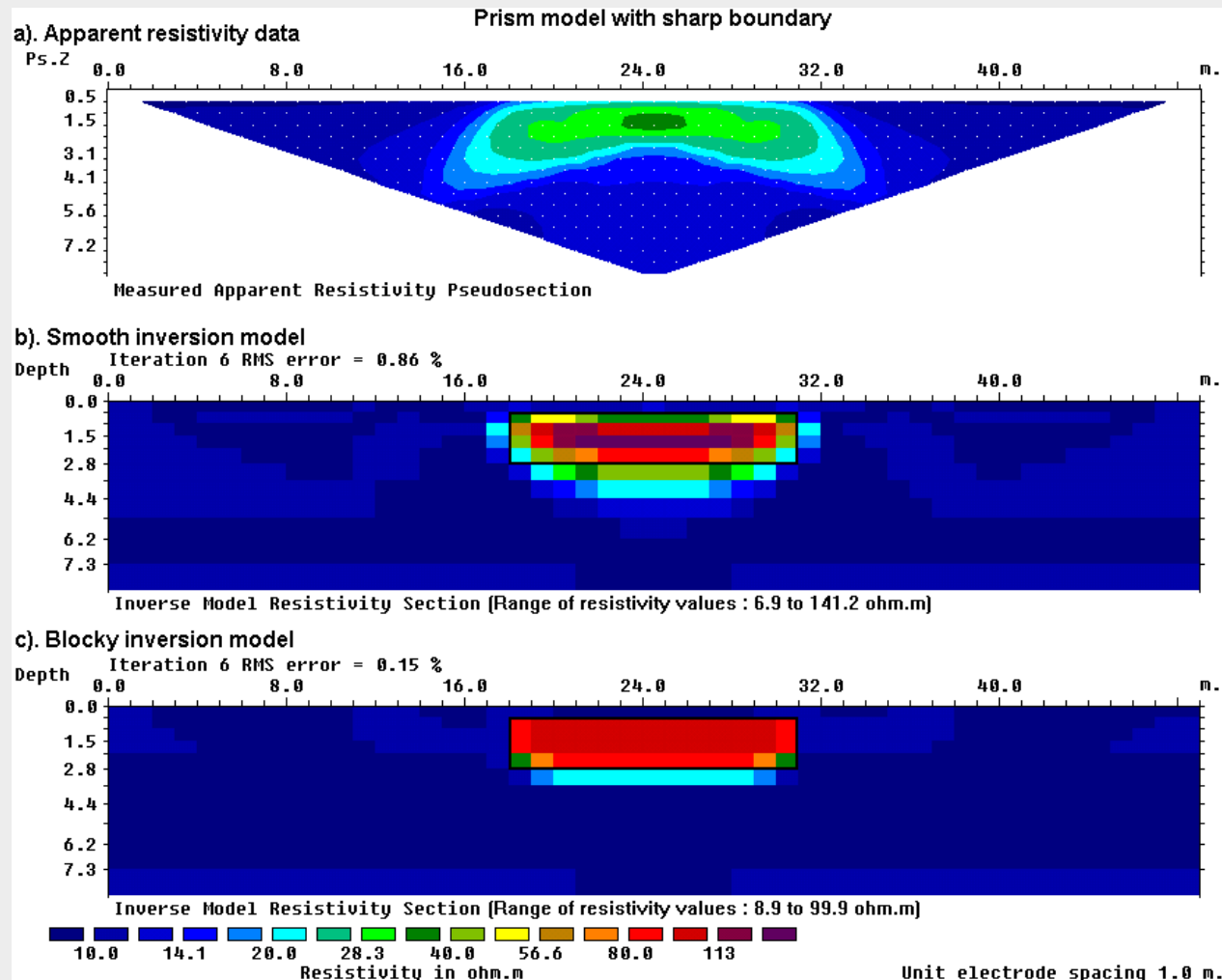
$$\mathbf{F}_R = \alpha_x \mathbf{C}_x^T \mathbf{R}_m \mathbf{C}_x + \alpha_y \mathbf{C}_y^T \mathbf{R}_m \mathbf{C}_y + \alpha_z \mathbf{C}_z^T \mathbf{R}_m \mathbf{C}_z$$

$\mathbf{R}_m$  is a weighting matrix used so that different elements of the model roughness matrix are given equal weights in the inversion process. It is a  $L_1$  norm (robust/blocky) method in that it attempts to minimize the absolute value of the model changes. It basically tries to minimize the sum of the absolute change  $\sum |q_{i+1} - q_i|$  in the resistivity from one layer to the next in a 1-D model.



# The blocky least-squares inversion method in 2-D

In the  $L_1$  norm 2-D model the high resistivity anomaly is concentrated in a smaller area within the actual boundaries of the block. There is a sharper transition to the low resistivity background.



# Example of $L_1$ and $L_2$ norms with a line fit problem

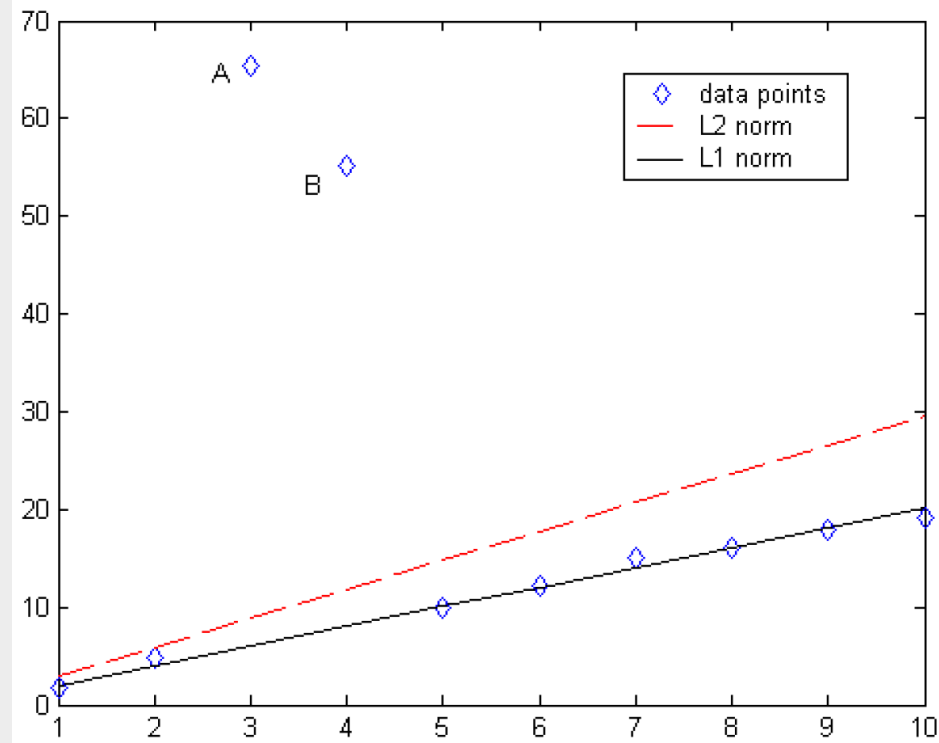
The example fits a straight line through 10 data points with  $(x,y)$  coordinates. The  $L_2$  norm method finds a line this minimizes the sum of the squares of the differences in the  $y$  values,

$$L_2 \text{ norm} : - \sum_{i=1}^m (y_i - f_i)^2$$

This is greatly affected by the 2 outlier data points **A** and **B**. The  $L_1$  norm method tries to minimize the sum of the absolute differences.

$$L_1 \text{ norm} : - \sum_{i=1}^m |y_i - f_i|$$

It is less affected by the 2 outlier data points. As an example, weight of distance of point **A** from the straight line is 60 units in  $L_1$  norm, but 3600 units in  $L_2$  norm.



# Other variations of the blocky least-squares method

There are other possible variations, usually made by adding different terms to the least-squares equation.

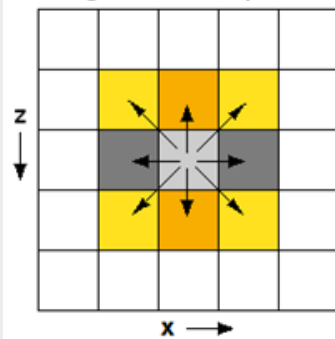
One common addition is to add a constraint so that the resulting model is “close” to some background model.

Another variation is to modify the roughness filters so that features in a desired direction are emphasized.

To avoid a bias in the vertical and horizontal directions, the filter can be modified to include diagonal components.

Another modification is to include a boundary that divides the model into separate regions.

Vertical roughness with diagonal x-z components

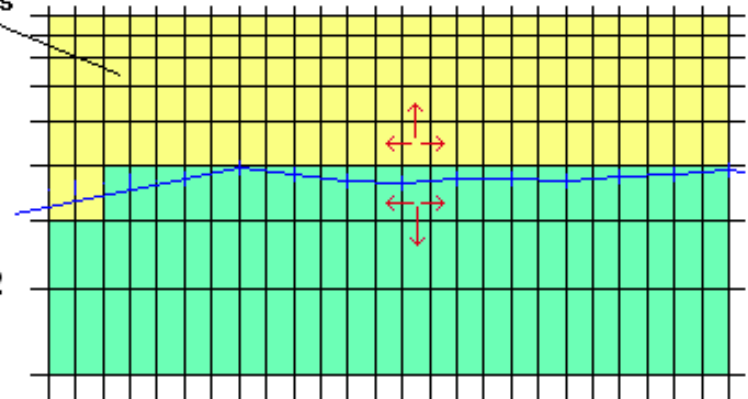


Model cells

Region 1

Region 2

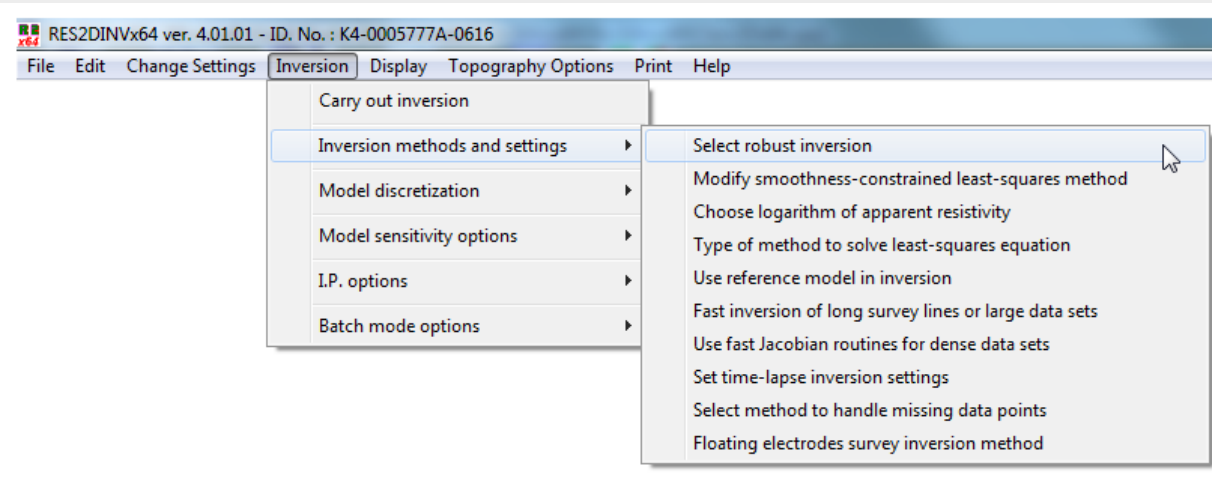
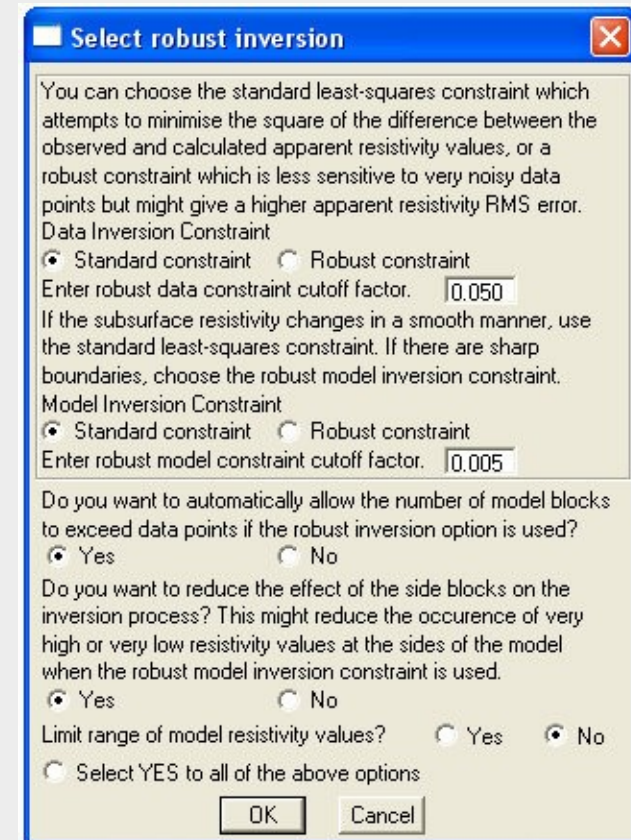
Boundary



# RES2DINV - Selecting inversion methods

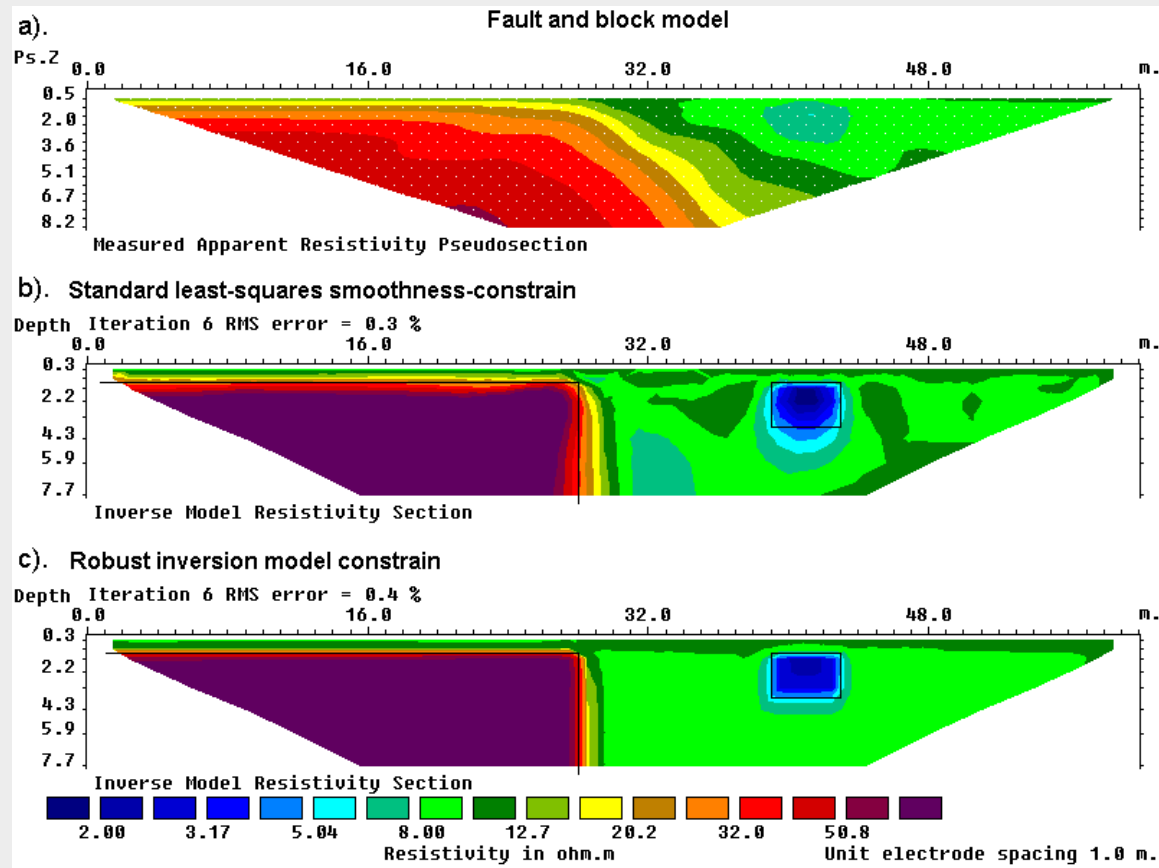
One commonly used option is the 'Robust' or 'Blocky' inversion method which should be used if the subsurface resistivity has sharp boundaries. Clicking the 'Select robust inversion' option will show the dialog box below. The 'Robust model constrain' will apply the blocky model inversion method. The 'Robust data constrain' should be used if the data is very noisy.

Standard =  $L_2$ , Robust =  $L_1$



# Example of robust or blocky model inversion

The figure below shows the inversion results for data from a synthetic model with sharp boundaries. In this case, the robust inversion method gives significantly better results since the true model consists of three regions with sharp boundaries between them. The model consists of a faulted block (100  $\Omega$ .m) and a small rectangular block (1  $\Omega$ .m) in a 10  $\Omega$ .m medium.



# Other inversion model settings

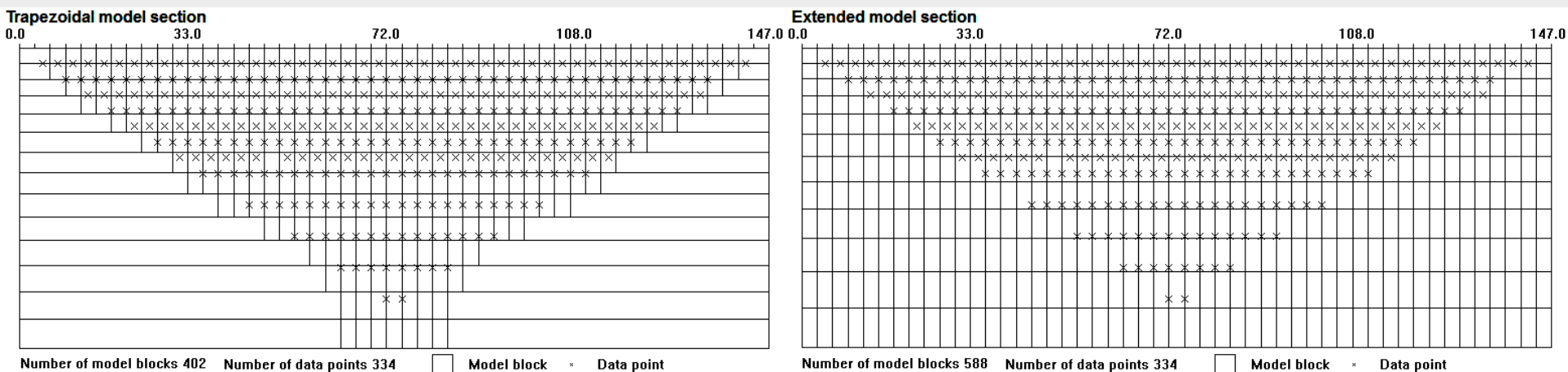
Settings that control the subdivision of the subsurface into model cells, and how they affect the inversion results.

- 1). Trapezoidal versus extended model sections
- 2). Model cell width
- 3). Topography modeling

# Trapezoidal and extended models

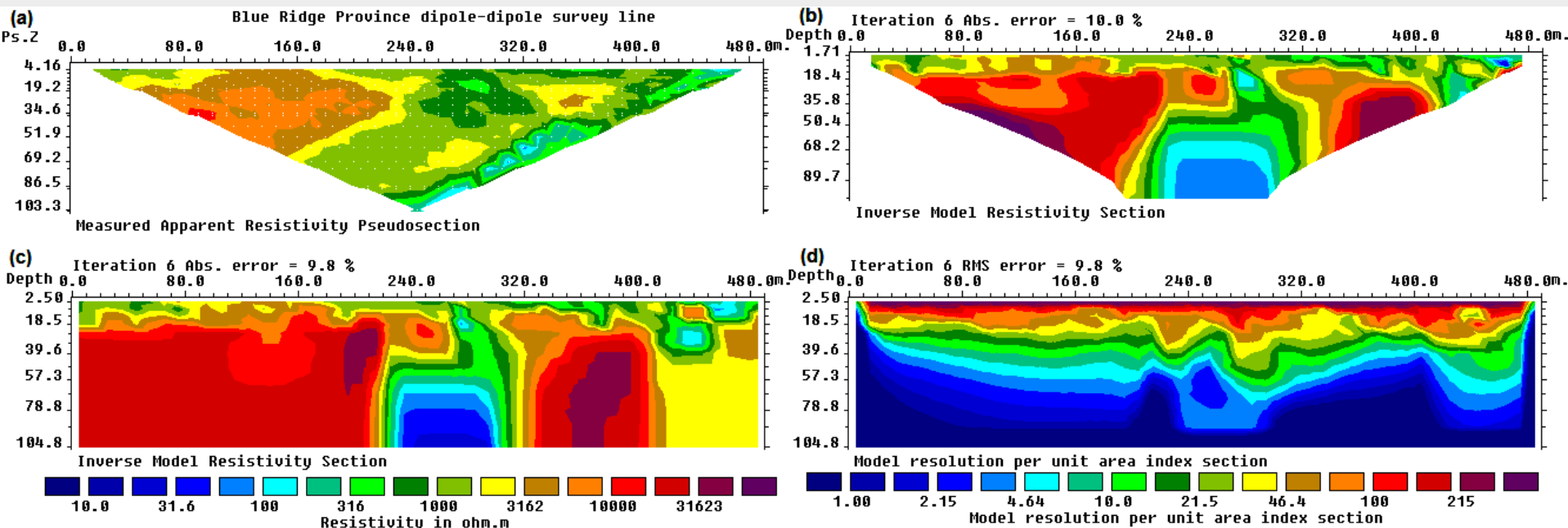
This controls the lateral extent of the model cells in the model. The two options are (i) use a distribution similar to the data points in the pseudosection, (ii) use an extended distribution that extends to the ends of the survey line.

The present preference is to use a uniform extended distribution, and use the model resolution section as a guide to highlight areas that are well constrained by the data. The pseudosection provides an approximate but crude guide to the lateral information in the data set, so using the trapezoidal shape might place too severe limits on the lateral extent of the model.



# Trapezoidal and extended models - example

The example below is from a dipole-dipole survey over a water-bearing fracture zone that occurs below the middle of the survey line. The trapezoidal model section (b) does not show the sides of the fracture zone clearly as they occur near the edges of the model section. They are more clearly shown in the extended model section (c). The model resolution section (d) shows there is significant information at depth below the 80 to 400 m. marks, while the pseudosection tapers to a point below 240 m.

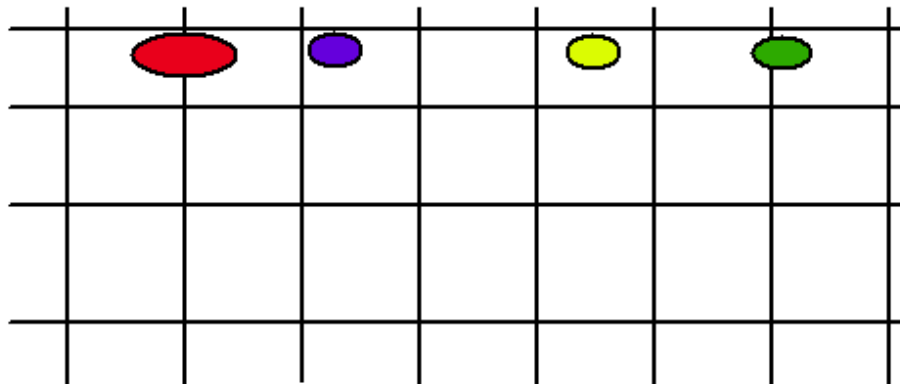


# MODEL DISCRETIZATION – Effect of model cell width

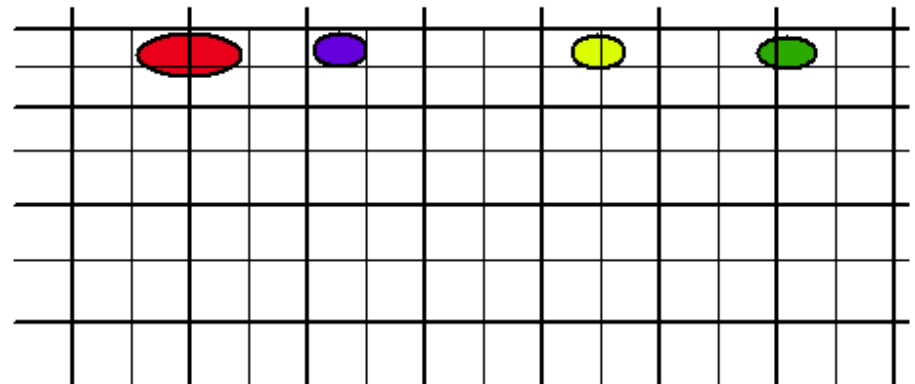
The default model uses model cells with the same width as the unit electrode spacing. In situations with large resistivity variations near the ground surface, better results can be obtained by using narrower model cells.

The model with cell width of one electrode spacing has a maximum misfit of one-half the electrode spacing for a near-surface inhomogeneity. The finer model with cell width of half the electrode spacing has a maximum misfit of one-quarter electrode spacing.

a). Default model with cell width of one unit electrode spacing



b). Finer model with cell width of one-half unit electrode spacing

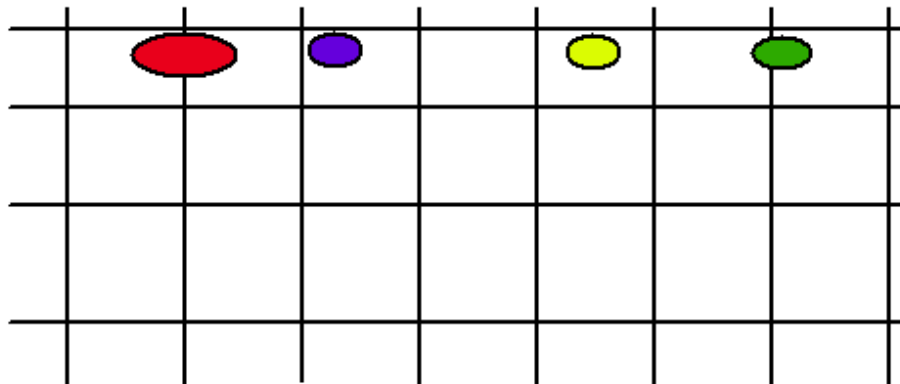


# MODEL DISCRETIZATION – Effect of model cell width

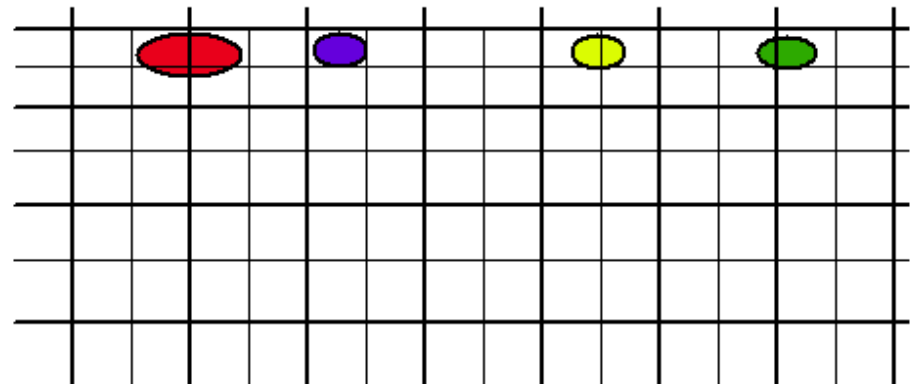
In theory, it is possible to reduce the cell width further, but the error due to the misfit becomes increasingly less significant. Reducing the cell width increases the number of model parameters, thus increasing the computer time and memory required.

We will look at the effect of using model cells with widths of one, one-half and one-quarter the electrode spacing to find the optimum model cell width.

a). Default model with cell width of one unit electrode spacing



b). Finer model with cell width of one-half unit electrode spacing

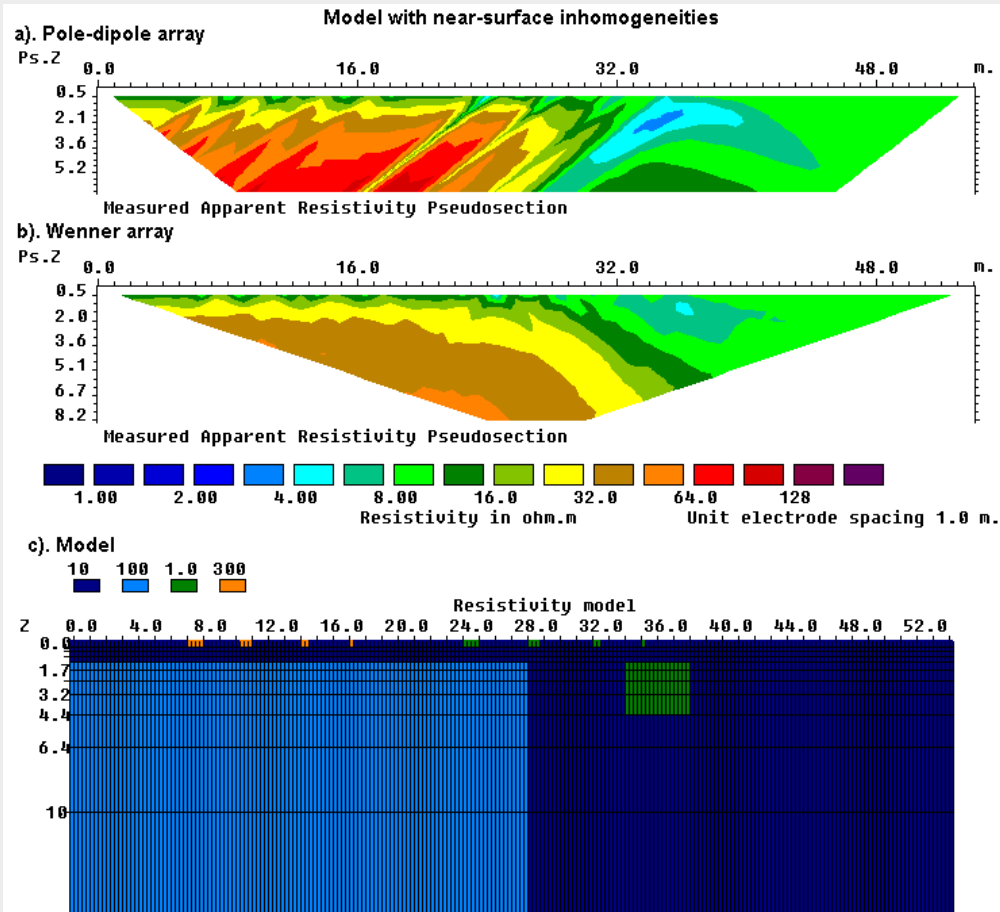


# MODEL DISCRETIZATION – Example test model

The model has a faulted block of  $100 \Omega.m$  and a rectangular prism of  $1 \text{ ohm.m}$  in a medium of  $10 \Omega.m$ . A series of small near-surface high resistivity blocks with widths of  $1.0$ ,  $0.75$ ,  $0.50$  and  $0.25 \text{ m}$ . and resistivity of  $300 \Omega.m$  are above the faulted block. A similar series of near-surface low resistivity blocks of  $1.0 \Omega.m$  are located on the right.

The pole-dipole array has the P1-P2 spacing (“ $\alpha$ ”) fixed at  $1.0\text{m}$ , but with “ $n$ ” factor ranging from  $1$  to  $16$ . Note the strong anomalies produced by the near-surface high resistivity blocks. The Wenner array is much less affected by the near-surface anomalies.

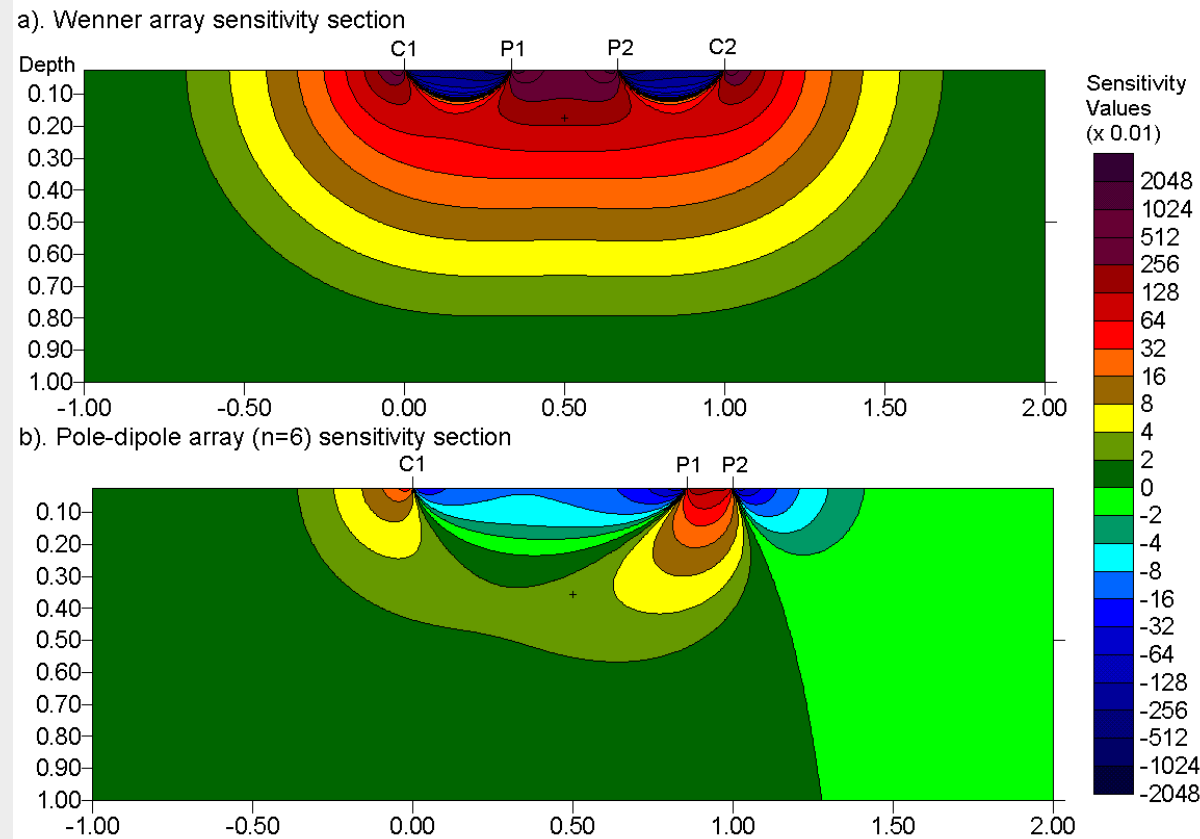
The reason lies in the sensitivity patterns of the two arrays.



# MODEL DISCRETIZATION – Sensitivity sections

The sensitivity sections for the Wenner and pole-dipole arrays with the same array length are shown below. The pole-dipole array has high sensitivity values concentrated below the P1-P2 electrodes. This makes it very sensitive to inhomogeneities below these electrodes. The Wenner array has relatively broad areas near the surface with high sensitivity values that are not as concentrated as the pole-dipole

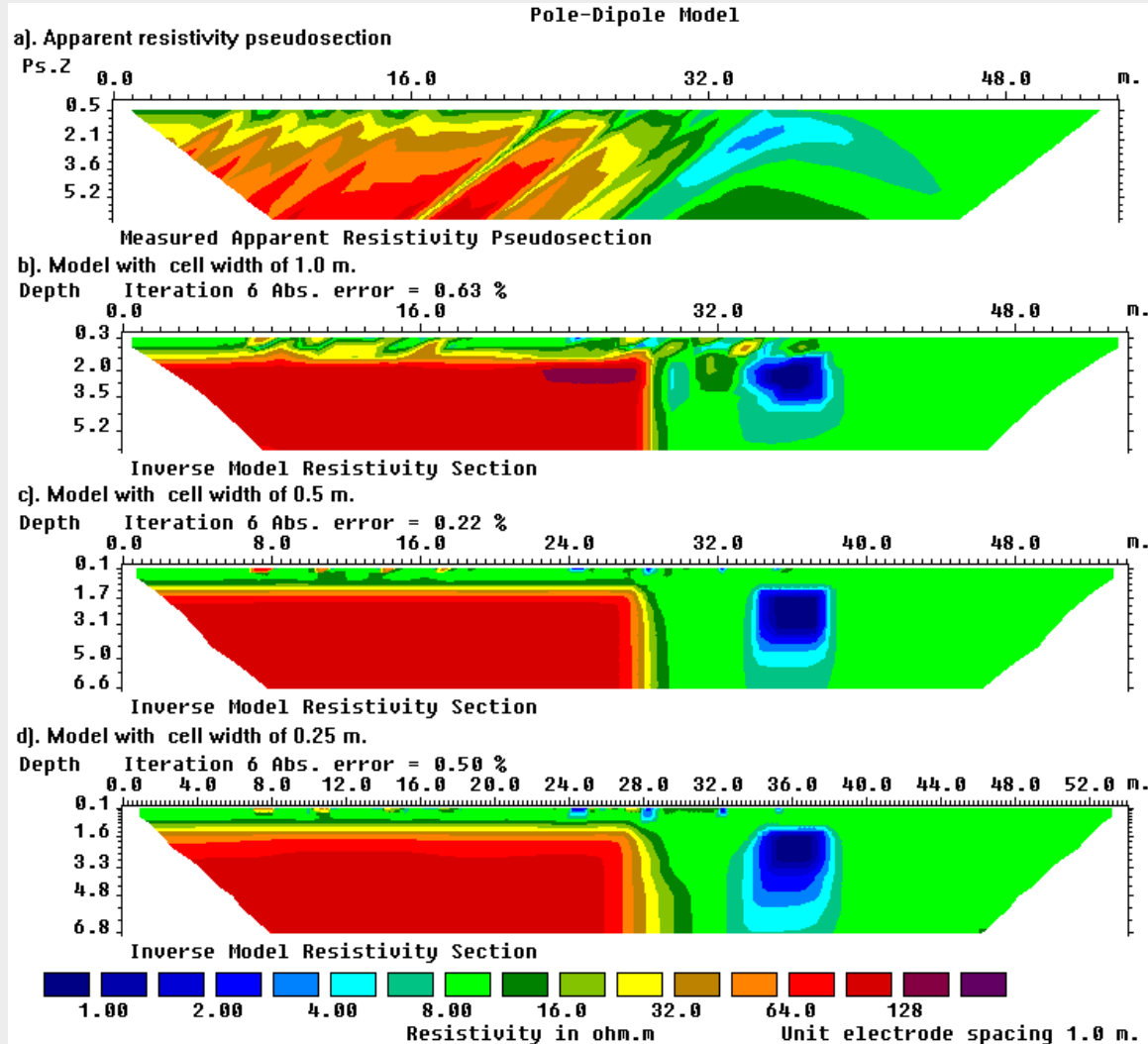
array. Thus it is less sensitive to small near-surface anomalies.



# Pole-dipole array model refinement

The model for the pole-dipole array with a cell width of 1.0 m. shows significant distortions near the top of the faulted block. Most of the distortions have been removed in the model with a 0.50 m. cell width.

The model with a 0.25 m. cell width does not show any major improvements over the 0.50 m. cell width model although it should more accurately model the near surface inhomogeneities of less than 0.50 m. width.

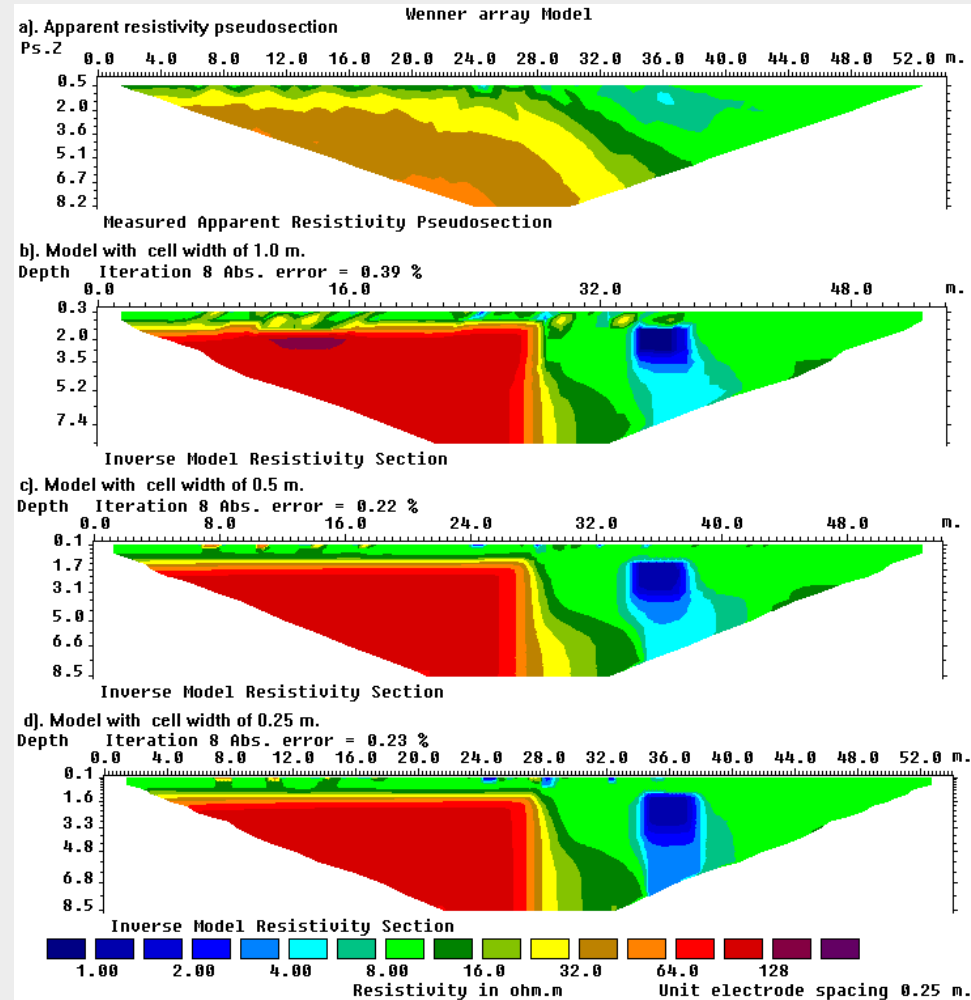


# Wenner array model refinement example

The model with a cell width of 1.0 m. shows significant distortions near the top of the faulted block. Note the near-surface high resistivity bodies near the 30 and 33 m. marks near the locations of the low resistivity near-surface inhomogeneities.

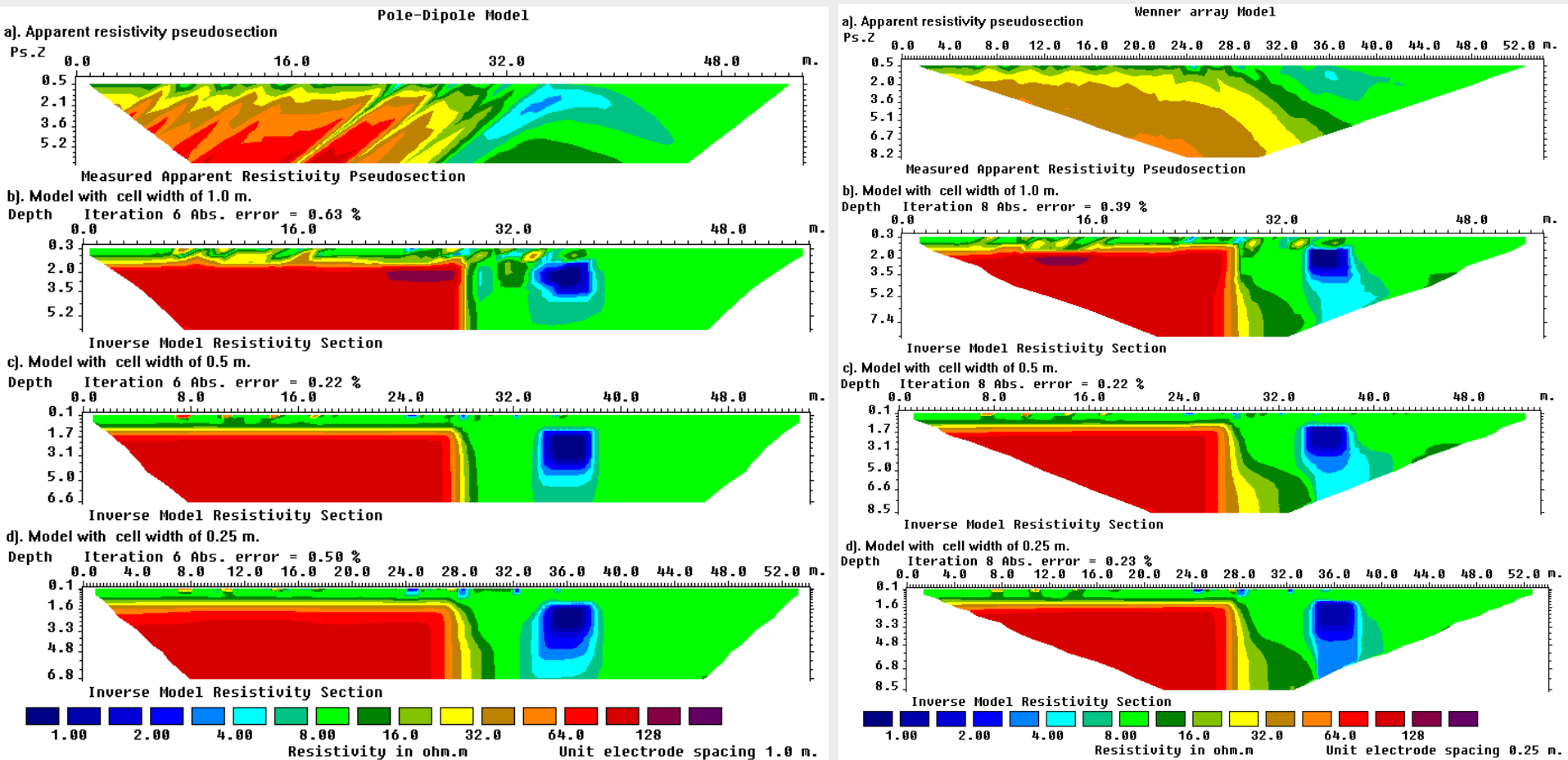
Almost all the distortions have been removed in the model with a 0.50 m. cell width.

The model with a 0.25 m. cell width does not show major improvements.



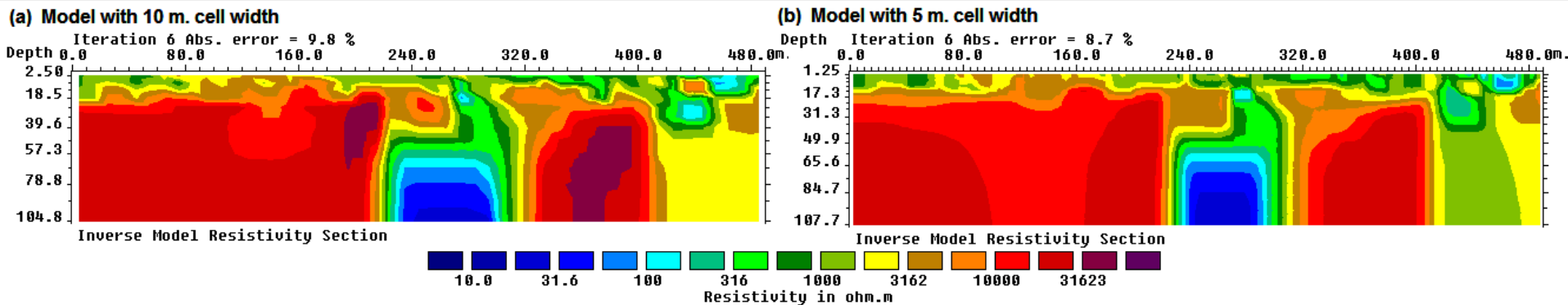
# Lateral resolution limit

The pole-dipole and Wenner array models show that reducing the cell width to less than half the unit electrode spacing do not significantly improve the results. The arrays are not sensitive to lateral variations of less than half the ' $a$ ' spacing. We can make use of this property to reduce the time to invert long survey data sets.



# Model refinement field data set example

The figure shows the models from the Blueridge survey using cell width of 10 m. (the survey electrode spacing) and 5 m. Note the 5 m. cell model has contours that are more regular and structures with the very high resistivity zones near the fracture zone are not present. They are probably caused by a discretization that is too coarse in the 10 m. model that cannot accurately model the large resistivity variations (with widths of less than 10 m) near the surface.



# MODEL DISCRETIZATION – General rules

In most cases, using a cell width of half the unit electrode spacing seems to give the optimum results.

Using a cell width of one-third the unit spacing seems to be beneficial only in certain cases with the pole-dipole and dipole-dipole arrays with very large ' $n$ ' values.

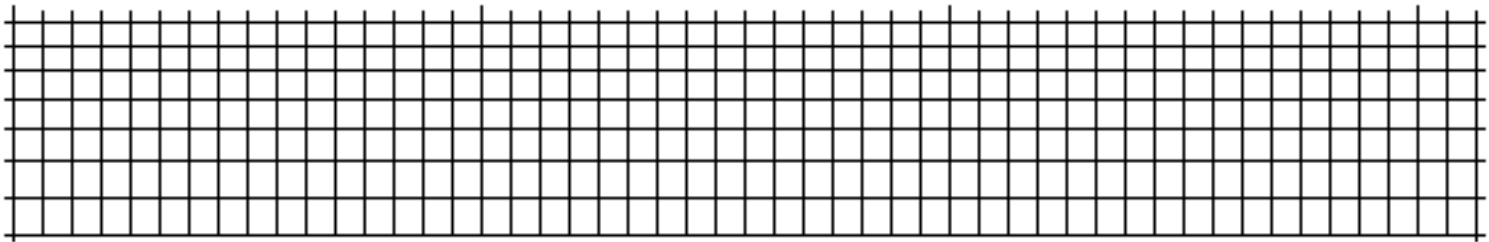
A cell width of one-quarter the unit spacing sometimes leads to instability with oscillating model values.

Using finer cells will lead to longer inversion times, so using a width of the half the unit spacing seems to provide the best trade-off. The resistivity method is unlikely to resolve structures less than one-third the ' $a$ ' spacing of the array used.

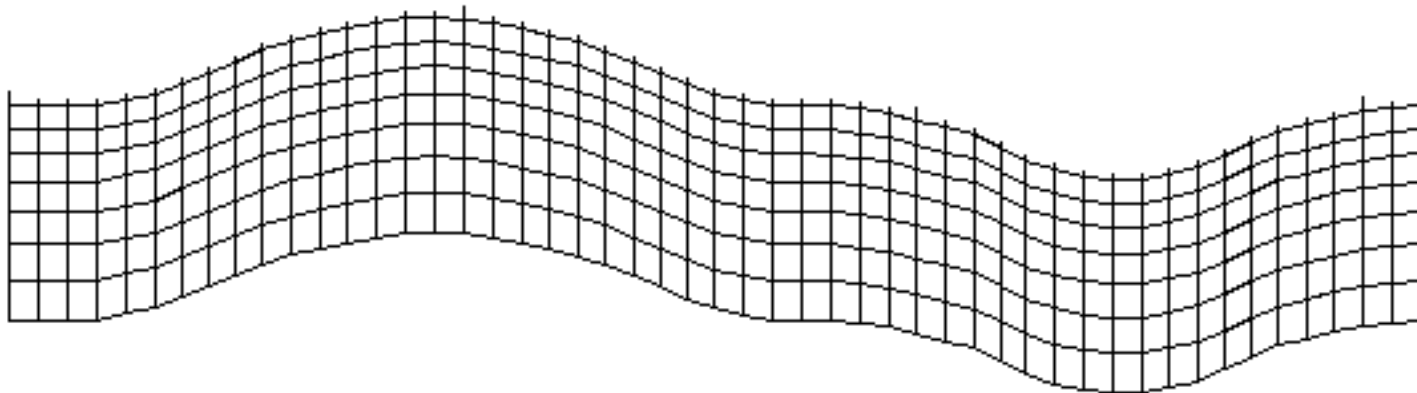
# Methods to handle topography

The RES2DINV program has 3 different methods to incorporate the topography into the inversion model. The surface nodes of the mesh are shifted up or down so that they match the actual topography. The topography becomes part of the mesh and is automatically included into the inversion model. The difference between these 3 methods is the way the subsurface nodes are shifted.

a ). Arrangement of model blocks without topography



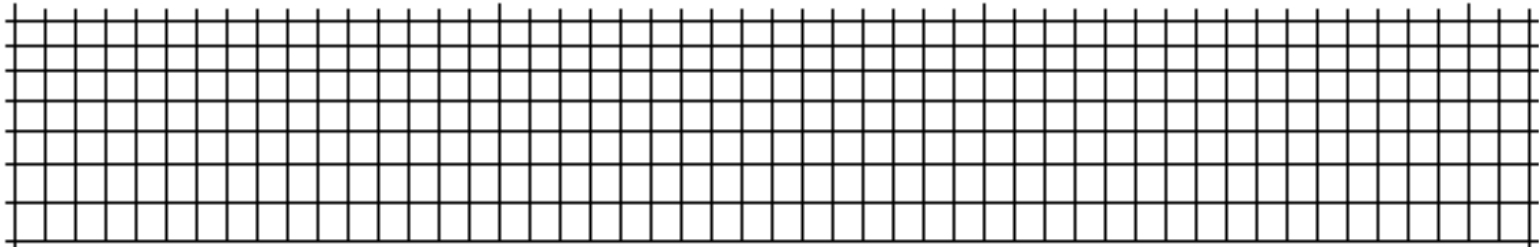
b ). Arrangement of model blocks with a uniformly distorted grid



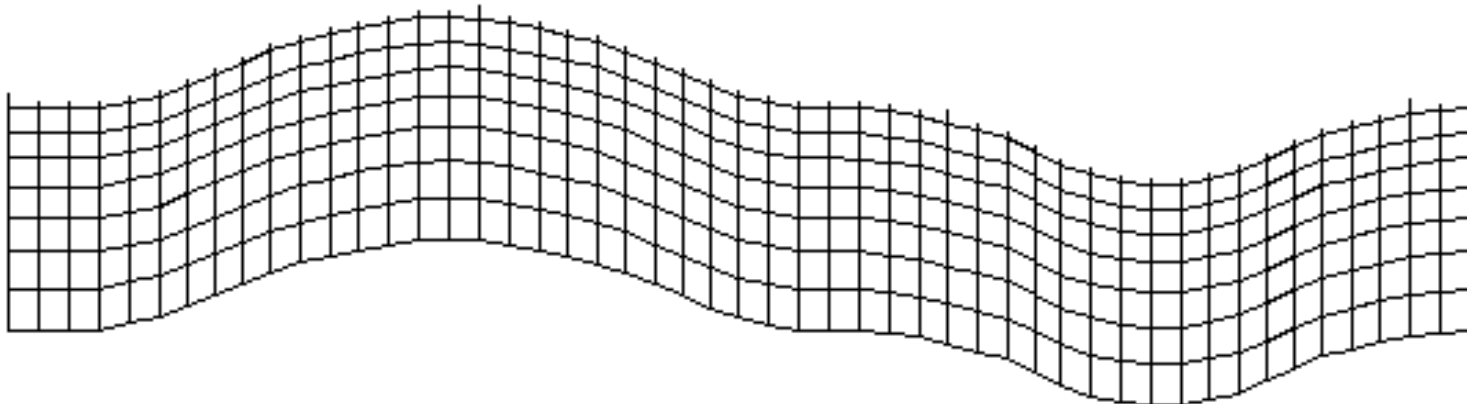
# Methods to handle topography – uniform grid

The simplest method is to shift all the subsurface nodes by the same amount as the surface node along the same vertical mesh line. This is probably acceptable for cases with a small to moderate topographic variations. The disadvantage is that every bend in the surface topography is reproduced in all the layers.

a ). Arrangement of model blocks without topography



b ). Arrangement of model blocks with a uniformly distorted grid

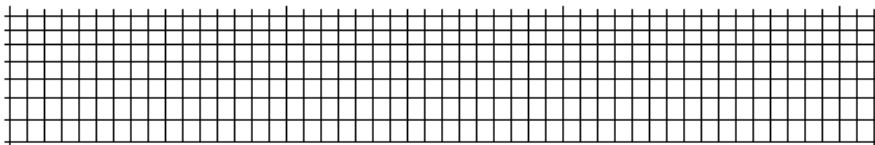


# Methods to handle topography – damped grid

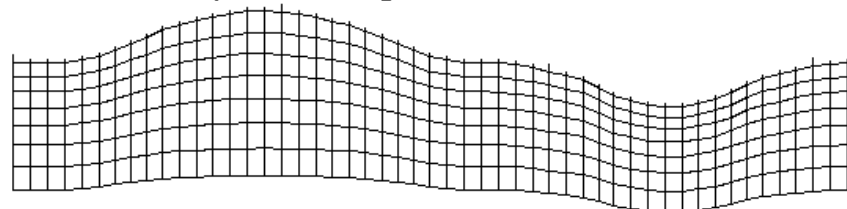
In the second method, the amount the subsurface nodes are shifted is reduced exponentially with depth. This is because the effect of the topography decreases with depth. One disadvantage of this method is that it sometimes produces a model that is too thick where the topography curves upwards, and too thin where it curves downwards.

The inverse Schwartz-Christoffel transformation method is used to calculate the amount to shift the subsurface nodes. This method takes into account the curvature of the surface topography and usually produces a more “natural” looking model section.

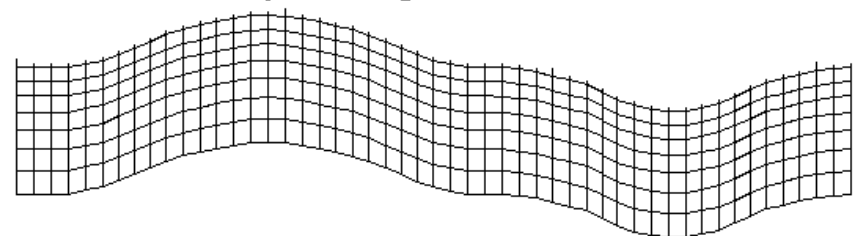
Arrangement of model blocks without topography



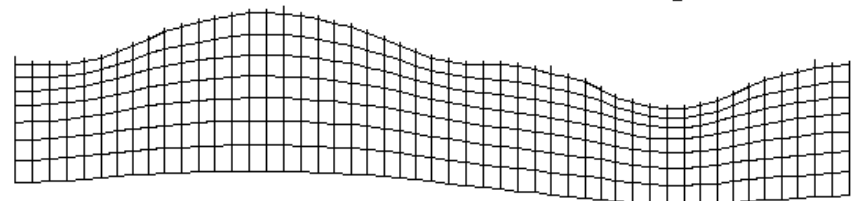
Method 2 - A damped distorted grid



Method 1 - A uniformly distorted grid



Method 3 - Inverse Schwartz-Christoffel transformation grid





# The 2-D ERT method : general conclusions

In most areas, the traditional 1-D sounding survey is probably not sufficiently accurate due to lateral changes in the ground resistivity.

The multi-electrode resistivity meter systems, fast microcomputers and software has made the use of 2-D resistivity imaging surveys possible. It has become a 'standard' geophysical exploration tool for engineering, environmental, hydrological and mineral surveys. The Wenner, Wenner-Schlumberger, pole-pole, dipole-dipole and pole-dipole arrays are the most common arrays used.

It gives sufficiently accurate results in areas of moderately complex geology where the 2-D assumption is reasonably accurate.

Choice of a proper electrode array, survey strategy, data processing and inversion method can significantly affect the results.

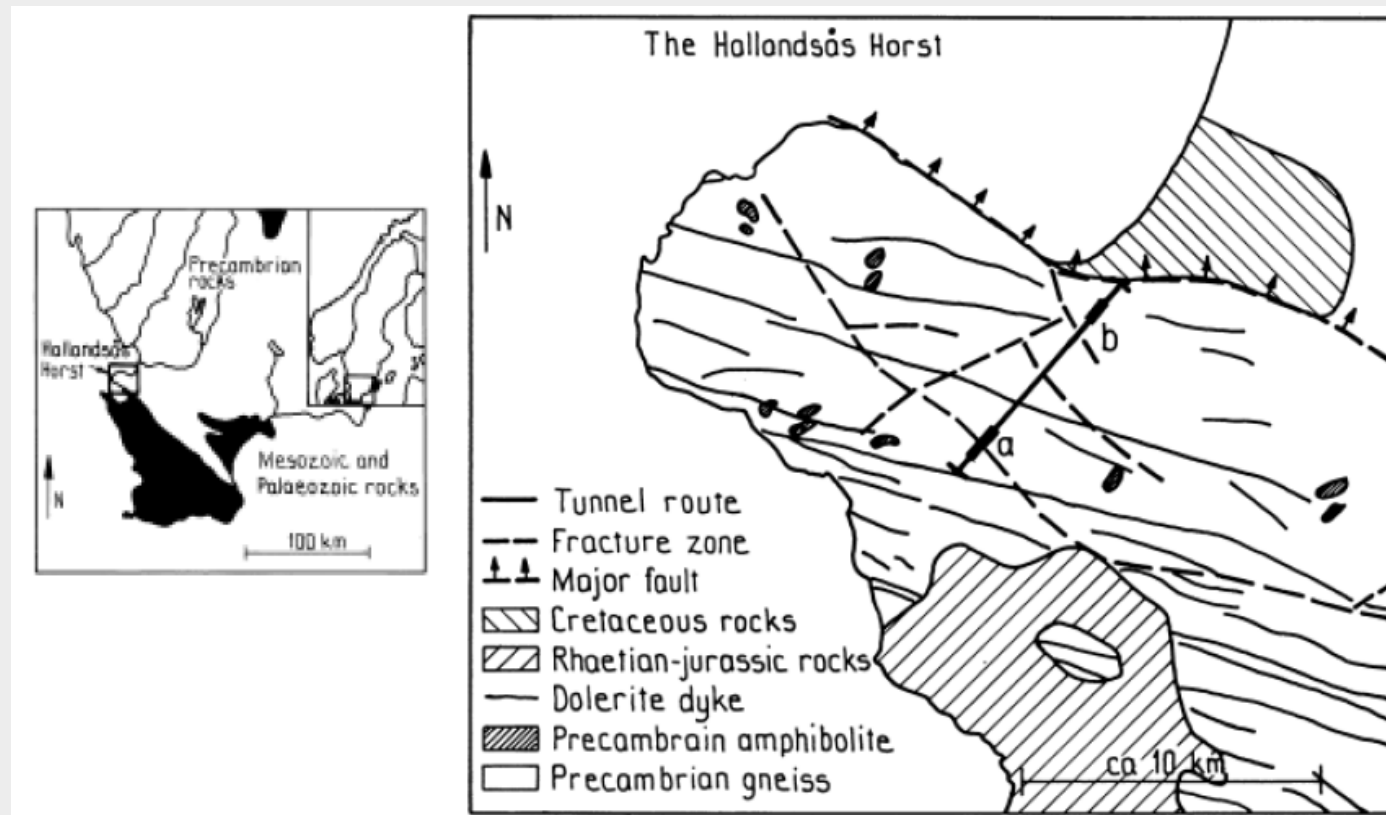
It is limited by the rapid decrease of resolution with depth, and in areas with significant 3-D variations near the survey line.

# 2-D case histories

Examples of 2-D surveys and results.

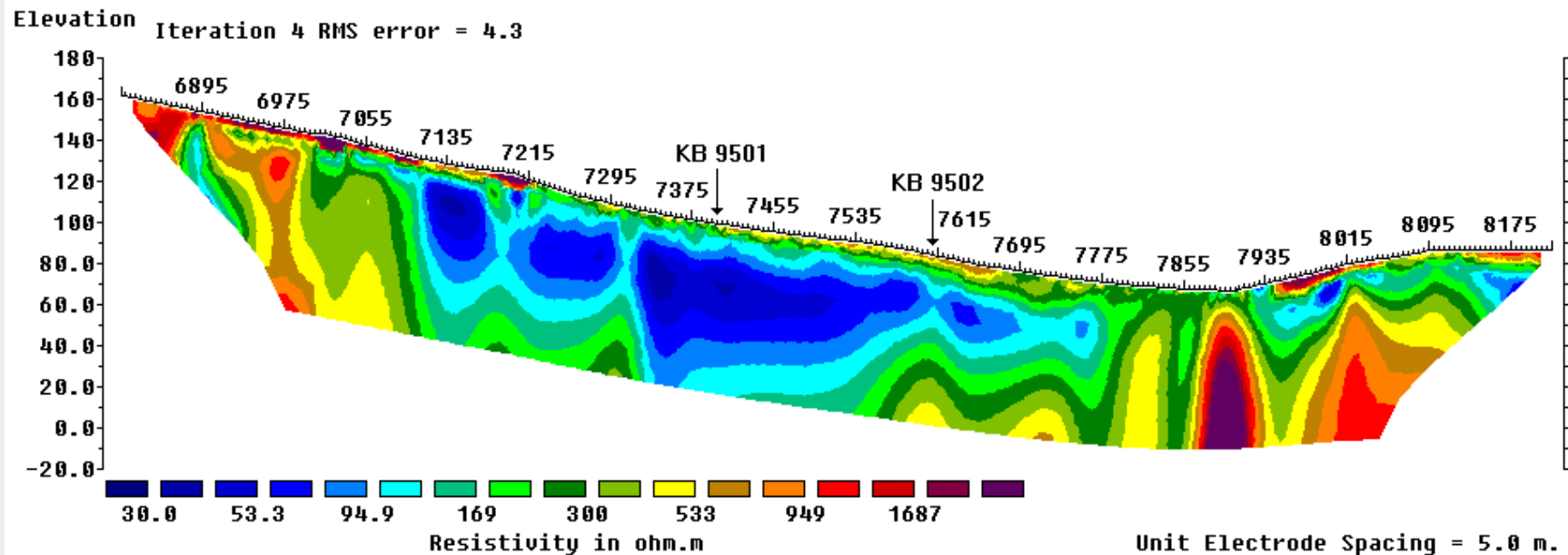
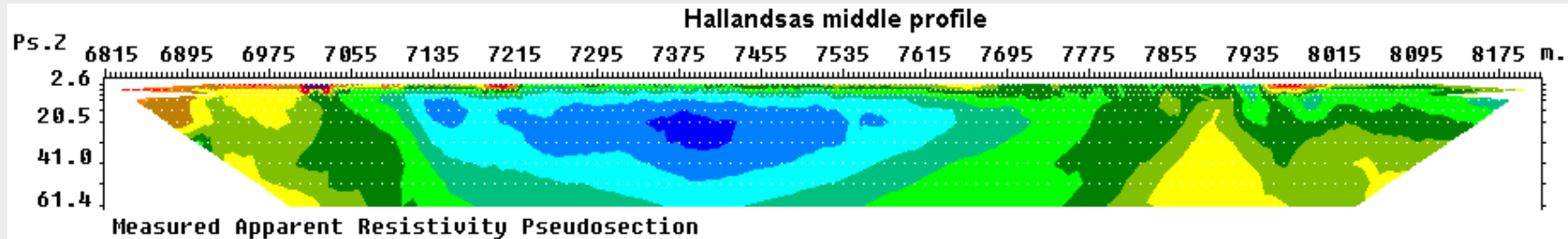
# Example 1 : Train tunnel project

This survey was carried out in south-west Sweden along a proposed railway tunnel route. The Hallandsås Horst is one of several uplifted blocks of the Earth's upper crust that are found in Skåne, the southernmost province of Sweden. The horst, composed of Precambrian rocks, is flanked by younger sedimentary rocks and some 8-10 km wide, 30-40 km long and trends NW-SE.



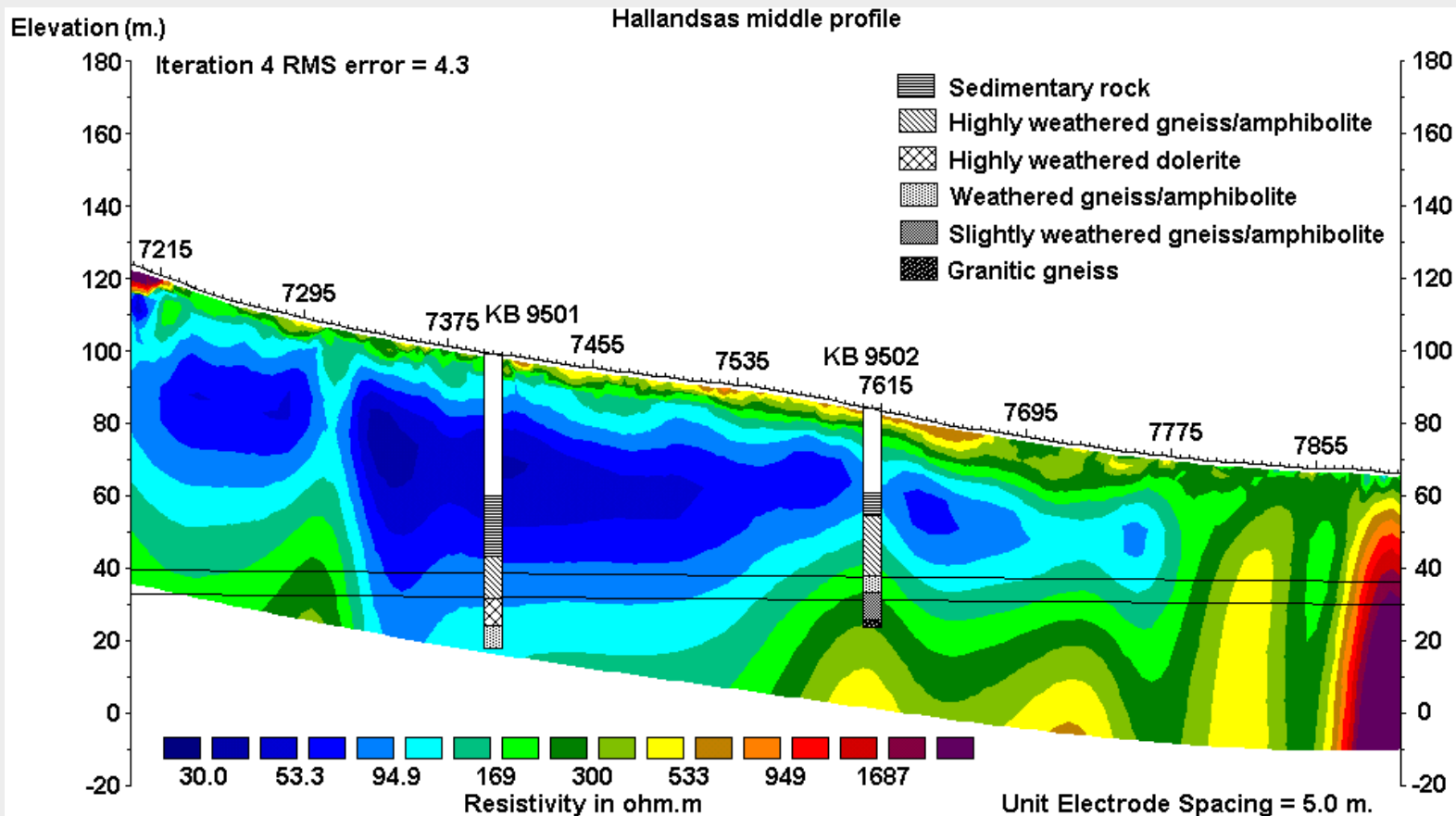
# Train tunnel project

The highly weathered sedimentary rocks poses greater problems to the tunnel construction compared to the higher resistivity metamorphic and igneous rocks. A large region with sedimentary rocks (blue region with resistivity values of less than 100  $\Omega.m$ ) was detected between the 7100 and 7800 m marks. The Wenner array was used in this survey.



# Train tunnel project

The figure below shows part of the inversion model obtained together with the lithology log from the two boreholes. There is a good correlation between the location of the low resistivity region and the weathered sedimentary and igneous/metamorphic rocks. The proposed tunnel route is shown by the pair of lines between elevation levels of about 20 to 40 m.



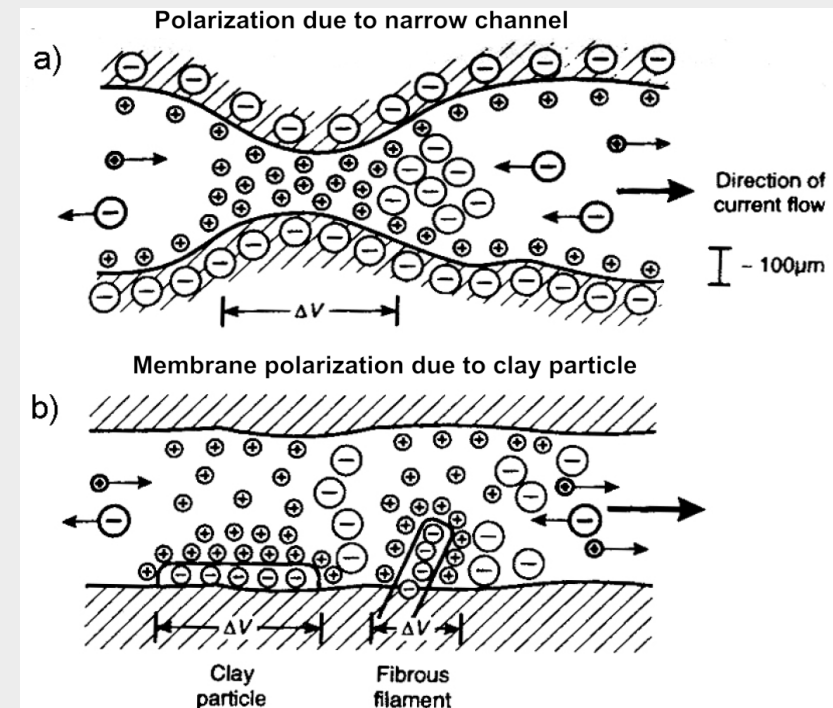
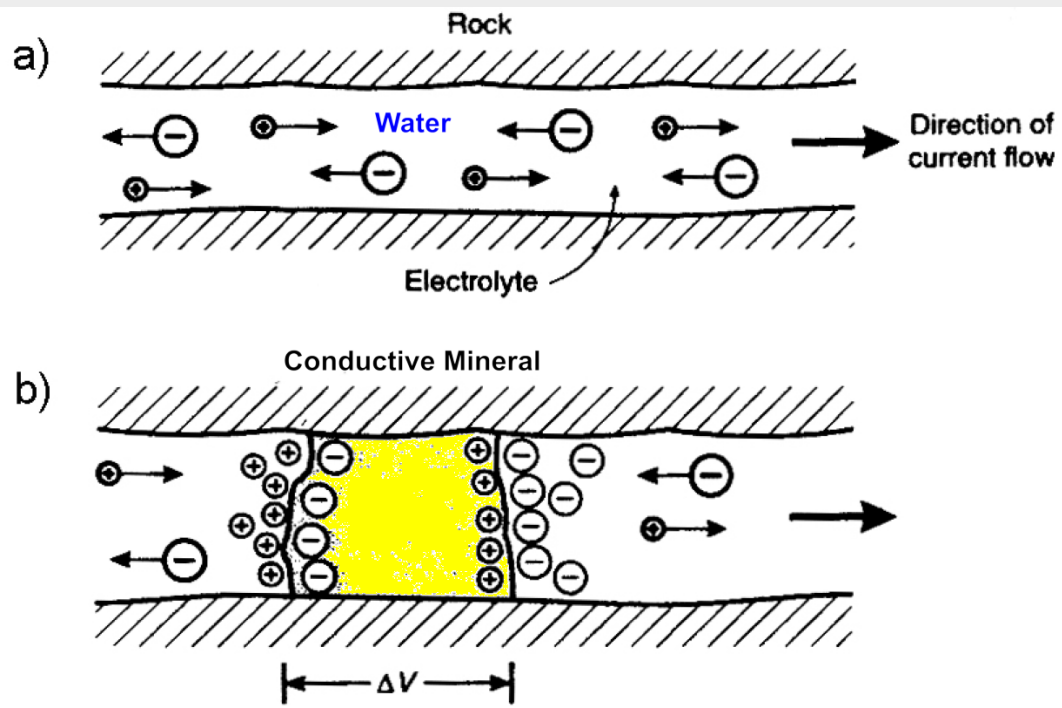
**Break for questions,  
discussion and consultation**

# I.P. surveys

**A brief look at the I.P. effect and its applications**

# The Induced Polarization (I.P.) effect

I.P. measurements are sometimes made simultaneously with resistivity surveys, particularly in mineral exploration. It has been used in environmental/engineering surveys for mapping clay bodies. The I.P. effect is caused by two main mechanisms, the membrane polarization and the electrode polarization effects. The membrane polarization effect is largely caused by clay minerals present in the rock or sediment. The electrode polarization effect is caused by conductive minerals in rocks.



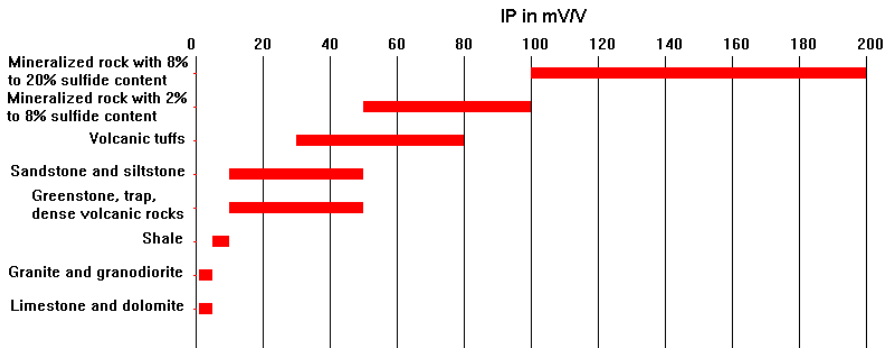
# I.P. properties of rocks and minerals

The I.P. method uses different parameters in the time and frequency domains used to represent the I.P. effect. One commonly used parameter is the time domain chargeability effect which is given in mV/V or milliseconds.

The figure below shows the I.P. values for some minerals and rocks. Note the I.P. effect for conductive minerals (sulfides) is much greater than that due to clay in sedimentary rocks and sediments.

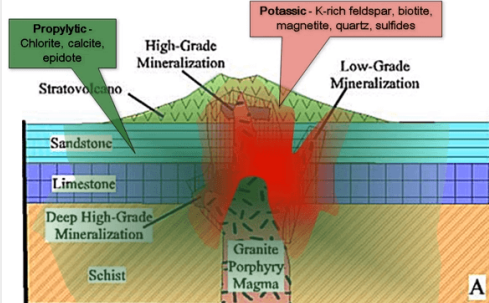
It is very useful for detecting disseminated minerals that is difficult to detect using resistivity alone. The magnitude of the I.P. anomaly depends on the surface area of the mineral rather than the volume.

## Disseminated Cu ore



## Porphyry deposit

Alteration provides clues to hidden ore bodies



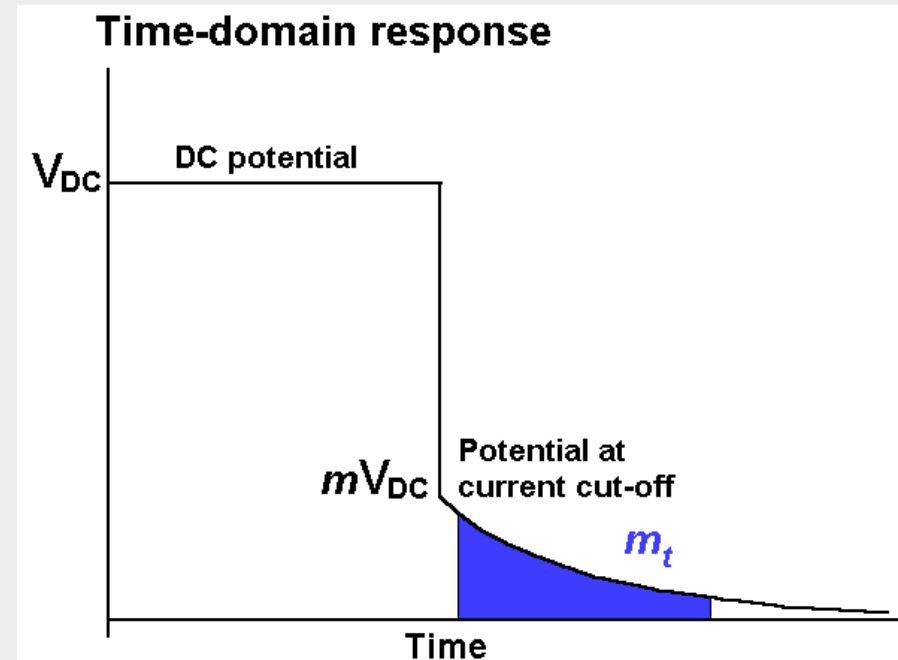
# I.P. time domain measurements

In the time-domain method, the residual voltage after the current cut-off is measured. Some instruments measure the amplitude of the residual voltage at several time intervals after the current cut-off.

A common method is to integrate the voltage electronically for a standard time interval. In the Newmont standard, the chargeability,  $m_t$ , is defined as

$$m_t = 1870 \frac{\int_{0.15}^{1.1} V_s dt}{V_{DC}}$$

The decay curve and the measurement of the I.P. value is shown in this figure. Normally the measured I.P. value is given in milliseconds (msecs).

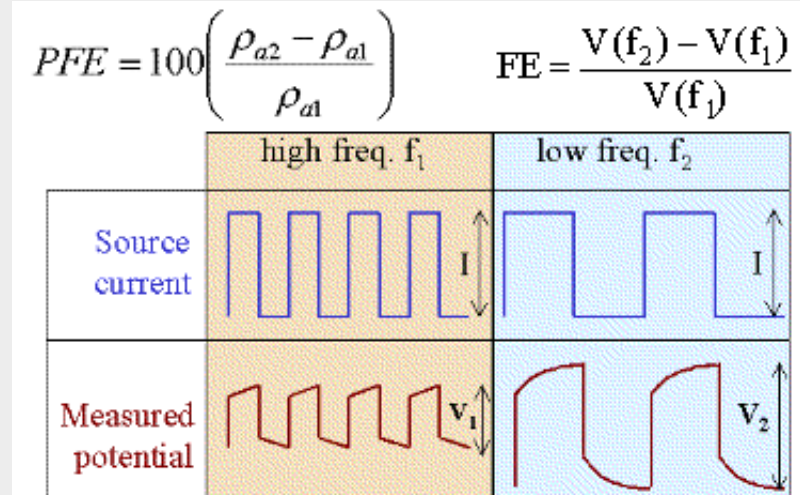
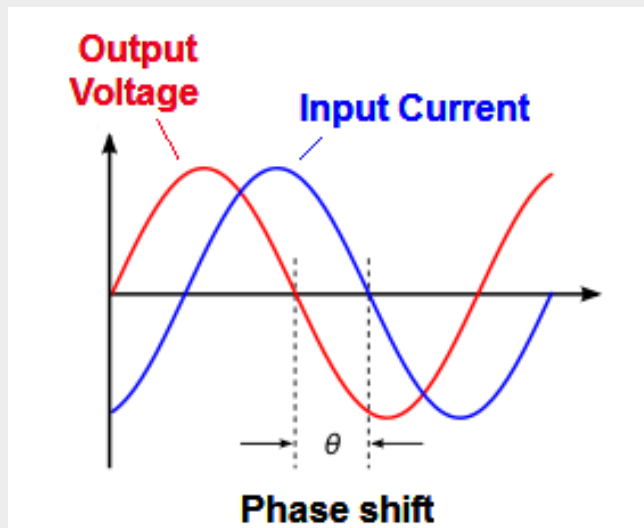


# I.P. frequency domain measurements

Frequency domain I.P. measurements use an alternating current source. In one method, the phase shift between the transmitted current and the measured voltage is used. The measured I.P. is given in terms of milli-radians (mrad).

Another technique compares the amplitudes of the voltage for two different AC frequencies, such as 1 Hz and 10 Hz. The I.P. value given as Percent Frequency Effect (PFE).

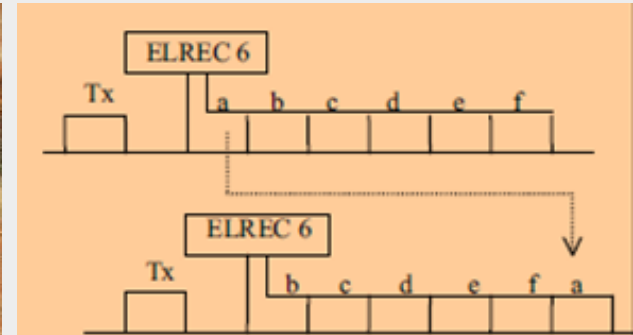
As a general rule, a chargeability value of  $M = 100 \text{ mV/V}$  is approximately equal to  $10PFE$ , or  $70\text{mrad}$ , or  $70\text{msec}$ .



# I.P. instrumentation

Many multi-electrode systems now offer an I.P. measurement option. The maximum current from battery-based systems is usually 1 Amp or less. This is usually too low to give reliable I.P. data when the electrode spacing is more than a few meters. However there has been recent improvements in the electronic circuitry and use of separate current and potential cables that have improved the quality of the I.P. data.

For large spacings of 10 m or more used in mineral exploration surveys, a more powerful current transmitter powered by a petrol based power generator and a series of separate I.P. receivers is normally used.



# I.P. survey with multi-electrode system

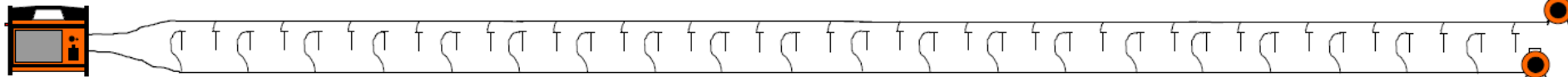
One method to improve the quality of I.P. data from conventional multi-electrode systems that has two separate cables is by using different cables for the current and potential electrodes. This reduces the EM coupling between the current and potential cables.

The possible current and potential electrodes positions are reduced and special control files are needed for this configuration. However, this method can be used with any multi-electrode system that uses a two cable arrangement.

Note the two cables are placed as far as possible from each other in the field survey.



Actual field layout during survey

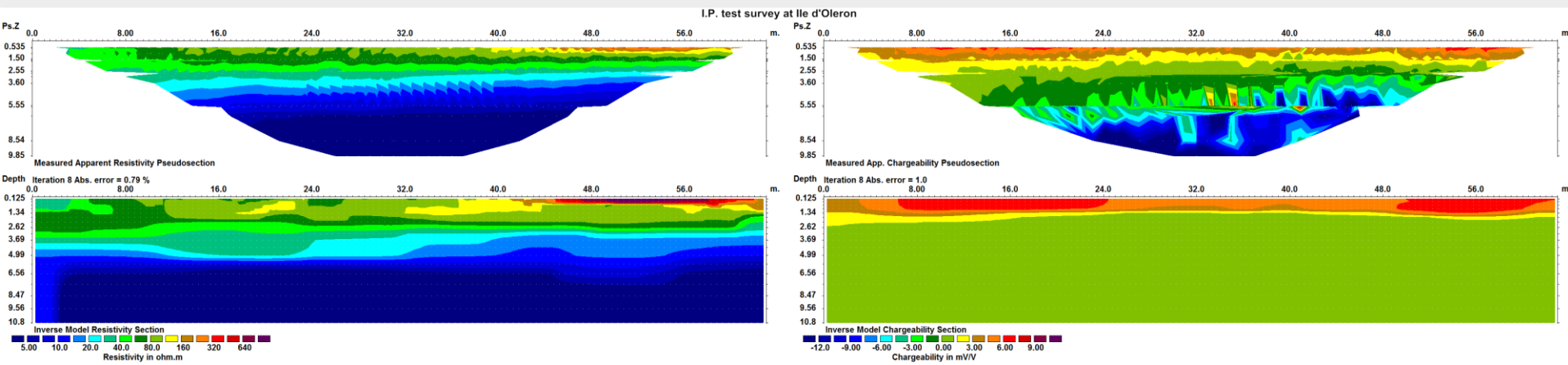


Sketch of cables setup with the Abem Terrameter LS system.

# Example of I.P. survey

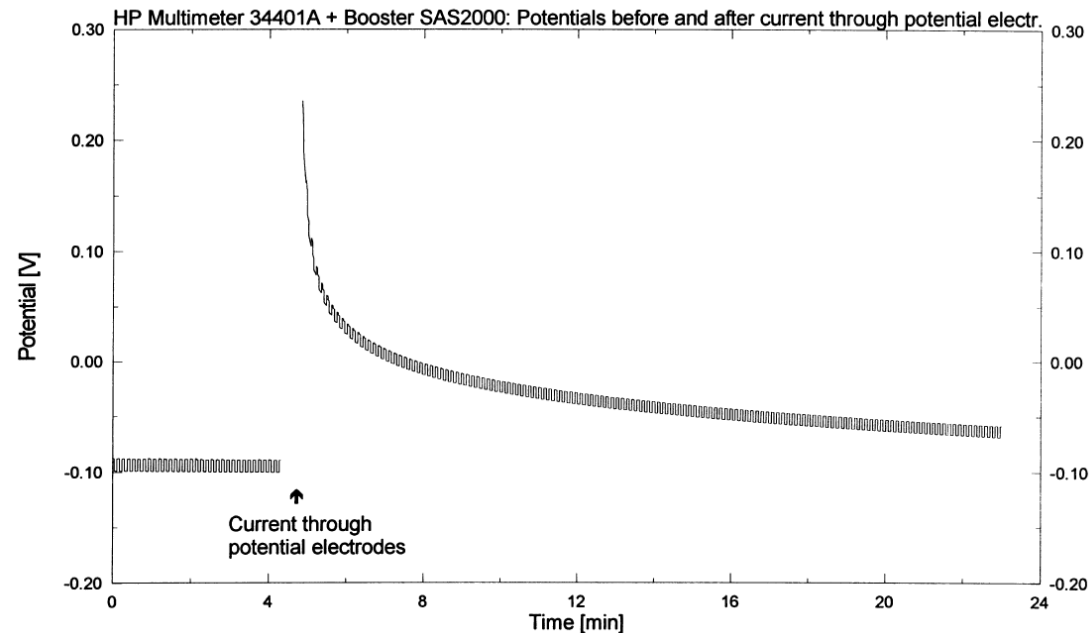
The results from a multi gradient array survey are shown below. The resistivity section shows an upper 3 to 4 meters sandy layer underlain by lower resistivity saline mud sediments. The I.P. section shows a top 1 to 2 meters layer with chargeability values of 4 to 8 mV/V which is probably sandy sediments with some organic content. The low I.P. values below this layer is probably due to high salinity that tends to reduce the I.P. effect.

Note the apparent resistivity pseudosection shows fairly regular contour patterns, whereas the bottom part of the I.P. pseudosection has noisier data due to larger electrode spacings and weaker signals.



# I.P. survey and the electrode polarization problem

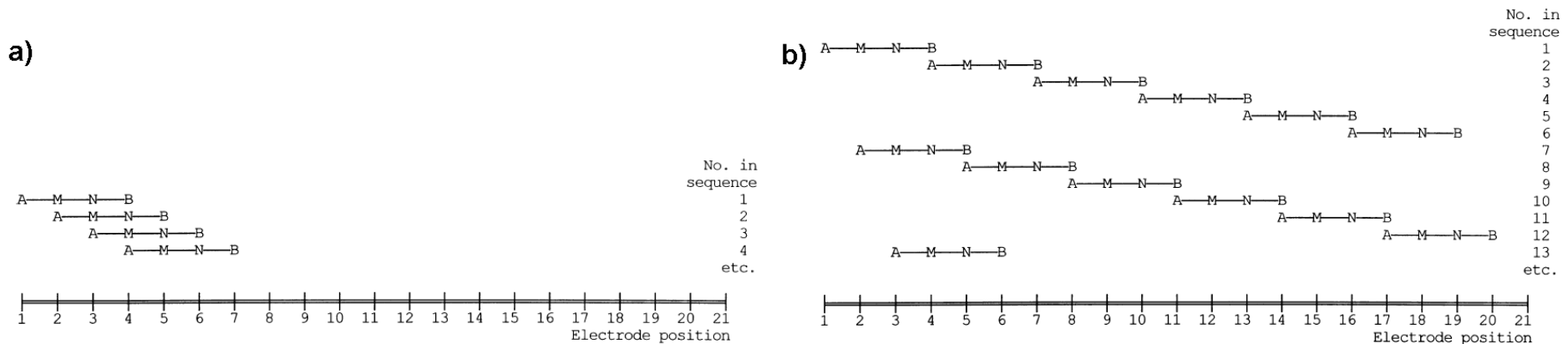
Due to the I.P. effect, some charge is stored in the ground near the current electrodes after switching off the current. This can cause a problem if the same electrode is used as a potential electrode shortly afterwards. Figure below shows the potential at an electrode after current cutoff where a current of 20 mA was used. The initial residual voltage is about 0.3 V. and takes more than 20 minutes to decay. The measurement sequence should be arranged so that the same electrode is not used as a potential electrode within that time.



# Avoiding the electrode polarization problem

In the first Wenner measurement sequence (A,B=curent, M,N=potential), the N potential electrode for the second reading is at the same location at as the B current electrode in the first measurement. This will cause severe noise due to the residual voltage at that electrode.

The second measurement sequence rearranges the readings so only after 5 readings a current electrode is used as a potential electrode, to provide sufficient time for the residual voltage to decay.



# Pitfalls in 2-D resistivity surveys and inversion

2-D resistivity surveys have made the mapping of many complex structures possible. However, we must be careful in interpreting the results from the data.

A list of some of the common problems are listed in the Tutorial Notes. Here we will look a few of them.

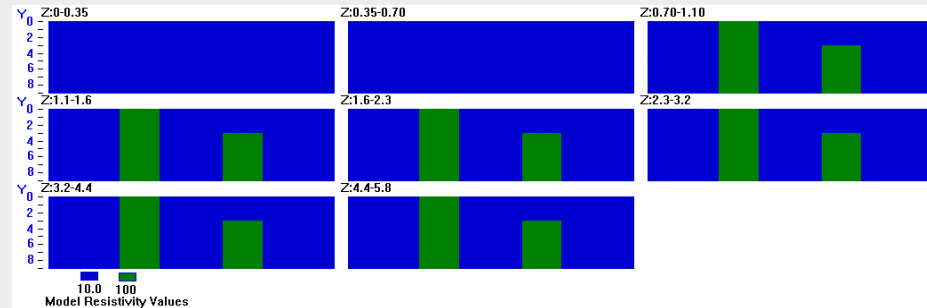
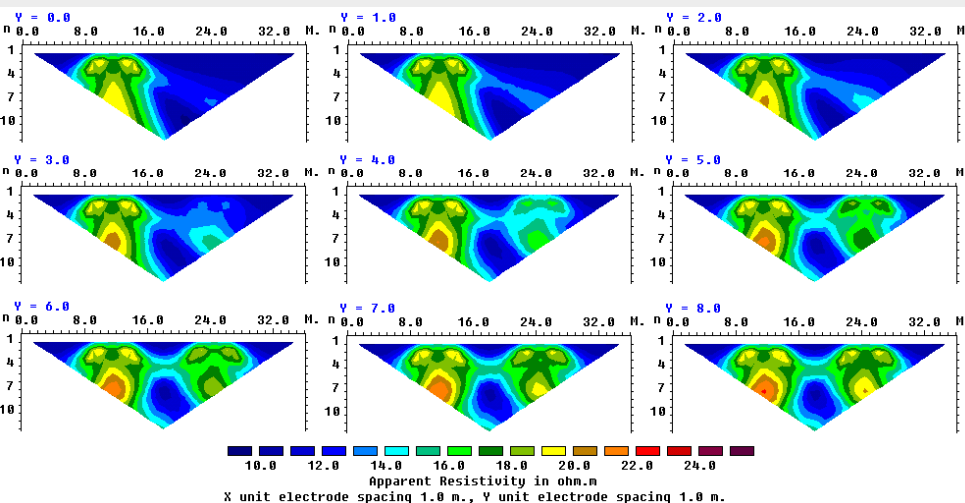
a) 3-D geology

b) Using large 'n' values with the pole-dipole and dipole-dipole arrays

c) Masking effect of a near surface anomaly

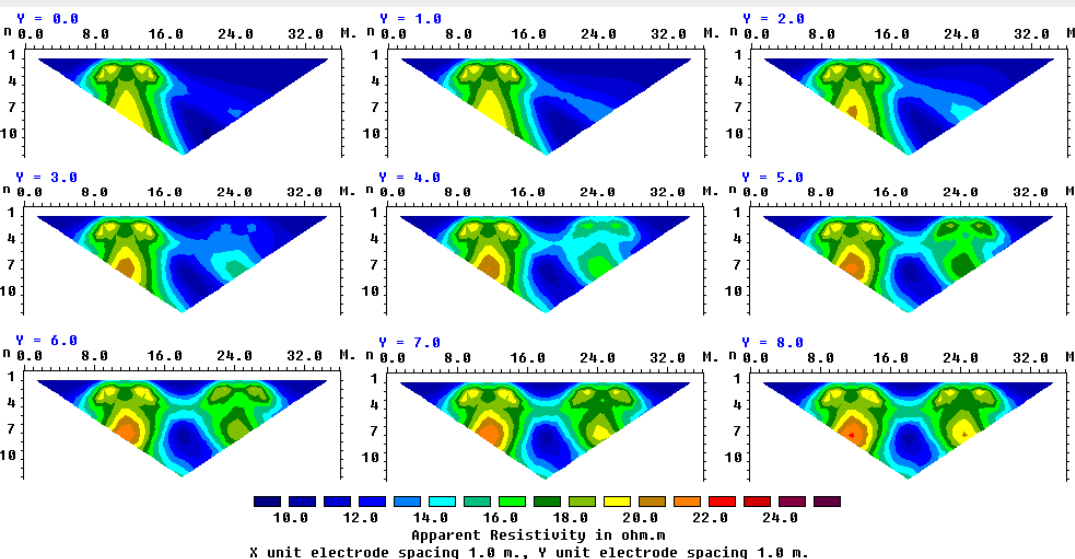
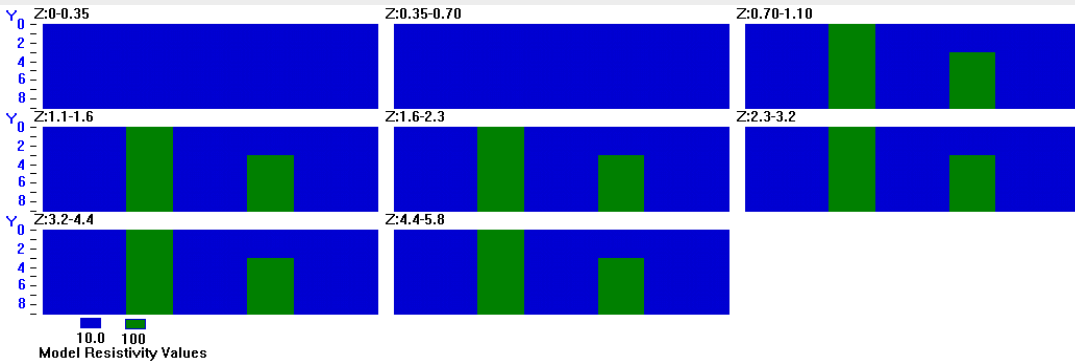
# Pitfalls in 2-D resistivity surveys – 3-D effects

3-D geology. It is assumed that the subsurface is 2-D when interpreting the data from a single line. This assumption is valid if the survey is carried out across the strike of an elongated structure. If there are significant variations in the subsurface resistivity in a direction perpendicular to the survey line, this could cause distortions in the lower sections of the model obtained. Measurements made with the larger electrode spacings are not only affected by the deeper sections of the subsurface, they are also affected by structures at a larger horizontal distance from the survey line.



# Pitfalls in 2-D resistivity surveys – 3-D effects

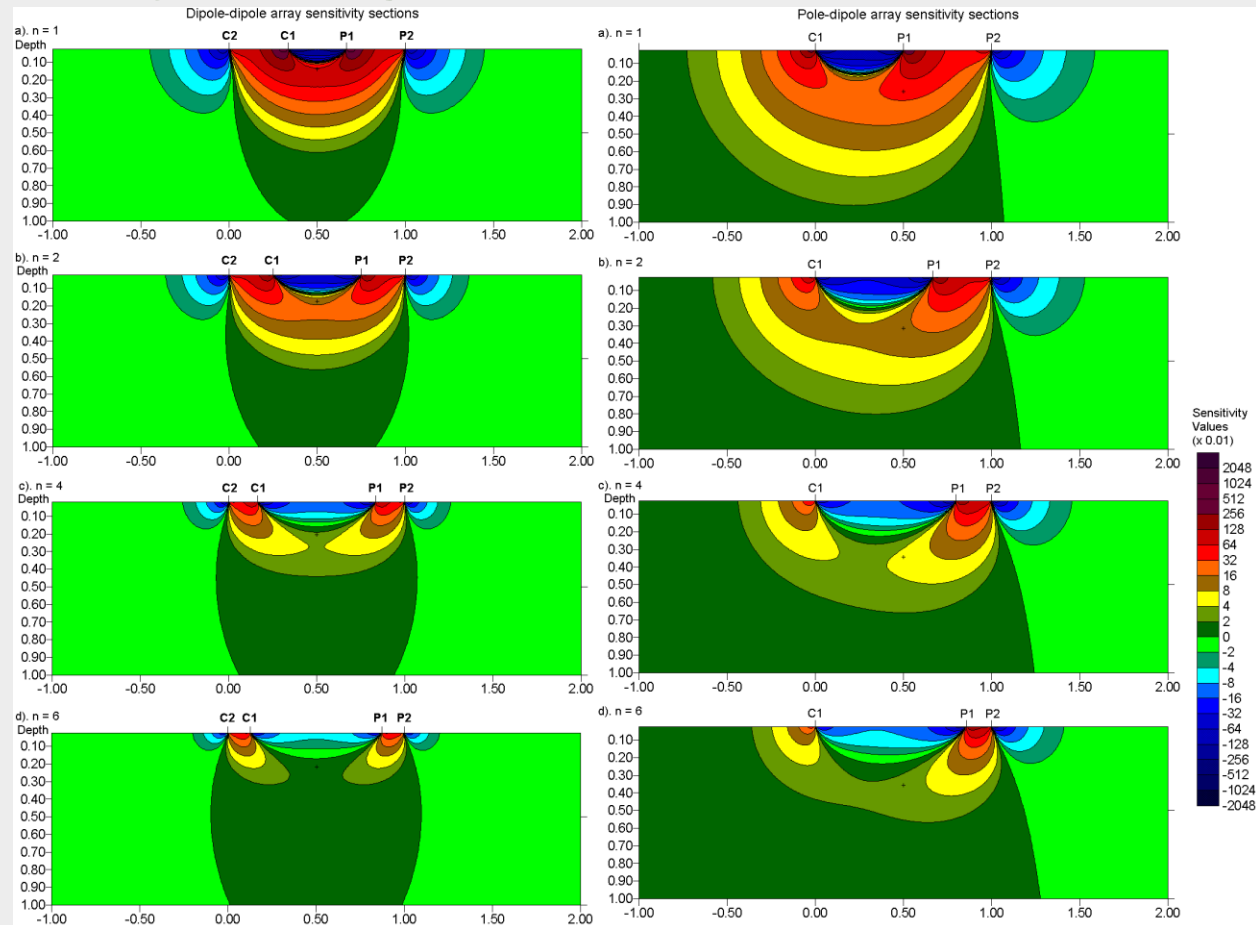
3-D effects are most pronounced when the survey line is placed near a steep contact with the line parallel to the contact. In general, the dipole-dipole array is more sensitive to 3-D effects than other arrays. The reason for this will be shown later when we look at the 3-D sensitivity pattern for this array.



# Very large 'n' values

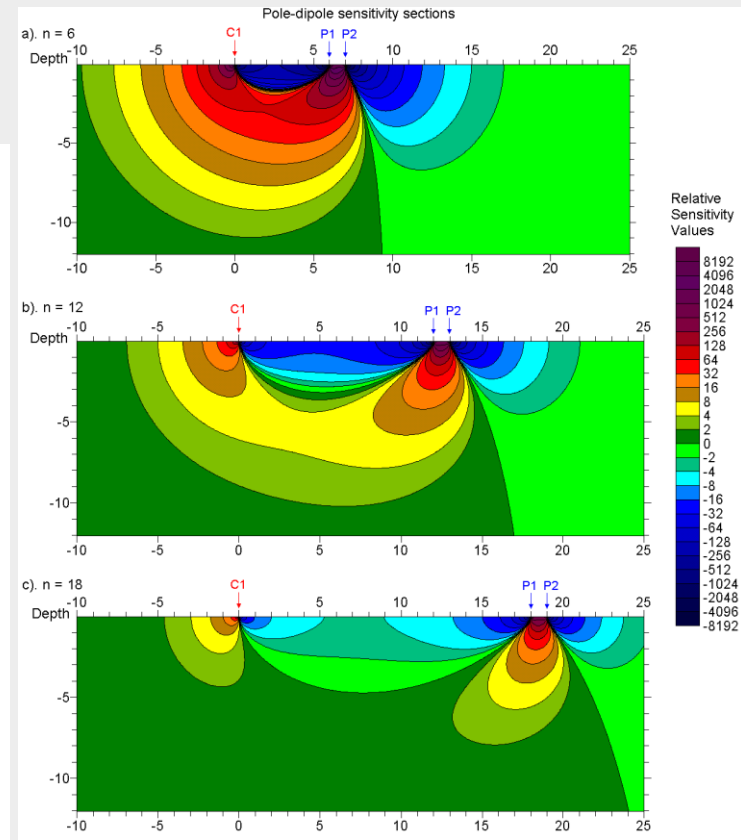
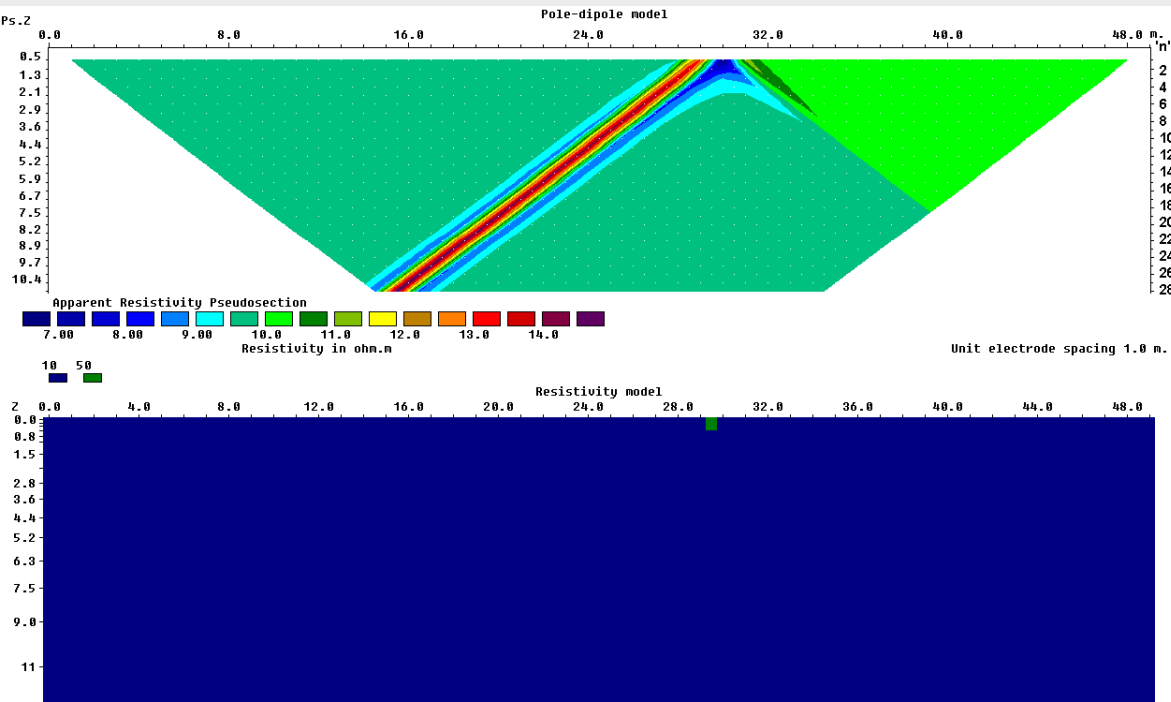
Increasing the electrode separation does not always increase the survey depth. For most arrays, as the separation between the electrodes is increased, the depth of the subsurface that is 'sensed' by the array also increases. However, this is not true of the pole-dipole and dipole-dipole arrays for large 'n' factors.

Note the region with high sensitivity values becomes increasingly concentrated near the surface between the dipoles as the 'n' factor increases.



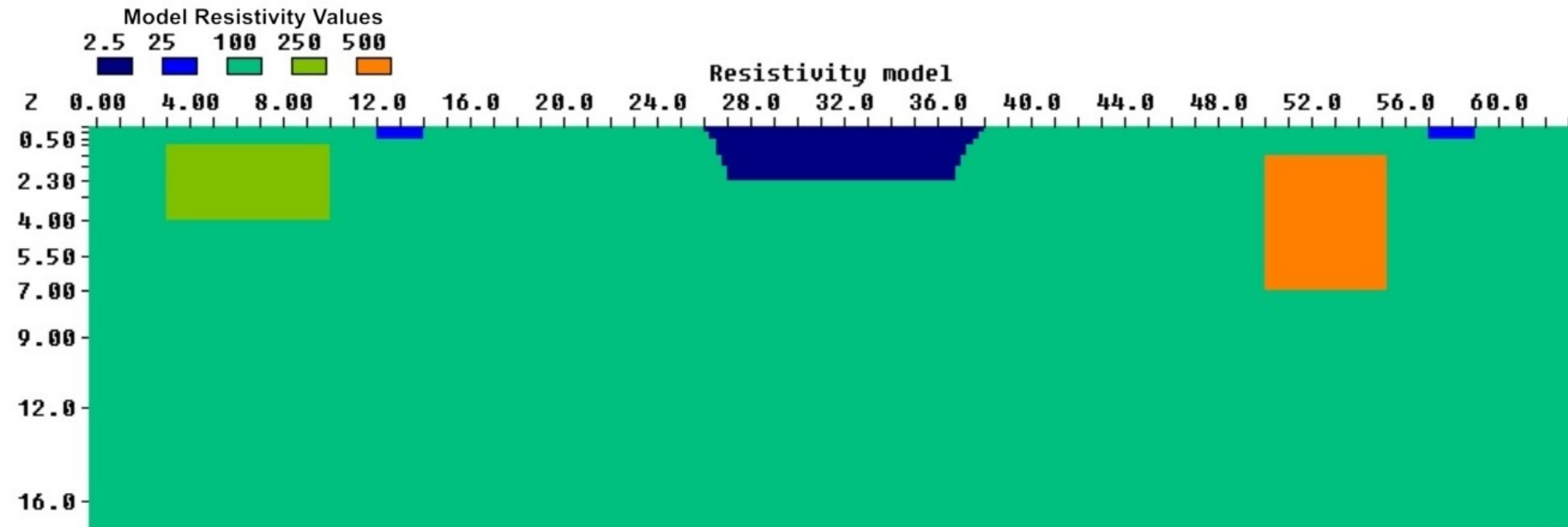
# Very large 'n' values : pole-dipole example

When the 'n' value is increased from 6 to 12, the zone of high sensitivity values becomes increasingly more concentrated below the P1-P2 dipole in a very shallow region. This means that the array with 'n' equals to 12 is less sensitive to deeper structures than the array with smaller 'n' values. This is shown by the positive anomaly due to the small near surface rectangular block that becomes stronger with increasing 'n'.



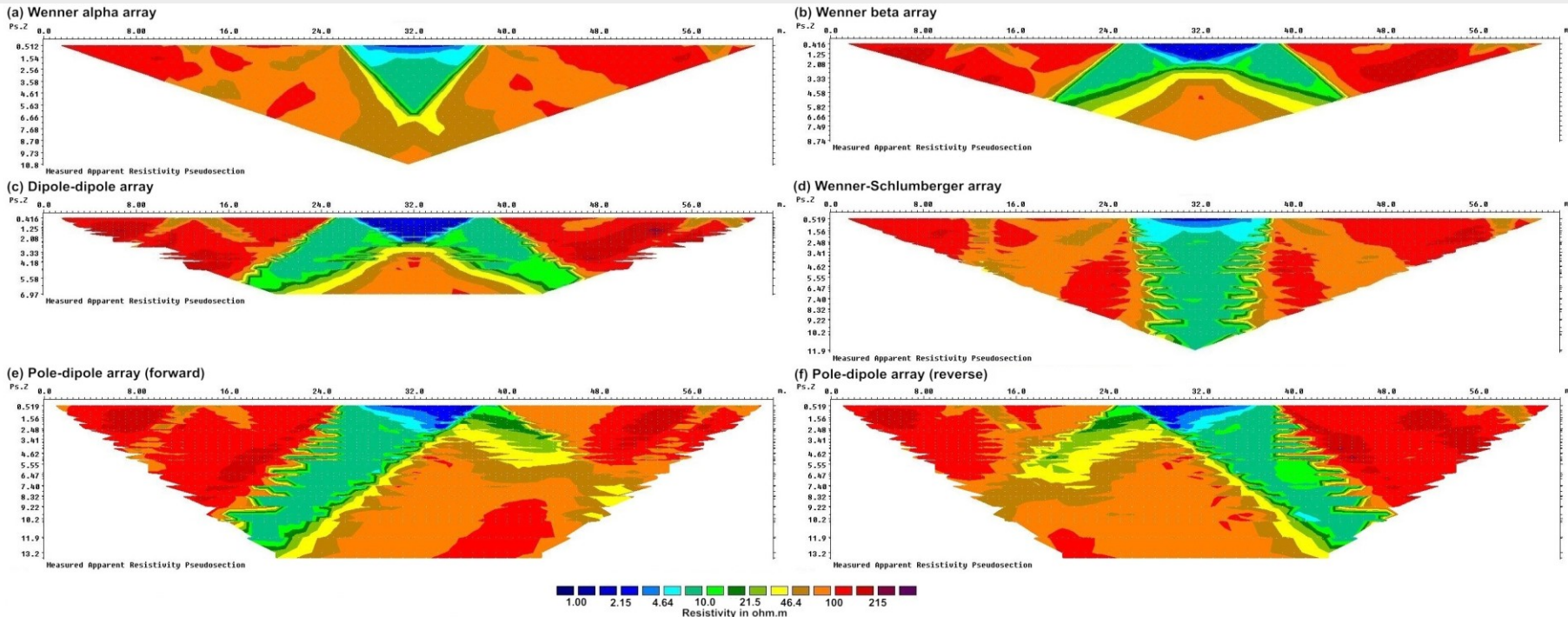
# Masking effect of a near surface anomaly

In some surveys, it has been observed that artifacts occur in the inverse model just below a very low or very high resistivity structure. For a low resistivity structure, the inverse model values tend to overshoot causing a high-resistivity artifact. Here we will look at an example of a low resistivity structure that could represent a landfill or tailings pond with low resistivity wastes. The pond is located between 26 to 38 m with a resistivity of 2.5  $\Omega$ .m that is much lower than the background of 100  $\Omega$ .m.



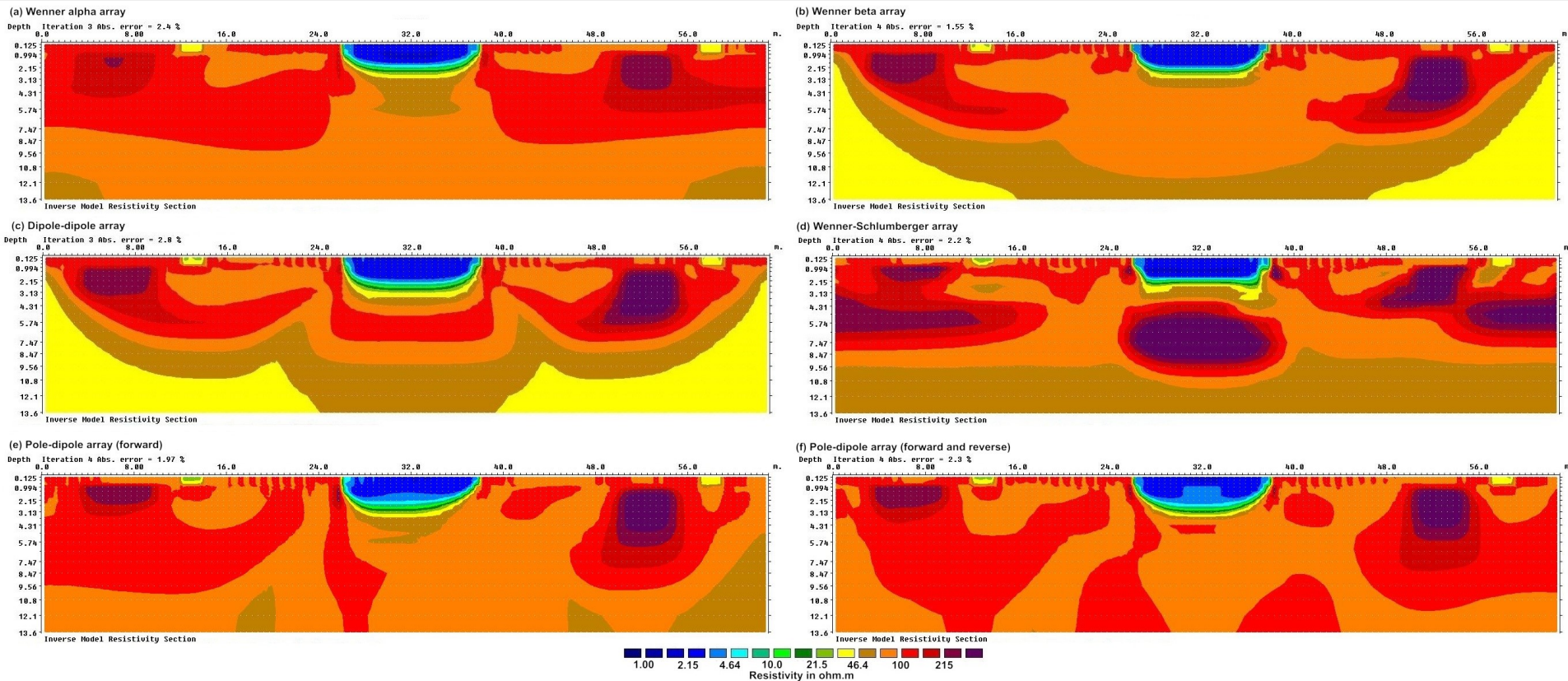
# Dump model apparent resistivity pseudosections

The apparent resistivity pseudosections with different arrays are shown. The Wenner-Schlumberger array (d) shows a broad low resistivity region below the dump site where the resistivity values do not recover back to the background value of 100  $\Omega.m$  towards the bottom of the pseudosection. The 'a' spacing for the Wenner-Schlumberger array range from 1 to 10 m. and the 'n' factor ranges from 1 to 6. The same set of 'a' and 'n' values are used for the pole-dipole arrays (e and f).



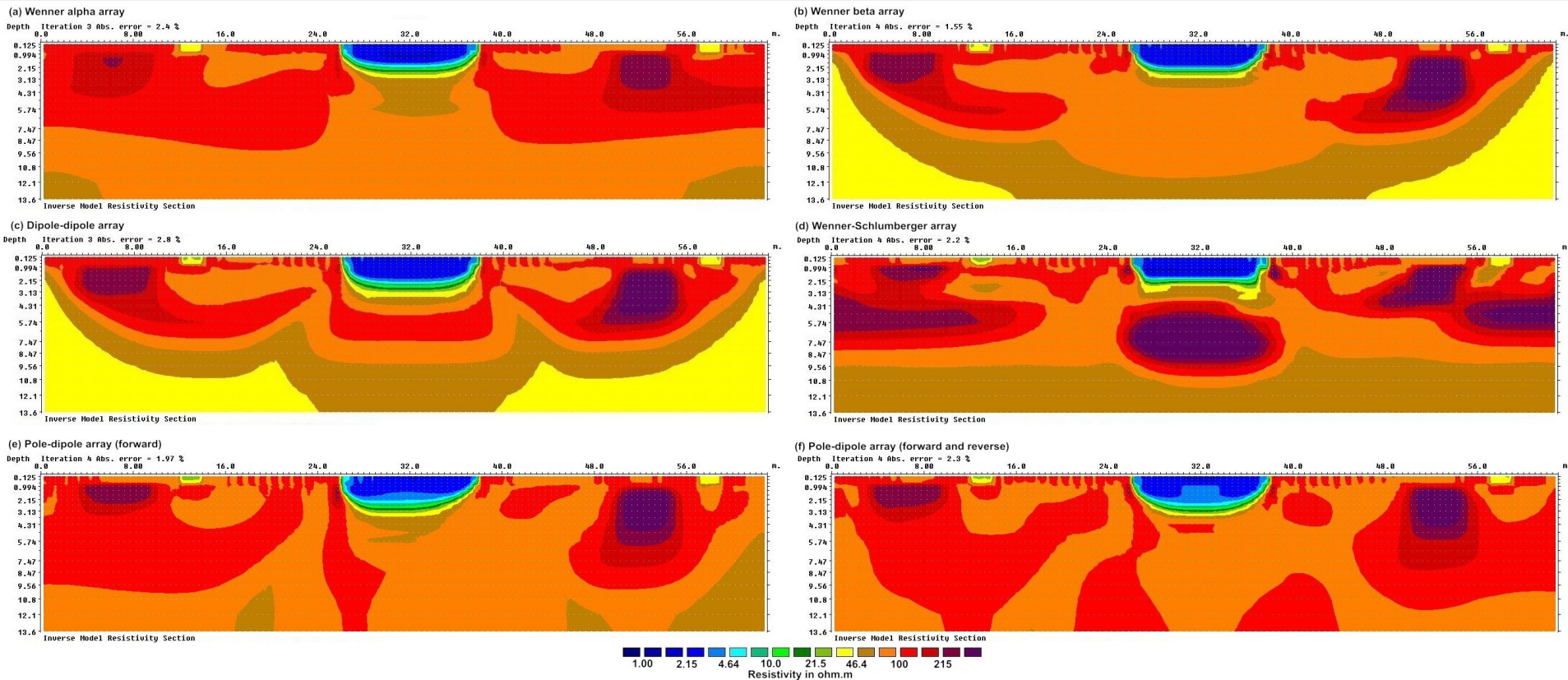
# Dump model inversion results

The Wenner alpha (a), beta (b) and dipole-dipole (c) models do recover the shape of the dump site. For the 3 models, the resistivity of the region below the low resistivity dump is close to the true value of 100  $\Omega$ .m. (the orange-red boundary). The Wenner-Schlumberger array model shows significant artifacts, particularly below the low resistivity dump where the resistivity values rise above 200  $\Omega$ .m (d).



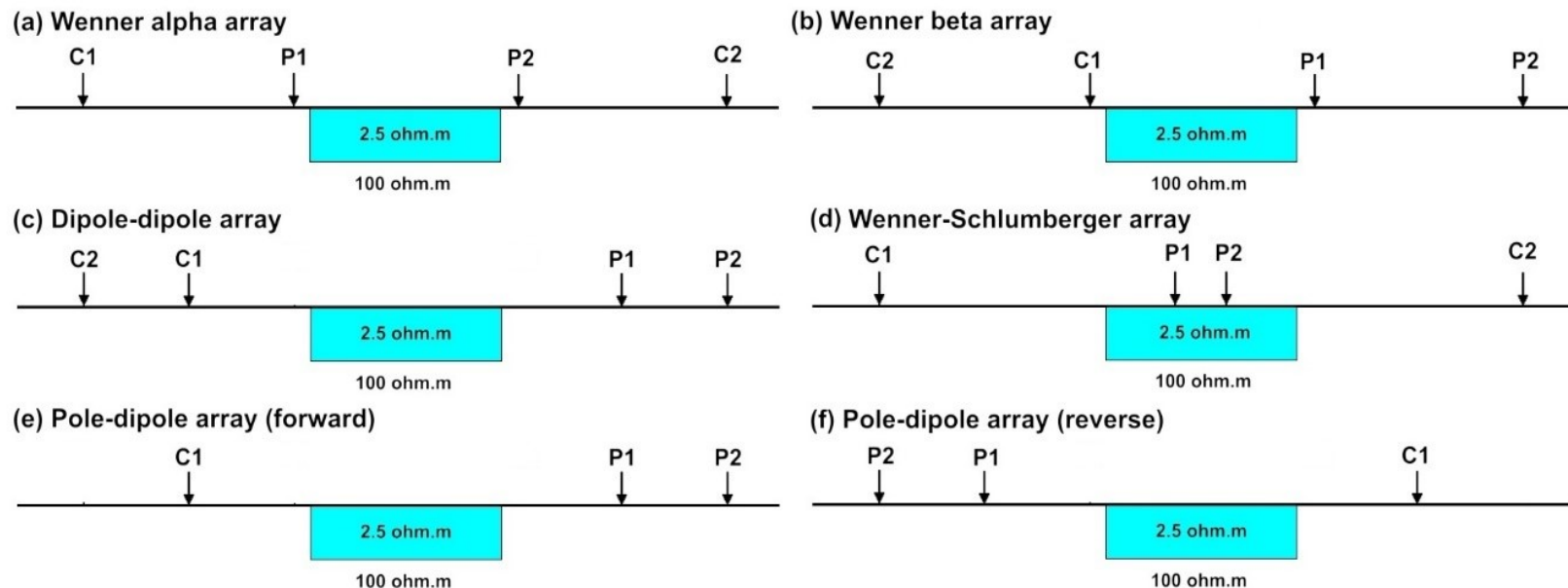
# Dump model inversion results

The model for the pole-dipole arrays using the forward measurements (e) alone is also free from the high resistivity artifact below the dump. There is a slight asymmetry in the shape of the dump due to the asymmetrical nature of the array. The model from the combined forward and reverse pole-dipole array measurements is free of this asymmetry.



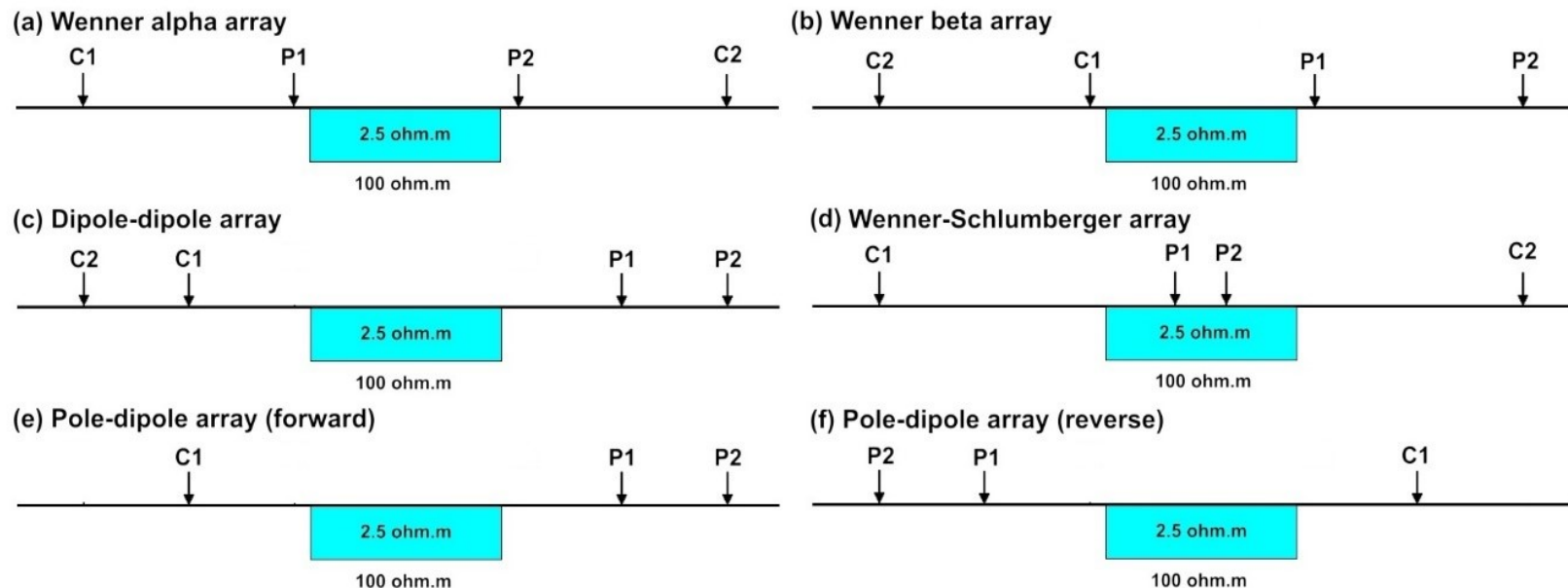
# Electrode positions for Wenner-Schlumberger array

The reason for the poorer performance of the W-S array is due to the arrangement of the electrodes. Although the C1 and C2 electrodes for the W-S array (d) are at the same positions as the Wenner array (a), both the potential electrodes (P1, P2) are within the low resistivity dump. The apparent resistivity measurement is dominated by the near-surface low resistivity structure, and the measurements has very little information about the region below the dump area. As the data set does not have much information about the material below dump area, it is impossible to accurately model this region.



# Electrode positions for other arrays

Figure below shows the positions of the electrodes for an array where the total length of the array is longer than the width of the dump site. For the Wenner array (a,b) all the potential electrodes can avoid the low resistivity dump site. For the dipole-dipole array (c), some of the measurements will have both dipoles outside the dump area. The pole-dipole arrays also have some measurements where all the electrodes are outside the dump area (e,f). These array measurements thus give more information about the material below the low resistivity dump.



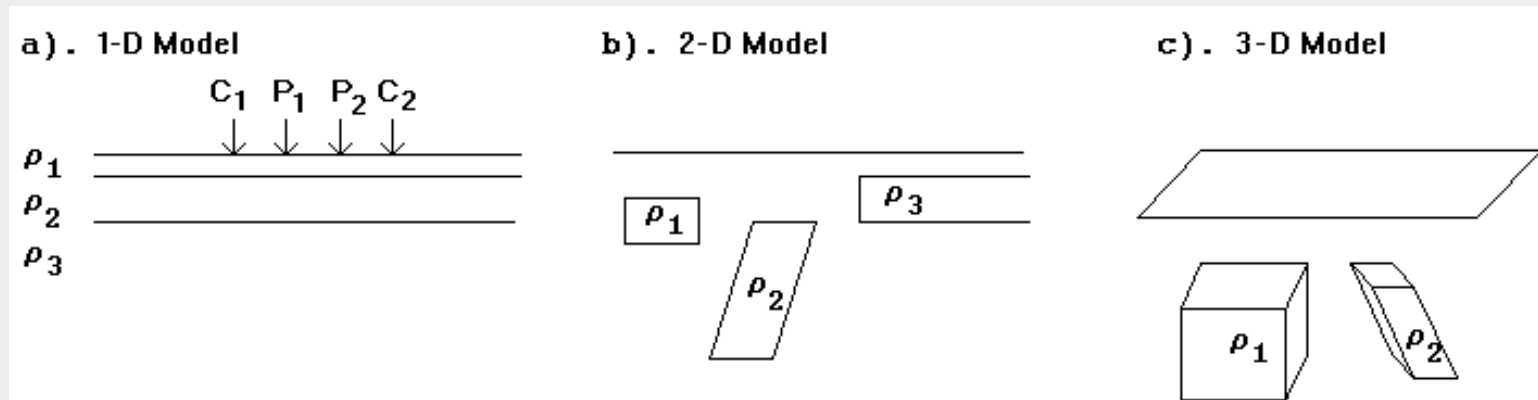
# Part 4

## 3-D surveys, data and inversion

# 3-D ERT Surveys

Since all geological structures are 3-D in nature, a 3-D resistivity survey using a 3-D inversion model should give the most accurate results. However 3-D surveys are not as commonly carried out as 2-D surveys due to higher costs. There are two new developments that makes 3-D surveys a more cost-effective option. Multi-channel resistivity meters significantly reduces the survey time, and faster microcomputers enable the inversion of very large data sets.

Many of the inversion concepts discussed for 2-D surveys are directly applicable for 3-D surveys and data inversion. This section will concentrate more on new features that are more relevant to 3-D surveys and models.



# Types of arrays for 3-D surveys

Most arrays that are used in 2-D surveys can also be used in 3-D surveys. However the following array types seem to be more widely used for 3-D surveys.

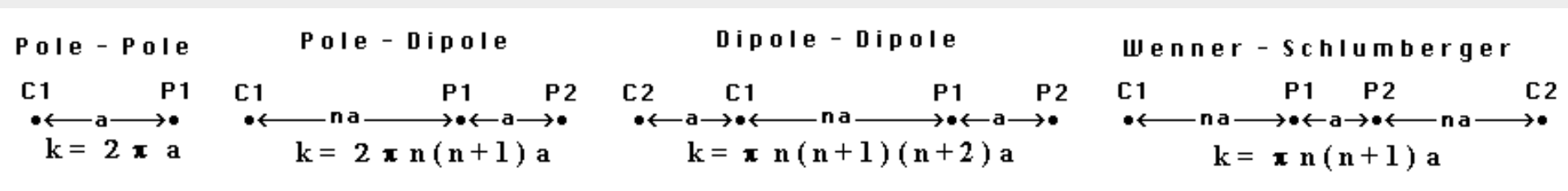
Pole-pole : 2 active electrodes

Pole-dipole : 3 active electrodes

Dipole-dipole : 4 active electrodes

Wenner-Schlumberger : 4 active electrodes

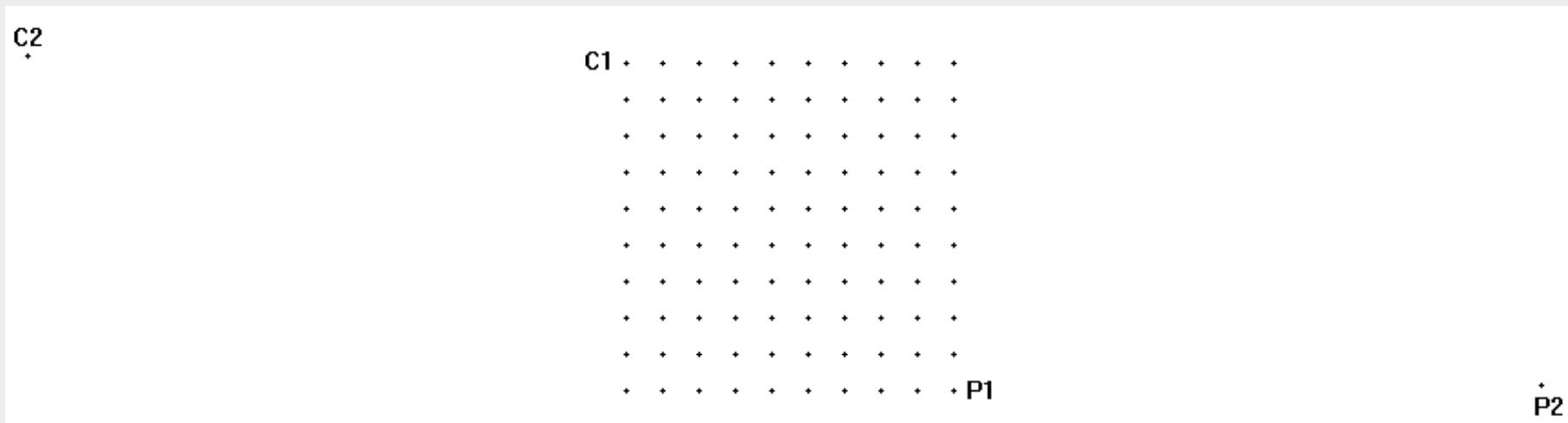
The arrangement of the electrodes for these arrays together with their geometric factors are shown below.



# The Pole-Pole array : Electrode layout

Only two active electrodes, C1 and P1, are used. The second current and potential electrodes, C2 and P2, are fixed throughout the survey and must be placed at a distance of at least 20 times the maximum C1-P1 spacing. If the distances of the remote electrodes is less, the positions must be recorded and included in the data file. Different pairs of electrodes in the grid are selected as the C1 and P1 electrodes.

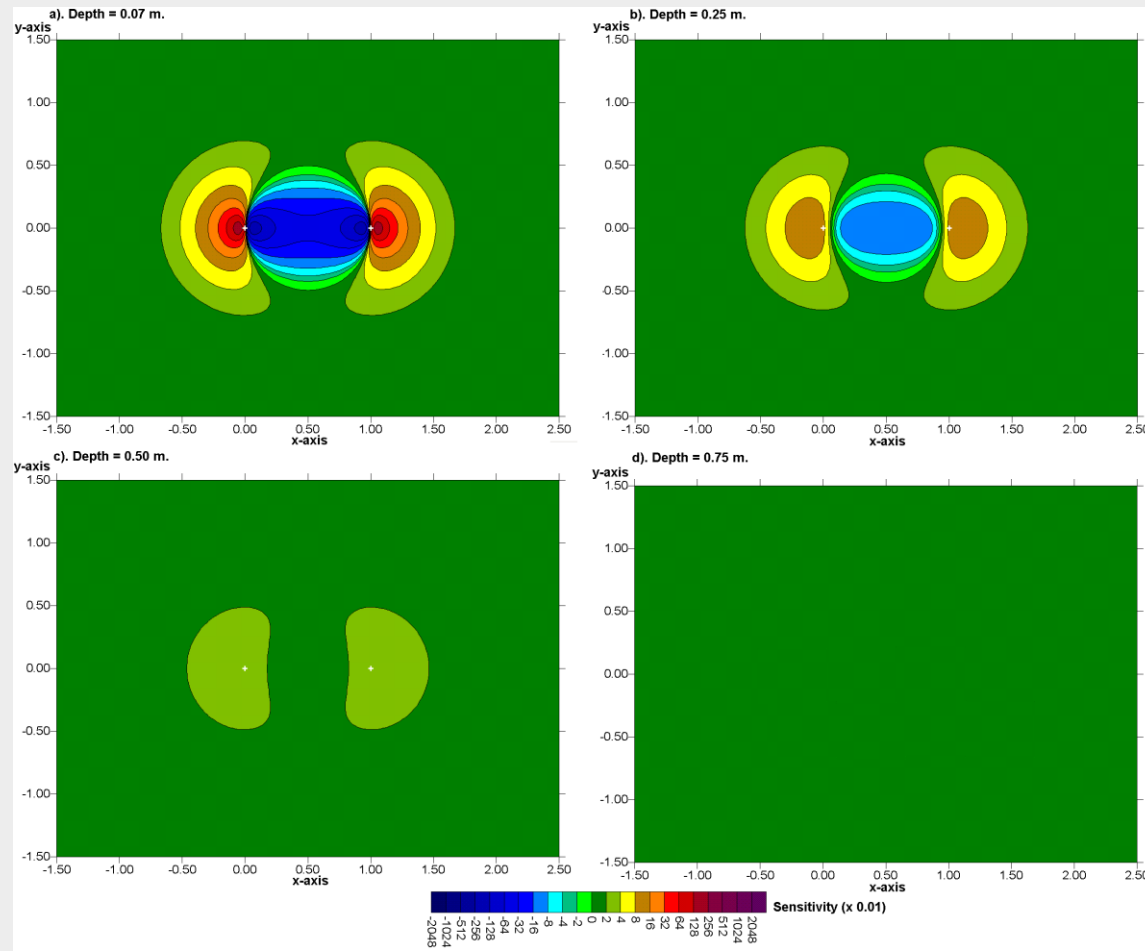
The depth of investigation is about 0.87 times the C1-P1 (or ' $a$ ') spacing.



# The pole-pole array - 3D sensitivity sections

The figure shows the sensitivity values on horizontal slices through the earth. The electrodes are at the 0 and 1 meter marks along the x-axis. Near the surface, there is an approximately circular region with negative sensitivity values in the top two slices at depths of 0.07 and 0.25 meter. The zone with the largest sensitivity extends in the y-

direction to slightly over half the electrode spacing. To get a complete 3-D coverage, if the measurements are only made in the x-direction, the spacing between the lines should not be much more than the smallest electrode spacing used.



# The pole-pole array for 3D surveys - summary

The pole-pole array has two main disadvantages.

Firstly it has a much poorer resolution compared to other arrays.

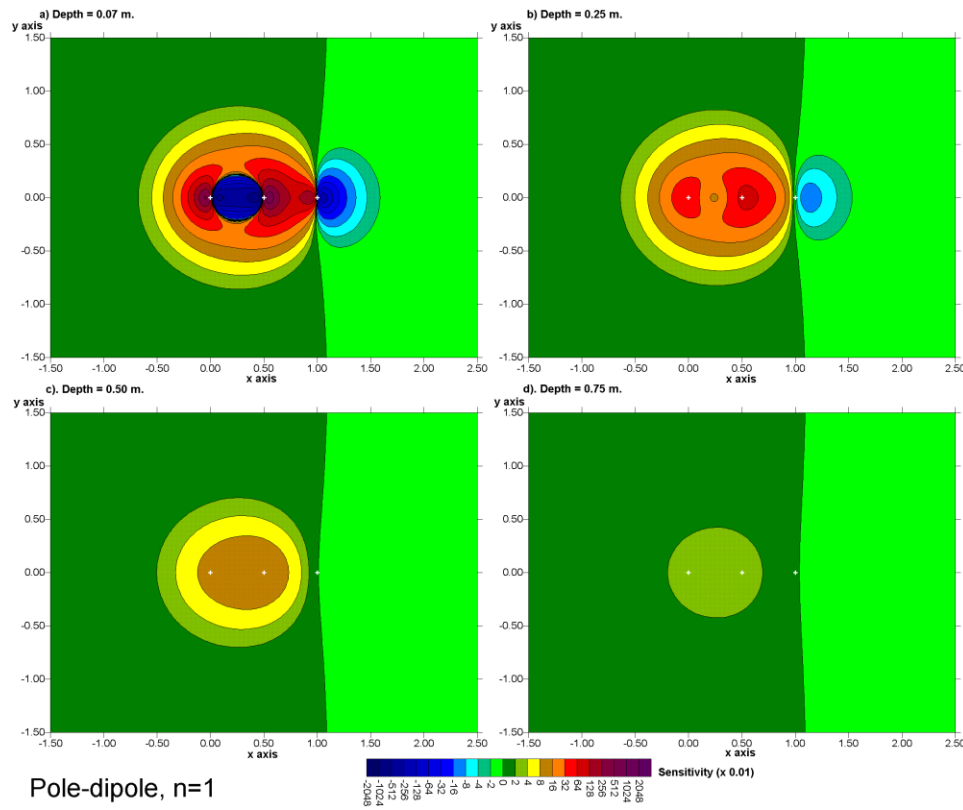
The second disadvantage is that the second current electrode C2 and potential electrode P2 must be placed at sufficiently large distances from the survey grid. This could be a challenging task for large grid sizes.

The main advantage of the pole-pole array is that it gives a better horizontal coverage than other arrays. It also has the deepest depth of investigation (0.87 times the C1-P1 spacing). For this reason, it is popular in small surveys grids.



# The pole-dipole array - 3D sensitivity sections

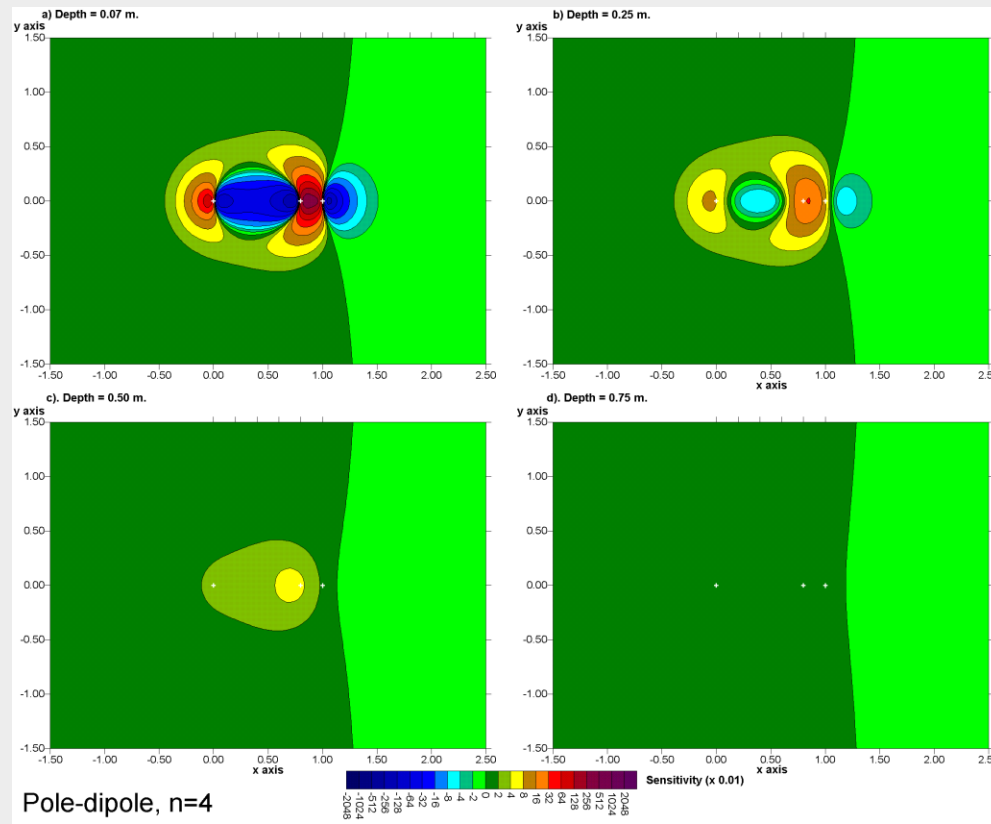
The figures below shows the sensitivity patterns with the dipole separation factor “ $n$ ” is equals to 1 and 4. There is prominent area with negative sensitivity values between the C1 and P1 electrodes. The array is more sensitive to structures off the array axis (i.e. in the  $y$ -direction) compared to the pole-pole array. The area with the higher sensitivity values extends to about 0.8 times the array length, or 1.6 times the unit electrode spacing for  $n=1$ .



# The pole-dipole array - 3D sensitivity sections

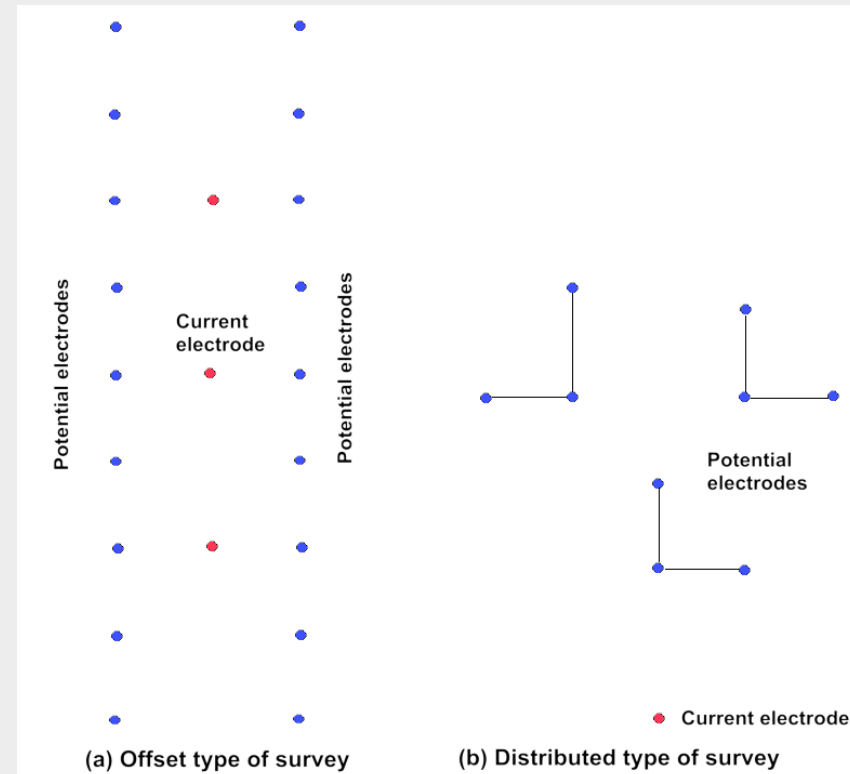
For  $n=1$  the area with the higher sensitivity values extends to about 0.8 times the array length, or 1.6 times the unit electrode spacing.

When  $n=4$ , the array is more sensitive to off-axis structures near the P1-P2 dipole. This sensitivity to off-axis structures is useful if the survey is conducted along a series of parallel lines. The distance between the lines should be within 2 times the unit electrode spacing.



# Offset variations of the pole-dipole array

Different variations of the pole-dipole arrays have been designed to maximize the area coverage with a small number of current electrode positions, particularly for I.P. surveys (due to heavy current transmitter system). The offset type of system use two parallel lines of potential electrodes which triples the area covered. The newer 'distributed' system uses groups of potentials electrodes arranged parallel and perpendicular to the current electrode.



# The pole-dipole array for 3D surveys - summary

This array is useful for surveys with medium and large survey grids.

It has a better resolving power than the pole-pole array, and is less sensitive to telluric noise since both potential electrodes are kept within the survey grid.

It has a stronger signal strength than the dipole-dipole array.

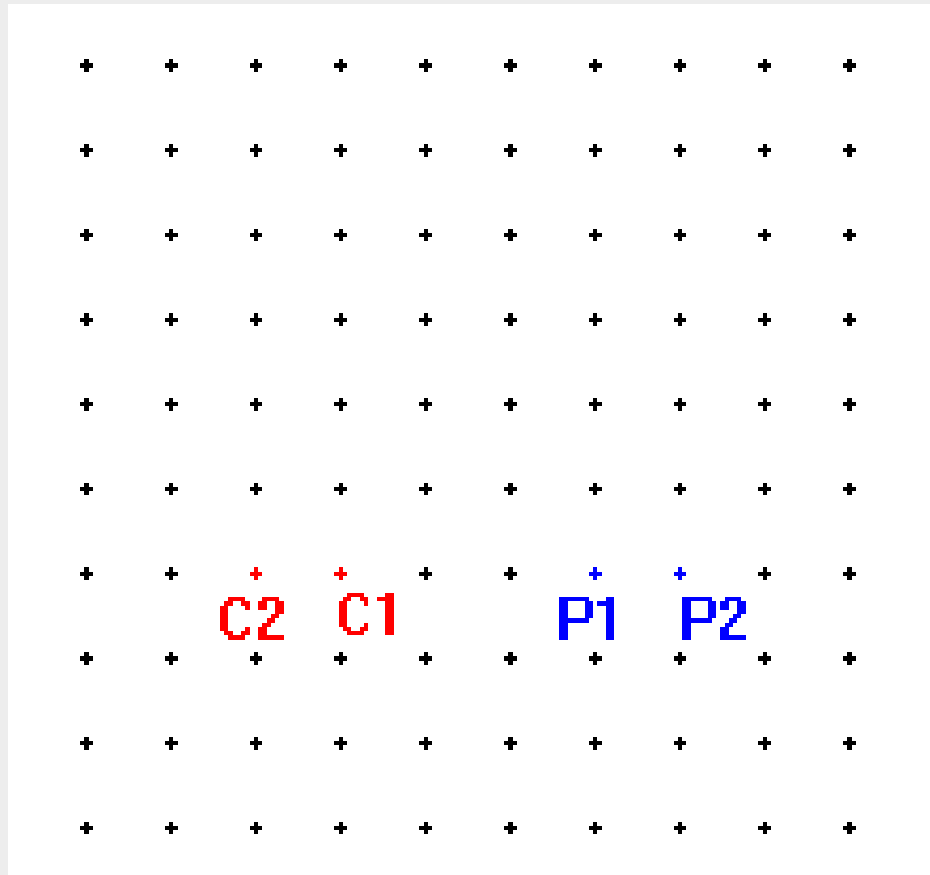
Although it has one “remote” electrode (the C2 electrode), the effect of this electrode on the measurements is much smaller compared to the pole-pole array. The effect can be included in the modeling by recording the position of this electrode.

This array is now widely used for 3-D I.P. surveys where very large survey grids (about 1000 electrodes and 50m spacing) are used. The offset or distributed arrangement, where the C1 electrode is on a different line from the P1-P2 electrodes, is frequently used.

# The Dipole-Dipole array : Electrode layout

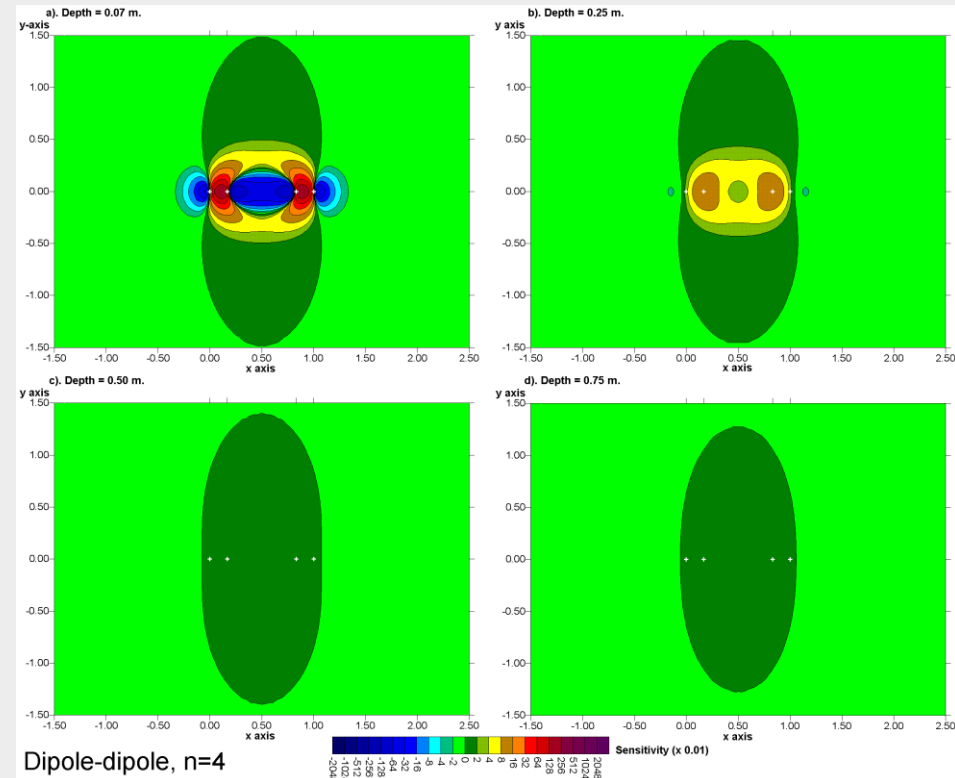
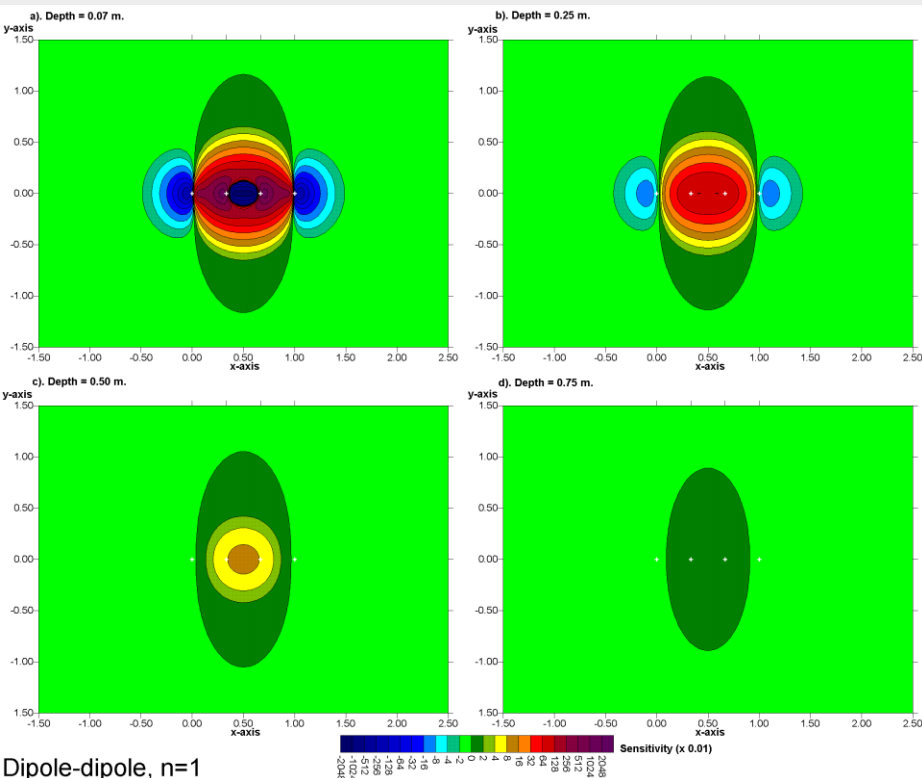
All four electrodes are used.

The depth of investigation is about 0.20 times the array length (C2-P2 spacing). Measurements are usually made along the x and y lines, frequently in only one direction.



# The dipole-dipole array - 3D sensitivity sections

The sensitivity contours are elongated in the  $y$ -direction, particularly for  $n=4$ . The high sensitivity area extends to about 1.5 times the array length in the  $y$ -direction. This sensitivity of the dipole-dipole array to off-axis structures is a problem in 2-D surveys, but is useful in 3-D surveys if the survey is conducted along a series of parallel lines. A larger spacing between the survey lines (to about 3 times the electrode spacing) can be used for 3-D surveys.



Dipole-dipole,  $n=1$

Dipole-dipole,  $n=4$

# The dipole-dipole array for 3-D surveys - summary

This array is widely used with large surveys.

The main problem that is likely to be faced with this array is the comparatively low signal strength. This problem can be overcome by increasing the “a” spacing between the P1-P2 dipole to get a deeper depth of investigation as the distance between the C1-C2 and P1-P2 dipoles is increased.

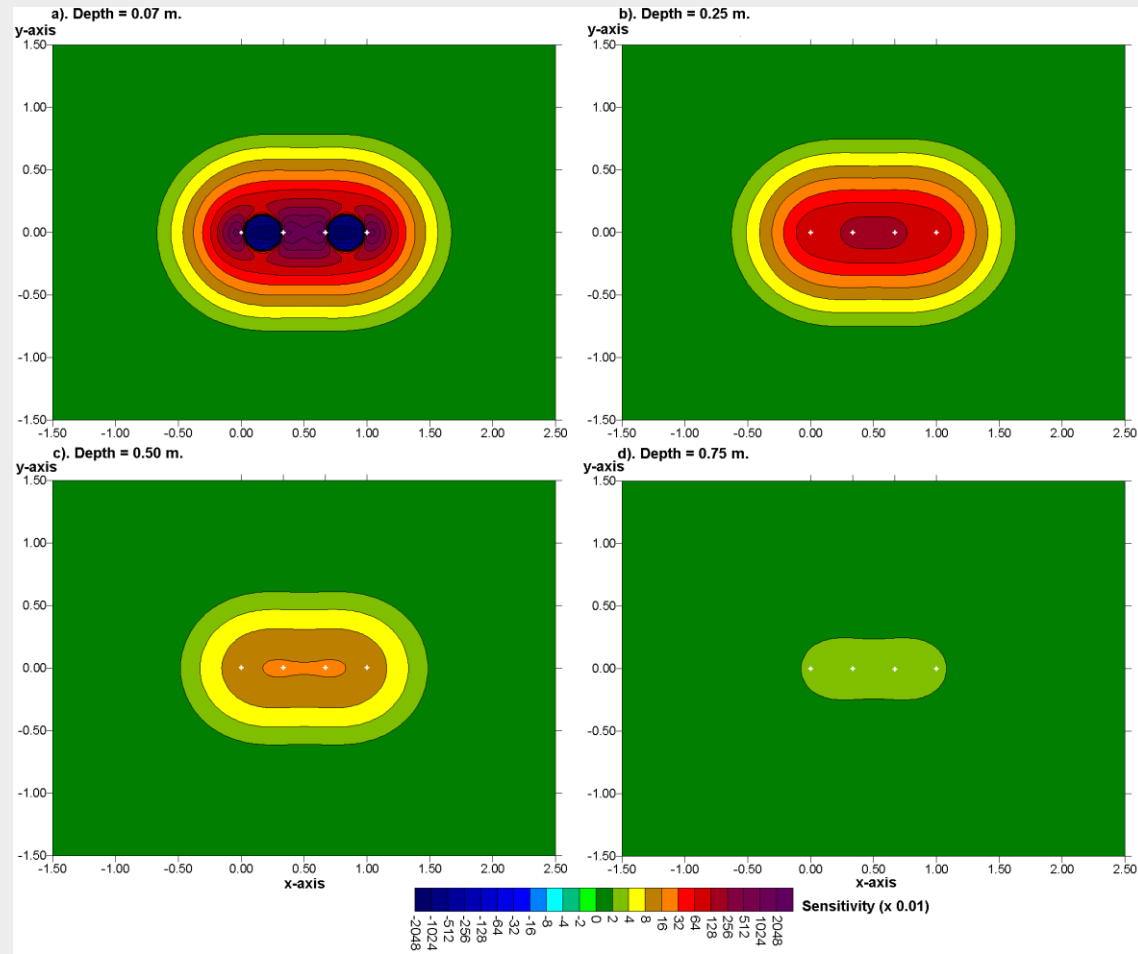
It might be a useful array if the “3-D” survey actually consists of measurements along a series of 2-D lines. It has a sensitivity pattern that is elongated perpendicularly to the array direction, and thus provide more information on structures that are off the line axis.

In some large 3-D I.P. surveys with multi-channel instruments, a non-symmetrical form of the dipole-dipole array is sometimes used. The P1-P2 dipole length can be increased at larger distances to get a stronger signal strength for the same C1-C2 current dipole. In some cases, the C1-C2 dipole is offset from the P1-P2 dipole.

# The Wenner array - 3D sensitivity sections

The sensitivity contours for the Wenner array (W-S with  $n=1$ ), outside of the immediate vicinity of the electrodes, are elongated in the direction of the line of electrodes. This means that the Wenner alpha array is less sensitive to off-line structures than the dipole-dipole array, i.e. it is less sensitive to 3-D effects.

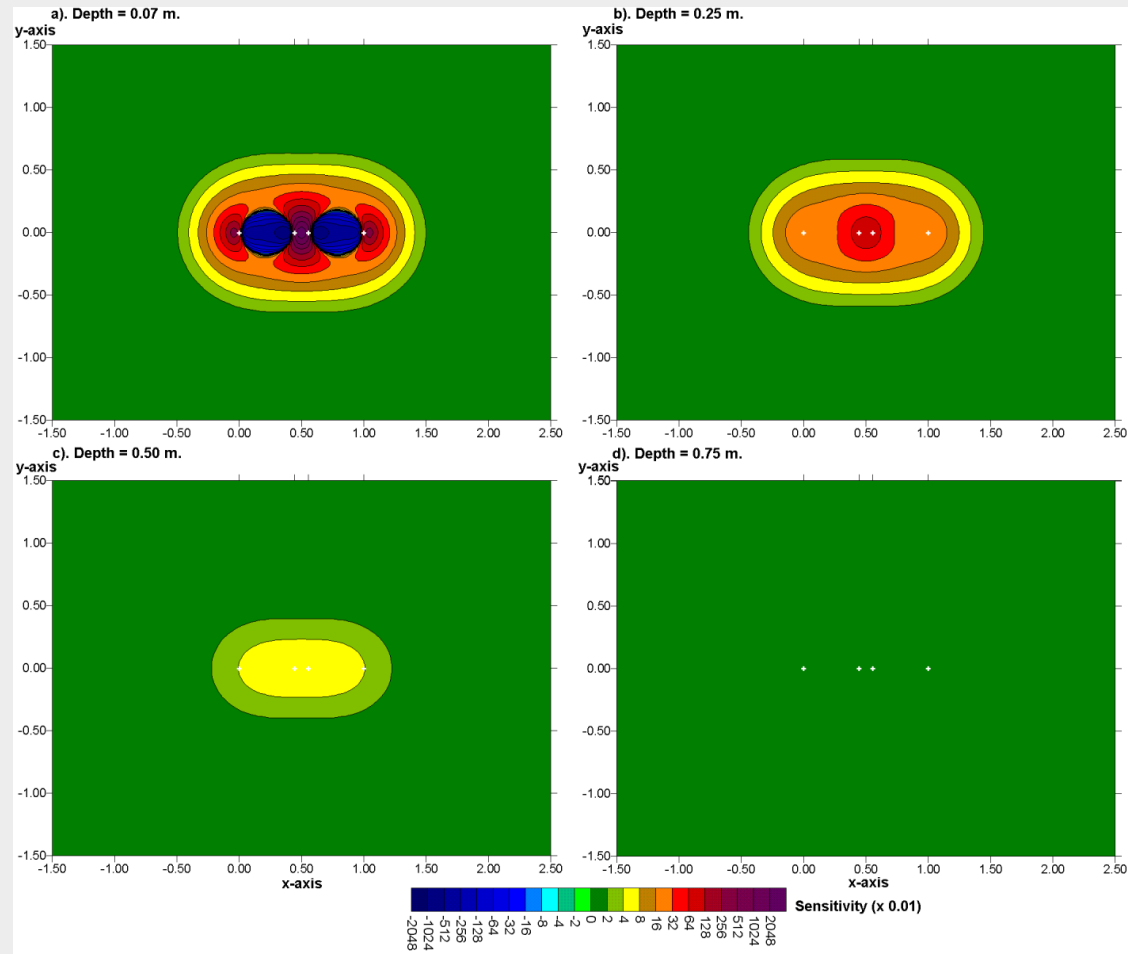
This is an advantage in 2-D surveys, but makes it less useful for 3-D surveys carried out with a series of 2-D lines.



# The Schlumberger array - 3D sensitivity sections

The sensitivity pattern for the Wenner-Schlumberger array ( $n=4$ ) is generally elongated in the direction of the line of electrodes with a slight bulge near the center of the array. It is less sensitive to off-line structures than the dipole-dipole array (i.e. it is less sensitive to 3-D effects). However, the wider zone of off-axis high sensitivity values

as the 'n' factor increases makes it is more useful for 3-D surveys than the Wenner ( $n=1$ ).



# Summary of array types for 3-D surveys

For relatively small survey areas, the pole-pole array is popular since it provides better horizontal data coverage compared to other arrays.

The pole-dipole array has been widely used in recent years with large survey grids, particularly the offset and distributed versions for I.P. surveys. It has a higher resolution than the pole-pole array. It requires only one remote electrode and is much less sensitive to telluric noise.

The dipole-dipole array is widely used for large survey grids, particularly if there is no convenient location for a remote electrode.

For very large survey grids with resistivity only surveys, the Wenner-Schlumberger has been used. This array is frequently used when the survey is carried out along a series of parallel 2-D lines, particularly in environmental/engineering surveys.

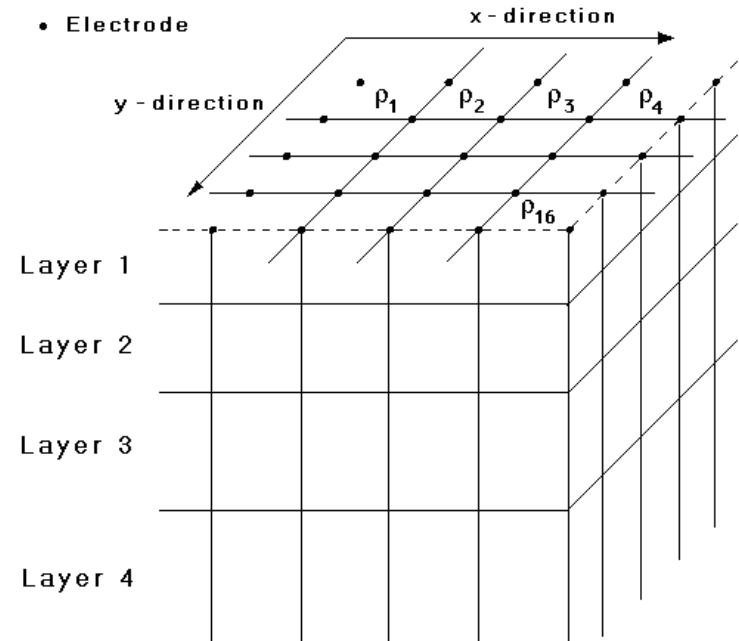
# **3-D surveys and data inversion**

**Methods for carrying out 3-D surveys, and different model discretizations used for data inversion**

# 3-D inversion models

What is 3-D inversion? An inversion model is 3-D if the resistivity values are allowed to vary in all three directions (in the  $x$ -,  $y$ - and  $z$ -directions) at the same time.

In 2-D inversion the subsurface resistivity is assumed to vary only in the  $x$ - and  $z$ -directions but constant in the  $y$ -direction. A model constructed from a series of 2-D inversions along parallel lines is not a true 3-D inversion model. A 3-D forward modeling subroutine (the finite-difference and finite-element method) is used to calculate the model apparent resistivity values.



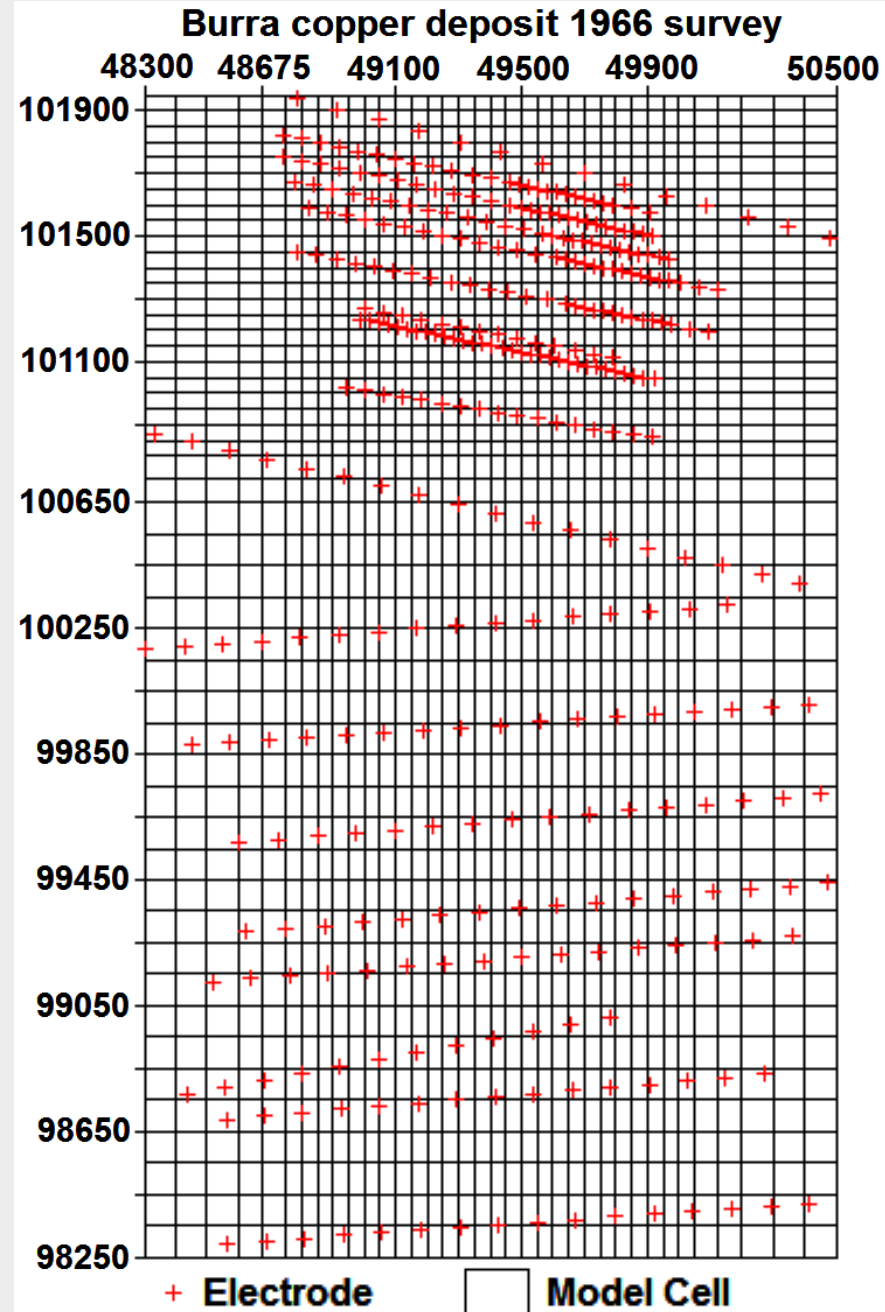


# 3-D data sets – non-rectangular layouts

Measurements can also be combined from 2-D lines that can run in different directions. This is common when the '3-D' data set was created from old 2-D surveys.

In this example, not only the lines have different directions, they also have different spacings.

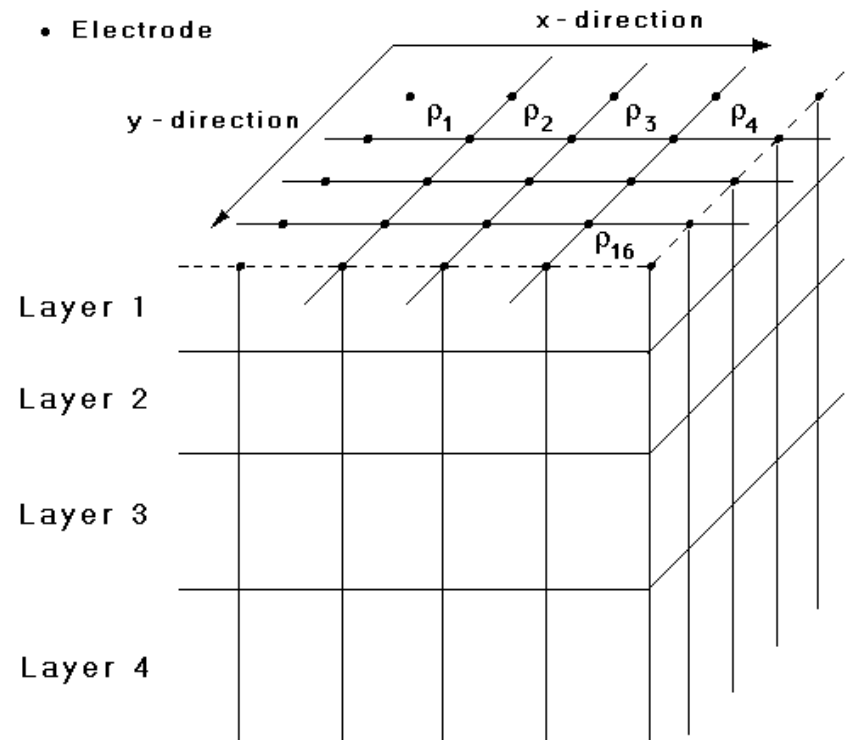
Note the model used in this example has smaller cells sizes in the areas with more data, and larger cells towards the left and right sides where larger electrode spacings are used.



# 3-D model discretizations

To convert the 3-D of field data set into a resistivity model for the subsurface, we divide the subsurface into a number of blocks. Depending on the complexity of the survey setup, there are a few methods used.

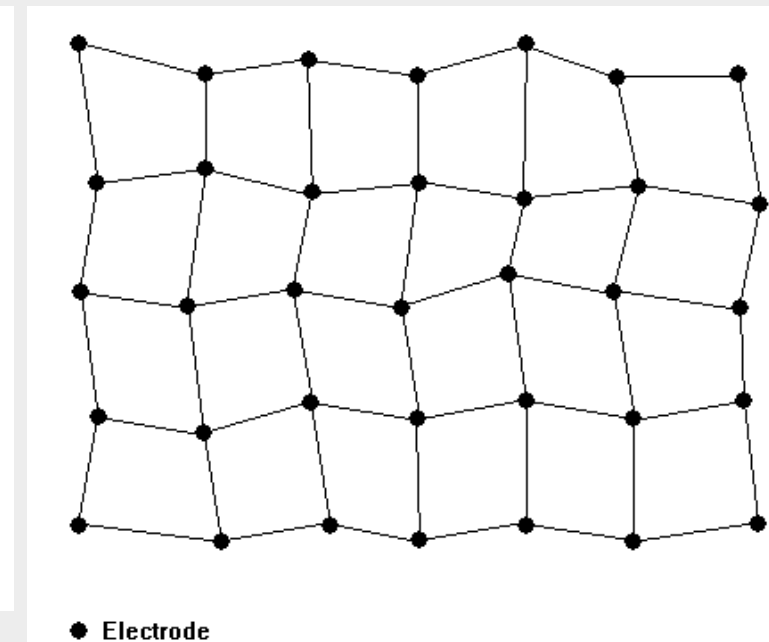
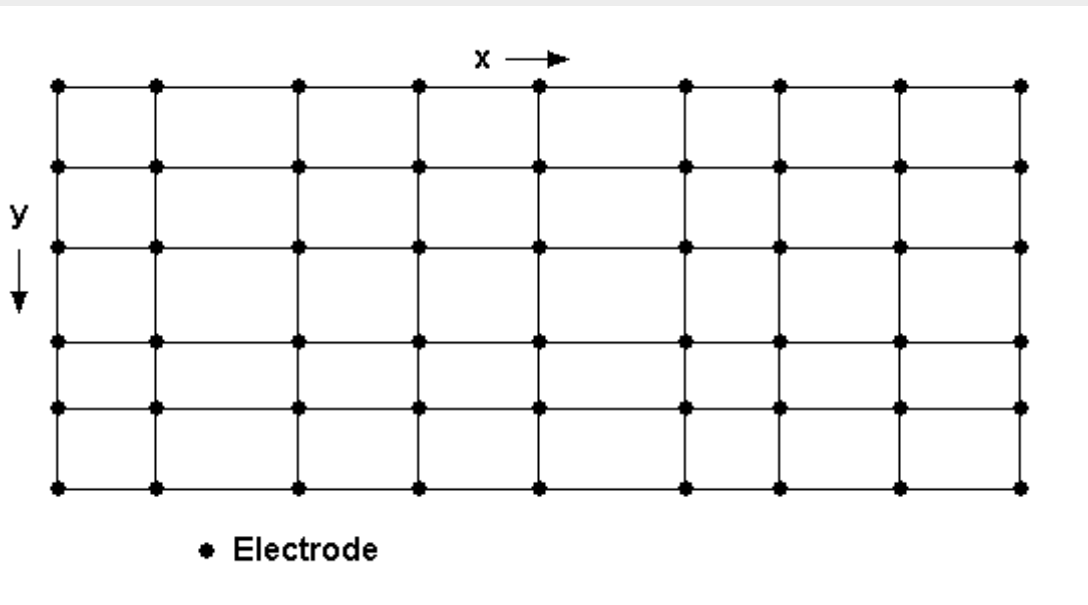
They range from simple rectangular grids, to trapezoidal grids and finally to arbitrary grids.



# Rectangular and Trapezoidal Grids

A rectangular grid, possibly with non-uniform spacing, can be used when the data was measured using electrodes in a rectangular grid, such as from a series of parallel 2-D lines.

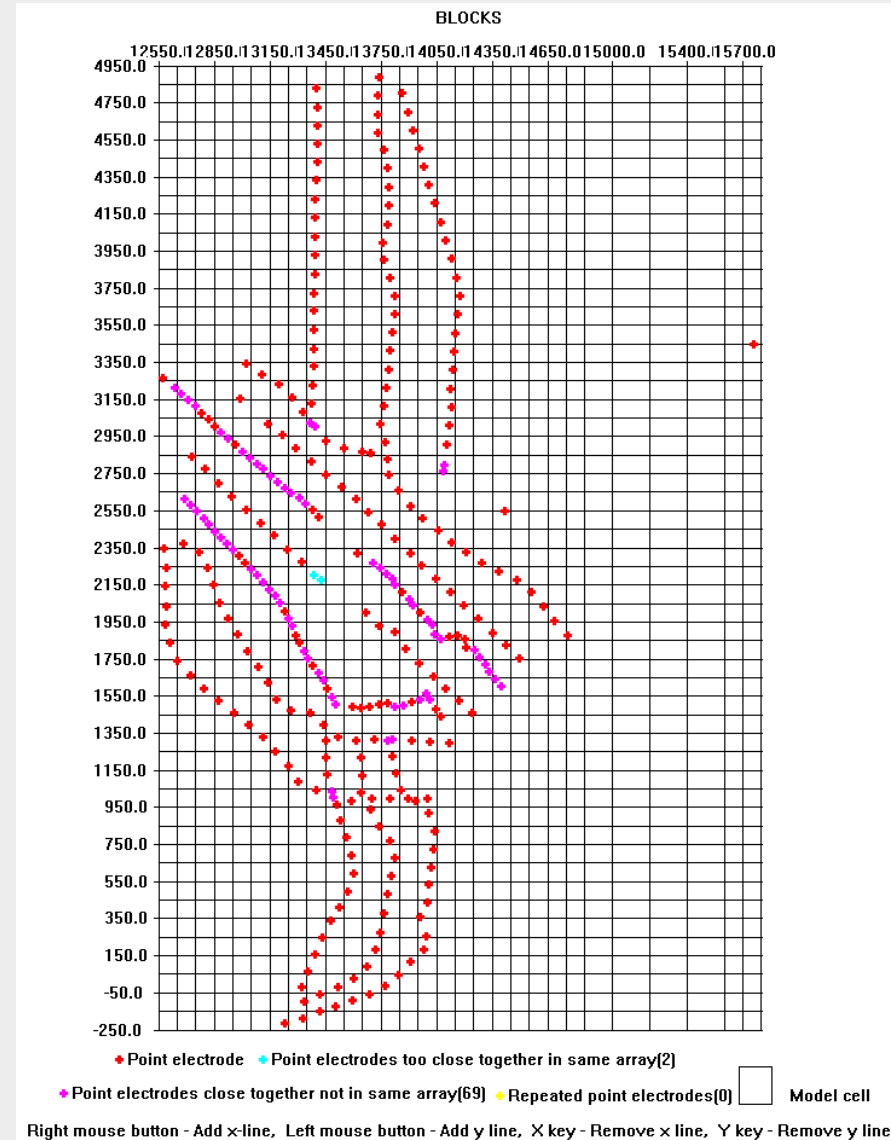
Due to physical obstructions, it is sometimes not possible to run straight survey lines. The next grid model allows for this. It still assumes each line has the same number of electrodes.



# 3-D surveys with arbitrary electrode positions

In some surveys, the positions of the electrodes cannot fit into a simple rectangular or even trapezoidal grid. This situation occurs because of physical obstructions such that straight survey lines cannot be used, or the data is collated from surveys over different periods.

This is particularly common in mineral exploration surveys where there were different survey phases, usually using a series of quasi-parallel 2-D survey lines. It is possible to invert such data sets by separating the model discretization grid from the survey grid.



Right mouse button - Add x-line, Left mouse button - Add y line, X key - Remove x line, Y key - Remove y line

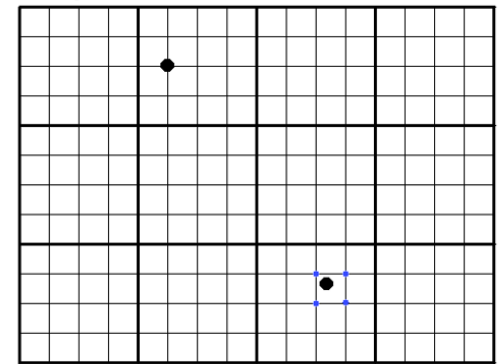
# Methods to handle arbitrary electrode positions

There are two methods to model the effect of an electrode at an arbitrary position. The first is to calculate the potential at the electrode by interpolating the potentials at the 4 nearest nodes in the mesh (or replace a current electrode by 4 current sources).

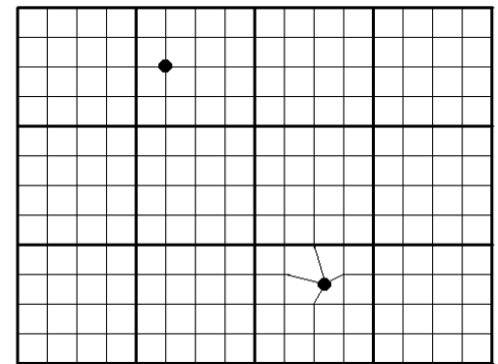
It's advantage is that the finite-difference method can be used (if there is no topography) which requires less computer time and memory than the finite-element method.

The second method moves the nearest node to the location of the electrode with a distorted finite-element mesh. It gives more accurate results for arrays such as the dipole-dipole that uses small potential differences between electrodes that are close together, but cannot be used if two electrodes are less than 2 nodes apart.

Interpolation Method

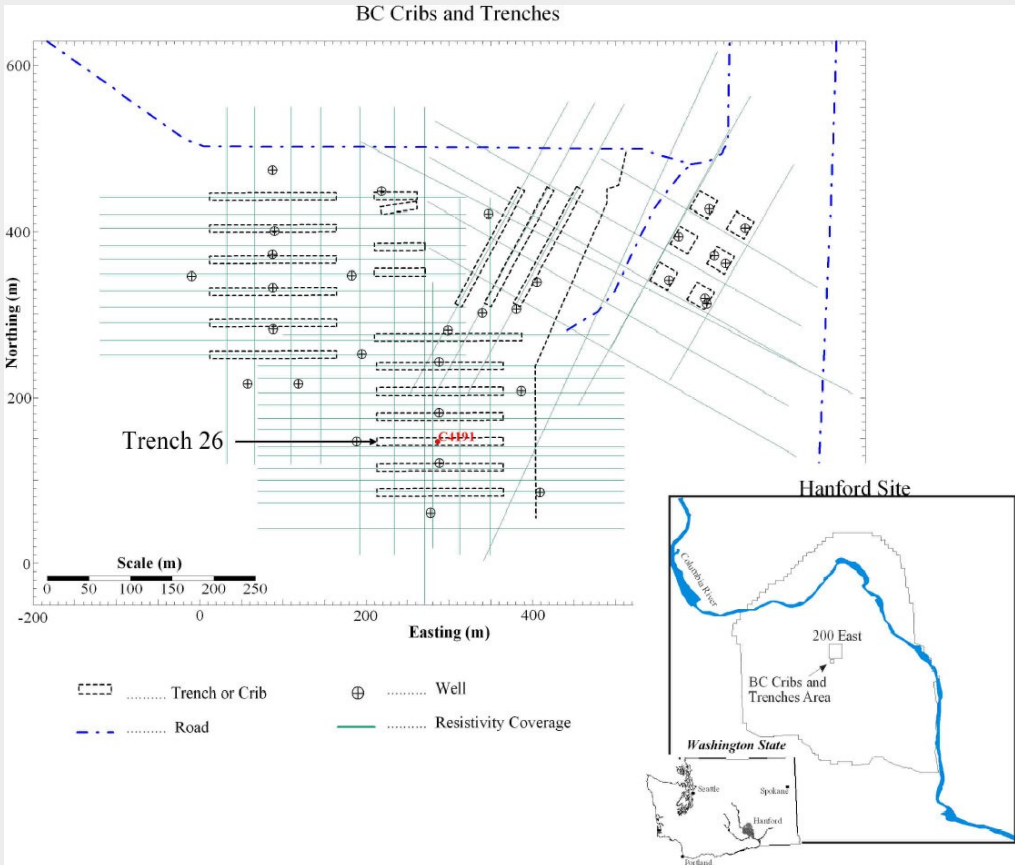


Distorted Grid Method



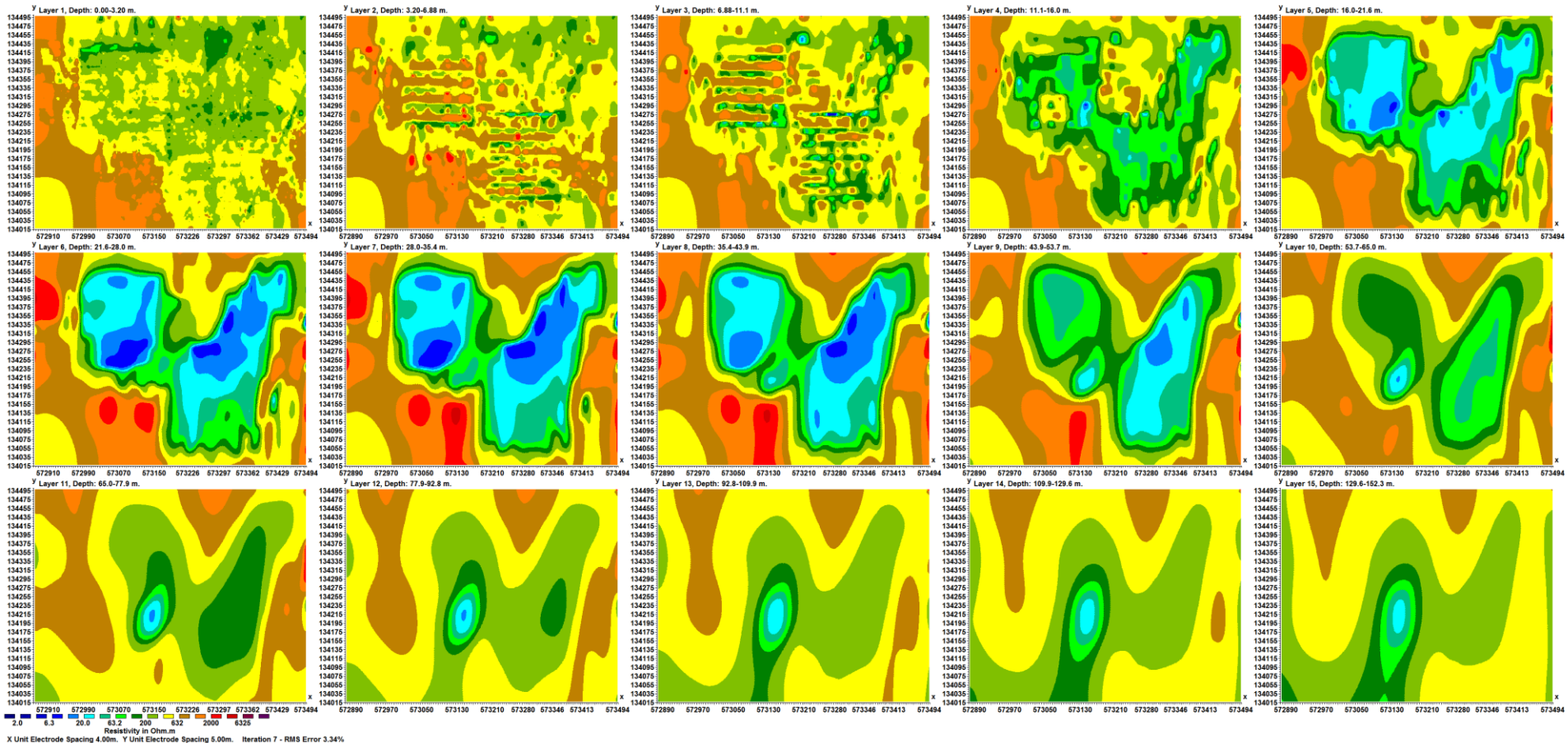
# Example field survey with lines in different directions

This example is from the Hanford site where the waste material was stored in trenches and concrete cribs. Different resistivity survey phases were carried out using 2-D lines. The distribution of the electrodes does not fit into a simple rectangular grid. This data set had 5598 electrode positions and 86697 data points. The pole-pole array was used in this survey. While most of the lines used an electrode spacing of 3 meters, there were some readings that had closer spacings due to survey site constraints.



# Inversion model for Hanford data set

Below is an inversion model of the data set. Note the prominent low resistivity zones indicating leakage zones. The linear features in the 2nd and 3rd layers are due to the trenches and concrete concrete cribs. The low resistivity anomaly that extends to the deepest layers is probably a metallic pipe.



# 3-D electrical imaging surveys : Summary

3-D surveys now play an increasingly important role in very complex areas, particularly for mineral exploration where the extra cost is justified. In many cases the 3-D data set is collated from a series of parallel 2-D survey lines to reduce the survey time and cost.

The pole-dipole and dipole-dipole arrays are widely used in mineral exploration surveys particularly with multi-channel I.P. systems. The Wenner-Schlumberger array is used in many engineering and environmental surveys, although the multiple gradient array will play an increasingly important role with multi-channel multi-electrode systems.

Fast computer software, and PCs with multi-core CPUs or multiple CPUs and at least 32 GB RAM, have reduced the computer processing time such that it has become practical to process 3-D data sets with thousands of electrode position, tens of thousands of measurements and model cells within hours.

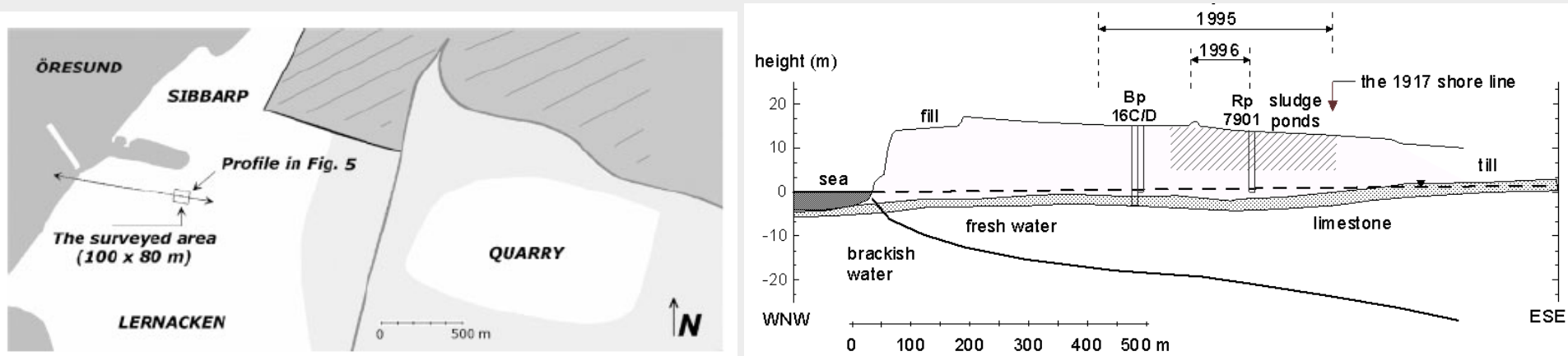
# **3-D Case Histories**

**Examples of 3-D field surveys**

# Example 1 – Landfill site, Sweden

The surveyed area is a former sludge disposal site, where liquid industrial waste was disposed in several shallow ponds. The site was later covered by earth resulting in a more or less flat surface. The site is situated in southern Sweden, at the abutment of the Öresund bridge, and has been previously investigated with DC resistivity imaging and electromagnetic profiling.

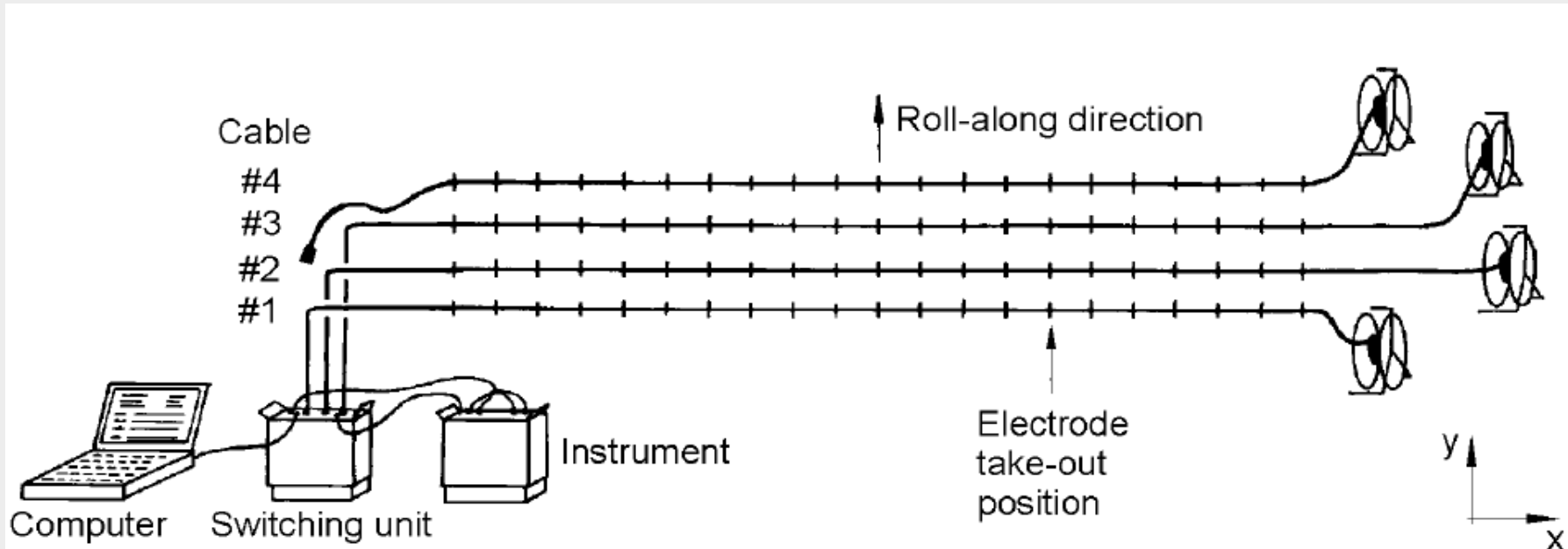
The figure below shows a geological cross-section of the survey site. Note the mound from the construction of the landfill site, and the boundary between the brackish and fresh water.



# Example 1 - Field survey procedure

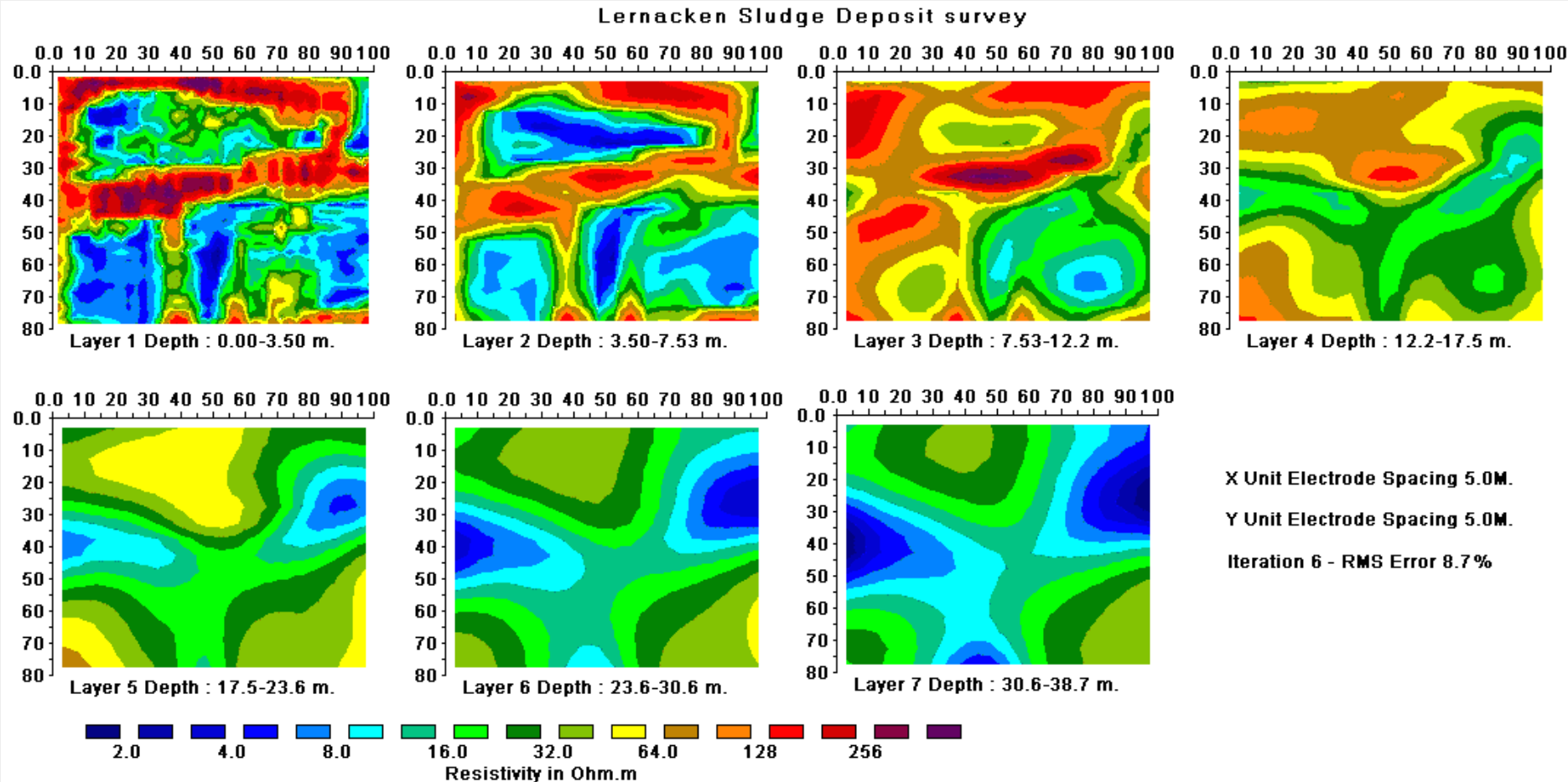
The Abem system was used with 3 cables each with 21 electrodes. The pole-pole array was used. The roll-along method in a direction perpendicular to the lines was carried out to extend the survey coverage.

Seven parallel multi-electrode cables were used to cover a 21 by 17 grid with a 5 m spacing between adjacent electrodes. There were a total number of 3840 data points in this data set.



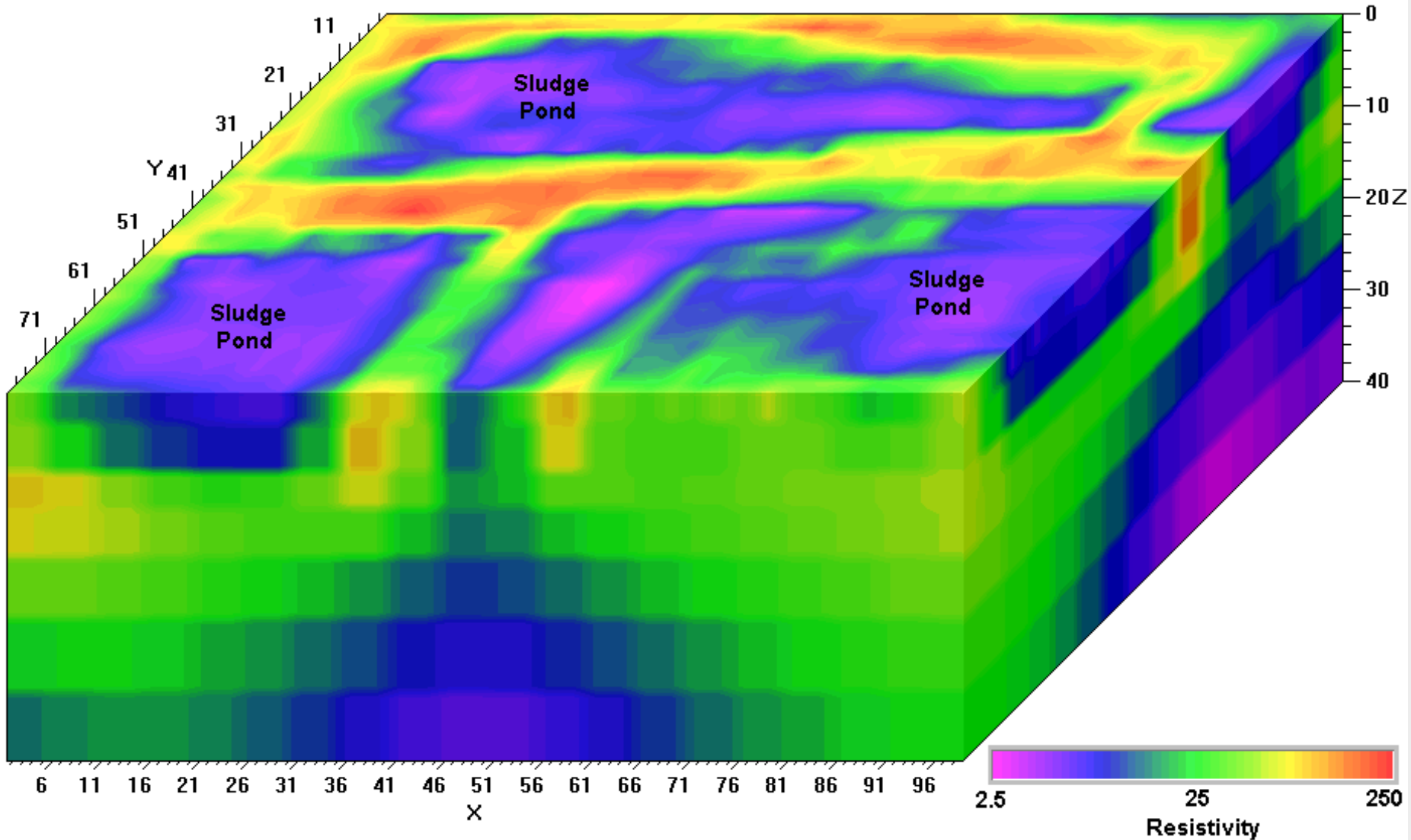
# Landfill site, Sweden (model depth sections)

The model obtained from the inversion of this data set is shown below. The former sludge ponds containing highly contaminated ground water show up as low resistivity zones in the top two layers. The low resistivity areas in the bottom two layers are due to saline water from the nearby sea.



# Landfill site, Sweden (Model 3-D view)

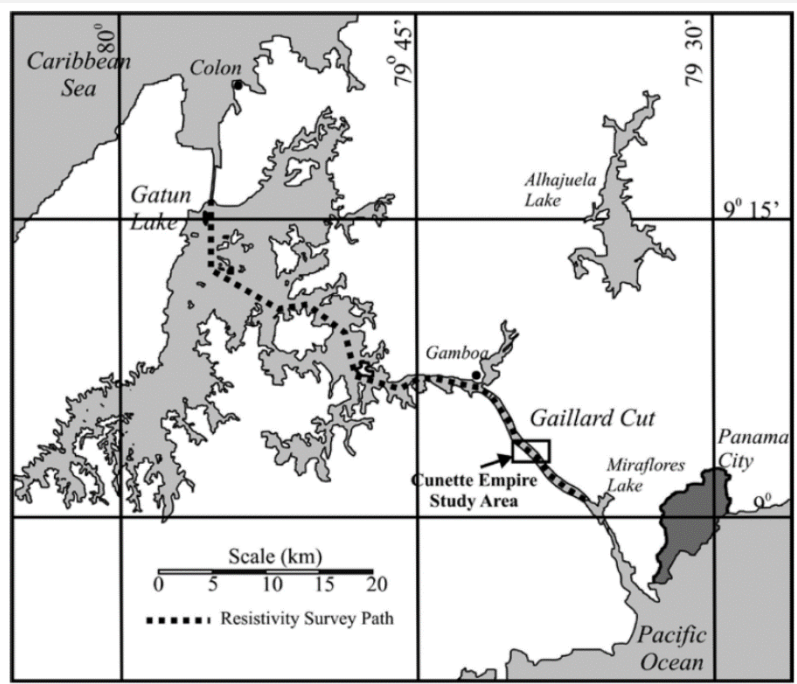
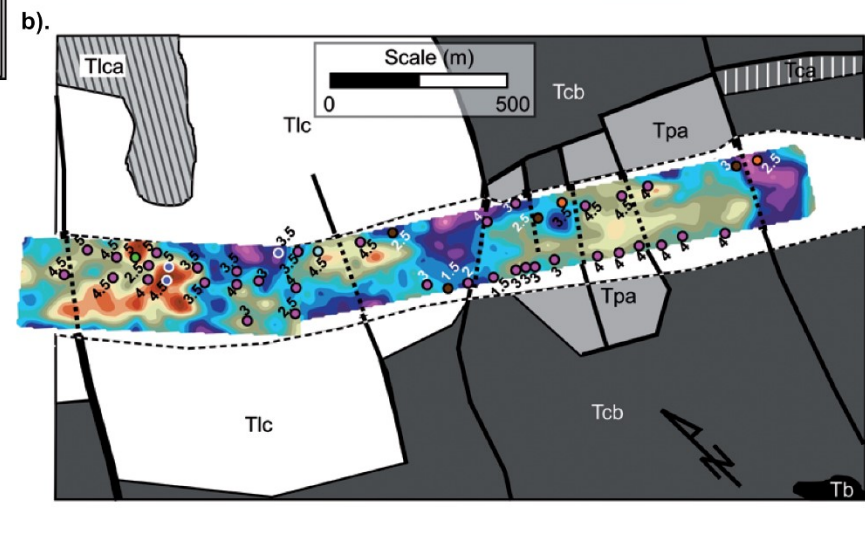
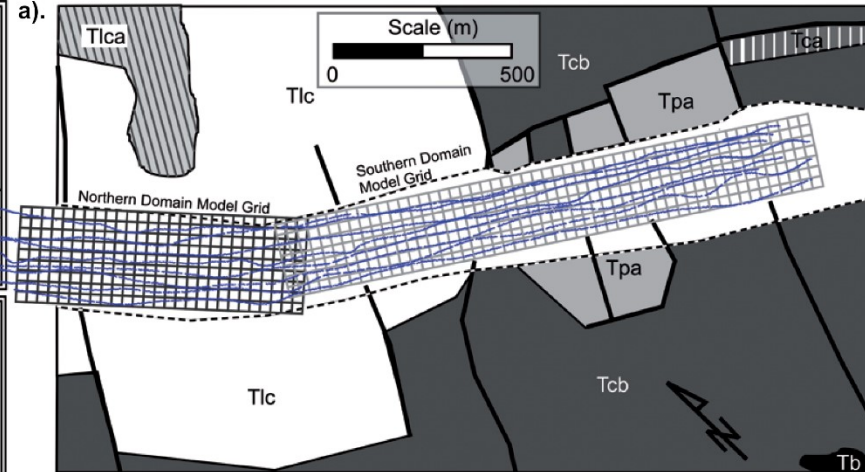
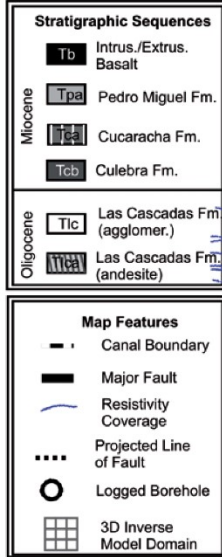
The figure below shows a 3-D plot of the inversion model using a 3-D contouring program.



# Example 2 – Streamer survey

This is from a survey with floating electrodes along the Panama Canal by HGI where sub-parallel lines were collated into a 3-D data set. The resistivity values of a section of the canal about 3 to 4 m below the canal bottom is shown. There is a positive correlation between resistivity and rock hardness.

Note the swaying of the survey lines with floating electrodes.

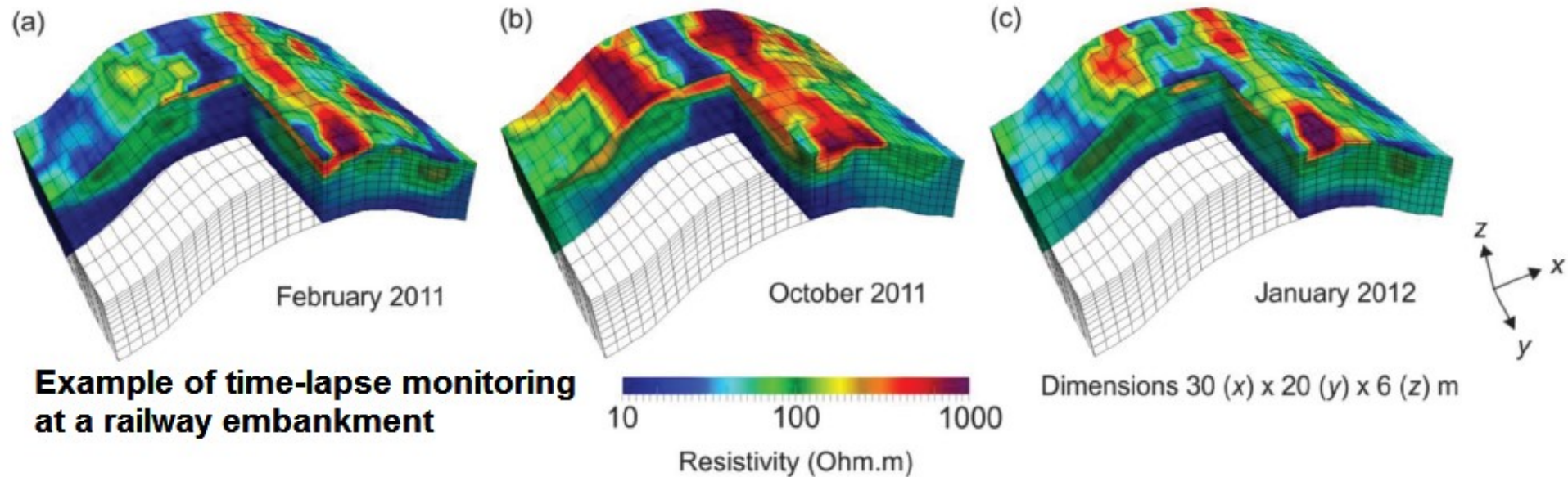


# Part 5

## 4-D surveys, data and inversion

# Time-lapse surveys

The measurements are repeated on the same site, using the same survey parameters, at different times. The surveys can be repeated along 2-D lines, or a grid of electrodes for a 3-D survey. The purpose is to monitor changes of the subsurface resistivity with time. Examples include mapping the flow of contaminants, change of water saturation due to water extraction, flow of water from the surface to the water table, production of methane gas in landfills, geological changes such as landslides.



# Time-lapse monitoring systems

Time-lapse surveys are used to monitor flow of fluids, possible landslides, landfill changes, leakages, aquifer drawdowns. Independent automatic systems that make the measurements at regular intervals and send the data over the Internet are now available, some with solar power. In some systems, the data are automatically processed and inverted in a central computer system that receives the data from the monitoring system.

Italy levee monitoring



U.K. landslide monitoring



Sweden landfill monitoring

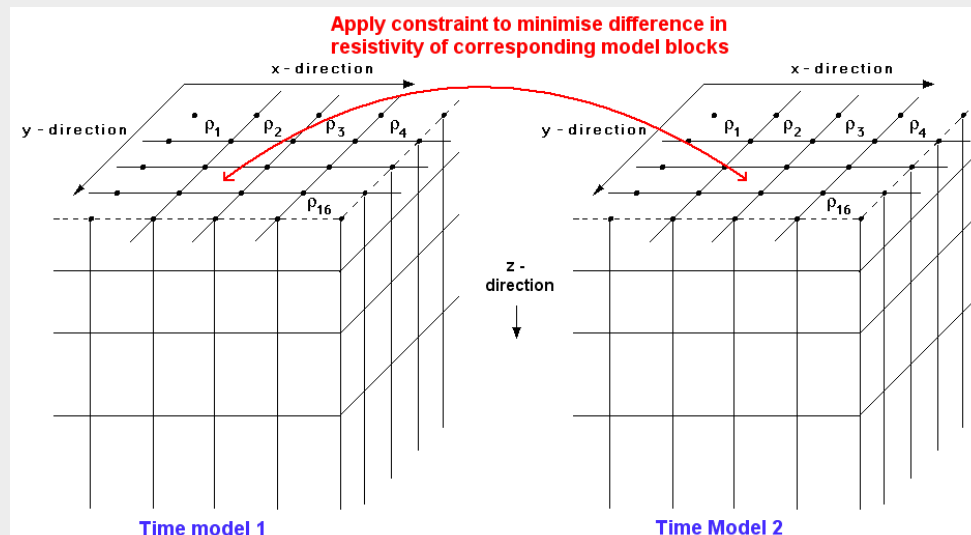


# Time-lapse surveys - inversion

The data from surveys at different times are inverted jointly using a constraint to minimize the change in the resistivity with time. We make use of the fact that the changes usually occur in a smooth manner with time. The equation used is as follows.

$$\left[ \mathbf{J}_i^T \mathbf{J}_i + \lambda_i (\mathbf{W}^T \mathbf{W} + \alpha \mathbf{M}^T \mathbf{M}) \right] \Delta \mathbf{r}_i = \mathbf{J}_i^T \mathbf{g}_i - \lambda_i (\mathbf{W}^T \mathbf{W} + \alpha \mathbf{M}^T \mathbf{M}) \mathbf{r}_{i-1}$$

The  $\mathbf{M}$  difference matrix is applied across the time models to minimize the difference in the resistivity of each model cell and the corresponding cell for the next temporal model. The parameter  $\alpha$  is the temporal damping factor that gives the relative weight for minimizing the change in the resistivity between one temporal model and the next model.



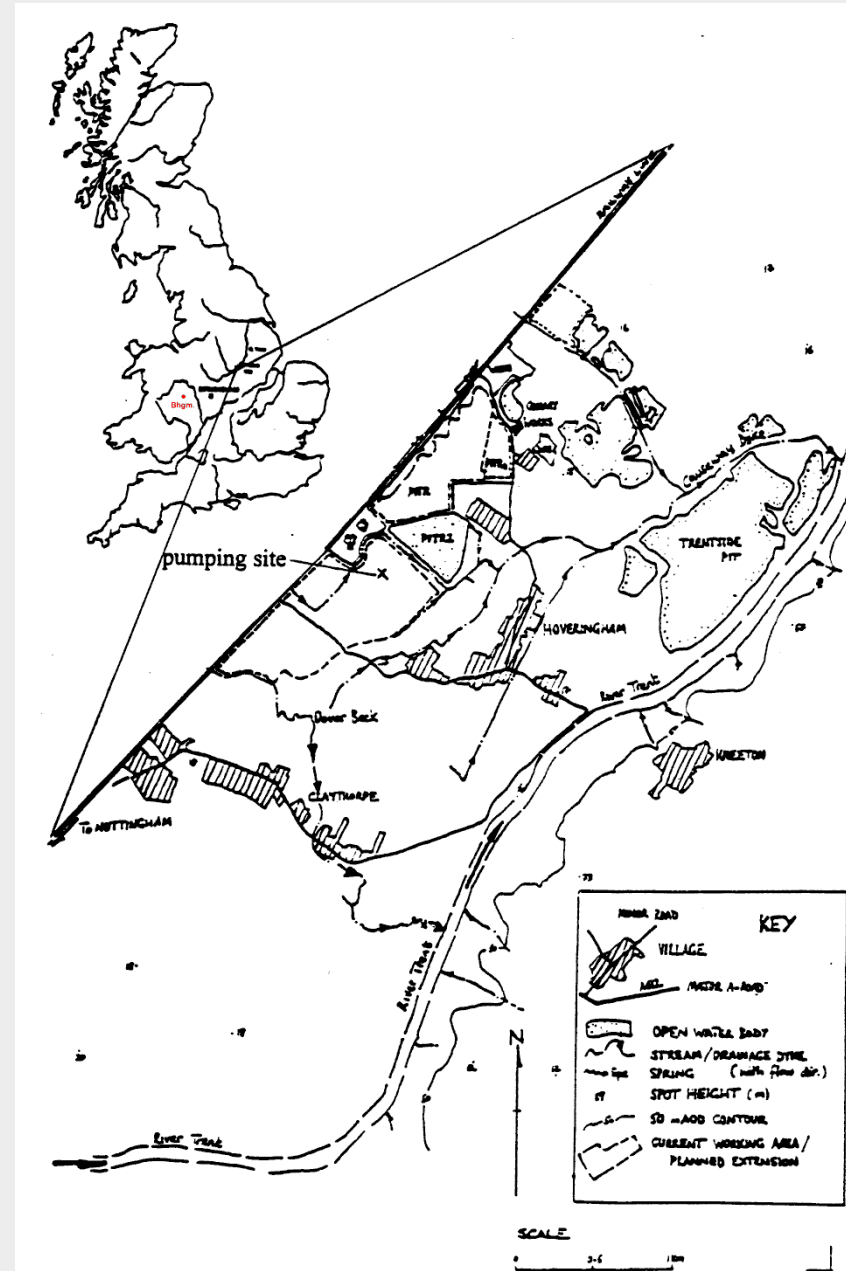
# **4-D Case Histories**

**Example of 4-D field surveys**

# Example 1 : Pumping test at Hoveringham area, U.K.

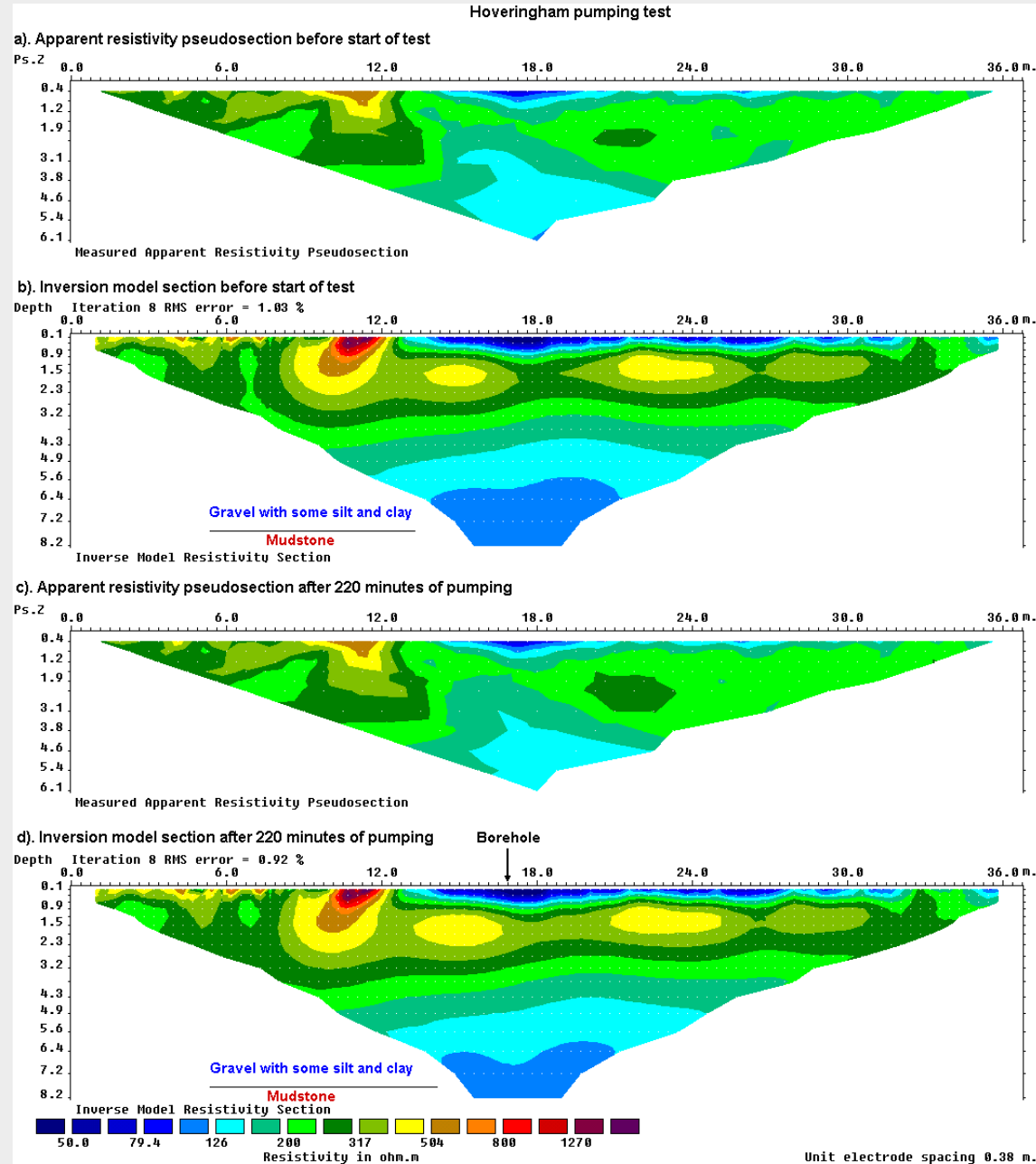
This survey was from an experiment to map the change in the groundwater level during a pumping test in a farm in Western Central England.

Water was pumped for about 220 minutes from a borehole. Measurements were made before, during and after the pumping.



# Hoveringham data set – data and models

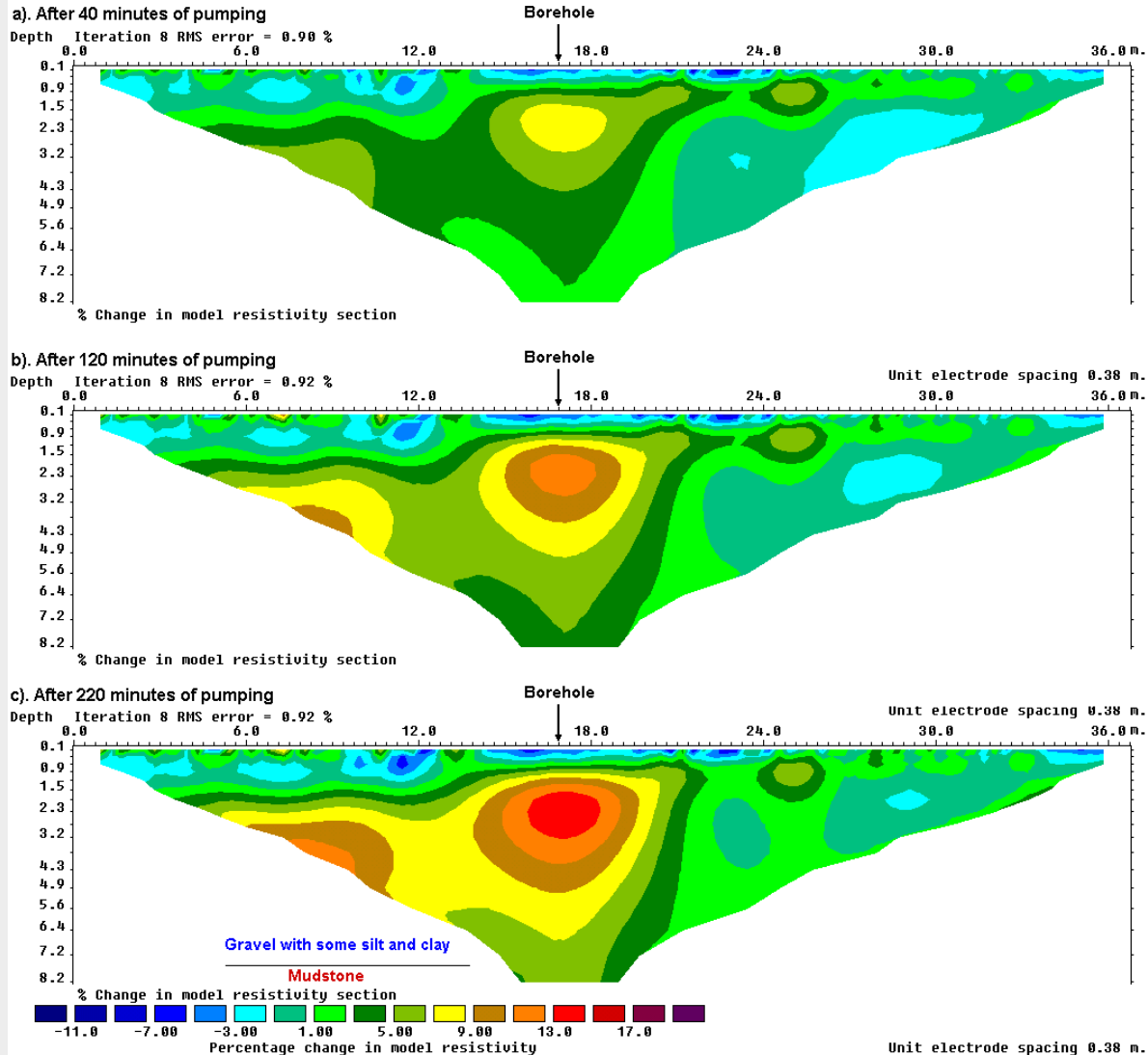
- (a) Apparent resistivity pseudosection and
- (b) inversion model for data set before the start of the pumping test.
- (c) Apparent resistivity pseudosection and
- (d) inversion model for data set after 220 minutes of continuous pumping.



# Hoveringham data set : change in resistivity

To show the change in resistivity more clearly, we take the difference in the logarithm of the model resistivity values.

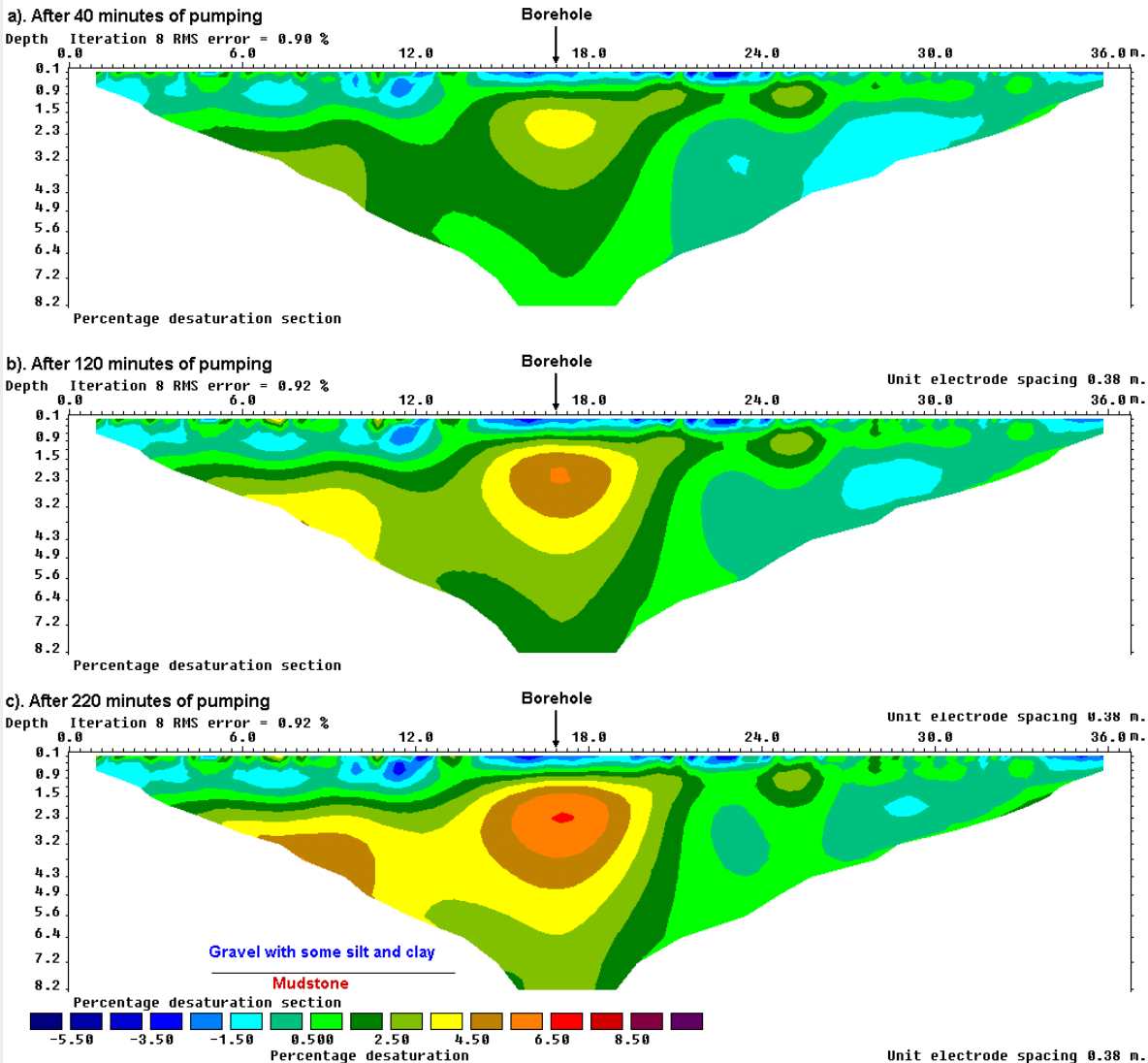
Sections showing the percentage change in the subsurface resistivity values with time obtained from the inversion of the data sets collected during the different stages of the pumping test.



# Hoveringham data set : change in saturation

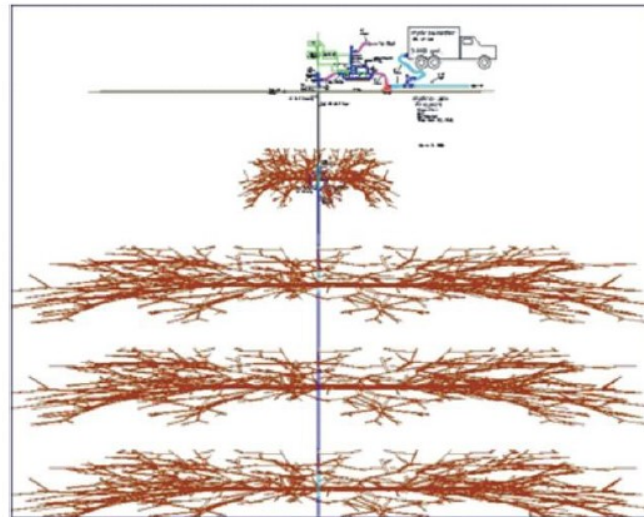
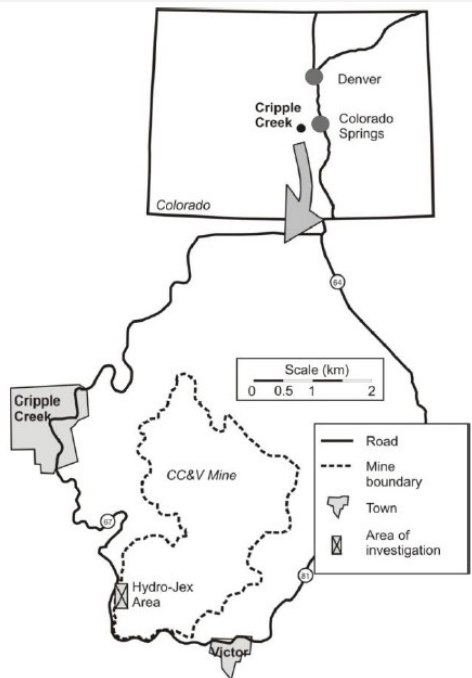
We can also calculate the change in the water saturation from the change in the resistivity using Archie's Law.

Sections showing the percentage desaturation values obtained from the inversion models of the data sets collected during the different stages of the pumping test.



# 3-D time-lapse example –AnglogoldAshanti USA

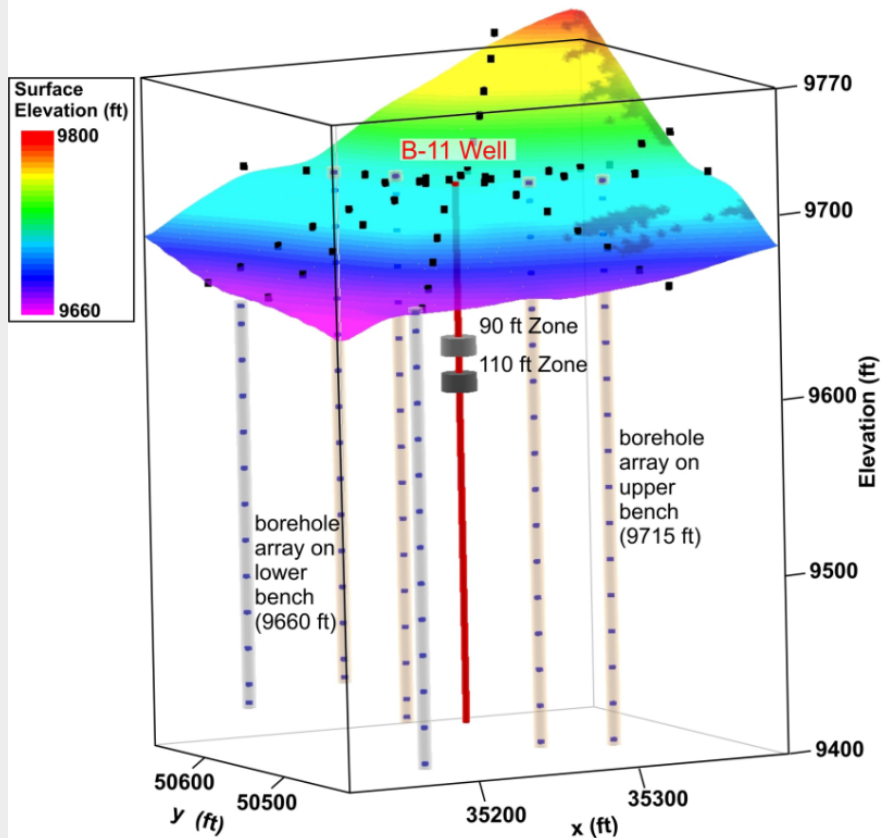
This example is from an injection experiment at the Cripple Creek and Victor Gold Mine, in Colorado, USA. A dilute sodium cyanide solution was injected at high pressures into an engineered rock pile to increase the extraction of gold as a means of secondary recovery after surface leaching had ceased. The figure shows an illustration of the Hydro-Jex method with four discrete injection zones. The picture shows Hydro-Jex unit.



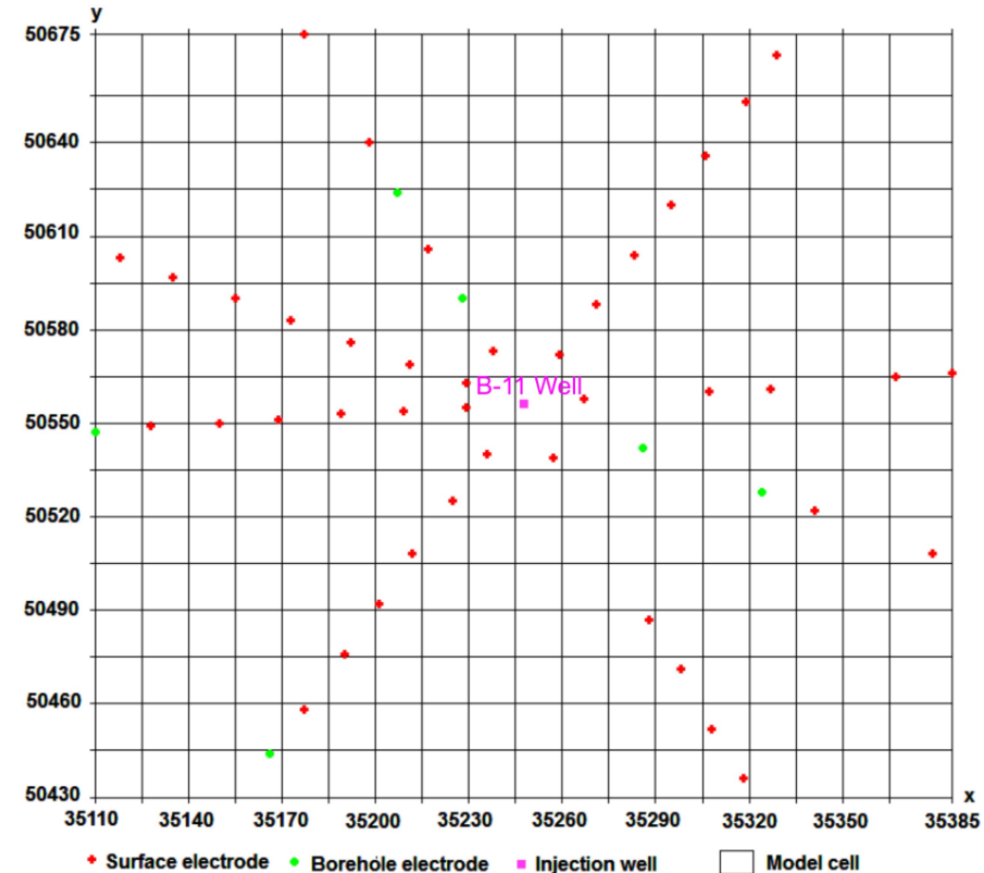
# AnglogoldAshanti USA – survey procedure

A resistivity survey was conducted to better understand the direction of flow and area of influence of the pressured injections. Resistivity measurements were made with the pole-pole array using 48 surface electrodes placed along 8 radials, 94 electrodes within 6 boreholes, and 8 long electrodes using steel-cased injection wells.

(a) 3D view of survey design



(b) Overhead view of model discretisation



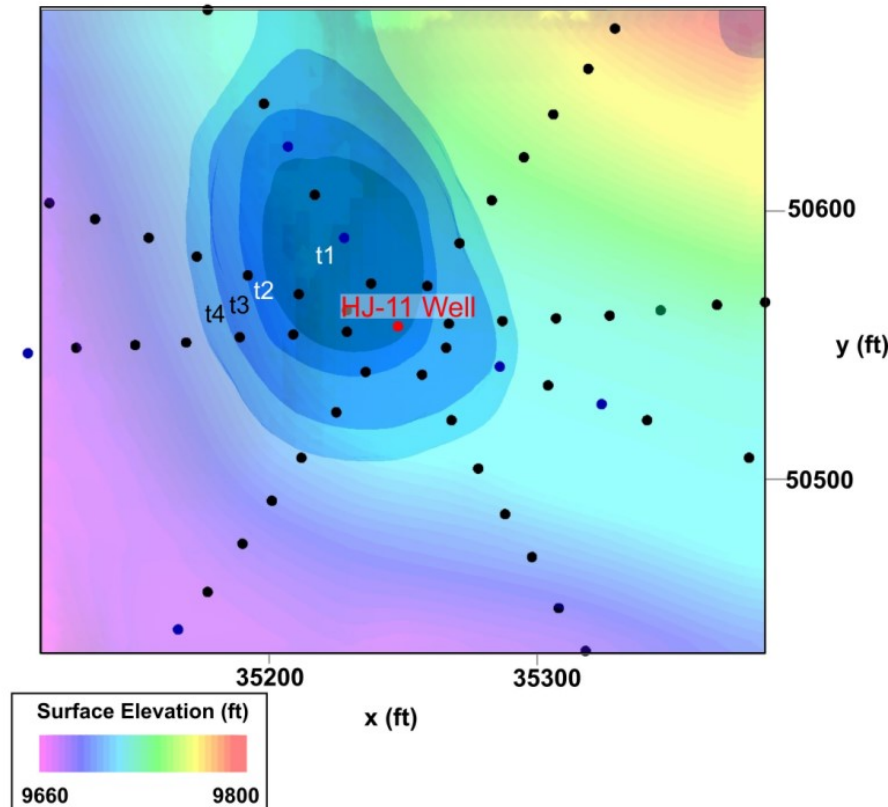
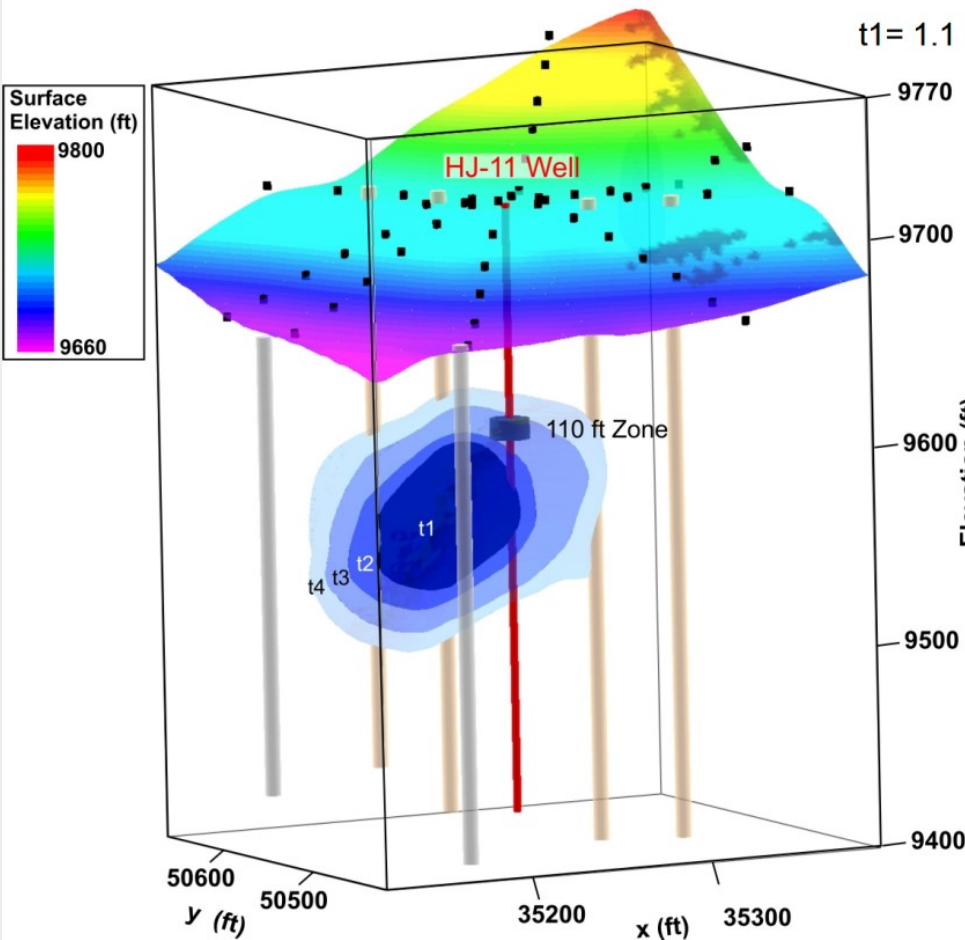
# AnglogoldAshanti USA - results

A sample of the injection results is shown. Injections were made at 90 ft and 110 ft below the ground surface. The figure shows the change in the resistivity (of -4%) in the form of 3-D iso-contours that better illustrates the migration of the solution.

(a) 3D view of inversion results

(b) Overhead view of inversion results

t1= 1.1 hours, t2= 2.4 hours, t3= 3.7 hours, t4= 4.9 hours



# Example 3 – AnglogoldAshanti USA

Below is a time-lapse video constructed from 137 snap-shots.



# Closing remarks on 2-D, 3-D and 4-D surveys

2-D surveys constitute the bulk of field surveys. They are simple and inexpensive to carry out.

3-D surveys are necessary to resolve complex structures. Most 3-D data sets are collated from 2-D surveys lines that are sufficiently close to each other. This provides a practical method to obtain a 3-D model of the subsurface in an inexpensive manner.

4-D surveys are used to map temporal changes in areas such as landslide monitoring, subsurface movement of fluids.

# Special Topics

For own reading.

1). Model reliability

2). Banding effects in 3-D surveys

# **Model reliability**

**Different estimates of model reliability**

**Sensitivity**

**Covariance matrix**

**DOI**

**Model Resolution**

# Model reliability

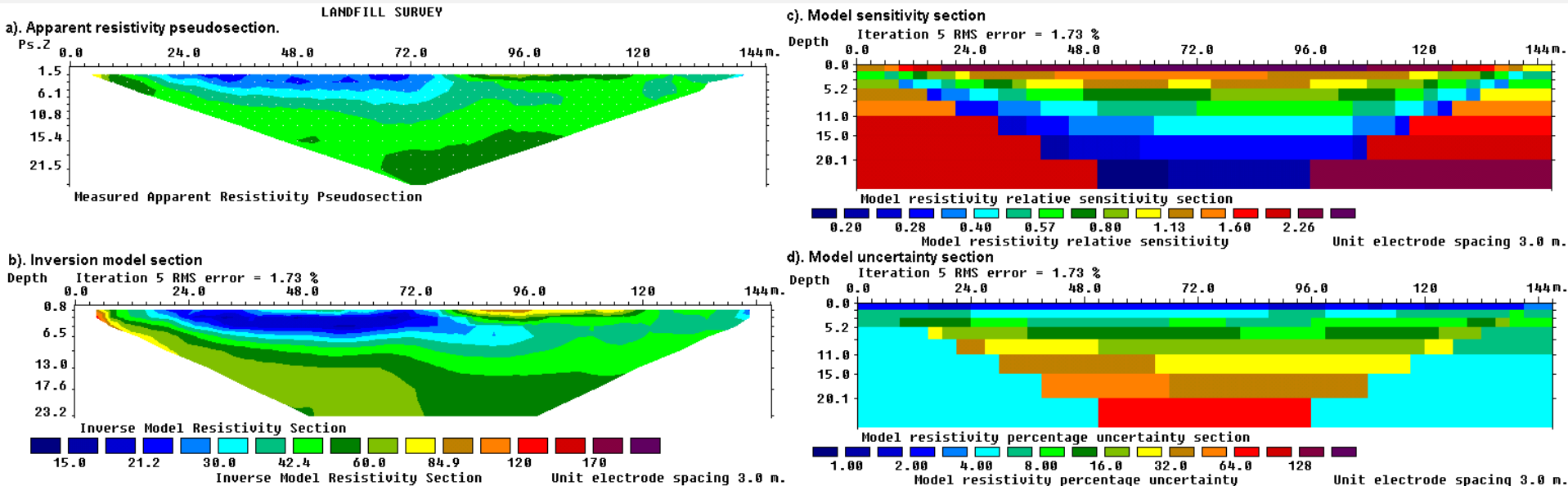
A 2-D survey typically has hundreds of data points collected with electrodes at different locations and spacings. We want to know the regions of the subsurface sensed by the survey, and the reliability of the results.

## Sensitivity values

One method is to use the 'sensitivity' values, i.e. elements of the Jacobian matrix associated with the model cells. In the RES2DINV and RES3DINV programs, the sum of the absolute values of the sensitivity values associated with the model cell is used. The sensitivity value is a measure of the amount of information about the resistivity of a model block cell in the measured data set. The higher the sensitivity value, the more reliable is the model resistivity value. In general, the cells near the surface usually have higher sensitivity values because the sensitivity function has very large values near the electrodes.

# Model reliability - sensitivity

Figure shows the model section obtained from the inversion of a data set for a survey to map leakage of pollutants from a landfill site. The model sensitivity section in shows high sensitivity values near the surface with decreasing values with depth. This is to be expected as the near surface materials have a larger influence on the measured apparent resistivity values. The large values at the sides are due to the larger sizes of the side model cells (the sensitivity values have not been normalized for the size of the cells).



# Model reliability – DOI

The depth of investigation (DOI) method carries out two inversions of the data set using different reference models using the following least-squares equation.

$$\left(\mathbf{J}^T \mathbf{J} + \lambda \mathbf{F}_R\right) \Delta \mathbf{q}_k = \mathbf{J}^T \mathbf{R}_d \mathbf{g} - \lambda \mathbf{F}_R (\mathbf{q}_k - \mathbf{q}_0), \text{ where } \mathbf{F}_R = \alpha_s + \alpha_x \mathbf{C}_x^T \mathbf{R}_m \mathbf{C}_x + \alpha_z \mathbf{C}_z^T \mathbf{R}_m \mathbf{C}_z$$

$\mathbf{q}_0$  is a homogeneous half-space reference model and  $\alpha_s$  is an additional “self” damping factor that has a value of about 0.01 times the  $\alpha_x$  and  $\alpha_z$  damping factors.

The DOI method carries out two inversions using different resistivity values for the reference model. The second reference model usually has a resistivity of 10 to 100 times the first reference model.

The DOI value is then calculated from the difference in the inversion models.

# Model reliability – DOI

The DOI value is calculated using the following equation.

$$R(x, z) = \frac{m_1(x, z) - m_2(x, z)}{m_{1r} - m_{2r}}$$

$m_{1r}$  and  $m_{2r}$  are the resistivity of first and second reference models,  $m_1(x, z)$  and  $m_2(x, z)$  are model cell resistivity obtained from the first and second inversions.

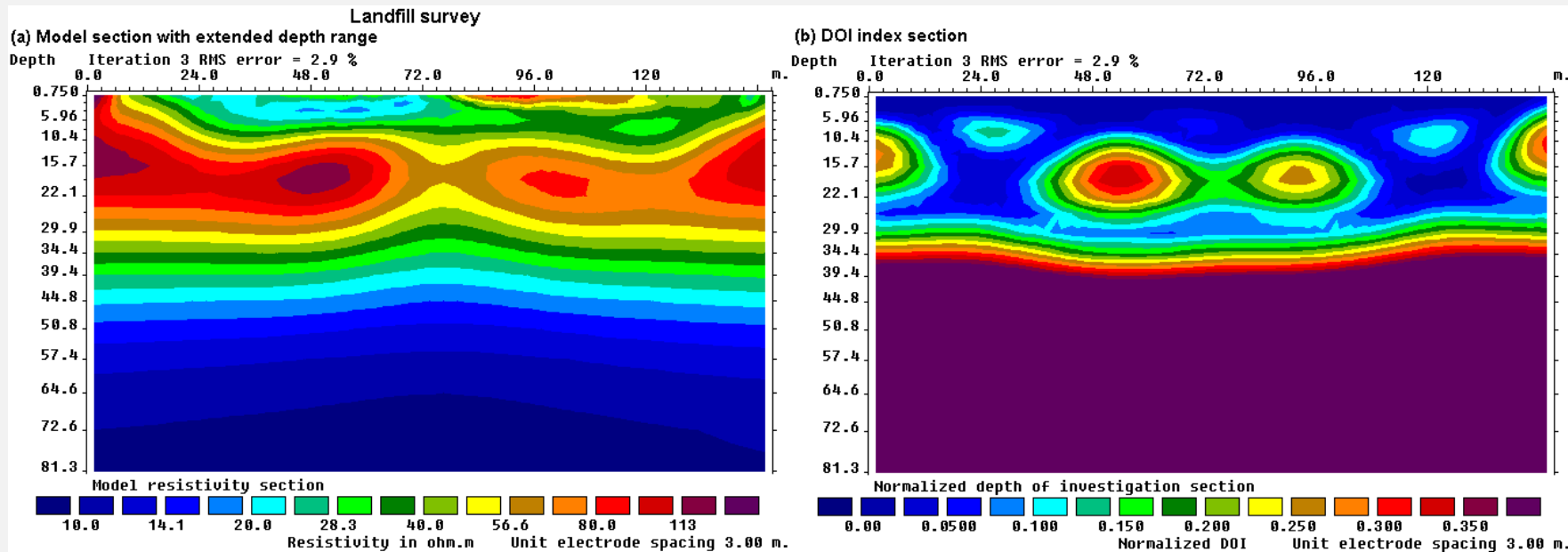
$R$  will approach a value of 0 where the inversion will produce the same cell resistivity regardless of the reference model resistivity. In such areas, the cell resistivity is well constrained by the data.

In areas where the data do not have much information about the cell resistivity,  $R$  will approach a value of 1 as the cell resistivity will be similar to the reference resistivity.

The model resistivity in areas where  $R$  has small values are considered to be “reliable”, while in areas with high  $R$  values are not reliable.

# Model reliability – Landfill DOI example

The figure below shows the inverse model and DOI section for the landfill survey data set. A value of 0.1 is used as the cut-off limit for the effective depth of investigation. The depth to the 0.1 DOI contour is about 27 m along most of the survey line, compared to 25 m for the maximum median depth of investigation. The shallower regions with high DOI values below the 50 m mark is probably due to the low resistivity plume that limits the amount of current flowing into the deeper sections below it. The regions at the sides of the section have high DOI values because of less data coverage.



# **DOI model reliability - remarks**

**The DOI method is useful in marking the regions where the model values are well constrained by the data set, and thus greater confidence can be placed on the model resistivity values at such regions.**

**The DOI method may be considered an empirical method to determine the regions where we can reasonably resolve the subsurface.**

# Resolution of data sets and models

**Use of model resolution to quantify the information in a data set and inversion model sections.**



# Model resolution equation

The model resolution equation is related to the least-squares equation which is given by

$$\left(\mathbf{J}^T \mathbf{J} + \lambda \mathbf{F}\right) \Delta \mathbf{q}_k = \mathbf{J}^T \mathbf{g} - \lambda \mathbf{F} \mathbf{q}_k$$

The relation between the calculated model resistivity and the true resistivity is approximately given by

$$\mathbf{q}_{\text{Model}} \approx \left(\mathbf{J}^T \mathbf{J} + \lambda \mathbf{F}\right)^{-1} \mathbf{J}^T \mathbf{J} \mathbf{q}_{\text{Actual}}$$

To show the relationship better, we rewrite it as

$$\mathbf{q}_{\text{Model}} \approx \mathbf{R} \mathbf{q}_{\text{Actual}}, \quad \mathbf{R} = \left(\mathbf{J}^T \mathbf{J} + \lambda \mathbf{F}\right)^{-1} \mathbf{J}^T \mathbf{J}$$

The R matrix is called the resolution matrix.

It can be considered as a ‘filter’ or ‘distorting lens’ through which we see the subsurface.

# Model resolution – seeing through a distorting lens

The effect of the model resolution matrix can be shown qualitatively below. Consider an original image, such as

The image shows the letters 'ABC' in a bold, black, sans-serif font. The letters are sharp and well-defined against a white background.

A person with less than perfect eyesight might see it as

The image shows the letters 'ABC' in a bold, black, sans-serif font. The letters are significantly blurred, with soft edges and some loss of detail, representing a lower resolution or a 'distorting lens' effect.

Someone with very poor eyesight might see it as

The image shows the letters 'ABC' in a bold, black, sans-serif font. The letters are extremely blurred and indistinct, appearing as soft, dark shapes, representing a very low resolution or a very poor 'distorting lens' effect.

The matrix  $R$  can be considered as a ‘blurring’ matrix that contaminates the calculated model value with values from nearby cells.

# Model resolution – simple example

Consider as simple model with only 4 cells.

The relationship between the calculated resistivity value for each cell and the true cell resistivity value is given by

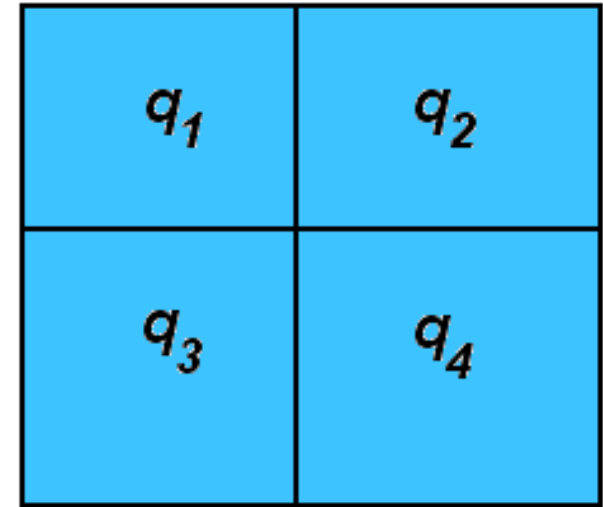
$$\mathbf{q}_{\text{Model}} \approx \mathbf{R} \mathbf{q}_{\text{Actual}}, \quad \mathbf{R} = (\mathbf{J}^T \mathbf{J} + \lambda \mathbf{F})^{-1} \mathbf{J}^T \mathbf{J}$$

This can be written in matrix form as

$$\begin{pmatrix} q_{M1} \\ q_{M2} \\ q_{M3} \\ q_{M4} \end{pmatrix} = \begin{pmatrix} R_{11} & R_{12} & R_{13} & R_{14} \\ R_{21} & R_{22} & R_{23} & R_{24} \\ R_{31} & R_{32} & R_{33} & R_{34} \\ R_{41} & R_{42} & R_{43} & R_{44} \end{pmatrix} \begin{pmatrix} q_{A1} \\ q_{A2} \\ q_{A3} \\ q_{A4} \end{pmatrix}$$

$\mathbf{q}_{\text{Model}} = \mathbf{R} \mathbf{q}_{\text{Actual}}$

Model with 4 cells



# Perfect model resolution example

So far we have the model resolution matrix

$$\begin{pmatrix} q_{M1} \\ q_{M2} \\ q_{M3} \\ q_{M4} \end{pmatrix} = \begin{pmatrix} R_{11} & R_{12} & R_{13} & R_{14} \\ R_{21} & R_{22} & R_{23} & R_{24} \\ R_{31} & R_{32} & R_{33} & R_{34} \\ R_{41} & R_{42} & R_{43} & R_{44} \end{pmatrix} \begin{pmatrix} q_{A1} \\ q_{A2} \\ q_{A3} \\ q_{A4} \end{pmatrix}$$

$\mathbf{q}_{\text{Model}} = \mathbf{R} \mathbf{q}_{\text{Actual}}$

Model with 4 cells

$q_1$	$q_2$
$q_3$	$q_4$

If the cells are perfectly resolved, the diagonal elements of the resolution matrix are 1.0 and other elements are 0.0.

This means the calculated value for each cell only depends on the true value.

$$\begin{pmatrix} q_{M1} \\ q_{M2} \\ q_{M3} \\ q_{M4} \end{pmatrix} = \begin{pmatrix} 1.0 & 0.0 & 0.0 & 0.0 \\ 0.0 & 1.0 & 0.0 & 0.0 \\ 0.0 & 0.0 & 1.0 & 0.0 \\ 0.0 & 0.0 & 0.0 & 1.0 \end{pmatrix} \begin{pmatrix} q_{A1} \\ q_{A2} \\ q_{A3} \\ q_{A4} \end{pmatrix}$$

# Imperfect model resolution example

In the case with imperfect resolution, the matrix might be like

$$\begin{pmatrix} q_{M1} \\ q_{M2} \\ q_{M3} \\ q_{M4} \end{pmatrix} = \begin{pmatrix} 0.7 & 0.1 & 0.1 & 0.1 \\ 0.1 & 0.7 & 0.1 & 0.1 \\ 0.1 & 0.1 & 0.5 & 0.3 \\ 0.1 & 0.1 & 0.3 & 0.5 \end{pmatrix} \begin{pmatrix} q_{A1} \\ q_{A2} \\ q_{A3} \\ q_{A4} \end{pmatrix}$$

$\mathbf{q}_{\text{Model}} = \mathbf{R} \mathbf{q}_{\text{Actual}}$

Model with 4 cells

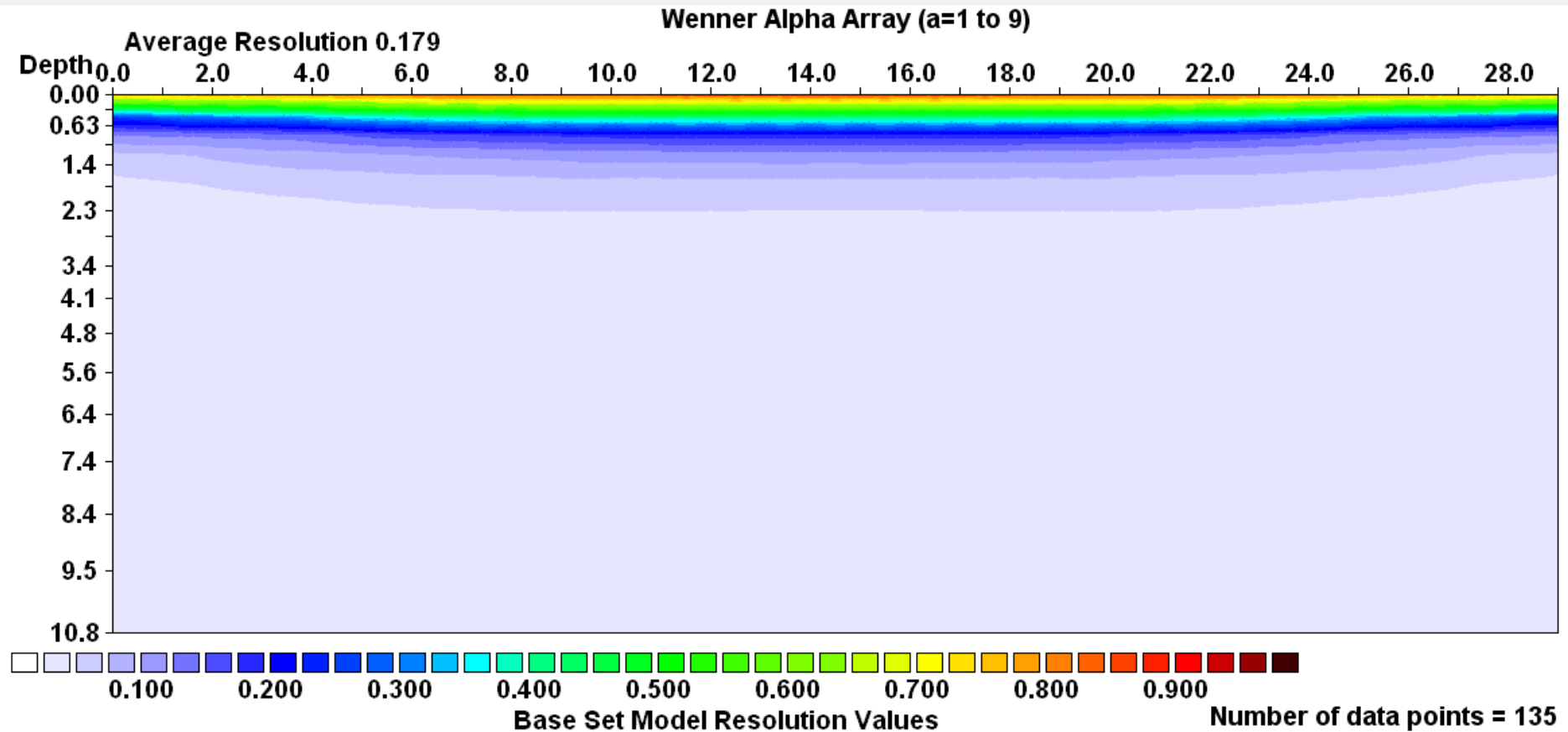
$q_1$	$q_2$
$q_3$	$q_4$

The diagonal elements give the ‘degree’ of resolution, while the off diagonal elements give the degree of ‘contamination’ or cross-correlation with the neighboring model cells.

One way to illustrate the resolution is to plot the values of the diagonal elements of the R matrix. This shows the degree at which the calculated model value depends on the true value. A value of about 0.05 (5%) is sometimes chosen as the ‘cutoff’ value.

# Model resolution – Wenner array survey

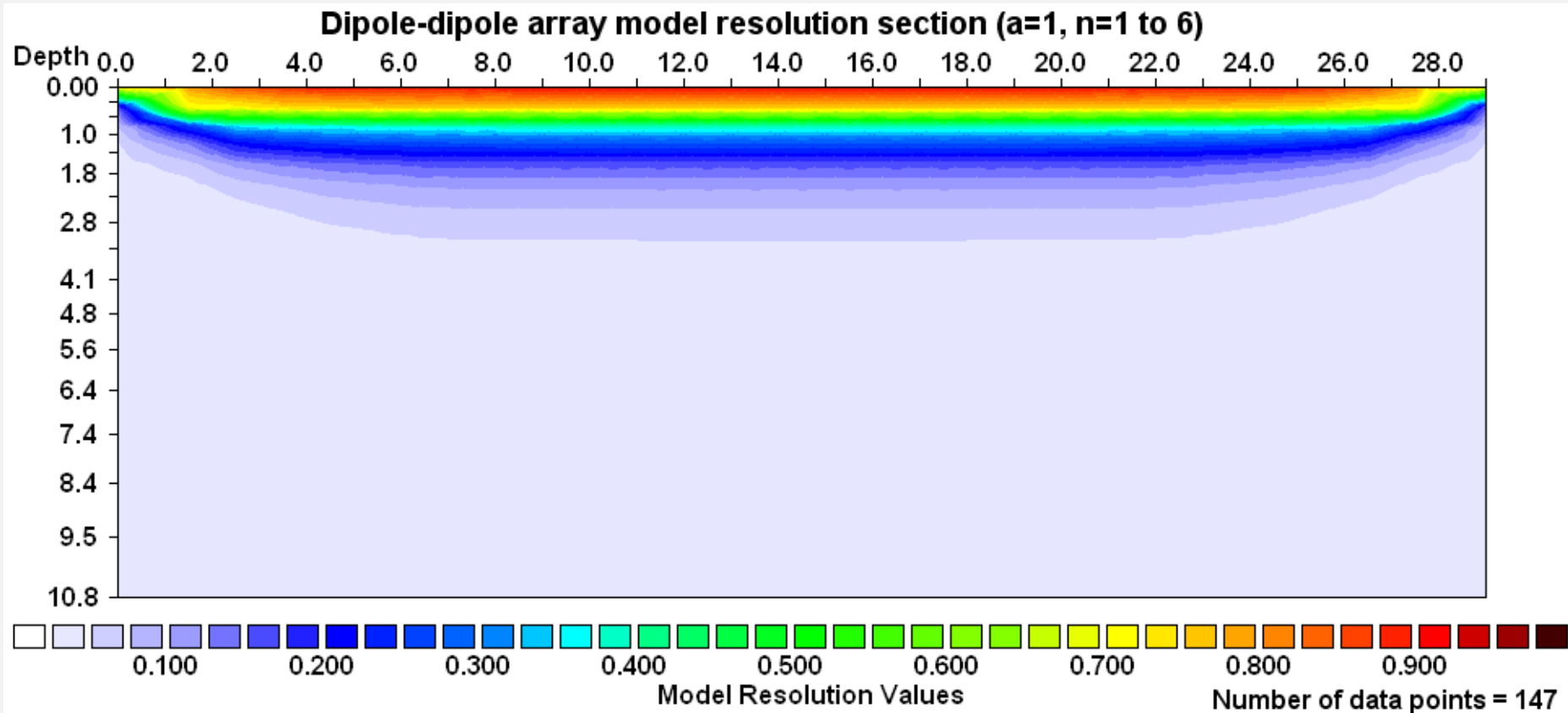
As an example, we use a survey line with 30 electrodes with 1 m spacing. First we look at the model resolution for a Wenner array survey with the ' $a$ ' spacing ranging from 1 to 9 m.



The resolution is greatest near the surface, decreases rapidly with depth, and is very small below a depth of about 2.0 m.

# Model resolution – dipole-dipole survey

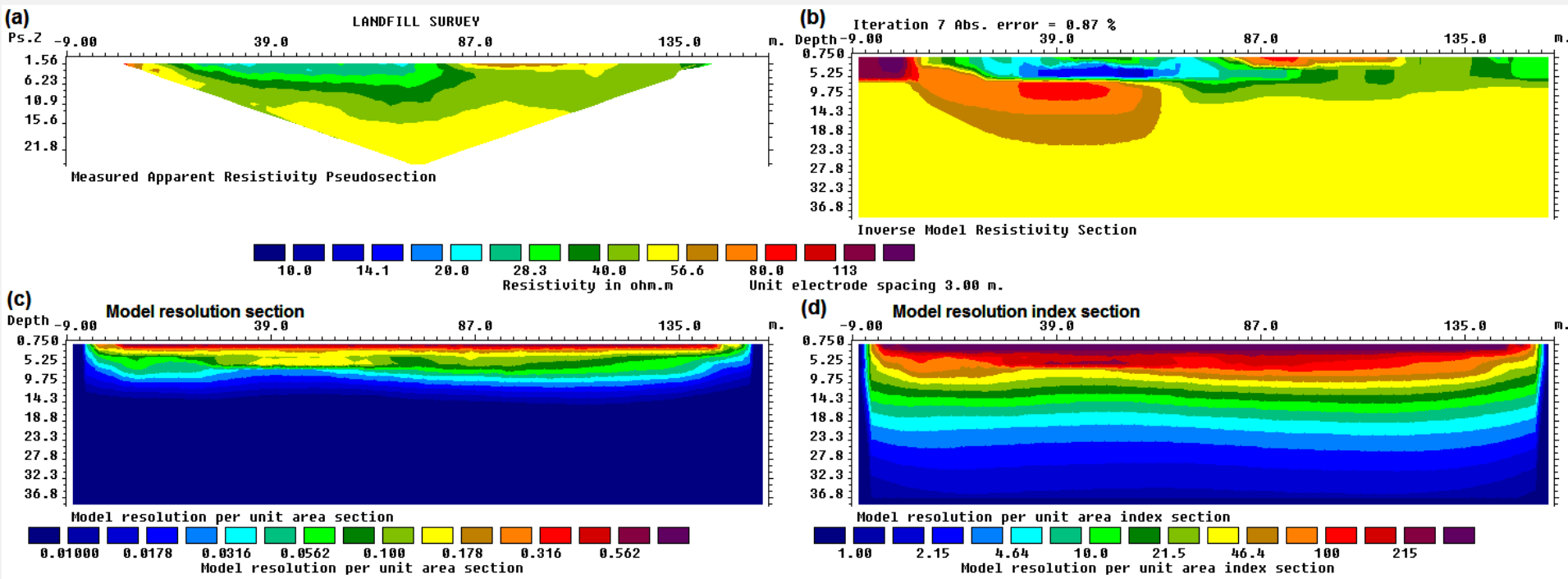
Next we check the resolution for a dipole-dipole survey carried out with  $a=1$ , and  $n=1$  to 6.



Note that the resolution is greatest near the surface, decreases rapidly with depth, and is not significant below a depth of about 3.0 to 3.5 meters. It has slightly more data points than the Wenner, and performs significantly better.

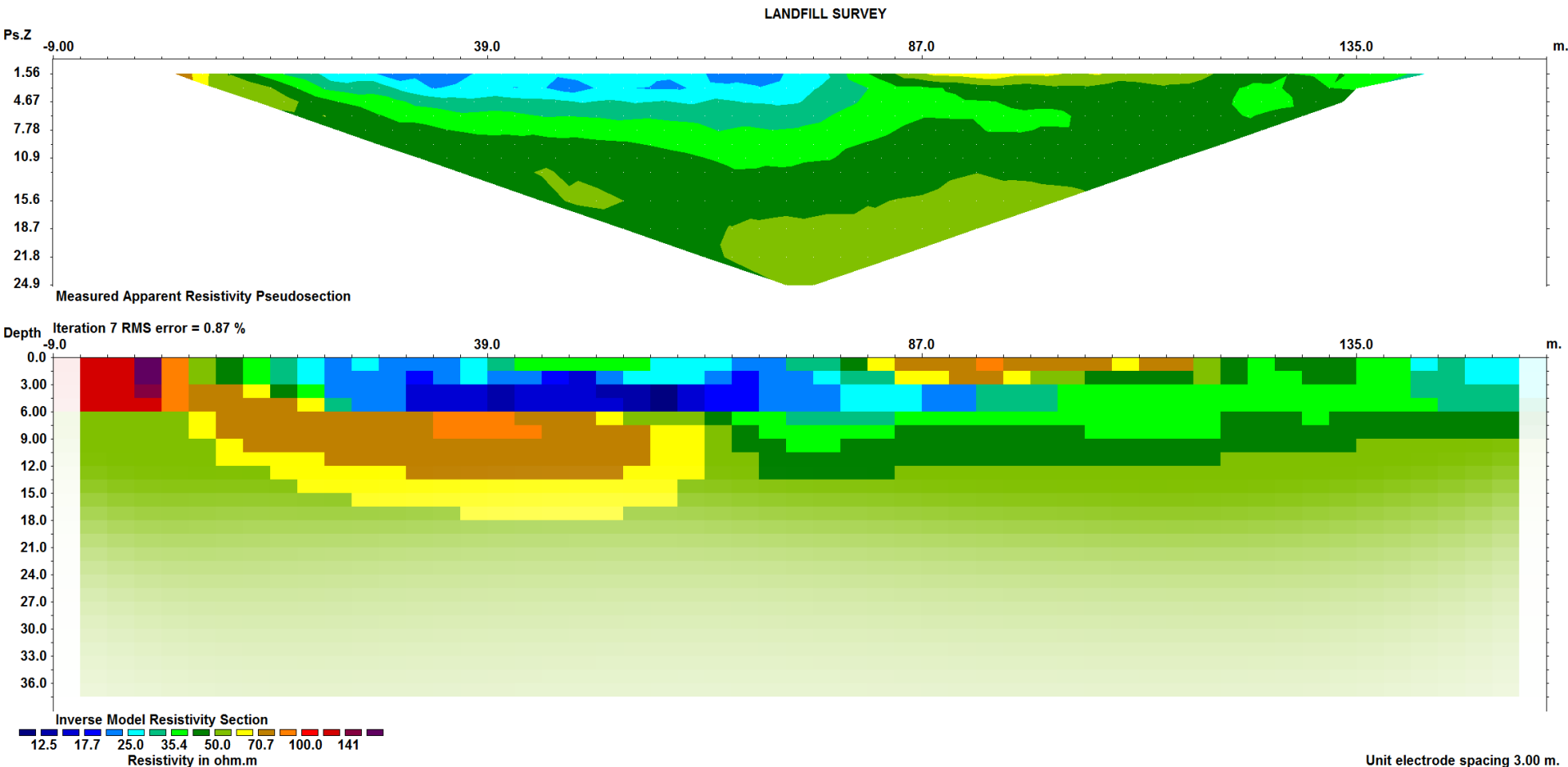
# Example of model resolution – landfill survey

The model resolution section is shown in (c). (d) shows the model resolution multiplied by the number of model cells to give an index value, i.e.  $R_{ij} \cdot m$ , to remove the effect of how finely we subdivide the subsurface. If a cut-off value of 5 is used for the index value, the depth with significant information is about 19 to 22 meters. Note the resolution values do not taper off towards the ends of the lines as rapidly as the pseudosection. The resolution values are slightly lower below the low resistivity landfill zone.



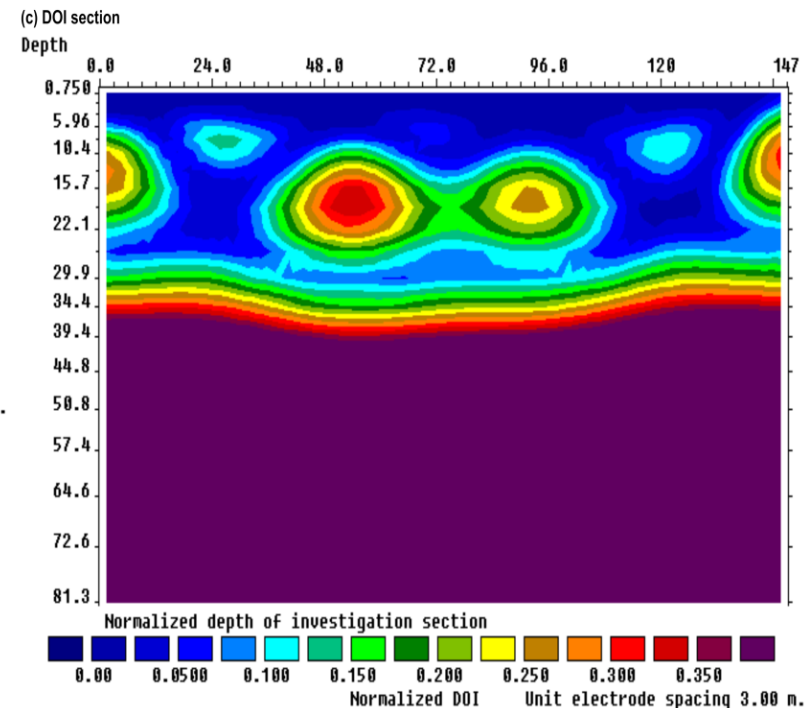
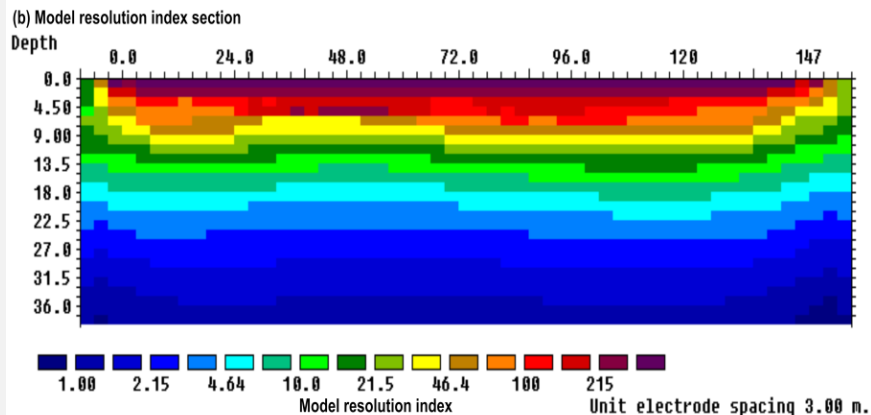
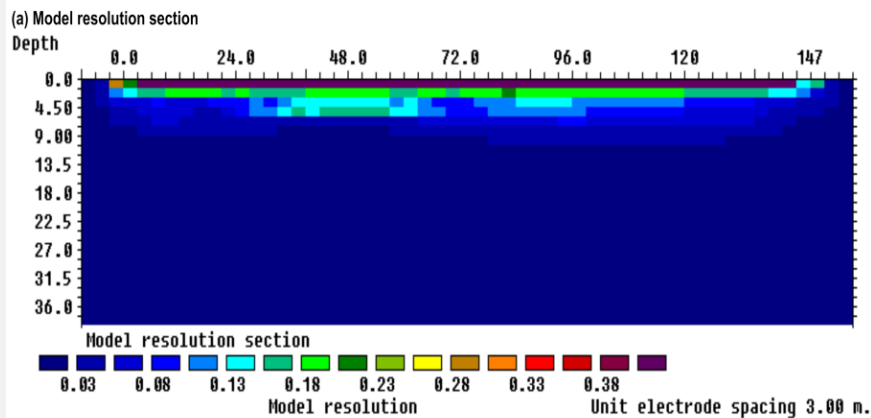
# Blanking out model using model resolution index

The model resolution values can be used to blank out parts of the model with low resolution values and are not reliable.



# Comparison of Resolution and DOI

The model resolution shows a more gradual change with depth (and also laterally) in the resolution values compared to the DOI. The 5 model resolution index contour (about 19 to 21 m depth) is slightly shallower than 0.1 DOI index lower contour at about 27 m. The model resolution section avoids the localized regions with high DOI index values. It is less empirical compared to the DOI index method.



# Comparison of methods to assess model reliability

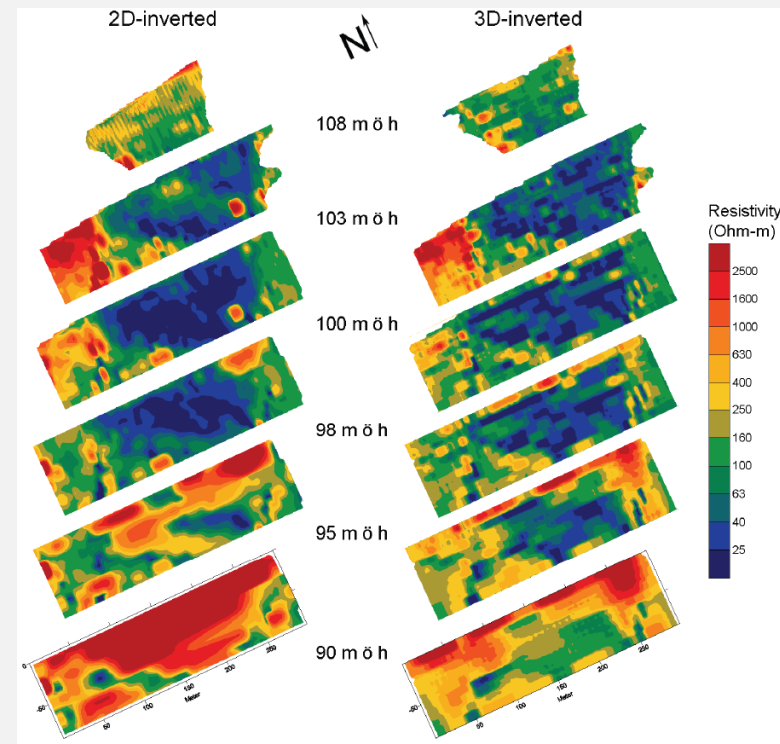
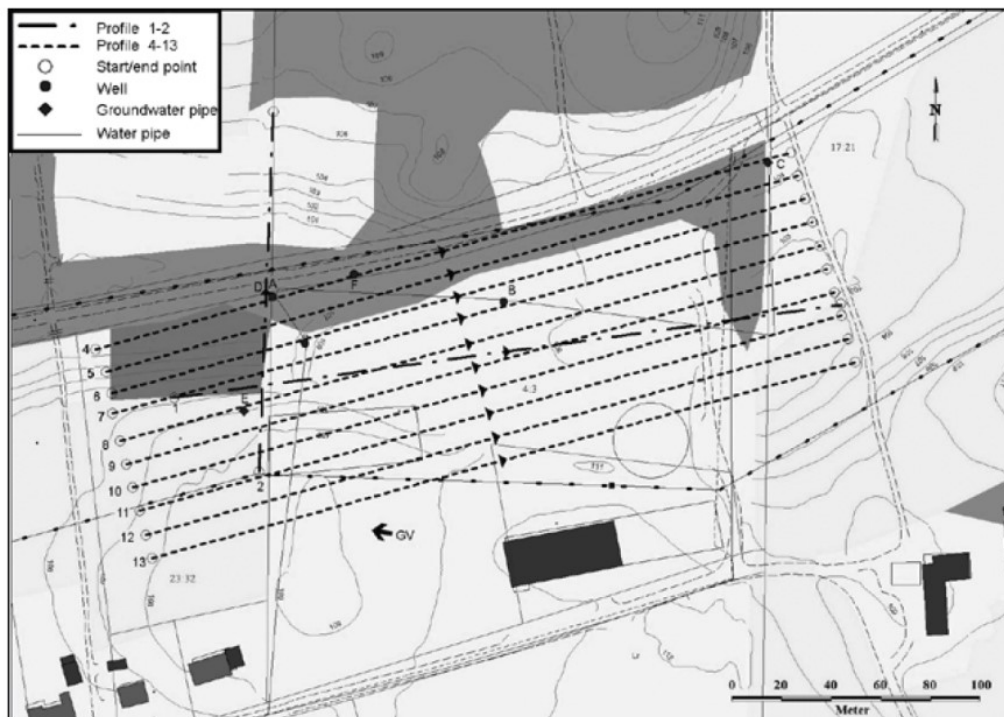
Method	Advantages	Disadvantages
<b>Sensitivity</b>	<b>Simple and fast to calculate.</b>	<b>A very crude measure. Does not take into account data redundancy.</b>
<b>DOI</b>	<b>Can be used for any inversion model. Only requires two inversions of the same data set. It can be used for very large 3-D models.</b>	<b>Can have localized regions with high or low DOI values, caused by noise or local anomalies. Sensitive to stability of inversion method used.</b>
<b>Resolution</b>	<b>Less subjective, shows a smoother variation than DOI.</b>	<b>Calculation time is proportional to <math>n^3</math> (<math>n</math>=number of model cells). Limitations in using for very large 3-D models</b>

# **Banding effects in 3-D models**

**Methods for reducing banding effects in 3-D inversion models for data collated from 2-D surveys lines.**

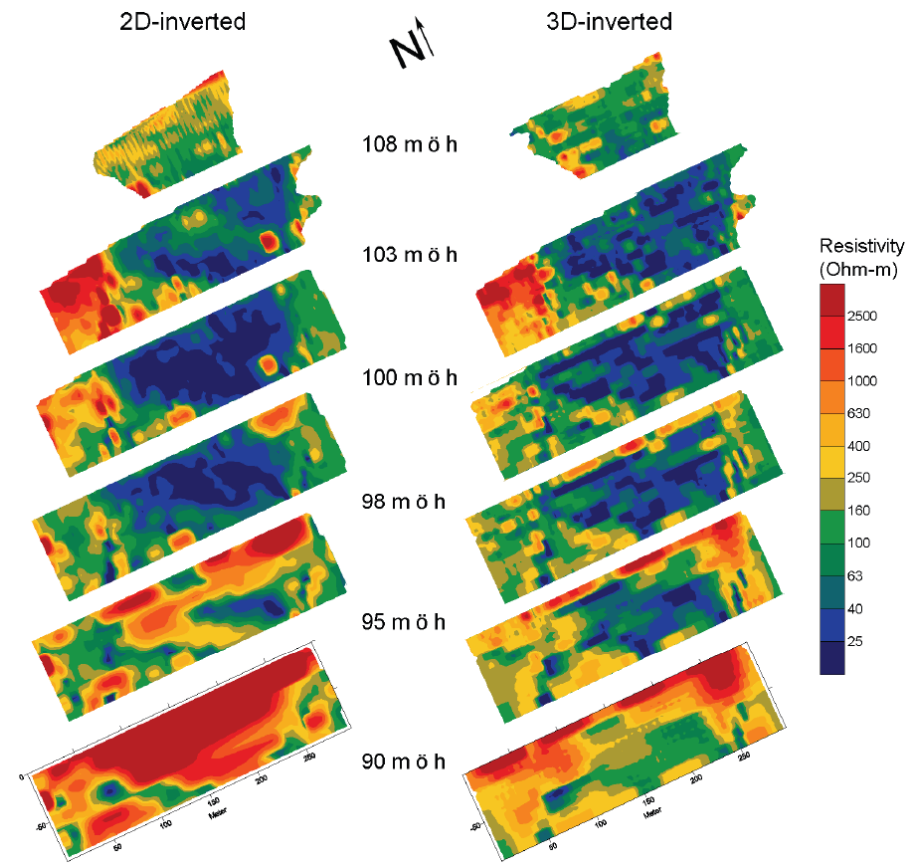
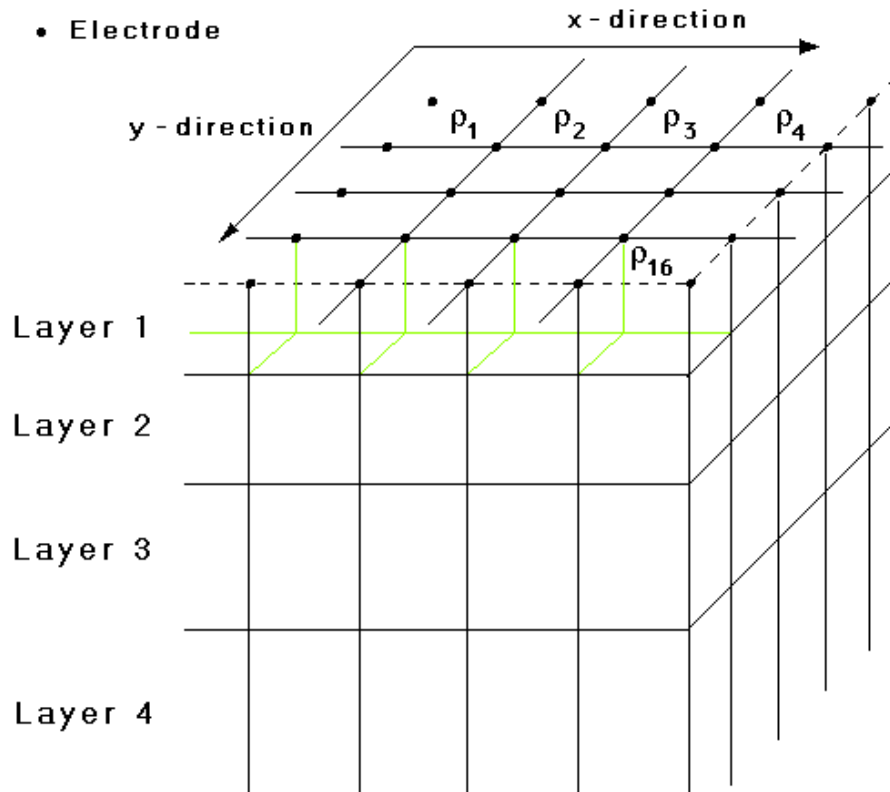
# Field example of 3-D banding effects

This survey was over the Ekeboda landfill (Sweden) has 10 parallel 2-D lines. The low resistivity area in the 2-D model due to leachate downward migration at 95 m. elevation is much smaller than the 3-D model. Other known structures such as a buried culvert on the eastern side at 98 m. elevation shows up better in the 3-D model. However the 3-D model shows prominent linear artefacts that are aligned along or perpendicular to the direction of the survey lines.



# Cause of 3-D banding effects

The artefacts are due to the survey setup and the arrangement of model cells and the smoothness-constrained least-squares method used. The measurements are made in only one direction. The  $x$  and  $y$  axis of the model cells are arranged along and perpendicular to the direction of the survey lines. There is a directional bias in both the data and the model cells setup in the  $x$  and  $y$  directions.



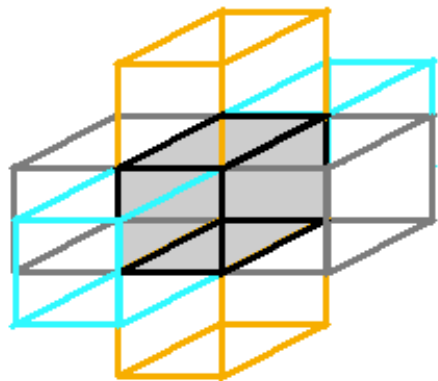
# Structure of the roughness filter

The roughness filter has the form 
$$\mathbf{F} = \delta\mathbf{x}^T \delta\mathbf{x} + \delta\mathbf{y}^T \delta\mathbf{y} + \delta\mathbf{z}^T \delta\mathbf{z}$$

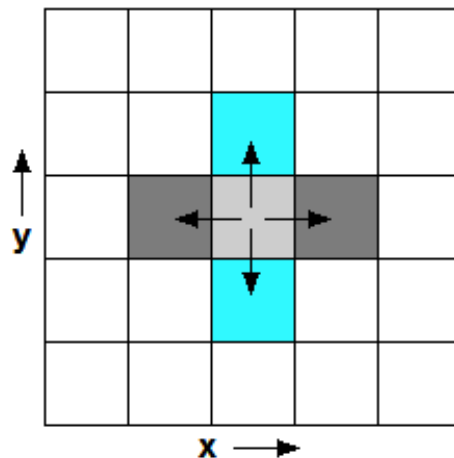
$\delta\mathbf{x}$ ,  $\delta\mathbf{y}$  and  $\delta\mathbf{z}$  are the first-order difference matrices in the  $x$ ,  $y$  and  $z$  directions. It minimizes the change the resistivity between adjacent model cells in the  $x$ ,  $y$  and  $z$  directions. It has a bias to produce structures that are aligned along the  $x$ ,  $y$  and  $z$  directions particularly if the  $L_1$ -norm (blocky) inversion method is used.

A modification to the horizontal roughness filter to include components in the diagonal  $x$ - $y$  directions is made to reduce the bias.

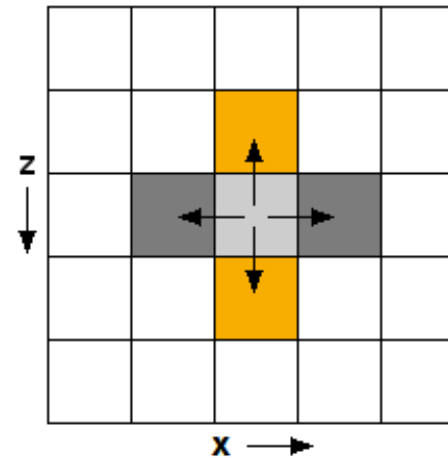
Coupling of 3-D model cells in roughness filter



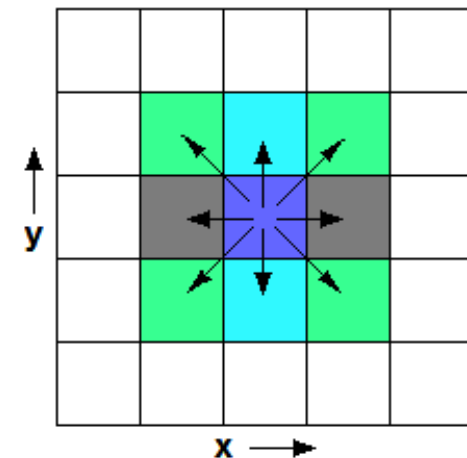
Normal horizontal roughness filter x and y components



Normal vertical roughness filter with z component

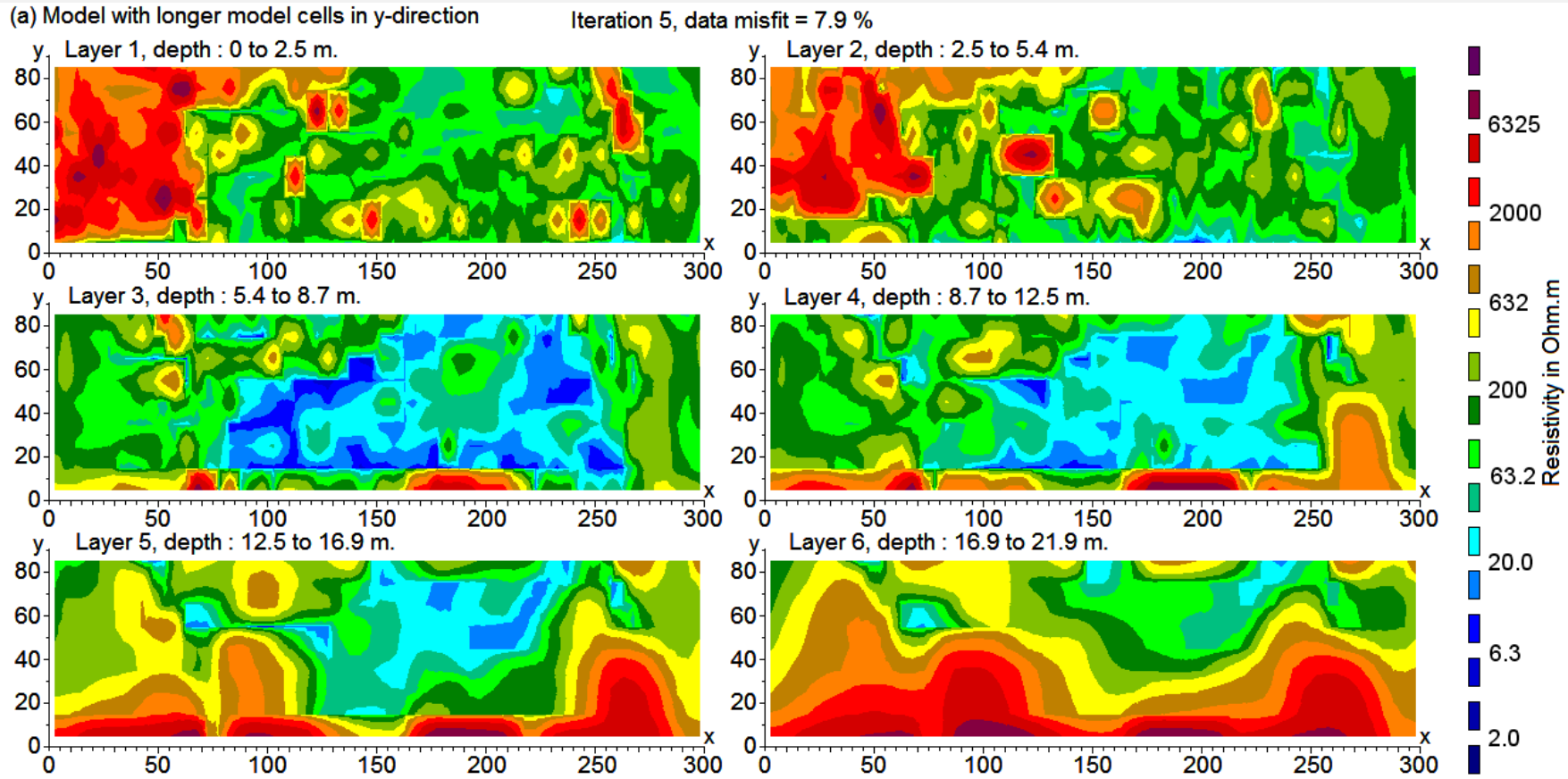


Horizontal roughness with diagonal x-y components



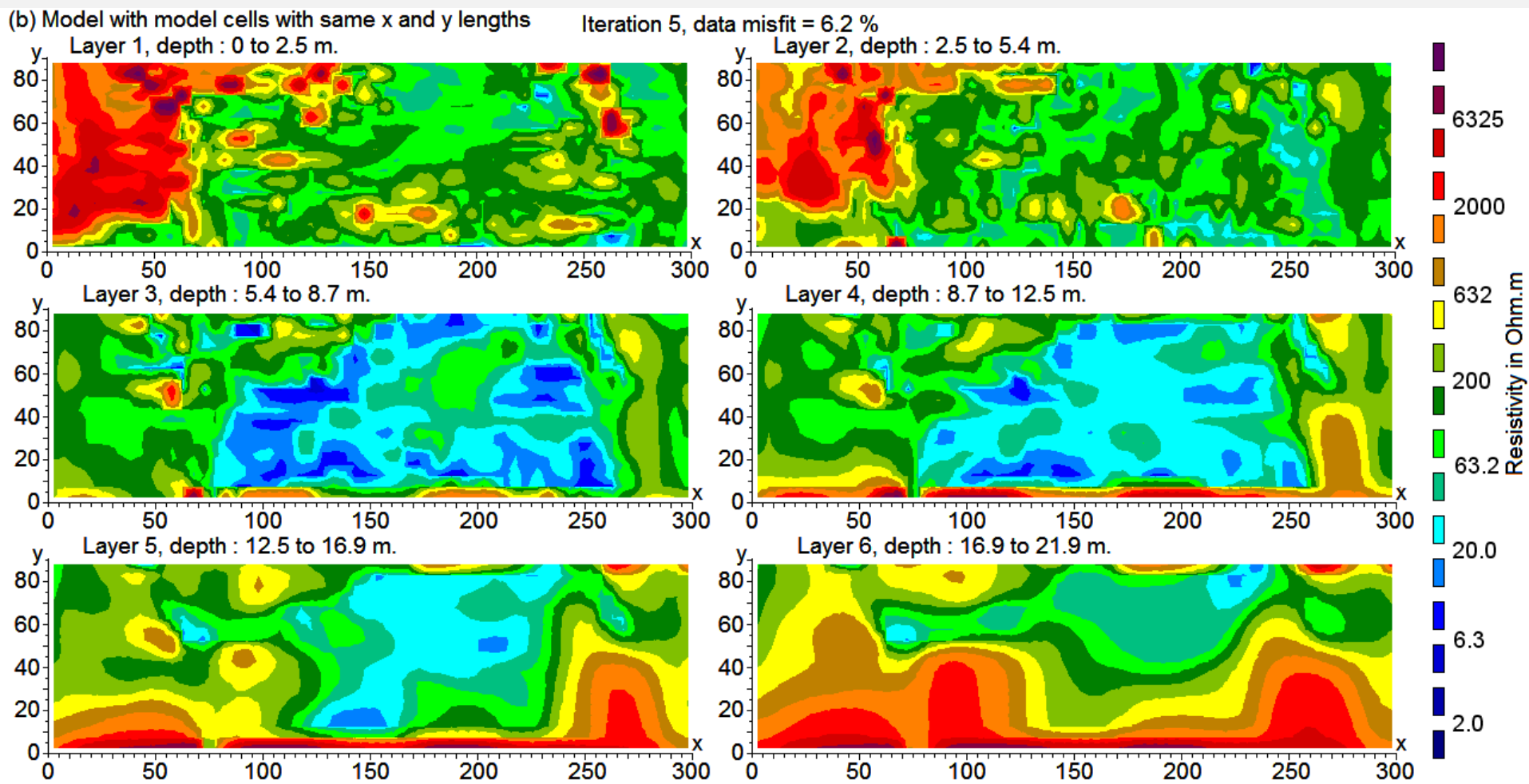
# Ekeboda landfill data set – default model

The field survey data set consists of 10 parallel lines with 61 electrode positions along each line using the multiple gradient array. The in-line electrode spacing is 5 m, and the spacing between the lines is 10 m. The model has prominent structures in the top two layers that are elongated in the  $y$  direction as the model cells are twice as long in this direction.



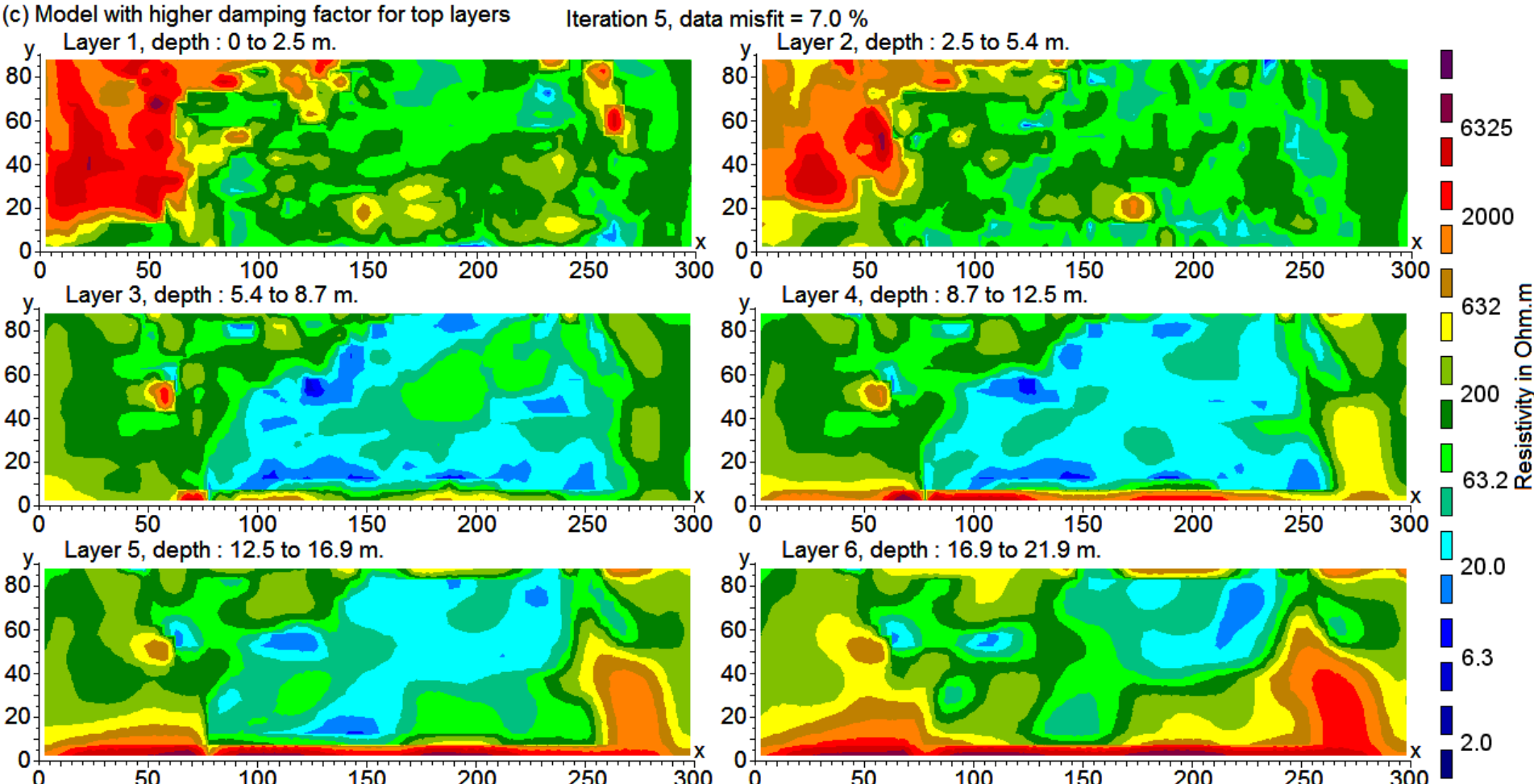
# Ekeboda landfill – model with uniform cell lengths

The inversion model with cells of the same lengths in the  $x$  and  $y$  directions removes the elongated structures in the  $y$  direction. The banding effect in the  $x$  direction is more clearly shown in the top three layers, such as in the low resistivity (blue) landfill.



# Ekeboda landfill – using higher damping factors

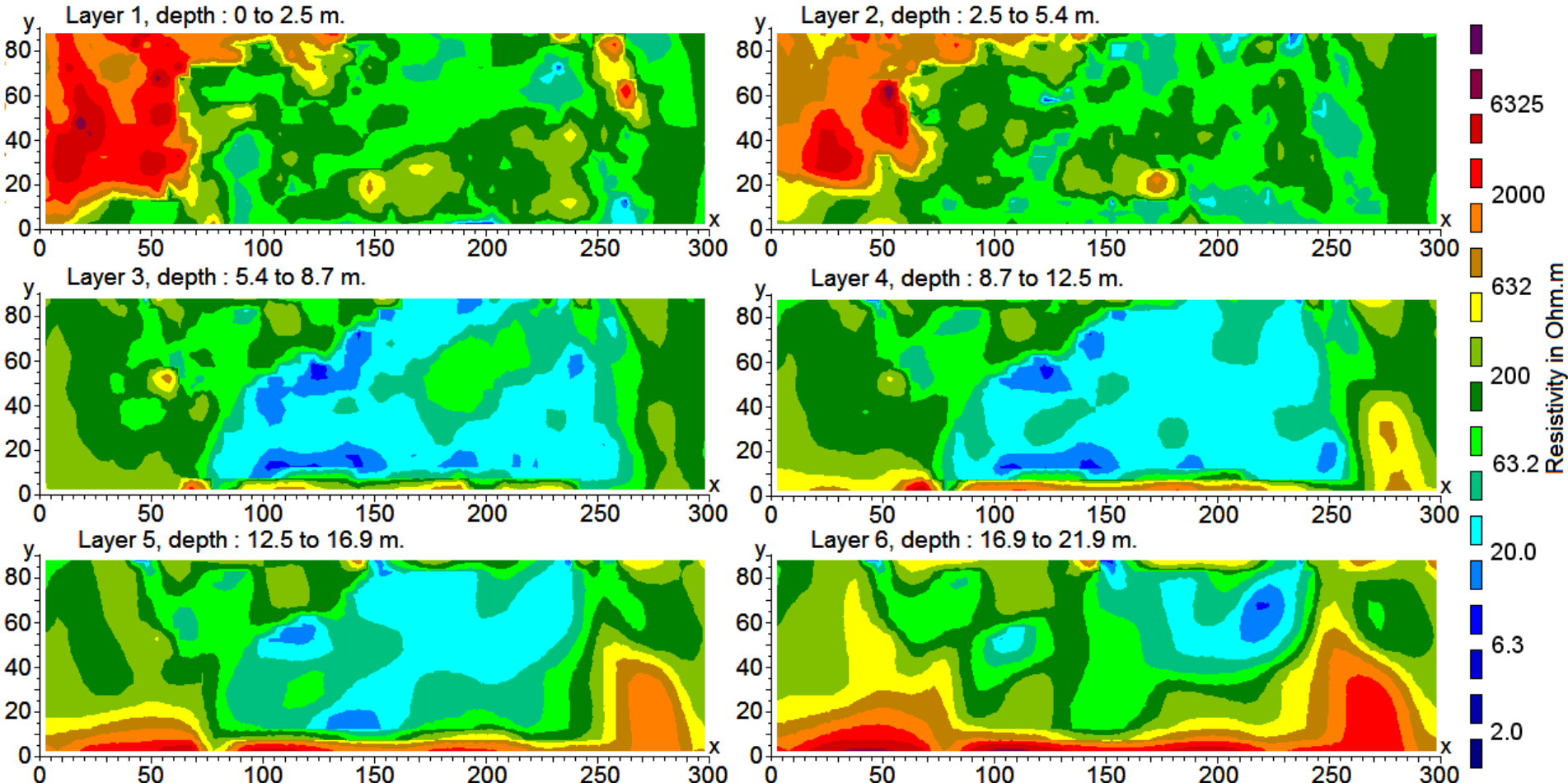
The elongated structures in the x direction are reduced by using a higher damping factor for the top layers. The more slanting left boundary of the low resistivity landfill is now more clearly shown.



# Ekeboda landfill data set – using diagonal filters

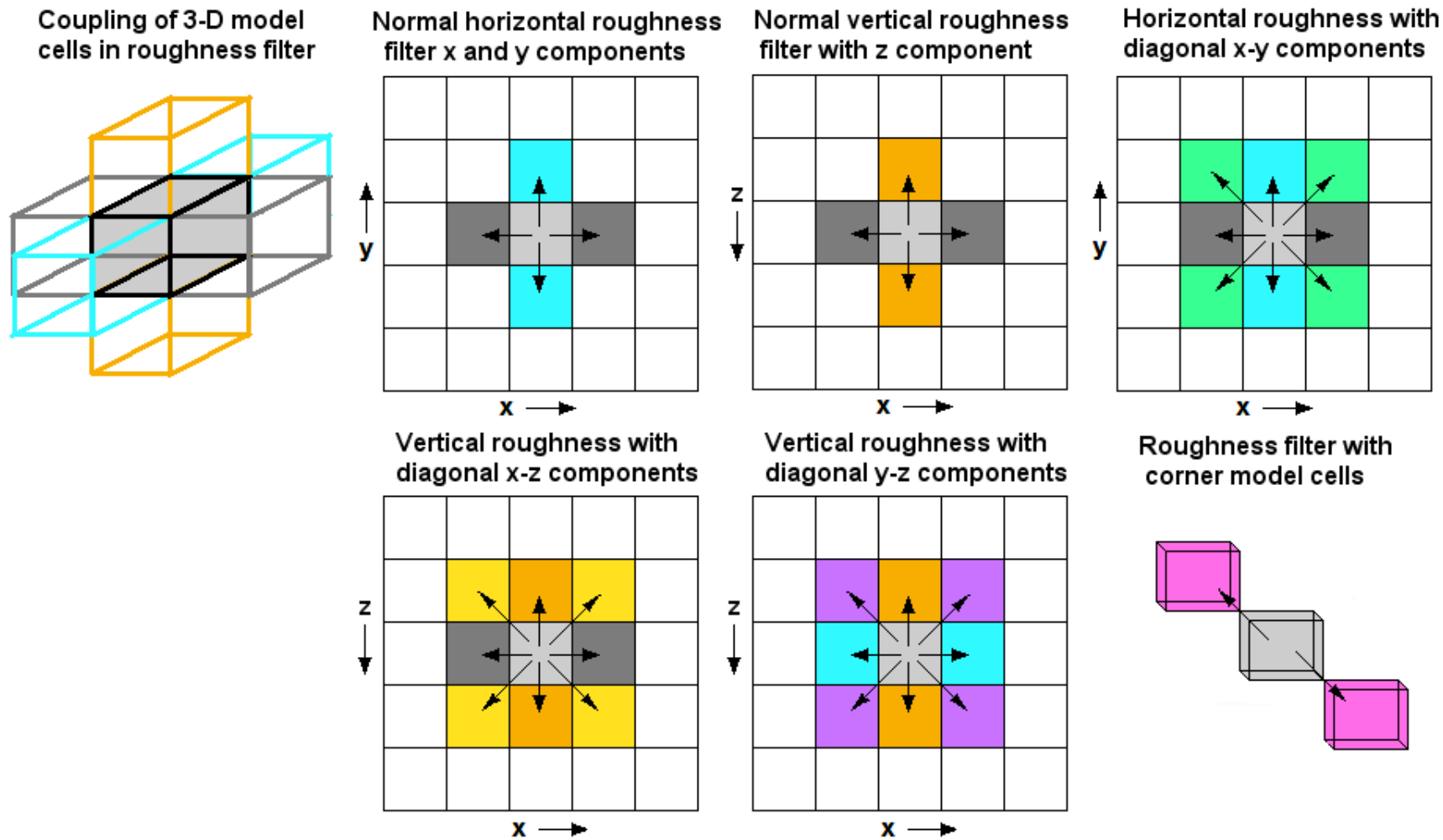
The elongated structures in the  $x$  direction are almost completely removed when the horizontal roughness filter with diagonal  $x$ - $y$  components is used.

(d) Model with higher damping factor for top layers and diagonal  $x$ - $y$  filter



# Other types of diagonal filters

Roughness filters with diagonal components in the  $x$ - $z$  and  $y$ - $z$  directions can be used to reduce bias in the vertical direction. The roughness filter can also be applied between the central and corner cells as well (only 2 out of 8 corner cells are shown).



# Banding effects conclusions

Many 3-D data sets are collated from a series of parallel 2-D survey lines. The distance between the lines is often two or more times the in-line electrode spacing.

Inversion models for such 3D data sets can display artefacts in the top layers elongated along the axes of the survey grid.

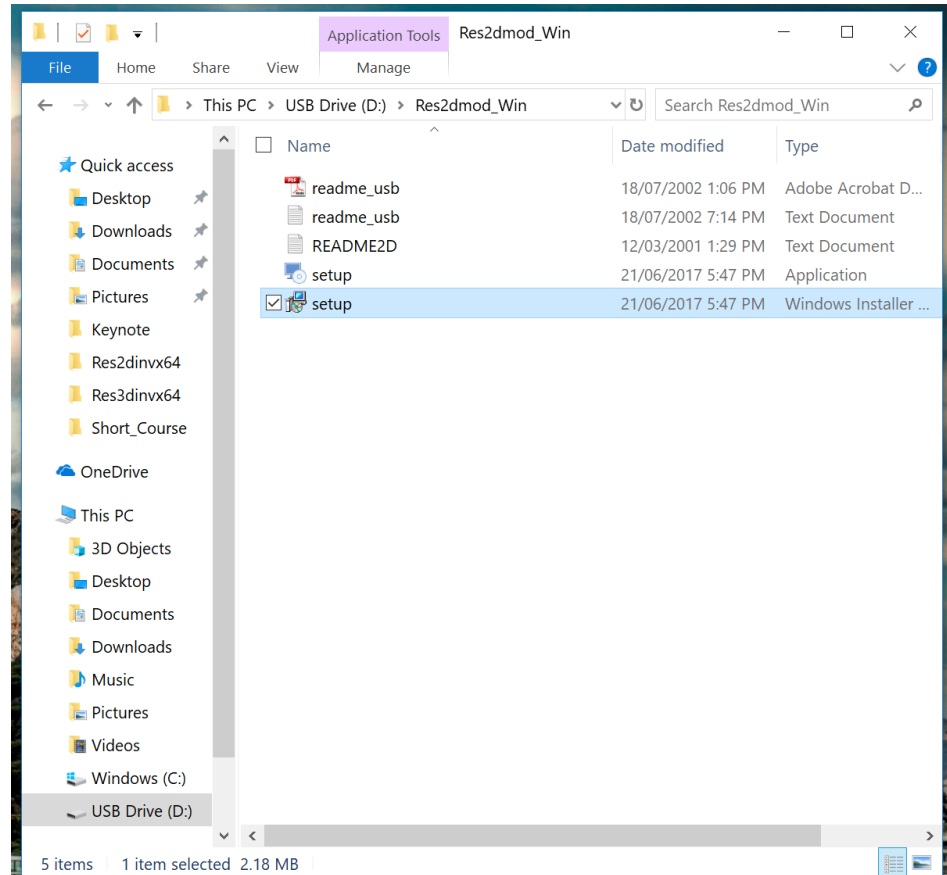
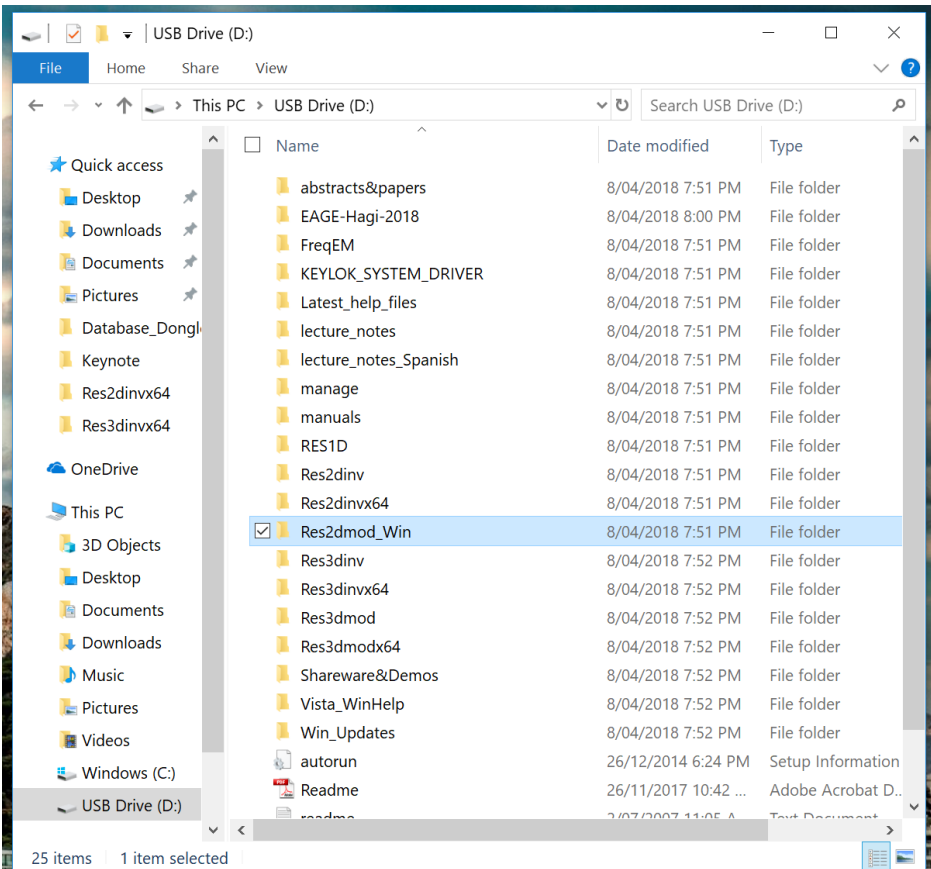
The artefacts are reduced by using a model discretization where the cells have about the same lengths in both horizontal directions.

Further reductions in the artefacts are achieved by using a higher damping factor for the top few layers.

Using a horizontal roughness filter with diagonal components will remove most remaining direction artefacts.

# Software installation – Res2dmod software

All the software and data files are in the USB drive provided. To install the programs, use the Windows File Explorer to list the folders in the USB drive. Go to the Res2dmod\_Win folder, and within the folder select the setup.exe file to install the Res2dmod program.



# Software installation – Res2dinvx64 software

Follow the same steps to install the Res2dinvx64, Res3dmodx64 and Res3dinvx64 programs.

